Universidade de Aveiro Departamento de Química
2010

Susana Cristina de Matos Fernandes

Novos materiais baseados em quitosano, seus derivados e fibras de celulose

Novel materials based on chitosan, its derivatives and cellulose fibres

Universidade de Aveiro Departamento de Química
2010

Susana Cristina de Matos Fernandes

Novos materiais baseados em quitosano, seus derivados e fibras de celulose

Novel materials based on chitosan, its derivatives and cellulose fibres

Dissertação apresentada à Universidade de Aveiro e à Université de Pau et des Pays de l'Adour para cumprimento dos requisitos necessários à obtenção do grau de Doutor em Química, realizada sob a orientação científica do Professor Doutor Alessandro Gandini, Investigador Coordenador do Departamento de Química da Universidade de Aveiro, Professor Doutor Carlos Pascoal Neto, Professor Catedrático do Departamento de Química da Universidade de Aveiro e do Professor Doutor Jacques Desbrières, Professor Catedrático do Departamento de Química da Universidade de Pau et des Pays de l'Adour.

texto Apoio financeiro do POCTI no âmbito do III Quadro Comunitário de Apoio.

texto Apoio financeiro da FCT e do FSE no âmbito do III Quadro Comunitário de Apoio.

Ciência.Inovação 2010 Programa Operacional Ciência e Inovação 2010

o júri

presidente

Doutor Aníbal Manuel Oliveira Duarte
professor catedrático da Universidade de Aveiro

Doutora Maria Helena Mendes Gil
professora catedrática da Universidade de Coimbra

Doutor Mohamed Naceur Belgacem
professor catedrático do Institut National Polytechnique de Grenoble

Doutora Carmen Sofia da Rocha Freire Barros
investigadora auxiliar da Universidade de Aveiro

Doutor Jacques Desbrières
professor catedrático da Université de Pau et des Pays de l'Aldour

Prof. Doutor Carlos Pascoal Neto
professor catedrático da Universidade de Aveiro

Doutor Alessandro Gandini
investigador coordenador da Universidade de Aveiro

Aos meus pais
Amélia e José

agradecimentos

A meta de um trabalho desta natureza só foi possível com o estímulo, ajuda e compreensão de algumas pessoas e instituições. São para elas estas palavras de agradecimento.

Em primeiro lugar, aos meus orientadores, ao Prof. Doutor Alessandro Gandini pela oportunidade, ao Prof. Doutor Carlos Pascoal Neto pelo incentivo e ao Prof. Doutor Jacques Desbrières pela dedicação. Aos três pela orientação paciente, pelo empenho, pela amizade e pela permanente compreensão demonstrados ao longo deste caminho. Ao Prof. Doutor Alessandro Gandini, por quem fui incentivada e encaminhada a fazer uma tese de doutoramento, ficarei eternamente grata.

À Doutora Carmen Freire e ao Prof. Doutor Armando Silvestre, mentores não formais, pelo vosso empenho, pelos vossos conselhos e pela vossa amizade e confiança.

Com as diferentes formas de ser e estar de cada um de vós aprendi muito sobre química, polímeros naturais, materiais e compósitos, mas também aprendi muito sobre relações humanas. Bem hajam!

Agradeço ao Prof. Doutor Inãki Mondragon, ao Prof. Doutor Mohamed Naceur Belgacem, à Prof. Doutora Maria Helena Gil e à Doutora Carmen Freire, examinadores e/ou membros do júri, por terem aceitado avaliar o meu trabalho de tese e pelo interesse demonstrado.

À Carmen, minha companheira incansável na realização deste trabalho, agradeço a dedicação, a amizade, a disponibilidade e o encorajamento prestados durante as dificuldades e imprevistos.

À Lúcia, colega de laboratório e depois amiga, que partilhou comigo as agonias da “produção” dos primeiros filmes transparentes, obrigada!

Aos meus colegas e amigos do Grupo de Materiais Macromoleculares e Lignocelulósicos, da Plataforma IDPoR e do CICECO, aos colegas e amigos do IPREM e às pessoas que me acolheram no Innventia AB pela amizade, pelo apoio, entusiasmo e boa disposição demonstradas ao longo da realização deste doutoramento, o meu bem hajam!

Ao Dominique Gillet (Mahtani Chitosan Pvt. Ltd., India) e ao Tör Håkonsen (Norwegian Chitosan AS., Noruega) pelo interesse e disponibilidade que sempre demonstraram e pela oferta das amostras de quitosano e quitina. Obrigada!

Agradeço ao Prof. Lars Berglund pela oportunidade de um estágio no KTH em Estocolmo, pela colaboração e oferta da NFC, e pela simpatia e disponibilidade.

À Drª Anne-Mari Olsson (Innventia AB), ao Prof. Lennart Salmén (Innventia AB), à Drª Sandra Magina (CICECO-Universidade de Aveiro), à Doutora Sylvie Blanc (IPREM), ao Doutor Ross Brown (IPREM), ao Doutor Laurent Rubatat (IPREM), à Drª Celeste Azevedo (Universidade de Aveiro), ao Dr Ricardo Pinto (CICECO-Universidade de Aveiro), à Doutora Márcia Neves (CICECO-Universidade de Aveiro), à Doutora Maria Rute Ferreira (CICECO-Universidade de Aveiro), ao Prof. Luís Carlos (CICECO-Universidade de Aveiro) pela colaboração e pela disponibilidade demonstrada.

Manifesto, aqui, o meu apreço ao Raiz - Instituto de Investigação da Floresta e Papel – pela disponibilidade das instalações, amostras de papel e equipamentos, e, claro, pela boa vontade sempre demonstrada por parte de todos. Em especial ao Engº. Amaral, ao Engº. Mendes Sousa, à Drª Fernanda Paula Furtado, ao José Carlos e a todas as pessoas dos diferentes laboratórios por onde passei, pela disponibilidade e boa vontade.

Ao Departamento de Química, CICECO, IPREM e Innventia AB agradeço a disponibilidade para a realização de parte deste trabalho nas suas instalações. À Plataforma IDPoR por todas as facilidades e oportunidades concedidas ao longo destes anos.

À Fundação para a Ciência e a Tecnologia (FCT) pelo apoio financeiro através da concessão de uma bolsa de Doutoramento (SFRH/BD/41388/2007) e pelo “National Program for Scientific re-equipment” Rede/1509/RME/2005 e REEQ/515/CTM/2005. À Peter Wallenberg's Foundation pelo suporte financeiro durante a minha estadia em Estocolmo.

E por fim, mas certamente não por menos, agradeço aos meus pais, ao meu irmão e a vocês, os meus mais próximos, que encontrei e reencontrei por Aveiro, Pau e por onde a vida me tem levado, que suportaram as presenças e as ausências, que se riram de mim e me puseram na ordem, que me ensinaram as virtudes e partilharam as fraquezas. Bem hajam!

palavras-chave

quitina, quitosano, celulose nanofibrilada, celulose bacteriana, nanocompositos transparentes, revestimentos de papel, oxipropilação.

resumo

O presente trabalho tem como principal objectivo o desenvolvimento de novos materiais baseados em quitosano, seus derivados e celulose, na forma de nanofibras ou de papel.

Em primeiro lugar procedeu-se à purificação das amostras comerciais de quitosano e à sua caracterização exaustiva em termos morfológicos e físico-químicos. Devido a valores contraditórios encontrados na literatura relativamente à energia de superfície do quitosano, e tendo em conta a sua utilização como precursor de modificações químicas e a sua aplicação em misturas com outros materiais, realizou-se também um estudo sistemático da determinação da energia de superfície do quitosano, da quitina e seus respectivos homólogos monoméricos, por medição de ângulos de contacto Em todas as amostras comerciais destes polímeros identificaram-se impurezas não polares que estão associadas a erros na determinação da componente polar da energia de superfície. Após a remoção destas impurezas, o valor da energia total de superfície (γ_s), e em particular da sua componente polar, aumentou consideravelmente.

Depois de purificadas e caracterizadas, algumas das amostras de quitosano foram então usadas na preparação de filmes nanocompósitos, nomeadamente dois quitosanos com diferentes graus de polimerização, correspondentes derivados solúveis em água (cloreto de *N*-(*3-(N,N,N*-trimetilamónio)-2-hidroxipropilo) de quitosano) e nanofibras de celulose como reforço (celulose nanofibrilada (NFC) e celulose bacteriana (BC). Estes filmes transparentes foram preparados através de um processo simples e com conotação 'verde' pela dispersão homogénea de diferentes teores de NFC (até 60%) e BC (até 40%) nas soluções de quitosano (1.5% w/v) seguida da evaporação do solvente. Os filmes obtidos foram depois caracterizados por diversas técnicas, tais como SEM, AFM, difracção de raio-X, TGA, DMA, ensaios de tracção e espectroscopia no visível. Estes filmes são altamente transparentes e apresentam melhores propriedades mecânicas e maior estabilidade térmica do que os correspondentes filmes sem reforço.

Outra abordagem deste trabalho envolveu o revestimento de folhas de papel de *E. globulus* com quitosano e dois derivados, um derivado fluorescente e um derivado solúvel em água, numa máquina de revestimentos ('máquina de colagem') à escala piloto.

Este estudo envolveu inicialmente a deposição de 1 a 5 camadas do derivado de quitosano fluorescente sobre as folhas de papel de forma a estudar a sua distribuição nas folhas em termos de espalhamento e penetração, através de medições de reflectância e luminescência. Os resultados mostraram que, por um lado, a distribuição do quitosano na superfície era homogénea e que, por outro lado, a sua penetração através dos poros do papel cessou após três deposições. Depois da terceira camada verificou-se a formação de um filme contínuo de quitosano sobre a superfície do papel. Estes resultados mostram que este derivado de quitosano fluorescente pode ser utilizado como marcador na optimização e compreensão de mecanismos de deposição de quitosano em papel e outros substratos. Depois de conhecida a distribuição do quitosano nas folhas de papel, estudou-se o efeito do revestimento de quitosano e do seu derivado solúvel em água nas propriedades finais do papel. As propriedades morfológicas, mecânicas, superficiais, ópticas, assim como a permeabilidade ao ar e ao vapor de água, a aptidão à impressão e o envelhecimento do papel, foram exaustivamente avaliadas. De uma forma geral, os revestimentos com quitosano e com o seu derivado solúvel em água tiveram um impacto positivo nas propriedades finais do papel, que se mostrou ser dependente do número de camadas depositadas. Os resultados também mostraram que os papéis revestidos com o derivado solúvel em água apresentaram melhores propriedades ópticas, aptidão à impressão e melhores resultados em relação ao envelhecimento do que os papéis revestidos com quitosano. Assim, o uso de derivados de quitosano solúveis em água em processos de revestimento de papel representa uma estratégia bastante interessante e sustentável para o desenvolvimento de novos materiais funcionais ou na melhoria das propriedades finais dos papéis.

Por fim, tendo como objectivo valorizar os resíduos e fracções menos nobres da quitina e do quitosano provenientes da indústria transformadora, estes polímeros foram convertidos em polióis viscosos através de uma reacção simples de oxipropilação. Este processo tem também conotação "verde" uma vez que não requer solvente, não origina subprodutos e não exige nenhuma operação específica (separação, purificação, etc) para isolar o produto da reacção. As amostras de quitina e quitosano foram pré-activadas com KOH e depois modificadas com um excesso de óxido de propileno (PO) num reactor apropriado. Em todos os casos, o produto da reacção foi um líquido viscoso composto por quitina ou quitosano oxipropilados e homopolímero de PO. Estas duas fracções foram separadas e caracterizadas.

keywords

chitin, chitosan, nanofibrillated cellulose, bacterial cellulose, transparent nanocomposites, paper coating, oxypropylation

abstract

The purpose of this study was to develop new materials based on chitosan and its derivatives and cellulose, in the form of nanofibres or paper sheet.
Firstly, the commercial chitosan samples were thoroughly characterized in terms of morphology and physicochemical aspects. Because of conflicting reports and unrealistic literature values, and because of the use of chitosan as mixtures component, or as precursor for chemical modifications, a systematic study of the surface energy of chitin, chitosan and their respective monomeric counterparts was carried out using contact angle measurements. All the commercial samples of these polymers were shown to contain non-polar impurities that gave rise to enormous errors in the determination of the polar component of their surface energy. After their thorough removal, the value of the total surface energy (γ_s), and particularly of its polar component, increased considerably.
Well characterized chitosan samples were then used to prepare transparent nanocomposite films based on different chitosan (CH) matrices (two chitosans with different DPs and corresponding water-soluble derivatives (*N*-(*3-(N,N,N*-trimethylamonium)-2-hydroxypropyl) chloride chitosan), nanofibrillated cellulose (NFC) and bacterial cellulose (BC) were prepared by a fully green procedure by casting a water based suspension of CH, NFC and BC. Different contents of NFC (up to 60%) and BC (up to 40%) were dispersed in 1.5% (w/v) CH solutions. The films were characterized by several techniques, namely SEM, AFM, X-ray diffraction, TGA, tensile assays, dynamic mechanical analysis and visible spectroscopy. The films obtained were shown to be highly transparent, displayed better mechanical properties than the corresponding unfilled chitosan films and showed increased thermal stability.
Another approach involved the coating of *E. globulus* based paper sheets with chitosan and two different chitosan derivatives, a fluorescent and a water-soluble derivative, on a pilot-size press machine.
First, a fluorescent chitosan derivative was deposited layer-by-layer onto conventional paper sheets and its distribution, in terms of both spreading and penetration, was assessed by emission measurements. The results showed that, on the one hand the surface distribution was highly homogeneous and, on the other hand, the penetration of chitosan within the paper pores ceased after a three-layer deposit, beyond which any additional coating only produced an increase in its overall thickness and film-forming aptitude. These results show that this modified chitosan can be used as probe to optimize and understand the mechanism of the deposition of chitosan onto paper and other substrates.

Then, the effect of chitosan and chitosan quaternization on the final properties of chitosan-coated papers was investigated. Different coating weights were attained by the deposition of 1-5 coating layers. The morphological, mechanical, surface, barrier and optical properties as well as the paper ageing and printability of the ensuing coated papers were investigated and assessed. In general, both chitosan and water-soluble chitosan coatings had a positive impact on the final properties of the coated papers, which was quite dependent on the number of deposited chitosan layers. The results obtained also showed that the water-soluble chitosan coated papers presented superior optical properties, inkjet print quality and better results on ageing measurements than chitosan coated papers. Therefore, the use of water-soluble chitosan derivatives on paper coating processes represents an interesting and sustainable strategy for the development of new functional paper materials or for the improvement of the end-user properties of paper products.
Finally, chitin and chitosan were converted into viscous polyols through a simple oxypropylation reaction, with the aim of valorising the less noble fractions or by-products of these valuable renewable resources. This process bears “green” connotations, given that it requires no solvent, leaves no by-products and no specific operations (separation, purification, etc.) are needed to isolate the entire reaction product. Chitin or chitosan samples were preactivated with KOH and then reacted with an excess of propylene oxide (PO) in an autoclave. In all instances, the reaction product was a viscous liquid made up of oxypropylated chitin or chitosan and PO homopolymer. The two fractions were separated and thoroughly characterized.

abreviations

AA: Acetic Acid Solution

AFM: Atomic Force Microscopy

BC: Bacterial Cellulose

CH: Chitosan

CHBC: Chitosan-Bacterial Cellulose

CHNFC: Chitosan-Nanofibrillated Cellulose

CS: Control Sheet

DA: Degree of N-acetylation

DDA: Degree of N-deacetylation

DMA: Dynamic Mechanical Analysis

DP: Degree of Polymerization

DSC: Differential Scanning Calorimetry

EA: Elemental Analysis

FITC: Fluorescein Isothiocyanate

FITC-CH: Fluorescent Chitosan

FTIR: Fourier-Transform Infra-Red Spectroscopy

GC-MS: Gas Chromatography- Mass Spectrometry

GlcNAc: N-acetyl-D-glucosamine

GlcN: D-glucosamine

GTMAC: Glycidyltrimethylammonium Chloride

HCH: High Molecular Weight Chitosan

HCHBC: High Molecular Weight Chitosan-Bacterial Cellulose

HCHNFC: High Molecular Weight Chitosan-Nanofibrillated Cellulose

HP: Homopolymer

I_{OH}: Hydroxyl Index Number

LCH: Low Molecular Weight Chitosan

LCHBC: Low Molecular Weight Chitosan-Bacterial Cellulose

LCHNFC: Low Molecular Weight Chitosan-Nanofibrillated Cellulose

$\bar{M}_w$**:** Average Molecular Weight

MFC: Microfibrillar Cellulose

MT: Mechanical Treatment

NFC: Nanofibrillated Cellulose

NMR: Nuclear Magnetic Resonance

PL: Polyol

PO: Propylene Oxide

PPO: Propylene Oxide Homopolymer

SEC: Size Exclusion Chromatography

SEC-MALS: Size Exclusion Chromatography Multi-Angle Light Scattering

SEM: Scanning Electron Microscopy

SR: Solid Residues

$\mathbf{Td_i}$**:** Initial Degradation Temperature

$\mathbf{Td_1}$**:** Maximum First Degradation Temperature

$\mathbf{Td_2}$**:** Maximum Second Degradation Temperature

TGA: Thermogravimetric Analisys

W: Water

WSCH: Water-Soluble Chitosan Derivative

WSHCH: Water-Soluble High Molecular Weight Chitosan Derivative

WSLCH: Water-Soluble Low Molecular Weight Chitosan Derivative

WSHCHBC: Water-Soluble High Molecular Weight Chitosan-Bacterial Cellulose

WSLCHBC: Water-Soluble Low Molecular Weight Chitosan-Bacterial Cellulose

WSHCHNFC: Water-Soluble High Molecular Weight Chitosan-Nanofibrillated Cellulose

WSLCHNFC: Water-Soluble Low Molecular Weight Chitosan-Nanofibrillated Cellulose

XRD: X-Ray diffraction

$[\eta]$: Intrinsic Viscosity

γ_s**:** Surface Energy

γ_s^d : Surface Energy, dispersive component

γ_s^p: Surface Energy, polar component

Contents

Introduction 1
The context 1
Objectives of the work 6

Part I
The state of the art 9

1 Chitin and chitosan 11
1.1 History 12
1.2 Occurrence 13
1.3 Processing of chitin and chitosan 15
1.4 Properties and functionalities 17
1.5 Chitosan derivatives 22
1.6 Applications 24

2 Cellulose 27
2.1 Properties and functionalities 28
2.2 Micro- and nanofibrillated cellulose 31
2.3 Bacterial cellulose 32

3 Chitosan-cellulose composites 35
3.1 Chitosan-cellulose: micro- and nanocomposites 36

4 Chitosan and cellulose in paper coating 39

5 Oxypropylation of natural polymeric substrates 43

Part II
Experimental 49

6 Materials and Methods 53
6.1 Chitin and chitosan 53
6.1.1 Purification of chitosan 54
6.1.2 Degree of N-acetylation 54
6.1.3 Molecular weight 57
6.1.4 Surface energy 58

6.1.5 Other properties 60
6.2 Cellulose substrates. 60
6.2.1 Bacterial cellulose 60
6.2.2 Nanofibrillated cellulose 61
6.2.3 Paper sheets 61

7. Synthesis of chitosan derivatives 65
7.1 Fluorescent chitosan 65
7.2 Water-soluble chitosan 66

8 Preparation of the chitosan-cellulose nanocomposite films 69
8.1 Blends 69
8.2 Nanocomposite films 70
8.3 Techniques used to characterize these materials 70

9 Coating experiments 73
9.1 General conditions 73
9.2 Preparation of the chitosan-coated papers using FITC-CH 74
9.3 Preparation of papers coated with CH and WSCH 76

10 Chitin and chitosan oxypropylation 77

Part III
Results and discussion 81

11 Chitosan and cellulose substrates: characterization 85
11.1 Chitin and chitosan 85
11.1.1 Degree of N-acetylation 85
11.1.2 Molecular weight 89
11.1.3 Surface energy 91
11.1.4 Other properties 98
11.2 Chitosan derivatives 102
11.2.1 Fluorescent chitosan 102
11.2.2 Water-soluble chitosan 106
11.3 Cellulose substrates 110
11.3.1 Bacterial cellulose 110
11.3.2 Nanofibrillated cellulose 111
11.3.3 Paper sheets 112

12 Chitosan-cellulose nanocomposite films 115
12.1 Morphology 117
12.2 Chemical structure 123
12.3 Crystallinity 125
12.4 Thermal stability 127
12.5 Optical properties 131

12.6 Mechanical properties 135
12.7 Final considerations 144

13 Chitosan-coated papers 145
13.1 Evaluation of the chitosan onto the paper sheets using a fluorescent chitosan 145
13.1.1 Reflectance 146
13.1.2 Luminescence 148
13.1.3 Final considerations 151
13.2 Effect of chitosan and chitosan quaternization on the final properties of chitosan-coated papers 151
13.2.1 Morphology 152
13.2.2 Mass properties 155
13.2.3 Roughness 156
13.2.4 Mechanical properties 157
13.2.5 Barrier properties 162
13.2.6 Optical properties 163
13.2.7 Paper lightfastness 164
13.2.8 Inkjet print quality 166
13.2.9 Final considerations 171

14 Chitin and chitosan oxypropylation 173
14.1 Structural properties 174
14.2 Elemental analysis 177
14.3 Thermal stability 178
14.4 DSC 180
14.5 Viscosity 181
14.6 I_{OH} 181
14.7 Final remarks 181

15 General conclusions and perspectives 183
15.1 Conclusions 183
15.2 Perspectives 186

References 189

Appendices

Introduction

The context

The exploitation of renewable resources as macromolecular materials precedes the use of conventional (fossil) counterparts by millennia. Renewable resources were always used by humans (e.g. fuel wood, fibres for textile and paper production or vegetable oils for illumination and lubricating), and their growth as materials began when men felt the need to develop activities and protect themselves from environmental conditions. For thousand of years a progressive sophistication of these materials and the enhancement of their properties and durability have been observed [1-3].

Nevertheless, the use of materials based on renewable resources declined in the 20th century first because of the development of the coal-based chemistry and after because of the petrochemical boom of the second half of the last century. As a result, the accessibility of an important number of cheap organic chemicals for the production of macromolecular materials originated the beginning of the well-known "plastic age" [1-2]. Nowadays, there are numerous well-developed and innovative technologies which are used to make sophisticated and multifaceted conventional polymers. These final products have been widely commercialized contributing for the life style of people around the world [1-2,4].

Over the past few decades, however, a renewed and growing interest on the exploitation of biomass resources for the development of new

materials, as well as a source of energy, has been observed.

This global tendency appears as a natural response for the expected scarcity of fossil resources (*viz*. petrol, natural gas and coal) in the next generations and also to the environmental concerns (mainly the massive plastic waste accumulation) associated with their continuous use during the last century and their non-biodegradable nature [1-2,4-8].

In this context, in the last decades, science and technology started to move in the direction of renewable raw materials that can overcome the well-known dependence on fossil resources. The aspiration is to develop chemicals, polymers, products and processes that are environmentally friendly and sustainable [3,9]. With the emergent interest in this topic a remarkable number of scientific publications (e.g. papers, patents, books and monographs), international meetings, industrial and public investments have been materialized.

Biopolymers, which are polymers produced by living organisms, are effectively vital in this question because of their renewable and recyclable nature, biodegradable character and abundance. Cellulose and starch, proteins and peptides, and DNA and RNA are all examples of biopolymers, in which the monomeric units are, sugars, amino acids, and nucleotides, respectively. It is estimated that the world vegetable biomass, which includes lignocellulosic materials, wood, agriculture residues, algae, among others, amounts to about 1.0×10^{13} tons (the solar energy renews about 3 per cent of it per annum) and the estimate yearly biosynthesis production from marine ecosystems is about 1.3×10^{9} tons to be compared with the annual production of synthetic polymers of about 1.4×10^{8} tons).

One of the most abundant and diversified groups of biopolymers are the polysaccharides. Cellulose and chitin are the most widespread natural polysaccharides, which perform structure-forming functions in flora and fauna, respectively.

Polysaccharides are polymeric carbohydrate structures, formed of repeating monosaccharides units joined together by glycosidic bonds. These structures are often linear, but may contain various degrees of branching as illustrated in Figure 0-1.

Cellulose, chitin and its derivative chitosan, and starch, used as such or modified, have been often assessed as alternative for petrol-based counterparts, not only as sustainable resources but also as attractive materials with specific properties and functionalities.

Despite the structural similarity of these polysaccharides (Figure 0-1), their properties (e.g. crystallinity, solubility and aptitude to chemical modification) are quite distinct, because of the only structural difference which reside in the replacement of an OH group at position C-2 in each saccharide unit of cellulose by an acetamido group in chitin, an amino counterpart in chitosan and by the presence of branched structures and different glycosidic linkages in starch, resulting in different functionalities that could be exploited for the development of new sophisticated materials.

Chitosan represents one of the most actively investigated materials from renewable resources because of its unique properties (biocompatibility, antimicrobial activity, biodegradability and excellent film-forming ability) and applications especially as biomaterial. The potential uses of chitosan derived from its exclusive chemistry, since it is a polycation contrasting with the other polysaccharides being usually neutral or anionic [10-13]. However, despite the enormous volume of publications dealing with chitosan (around 17 000), there is a lack of studies that permit to understand the physicochemical phenomena in systems where chitosan is used as a polymeric matrix, in blends and as a coating material.

Cellulose, the most abundant natural polymer and the oldest used on Earth, also presents unique advantages and properties, such as biodegradability, recyclability, biocompatibility, high diversity of fibres, relatively high resistance and stiffness, among others.

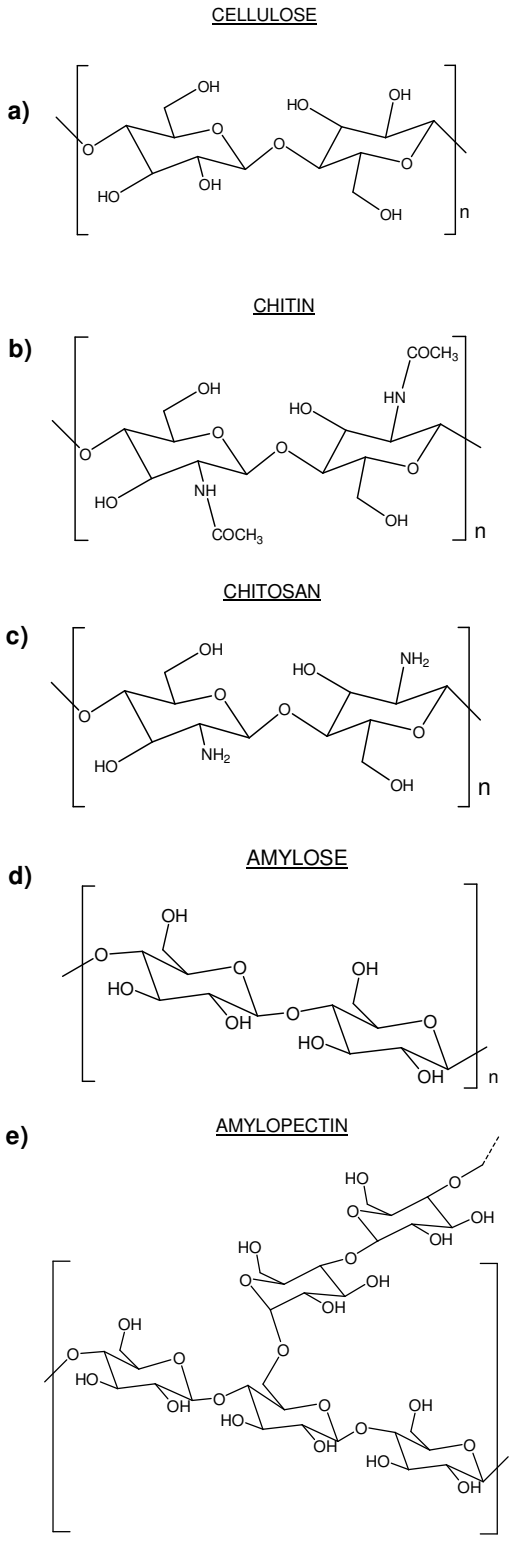

Figure 0-1. Chemical structures of cellulose a), chitin b), chitosan c) and starch (amylose d) and amylopectin e)).

This biopolymer has been widely explored, especially for making paper and textile materials, and more recently also as reinforcing element in polymeric composites. The blending of polymers to improve their chemical and physical properties has been received extensive attention in the past decades [14-19]. Despite their attractive properties, cellulose fibres are used only to a limited extent in such industrial applications due to difficulties associated with surface interactions (low interfacial compatibility and inter-fibre aggregation by hydrogen bonding). The inherent polar and hydrophilic nature of polysaccharides and the nonpolar characteristics of most thermoplastics result in difficulties in compounding the filler and the matrix [18-19] and, therefore, in achieving acceptable dispersion levels, which results in inefficient composites.

Considering the similarity in the chemical structure of chitosan and cellulose, it is expected that the blending of these polymers might improve the chemical, physical, mechanical and biological properties of the ensuing materials because of their high compatibility and interfacial adhesion. Compared to the studies in the field of conventional micro- and nanocomposites based on synthetic nonbiodegradable materials, only limited work has been reported in the area of bionanocomposites.

Moreover, taking into account the considerable attention to the economical and environmental problems associated with the use of fossil counterparts, the vast quantities of by-products arising from marine activities represent a very promising first generation of natural resources available for specific chemical modifications aimed generating novel materials. It is relevant, in the case of chitin and chitosan, to select only the less noble parts for the modifications, leaving the more valuable ones for well-established uses. Indeed, a growing number of studies show that the so-called by-products can in fact be the precursors to materials with remarkable properties and high added value.

Objectives of the work

Thus, the objective of this work was to develop novel materials based on chitosan (and its derivatives) and cellulose fibres (namely bacterial cellulose, nanofibrillated cellulose and paper) by simple and green approaches. Specifically, it was investigated the preparation of new transparent nanocomposite films and also new paper coating formulations based on these two biopolymers.

This investigation also aimed to valorise the less noble fractions or by-products of chitin and chitosan, transforming these valuable renewable resources into viscous polyols through a simple oxypropylation reaction.

This manuscript is divided in three parts. In the first part fundamental aspects are briefly reviewed. The second part is a presentation of the scientific approach. It lists the raw-materials, the most important procedures used, the main experiments and the equipment involved. The third part and last part is a presentation of results, discussions, conclusions and suggestions for further work.

The content of this thesis intends to gather ideas in order to better understand the interactions and behaviour of some polymers from renewable resources, and thereby contribute to a better world.

Part I

The state of the art

1 Chitin and chitosan

Chitin is derived from the Greek word χιτωμγ, which means tunic or cover. It is a high molecular weight linear polymer composed of *N*-acetyl-2-amido-2-deoxy-D-glucose units linked by β(1→4) bonds. A point of difference from other polysaccharides is the presence of nitrogen [20].

Chitosan (CH), the major, simplest and least expensive chitin derivative, is also a high molecular weight linear polymer obtained by deacetylation of chitin and is therefore composed of 2-amino-2-deoxy-D-glucose units linked through β(1→4) bonds [20].

These two polysaccharides should be considered as copolymers containing two types of β(1→4) linked structural units *viz.* *N*-acetyl-D-glucosamine (GlcNAc) and D-glucosamine (GlcN) as shown in Figure I-1.

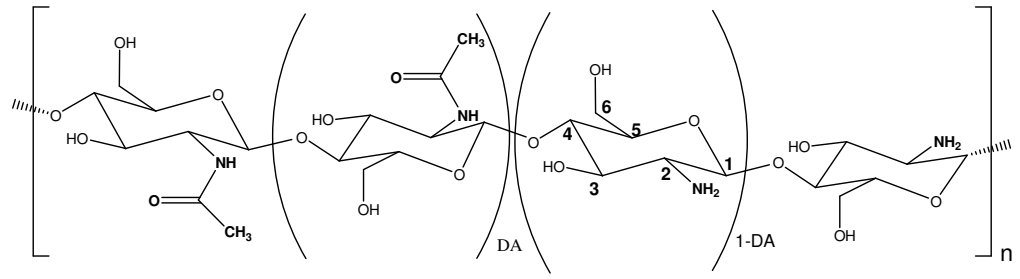

Figure I-1. Representation of the chemical structure of copolymers (chitin (DA>>1-DA) and chitosan (1-DA>>DA)) of *N*-acetyl-D-glucosamine (molar fraction=DA) and D-glucosamine units (molar fraction=1-DA). Conventionally, chitin DA> 0.50 and chitosan DA<0.50.

Isolated chitin is a highly ordered copolymer of GlcNAc as the major component and GlcN as a minor constituent. These residual monomers are present in the native chitin

or are formed through hydrolysis of some acetamido groups during the isolation and purification processes. Since it is almost impossible costly and impractical to completely deacetylate chitin, the major chitosan component is GlcN and the GlcNAc is the minor constituent [10,12,20-25].

The terms chitin or chitosan do not therefore refer to a single well-defined structure, since they can differ in molecular weight, degree of *N*-acetylation (DA) and sequence (*i.e.*, acetylated residues are distributed along the backbone in a random or blocky manner). Due to these structural differences, their properties can vary drastically, as will be discussed in detail in the appropriate sections below.

1.1 History

It is normally accepted that chitin was first isolated in 1811 from mushrooms by Bracconot, a French Professor in Natural History. However, A. Hachett, an English scientist, had previously isolated from arthropod cuticle in 1795 an organic material particularly resistant to the usual chemicals [26]. Nevertheless, Hachett did not investigate this new material and it was Braconnot that carried out further chemical analysis and reported the formation of acetic acid when treating this material with a hot acid [20]. Therefore, Bracannot is considered the discoverer of chitin, even if his name for the new material, “fungine”, was replaced by its current name in 1823 as proposed by Odier.

Years latter, Odier identified chitin in demineralised crab carapace and suggested that it is the basic material of the exoskeletons of all insects. Rouget presented a study about the existence of a “modified chitin” soluble in diluted acids. It was however Hoppe-Seyler who in 1894 proposed the name chitosan for the product obtained when chitin from shells of crabs, scorpions and spiders was heated at 180ºC in KOH. This product was soluble in acetic and hydrochloric acid solutions and could be precipitated from such solutions by addition of an alkali [20].

Even if the isolation of chitin by Bracannot preceded Payen’s isolation of cellulose by some 30 years, the development of chitin chemistry and its industrial applications had lagged far behind that of cellulose. The initial interest in chitin was cultivated principally by zoologists, marine entomologists and physiologists, and it was only in the late 1970s

that chemists looked at chitin with scientific curiosity [20,27]. Immediately, chitin was recognized as an abundant source of chitosan, the unique cationic polysaccharide [27]. However, the increasing interest in the use of chitin and chitosan in several applications only started at the beginning of the 1980s because of the recycling requirements of the organic solid wastes and by-products generated by the food industry (principally in crustacean canning factories in Japan and USA), resulting in the valorisation of added-value products.

The advances in chitin and chitosan science in the last 30 years followed different periods dominated by specific topics related to: (i) biochemical significance (e.g. bone regeneration, blood coagulation); (ii) technological advances (e.g. spinning, cosmetic functional ingredients); (iii) inhibition of biosynthesis (e.g. insecticides); (iv) chitin enzymology; (v) combinations of chitosan with natural and synthetic polymers (e.g. blends, coatings, grafting, polyelectrolyte complexation); (vi) use of chitosan as a dietary supplement and food preservative; and (vii) drugs delivery.

Unquestionably, chitin, and in particular chitosan, are, among the biological macromolecules, those that registered the most significant and progressive development in several areas. The key consideration that justifies this interest is their ubiquitous character and specific properties.

The following sections are essential for a better understanding of chitin and chitosan.

1.2 Occurrence

Chitin is biosynthesised by a vast number of living organisms and it is estimated that at least 1.0×10^{10} tons of this biopolymer are constantly present in the ecosystem [28].

It occurs in nature as ordered crystalline microfibrils, forming structural components in animals, algae and fungi in which chitin acts as a supportive and protective component (Figure I-2). In animals, chitin occurs essentially in crustacean, molluscs and insects, where it is the main constituent of their exoskeleton, associated with organic substances, mainly proteins, and impregnated with inorganic substances, such as calcium salts.

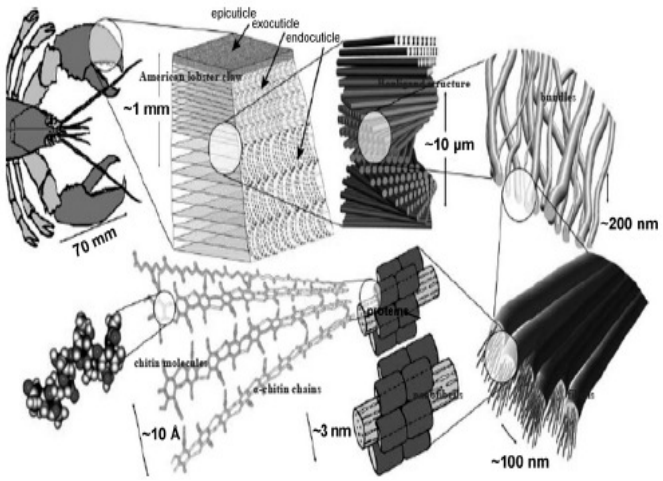

Figure I-2. Source and hierarchical structure of crustaceans cuticle showing the ordered structural chitin (reproduced from ref [29]).

It is essentially found as α–chitin in the calyces of hydrozoa, the egg shells of nematodes, the radulae of molluscs and cuticles of arthropods, and as β–chitin in the shells of brachiopods and molluscs, cuttlefish bone and the squid pen, for instance. In vegetable, chitin occurs in algae associated with cellulose and also in certain fungi where it is the principal fibrillar polymer of the cell wall associated with glucans and mannans [12,20,30-31]. All these organisms synthesise chitin according to a common pathway that ends with the polymerization of *N*-acetyl-D-glucosamine from the activated precursor uridine diphosphate-*N*-acetyl-D-glucosamine [32].

Chitin biodegradation is also performed by enzymatic action by three different ways: (i) deacetylation, where chitosan, chitobiose and glucosamine could be final materials; (ii) hydrolysis, that permits obtaining oligomers of poly[β-(1→4)-2-acetamid-2-desoxy-D-glucopyranose]; and (iii) deamination, where cellobiose or glucose could be the final products [20].

There are also some fungi that produce chitosan at significant yields (28-30%, on dry cell wall basis). However, even if the number of advantages of fungal sources is more than crustacean sources (uniform composition of the raw material, availability throughout the year, among others), the culture systems are slowly and produced low-density cultures. So, up to now, the main commercial sources of chitin and chitosan have been crustacean exoskeletons obtained as waste biomass from the shellfish processing industry [10,12-13, 20].

1.3 Processing of chitin and chitosan

At an industrial level chitin and chitosan are easily obtained from crustaceans. Shells of crabs, shrimps, and lobsters coming from the peeling machines in canning factories are used for the industrial preparation of chitin and chitosan. Considering that crustacean shell waste consist of protein (20-40%), calcium and magnesium salts (30-60%), chitin (20-30%) and lipids (0-14%) [33], chitin isolation involves several different operations. Conventional chemical processes involve three basic operations: deproteinization, *viz.* removal of residual proteins by treatment with dilute alkali (NaOH), demineralization**,** *viz.* removal of mineral salts by acid treatment (HCl) and finally decolouration, *viz.* removal of lipids and pigments by typical bleaching treatments (H_2O_2 and NaClO) [20,22,33-34]. In some cases, the demineralization operation can precede the deproteinization operation.

Chitosan, the main derivative of chitin, is obtained by deacetylation of chitin, *i.e.* the cleavage of the *N*-acetyl group at C-2 position. The removal of the *N*-acetyl groups from chitin is a severe alkaline hydrolysis treatment usually carried out with concentrated NaOH or KOH and high temperatures [20-22,34]. Two methods of preparing chitosan with various degrees of acetylation dominate, namely heterogeneous deacetylation of solid chitin and homogenous deacetylation of pre-swollen chitin, both in an aqueous media [20-21, 34]. However, these standard aqueous alkali treatments cause a partial degradation of the polysaccharide, so attempts have been made to develop other methods in order to avoid this problem. These methods involve the use of water-miscible solvents, such as 2-propanol or acetone, to guarantee a good stirring, and as a transfer medium to ensure uniform distribution of the aqueous alkali throughout the chitin mass [20]. The conventional purification process of chitin and the preparation of chitosan is outlined in Figure I-3.

Enzymatic hydrolysis processes have also been applied to chitin [21]. The enzymatic hydrolysis of chitin can occur through the action of chitinases, chitosanases, lysozymes and cellulases [35], and the process is environmentally friendly. The chitosans from chemical and enzymatic methods are different with respect to their characteristics (degree of deacetylation, distribution of acetyl groups, degree of polymerization (DP),

molecular weight among others). For example, the products of chitin enzymatic hydrolysis have in general a higher degree of polymerization.

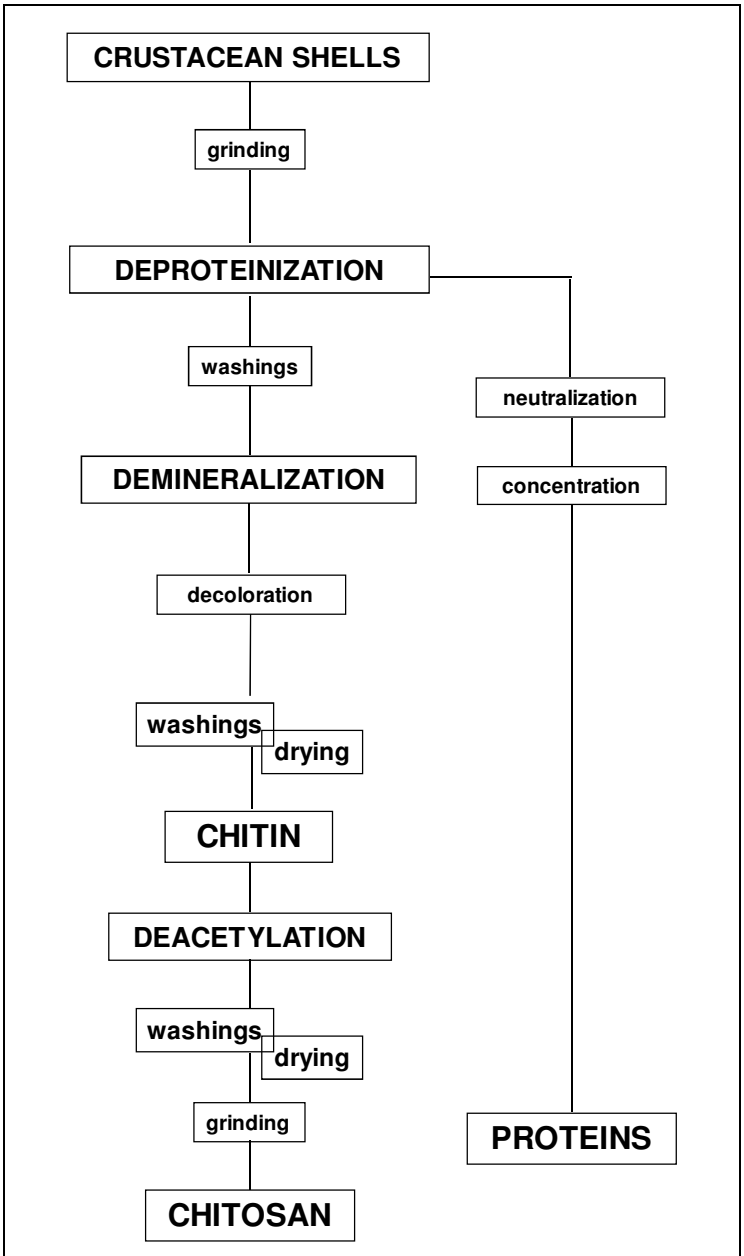

Figure I-3. Schematic representation of purification process of chitin (and proteins) and of preparation procedures of chitosan (based on ref [10]).

Alternatively, enzymatic chitin deacetylation takes place in certain bacteria and fungi. Deacetylases have been isolated from various types of fungi, but the lack of solubility of chitinous substrates with a high degree of acetylation in aqueous solvents is

still a practical limitation for the preparation of chitosan using chitin deacetylase systems [21,36].

The production of chitosan-glucan complexes is associated with a fermentation process, which involves alkali treatment yielding chitosan-glucan complexes. The alkali removes the protein and simultaneously deacetylates the chitin [21,37].

1.4 Properties and functionalities

Numerous parameters, such as the origin and the manufacturing process of the materials, the composition and dimension of the polymer chain, among others, determine many of the characteristics of these macromolecules, namely the degree of *N*-acetylation and the molecular weight. Other characteristics such as crystallinity, moisture, ash percentage, colour and insoluble materials percentage are also important. For medical, pharmaceutical and food applications the residual protein, toxicity and heavy metal content are also quite relevant [10,20,38-39]. As the relative importance of each characteristic depends on the intended use, in this section only those most relevant for the present study are described.

Degree of N-acetylation

The degree of *N*-acetylation (DA) of chitin and chitosan is the most important parameter which influences in its various physicochemical properties, such as solubility, and biological activity, like biodegradation [35], and has been employed to differentiate chitin from chitosan.

The DA is defined as the average molar fraction/percentage of *N*-acetyl-D-glucosamine units within the macromolecular chain [25] and varies from 1/100 (chitin) to 0/0 (fully deacetylated chitin). Thus, to determine the *N*-acetyl-D-glucosamine units content in chitin and chitosan samples, appropriate techniques giving acceptable and reasonable results for the DA are essential. Several methods are used to evaluate the average DA, including IR spectroscopy [40-43],

UV-spectroscopy [31,44-45], ^{1}H NMR spectroscopy [46-49], ^{13}C solid state NMR [47,50-54], thermal analysis [55], various titrations methods [51,56], elemental analysis [56-57], among others [58].

^{1}H NMR spectroscopy offers the most precise value, but the preparation of a perfect low viscosity solution is mandatory. Meanwhile, IR spectroscopy remains the simplest and reliable method for samples in the solid state and the UV-method gives very good results for chitosan solutions.

Molecular weight

The molecular weight of native chitin is usually larger than one million, while those of commercial chitosan products fall between 100 000 and 1 200 000, because of the harsh conditions of the manufacturing process that can lead to degradation of polymer chain. The weight-average molecular weight ($\overline{M}_w$) of chitin and chitosan has been determined by light scattering [59-61], gel permeation chromatography (GPC) [62-63] and viscosity [20,64-65]. Among these, intrinsic viscosity, using the Mark–Houwink relation (Equation I-1) with known values of the *K* and *a* parameters, is the simplest and rapid method.

$$[\eta] = K\,Mv^{a} \qquad \text{Equation I-1}$$

Where, [η] is the intrinsic viscosity and *K* and *a* are the constants, that depends on the polymers/solvent/temperature system [20].

The first difficulty encountered in this determination concerns the solubility of the samples and the dissociation of aggregates often present in polysaccharide solutions. Various solvents systems have been proposed [64,66-67]. Additionally, this method is not an absolute method, since it requires the determination of constants (*K* and *a*) through correlation of the intrinsic viscosity with molecular weight values measured by an absolute method.

Crystallinity

In nature, chitin forms a hydrated solid matrix made of amorphous regions where crystallites co-exist to form assemblies of strong extended fibres, as cellulose in plants. These fibres provide support to the exoskeleton of crustaceans and insects, as well as to cell wall of fungi. Depending on its source, this natural polymer can occurs in three different allomorphs, namely the α, β and γ-forms [12,20], which differ in the arrangement of the chain within the crystalline regions. Infrared and solid-state NMR spectroscopy, together with X-ray diffraction, can be used to differentiate these chitin forms.

α–Chitin is by far the most stable, ubiquitous and widely available form. The unit cell is orthorhombic and the individual chains are arranged in anti-parallel fashion (Figure I-4a). Thus, adjacent chains are oriented in opposite directions [12,20,68]. α–Chitin is found where extreme hardness is required, as in arthropod cuticle.

β-Chitin (Figure I-4b) and γ-chitin are instead found where flexibility and toughness are required, as in skeletal pen and in the thick cuticle coating the stomach. β-chitin displays a parallel arrangement of the chains, while γ-chitin possesses two parallel chains in association with one anti-parallel chain. Both β-chitin and γ-chitin may be converted to the thermodynamically stable α–form by treatment with 20% NaOH followed by washing with water [20].

In these structures, the chitin chains are organized in packs, where they are strongly held by a number of intra-pack hydrogen bonds. This tight network, dominated by strong C–O….HN hydrogen bonds, maintains the chains at a distance and gives rise to extended ordered regions [12,69].

Chitosan is usually less crystalline than chitin, which presumably makes chitosan more accessible to reagents. In the solid state, chitosan molecules, as chitin, also partly organise themselves into ordered crystalline regions co-existing with amorphous phases. Chitosan crystallinity is strongly dependent on the origin and preparation mode of the sample. For instance, chitosan produced under homogenous conditions presents a more amorphous and randomly distributed fine structure in terms of *N*-acetyl-D-glucosamine and D-glucosamine groups [70]. Its morphology has been investigated, and many polymorphs are mentioned in the literature.

The first documented crystal structure of chitosan was reported by Clark and Smith in 1937 [71] (orthorhombic unit cell with dimensions b (fibre axis) = 1.025 nm, c = 1.7 nm and a = 0.89 nm and β = 90º). Some years later, distinct polymorphic arrangements I and II form were identified in chitosan films depending of the way of crystallization (as-cast or precipitation) [72]. Both forms were assigned to an orthorhombic unit cell ($P2_12_12_1$) with two antiparallel chitosan chains. The degree of crystallinity and molecular structure are parameters that influence solubility, mechanical strength and other functional properties of chitosan.

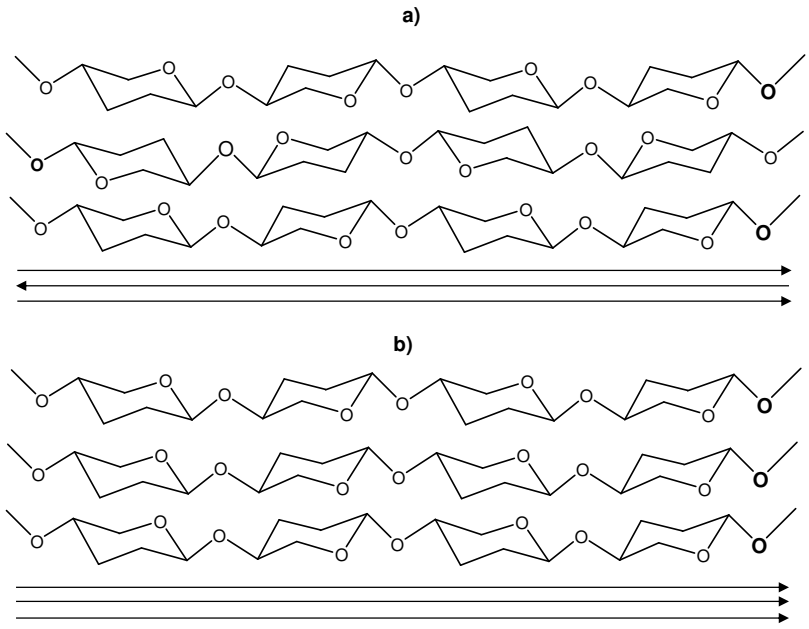

Figure I-4. Anti parallel and parallel chain arrangement of α–chitin a) and β-chitin b) (reproduced from ref [73]).

Solubility and solution properties

The most remarkable difference between chitin and chitosan is their solubility characteristics. Chitosan is soluble in dilute acidic solutions contrary to chitin which is very difficult to dissolve. For a long time, chitin was considered as an intractable polymer and, despite its structural similarity to cellulose, it is insoluble in some typical

cellulose solvents. Only a limited number of known solvents are applicable as chitin solvents without any appreciable polymer degradation [13]. Roberts has grouped the solvents for chitin in three categories: (i) aqueous solutions of neutral salts like LiCNS, CaI_2, among others; (ii) acid solvents like H_2SO_4, HNO_3, etc; and (iii) organic solvents like systems composed by dimethylacetamide containing lithium chloride (DMAc/LiCl), dimethylformamide containing lithium chloride (DMF/LiCl) and *N*-methylpyrrolidone containing lithium chloride (NMP/LiCl) [20]. Most solvents used for the dissolution of chitin are toxic and hence cannot be used in food processing and biomedical applications.

In contrast, the presence of free amine groups along the chitosan chain allows this macromolecule to dissolve in dilute aqueous acids through their protonation, giving the corresponding chitosan salts in solution. In dilute acidic media, the following equilibrium takes place [21,38]:

$$\mathbf{-NH_2 + H_3O^+ \Leftrightarrow -NH_3^+ + H_2O}$$

As a consequence, the emergence of positive charges on the chains (polyelectrolyte character of chitosan), influences the chitosan hydrodynamic, acid-base, conductimetric and rheological properties, among others [74-75].

Therefore, the pH substantially alters the charged state and properties of chitosan. At low pH (less than about 6), the amine groups are protonated and positively charged, thus conferring a polycationic behaviour to chitosan. At high pH (above 6.5), chitosan amine groups are deprotonated and the polymer becomes insoluble. Depending on DA, chitosan's soluble-insoluble transition occurs at pHs between 6 and 6.5, which is a particularly suitable range for biological applications [74,76-77]. Also at pH above 6.5 chitosan electrostatic repulsions are reduced, permitting the formation of inter-polymer associations that can lead to fibres, films, networks and hydrogels, depending on the conditions used to initiate the soluble-insoluble transition [78].

Film forming properties

Unquestionably, one of the most interesting properties of chitosan is its ability to form films. Since chitosan can be dissolved under slightly acidic aqueous conditions, it can be readily cast into membranes or films with good mechanical and permeability properties [13,21,79]. In some cases, chitosan serves simply as a matrix to entrap components within the film network. Examples include the entrapment of nanoparticles (e.g. carbon nanotubes [80], silver nanoparticules [81]) and biologically active components (e.g. enzymes [82]).

Biodegradability

Chitin and chitosan are polymers of great interest in biomedical and food applications, and therefore their biodegradation is considered as one of the most important property. Chitin and chitosan can be easily depolymerised by enzymatic means using a variety of hydrolases, including chitinase, chitosanase, lysozyme (present in human body fluids), cellulase, hemicellulase, lipases, amylases, among others [20,83-84].

Apart from their complete biodegradability, these biopolymers also show low toxicity, excellent biocompatibility and antifungal and antimicrobial activity [12,31]. The antimicrobial activity of chitosan is partially attributed to the protonation of chitosan in solution. The positive charge attracts the negatively charged bacterial cell walls, and the interaction between the two charges breaks the cell wall of bacteria leading to leakage of their cytoplasm, eventually causing death [85]. However, the exact mode in which chitosan exhibits antimicrobial activity is still not clear.

1.5 Chitosan derivatives

The chemical modification of these unique polysaccharides has been applied in order to improve their properties and biological functions, including solubility, and to develop new advanced materials. Chitin and chitosan are quite interesting because of the presence of the functional groups in their monomer units *viz.* one amino group (primary

amino function C-2) and two hydroxyl functionalities (primary C-6 and secondary C-3 hydroxyl groups) on each deacetylated unit [12-13,20,73,86-92]. Figure I-5 illustrates the possible reaction sites for chitin and chitosan.

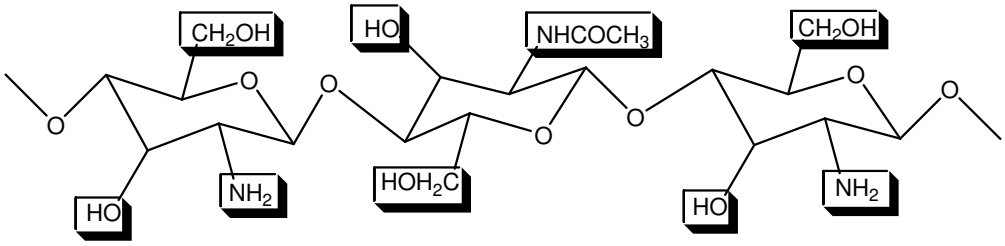

Figure I-5. Possible reaction positions of chitin and chitosan (reproduced from ref [87]).

Chitin and chitosan, as cellulose, can suffer many reactions such as etherification, esterification [89,93], cross-linking [94-95], graft copolymerization [95], among others. Both amino and hydroxyl functional groups provide specific chemical reactions. The amino functionality provides amidation, quaternization (e.g. *N*,*N*,*N*-trimethylamonium chloride chitosan derivative), alkylation (through reductive amination), grafting and chelation of metals (e.g. palladium, copper, silver). The hydroxyl groups give reactions such as *O*-acetylation (e.g. *O*-carboxymethyl, cross-linked *O*-carboxymethyl chitosans) esterification, grafting, and also H-bonding [11,73,87]. The final derivatives could present different characteristics namely antibacterial, anti-fungal, anti-viral, non-toxicity and non-allergenic properties and total biocompatibility and biodegradability, solubility, etc.

Chitosan is much easier to modify than chitin due to its higher accessiblility to reagents [12-13]. Nevertheless, the stability of chitosan derivatives is generally lower, because of their more hydrophilic character and pH sensitivity.

Cationic chitosans are the most important chitosan derivatives, because they are water soluble over the whole practical pH range. Quaternary ammonium chitosan salts can be obtained using two different ways namely, (i) by addition of a substituent which contains a quaternary ammonium group (using quaternary ammonium epoxides like glycidyltrimethylammonium chloride) [96-99] and (ii) by quaternization of the amino groups of chitosan by means of a suitable alkylating agent [11,100]. A water-soluble chitosan derivative obtained by its reaction with an epoxy derivative is illustrated in Figure I-6a).

Chitosan solubility in the absence of acids is frequently required when acids are undesirable substances in the final products, such as cosmetics, medicines and food. These polymers show good flocculating properties with kaolin dispersions, suggesting also applications in papermaking [101].

Other interesting biomedical applications of modified chitosans have also been reported. For example, fluorescent chitosans have been applied as probes in some biologically and medical related systems [102-106]. Figure I-6b) shows the chemical structure of a fluorescent chitosan synthesised with fluorescein-isothiocyanate (FITC).

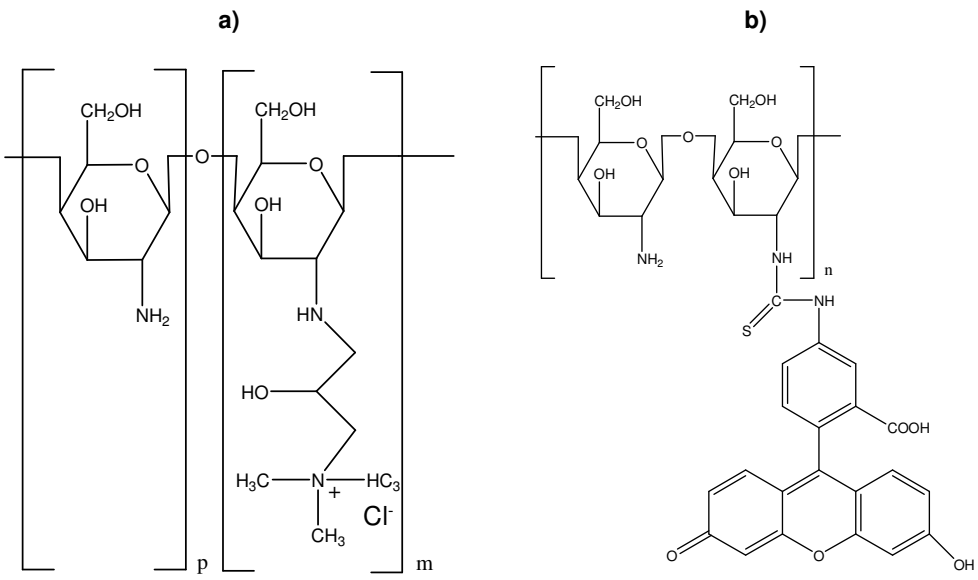

Figure I-6. Chitosan derivatives: a) water soluble chitosan derivative obtained by reacting with glycidyltrimethylammonium chloride and b) chemical structure of FITC-labelled chitosan obtained by reacting with fluorescein isothiocyanate.

1.6 Applications

The unique physicochemical properties and functionalities of chitin and chitosan, as such or modified, are the driving force for the multiple applications where these biopolymers are implied. The present tendency is to produce high value products, like cosmetics [107], feed additives [108], drugs carriers and pharmaceuticals [27]. However, a larger number of chitosan applications are focused on sludge dewatering, food processing and removal of heavy metal ions through chelation [12,22,24,37,39,109-110].

In spite of the reduced solubility of chitin, that limits its utilization, this natural polymer has been used to produce fibres for textiles [87,111-112] and for absorbable suture materials [113-114].

In agriculture, chitosan is used as inhibitor of fungal pathogens, to improve germination and as enhancer of plant-resistance against infections [113,115]. Chitosan is also exploited in agrochemicals, like fertilizers, herbicides and pesticides [39]. The beneficial use of chitosan as animal feed supplement has also been the subject of many studies [108].

Due to its high chelating and coagulating ability, chitosan has been widely utilized in food industry, as gelling, stabilizer, and thickener, and to improve the nutritional quality of various foods. Other applications in the food industry include the use as packaging films or edible food wrappings [116-119].

One of the oldest applications of chitosan was as effective biosorbent due to its low cost, compared to activated carbon, and its high contents of amino and hydroxyl functional groups showing high adsorption potential for various aquatic pollutants [35,120-122]. The removal of metal ions, different classes of dyes, radioactive materials, proteins and solids from water and wastewater is feasible using chitosan. However, the treatment of wastewater remains the most important applications from an economic perspective.

Chitosan has been reported to improve the final properties of paper, as bulk (imparting wet strength to paper) and as surface (improving antistatic properties since electrostatic discharge can cause a serious decrease in printing quality) treatment [123-126]. Hydroxymethyl chitin and other water soluble derivatives are useful end additives in papermaking for better finish paper properties. However, this polymer, although potentially available in large quantities, has not become a commercially significant product [37].

In medical and pharmaceutical domains, chitin and chitosan derivatives are exploited in their different forms, such as films, membranes, fibres, microcapsules, solutions, powders, etc. The biological properties of chitosan as hemostatic agent, bacteriostatic, anticoagulant, spermicide, joined to its physicochemical properties show its potencial for the production of biomaterials [27,37,79,109].

Cosmetic applications are also important fields where the specificity of chitosan must be recognized, especially for hair care in relation to electrostatic interactions [37,107].

2 Cellulose

In 1838 Anselme Payen, a French chemist, isolated a resistant fibrous material by treating various plant tissues alternately with nitric acid and sodium hydroxide solutions [127]. "Cellulose", was the name attributed to this plant constituent in 1839. The precise chemical formula was established by R. Weillstatter in 1913 and in 1933 cellulose was recognised as having a macromolecular character by Staudinger [127].

It is a linear homopolysaccharide composed of D-glucose units, joined by β(1→4) bonds. At the positions C-2, C-3 and C-6 of the β-D-glucose unit are placed hydroxyl groups, which are in general accessible to the typical reactions of primary and secondary alcoholic OH groups (Figure 0-1a) [19,128-130].

This biopolymer is known to occur in a wide variety of living species mostly from the world of plants (in their cellular walls), but also occasionally from animals, and bacteria as well as some amoebas. In many of these, the main function of cellulose is to act as a reinforcement structural component. It has been estimated that globally between 1.0×10^{10} and 1.0×10^{11} tons of cellulose are biosynthesized each year [131].

During cellulose biosynthesis, the individual polymers pile onto each other forming microfibrils, with typically a diameter of 2-30 nm, which form both crystalline and amorphous regions. The microfibrils further aggregate into fibrils, with diameters of 30-100 nm and lengths of 100-500 μm, and finally into cellulose fibres, with diameters of 100-400 nm and lengths of 0.5-4 mm [1,128-130,132-133].

Native cellulose (*i.e.* cellulose without any transformation after its biosynthesis) exists naturally in two forms *viz.*, *cellulose in a pure state*, which includes cellulose produced in their natural state, such as cotton, bacterial cellulose and those present in some

algae and some marine animals like tunicates, and *cellulose associated with other components*, which includes most of the celluloses present in nature, as the fundamental component of the cellular wall of higher plants [134].

All the natural manifestations of cellulose are in the form of fibres, whose morphology and chemical composition can vary greatly from species to species, climatic conditions, age and digestion process. Natural fibres can generally be classified into several groups according to their sources *viz.* (i) wood fibres (softwoods and hardwoods) and (ii) vegetable fibres (annual plants like cotton, jute, kenaf, sisal, among others).

Cellulose main sources, however, are wood and cotton. Wood is a natural composite, where cellulose (representing 40-45% of the dry weight in most wood species [128-129]) is enclosed in combination with lignin, hemicelluloses and sometimes with pectin in a texture which certainly represents a masterpiece of natural architecture [4,135-136]. For this reason, natural fibres are also referred as lignocellulosic fibres, or as cellulosic fibres, related to their main chemical component [18]. The selected separation process and its conditions are crucial to maintain the high quality of the fibres when they are detached from the original plant. Among the separation methods, retting, scrapping and pulping are the most commonly used [135].

2.1 Properties and functionalities

From one form of cellulose to another, the degree of polymerization, which can extent from hundreds to thousands of units, may vary as well as the supramolecular organization of its chains, which can give rise to amorphous and several types of crystalline structures.

In nature, cellulose chains have a DP of approximately 10 000 in wood, 15 000 in cotton and 50 000 in same algae [128,137], but separation and purification methods usually reduce it to the order of 2 500 [138].

The formation of intra- and intermolecular hydrogen bonds results in a highly crystalline structure, with 55-70% crystalline regions in most plants [137], which is responsible for the chemical stability, structure rigidity and tensile strength of cellulose. In addition to the crystalline phases, native fibres contain disordered domains which can be

considered as amorphous. Disordered domains can be found in the primary wall, while the oriented domains are mainly found in the secondary wall of the cell (Figure I-7).

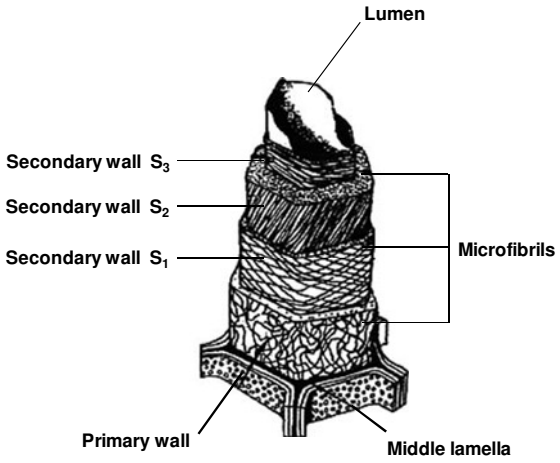

Figure I-7. Organization of cellulose chains in fibre cells (reprinted from ref [1]).

Native cellulose can be considered as a semicrystalline fibrillar material [139-141]. The crystalline structure of cellulose displays four different polymorphs, namely I (native cellulose), II, III and IV [140,142-143]. The conversion of native cellulose to cellulose II depends of the treatment conditions, such as the regeneration of cellulose derivatives or mercerisation (alkaline conditions). A parallel chain packing is proposed for cellulose I [144], and regenerated cellulose II is supposed to assume an antiparallel chain packing [145]. The transformation of cellulose I into cellulose II is irreversible, meaning that the II form is thermodynamically stable, whereas the I form is metastable. Cellulose III is obtained when cellulose I or II are treated with liquid ammonia, monomethylamine, or monoethylamine. The structure known as cellulose IV is produced by heating cellulose I or II in glycerol at 280 ºC or by boiling the cellulose-ethylene diamine complex in dimethylformamide.

Native cellulose (cellulose I) is composed of two crystalline forms, namely triclinic Iα and monoclinic Iβ [146], as revealed by ^{13}C NMR. The ratio of these two allomorphs varies with the origin of the native cellulose. Iα is the major crystalline form in algae and bacteria, while the Iβ is the main form in higher plants.

The disordered phases of cellulose are the preferred attack sites by solvents and chemical reagents. Cellulose is difficult to be processed in solution because of the highly organized network system surrounding the single polyglucan chain [147]. The key for cellulose dissolution and following applications is that the solvent can effectively destroy the intra- and intermolecular hydrogen bonding in polymer chains. There are two basic systems for cellulose dissolution *viz. indirect solvent systems* (called derivatizing solvents), such as *N*,*N*-dimethylformamide/pyridine, *N*,*N*-dimethylformamide/N_2O_4 and dimethyl sulfoxide/N_2O_4, where cellulose forms derivatives during dissolution; and *direct solvent systems* (called nonderivatizing solvents), such as trifluoroacetic acid/dichloromethane and dimethylacetamide/LiCl, that form complexes with cellulose without altering its molecular structure [147-148].

The reactivity of cellulose arises mainly from the presence of three hydroxyl groups at the C-2, C-3 and C-6 of each glycosidic unit. Generally, the functionalization along the cellulose chain takes place in a statistical way, in spite of the different reactivities of these three OH groups. They react easily with various reagents, allowing the synthesis of cellulose derivatives by esterification, etherification, urethane formation and crosslinking or graft-copolymerization reactions [2,4,148]. Cellulose esters of inorganic and organic acids, and cellulose ethers, are pioneer compounds of cellulose chemistry and remain the most important cellulose derivatives. Examples of cellulose derivatives and their corresponding applications include: (i) sodium carboxymethyl cellulose (CMC), which is water soluble, and widely used as a sizing agent, in food products, textiles, adhesives and detergents [149]); (ii) cellulose acetate (a generic term for a wide range of materials with varying degrees of esterification) which is used in cigarette tow, textile fibres, films, plastics, packaging, fabrics, etc [150]; (iii) methyl cellulose can be used as an additive in adhesives, cosmetics, agricultural chemicals, paper products, building materials, pharmaceuticals, printing inks, resins, textiles and tobacco [151]. Recently, these cellulose derivatives have been used in blends with other natural polymers, in order to obtain new materials with multiple applications [147]. However, cellulose is still extensively used as such in paper making and textile industries. One of the more recent and exploited applications of natural cellulose fibres, replacing inorganic/mineral based fibres, is their use as reinforcing elements in composite materials with thermoplastic or thermosetting

polymeric matrices [18-19,132,135-136,138,152-153], after required surface modification [154-157].

2.2 Micro- and nanofibrillated cellulose

The cellulose I hierarchical structure, made up of smaller and mechanical stronger entities encourages the utilization of nanoscale native cellulose elements for potential novel applications [138]. As mentioned before, within the different cell wall layers of fibres, cellulose exists as a system of fibrils embedded in a matrix of hemicelluloses and lignin. Each fibril can be considered as a chain of crystalline units, linked together by amorphous domains (Figure I-8) [158]. Using new effective methods, these fibrils can be disintegrated from the fibres to form a uniform micro- or nano-sized material.

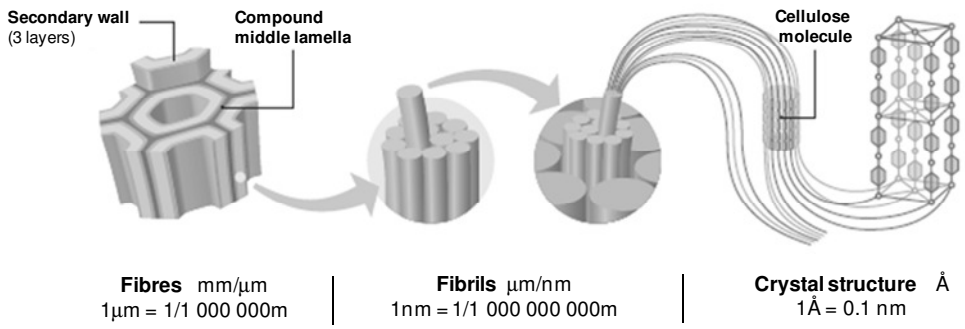

Figure I-8. Wood cell wall with the compound middle lamella and three layers of the secondary wall (reprinted from ref [159]).

The first production of microfibrillar cellulose (MFC) from wood fibres was reported in 1983 by Turbak et al. [160-161]. More recently, the term nanofibrillar cellulose (NFC) is more applied because the optimization of the processes allows to obtain nanoscale cellulose fibres.

NFC, which is distinctly different from microcrystalline cellulose (MCC) obtained by acid hydrolysis, arise from the mechanical disintegration of cellulose pulp fibres into micro- or nano-fibrillar cellulose using high-pressure homogenizers [159-160,162]. However, such methods are energetically costly and tend either to damage the microfibril structure by reducing the molar mass and the degree of crystallinity, or fail to disintegrate

sufficiently the pulp fibre. Recent studies have attempted to improve the disintegration of cellulose at reasonable cost without severe degradation using an additional enzymatic hydrolysis treatment [163-164] and/or the combination of different methods [159].

The ensuing cellulose I fibril suspensions bear the appearance of highly viscous, shear-thinning transparent gels. The fibrils have high aspect ratios and specific surface areas combined with remarkable strength and flexibility. Depending on the disintegration process, their dimensions vary, and fully delaminated NFC consists of long (in the micrometer range) nanofibrills (diameter =10-20 nm).

The uses of NFC include nanocomposites reinforcement [159,162,165-175], as well as a host of other ones, including papermaking applications [176] and dispersion stabilizers [177].

2.3 Bacterial cellulose

Bacterial cellulose (BC), also known as microbial cellulose, is produced by the biosynthesis of different genus of bacteria, such as *Glucanacetobacter* (formerly *Acetobacter*), *Rhizobium*, *Sarcina*, *Agrobacterium*, *Alcaligenes*, etc. Among them, *Glucanacetobacter xylinus* (also called as *Acetobacter xylinum*) is the most studied due to its efficiency to produce cellulose [178-179]. These are gram-negative aerobic and non-photosynthetic bacteria, capable of converting glucose, glycerol and other organic substrates into cellulose within a period of a few days [134,180]. The production of cellulose from *Acetobacter xylinum* was first reported in 1886 by Brown, who observed that the resting cells of *Acetobacter* produced cellulose in the presence of oxygen and glucose [180]. These microorganisms are usually found in fruit, vegetables, vinegar and alcoholic beverages.

The biosynthesis of bacterial cellulose is a precisely regulated multi-step process that may occurs in static or agitated culture systems. The static culture result in the accumulation of a gelatinous membrane of cellulose at the air/liquid interface, while the agitated culture results in fibrous suspensions. The growing time depends on the desired thickness of the ensuing cellulose material. In bacterial cellulose biosynthesis, the cellulose chains interact through hydrogen bonds resulting in crystalline domains. Thus, *Acetobacter*

xylinum cellulose consists of ribbons of microfibrils generated at the surface of the bacterial cell (Figure I-9). The bacteria first segregate a structurally homogeneous slimy substance within and, after a short time, the cellulose fibres are formed [134,180].

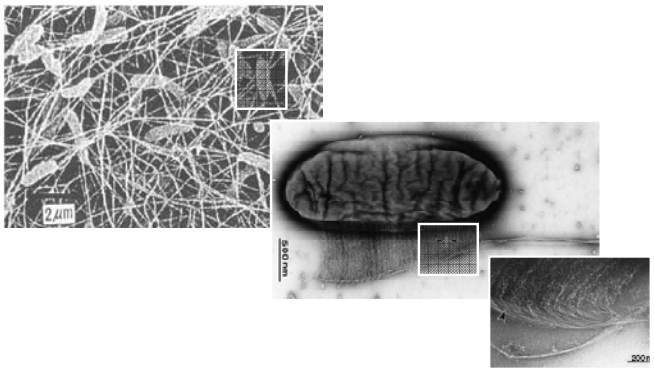

Figure I-9. SEM images of *Acetobacter xylinum* producing cellulose fibres (reproduced from refs [181-182]).

The bacterial cellulose forms a 3D network of nano- and microfibrils with 3-4 nm thick and 70-80 nm wide (Figure I-10), *i.e.* about 100 times thinner than typical vegetal cellulose fibres.

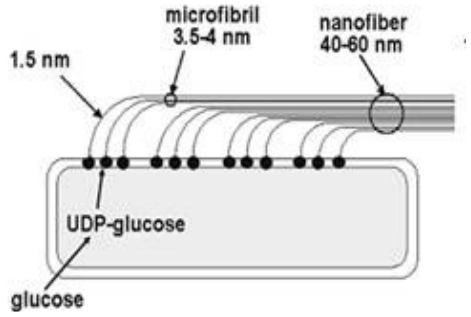

Figure I-10. Scheme showing the assembly of cellulose microfibrils by *Acetobacter xylinum* and the dimension of the fibrils (reproduced from ref [183]).

The microfibrillar structure of bacterial cellulose is responsible for most of its properties. Bacterial cellulose possesses very high purity (free of lignin, hemicelluloses and the other natural components usually associated with plant cellulose, except for cotton) a high degree of polymerization and crystallinity (presence of crystalline cellulose I and

II), extremely high water binding capacity, high tensile strength and of course a higher surface area, as compared to the widespread plant-based counterparts [184-185]. Table I-1 contrasts the main properties of bacterial and wood cellulose.

One of the most attractive features of bacterial cellulose production is the ability to control and modify the physical characteristic of the material [180]. Structural modifications can also be accomplished in a post-production step, since it is possible to functionalize the hydroxyl groups.

Table I-1. Properties of bacterial and plant cellulose [134, 180].

Property	Bacterial Cellulose	Wood Cellulose
Crystallinity	65-80%	55-70%
Degree of polymerization	2 000-6 000	13 000-14 000[a]
Young's modulus	15-30 GPa	5.5-12.6 GPa
Fibre width	40-80 nm	14-40 µm

[a] These values correspond to the native cellulose chains.

Bacterial cellulose, produced by *Acetobacter Xylinum,* is becoming a promising biopolymer of choice for several applications, including optical transparent nanocomposites [186-189], papermaking [190-192], electronic paper [193], food [194-195], pharmaceutical and medical devices [196].

3 Chitosan-cellulose composites

The main purpose of the development of composite materials is the possibility of obtaining products with properties that cannot be attained from the individual constituents. Like numerous petroleum-based polymers, those from renewable resources are also not often used by themselves. The history of composites from renewable resources is quite ancient. For instance, in the biblical Book of Exodus, Moses' mother made a basket from rushes, pitch and slime, a kind of fibre reinforced composite, according to the modern classification of materials [4,8]. Other typical examples, like paper, silk, skin and bone arts, can be found in many museums in the world [8].

Despite the numerous advantages and unique properties of chitosan, the mechanical performance of its films is often not satisfactory for several applications. One way to improve those properties (and other functionalities) of chitosan films, is to prepare composites with other polymers. In the past few years, a considerable number of studies dealing with the blending of chitosan with various synthetic and natural polymers, such as poly(vinyl alcohol) [197-199]; poly(*N*-vinyl pyrrolidone) [200], polyethylene glycol [201], poly(ethylene oxide) [202], poly(lactic acid) [203], starch [199,204], collagen [205-206], water soluble tertiary polyamides [207], cellulose [208-211] and its derivatives [198-199], has been published. These new materials are extending the utilization of polymers from renewable resources into new value-added products, such as in pharmaceutical and biological areas, and in cosmetics.

The advantage of chitosan in these materials is not only its biodegradability and antibacterial activity, but also the presence of groups able to form secondary interactions involving hydrogen bonds with other polymers, in particular cellulose. As mentioned

before, chitosan–cellulose mixtures are of particular interest because of their structural similarity, resulting in homogeneous composite materials that combine the physicochemical properties of chitosan with the excellent mechanical properties of cellulose fibres [14-16,212].

One practical application of chitosan-cellulose mixtures is their processing into films, having high strength parameters and also good biocompatibility, biodegradability and hydrophilicity. These properties are determined by the type of bonds between the two components, their compatibility, and the features of the ensuing supramolecular structure [17]. Several authors have studied the structure of these mixtures, obtained in solution [14,208-209], in the solid phase [17] or using the cellulose fibres in solid state [172-173], and found evidence of interactions, mainly on the interfacial region between chitosan and cellulose [213].

3.1 Chitosan-cellulose: micro- and nanocomposites

Recently, the incorporation of micro and cellulose nanofibres into several polymeric matrices, including chitosan, gave materials with superior mechanical, thermal and barrier properties and transparency [174,214-216]. The search for new renewable transparent films for several applications, such as electronic devices and packaging materials, is a very recent and promising research field [217-219].

Cellulose nanofibres offer unique possibilities as reinforcing materials due to their fine scale, and consequent high aspect ratio (*i.e.*, the ratio between average length and the diameter of the fibres), high stiffness and strength, as well mechanical percolation effects [216], imparting the novel nanocomposites with unique properties. Percolation theory predicts a maximum improvement in nanocomposite properties when there are just enough fillers to form a continuous structure, considering that they are properly dispersed within the matrix. Therefore, the modulus and strength are expected to be improved when each nanofibre is in contact with two other, on average [216,220]. Zimmermann et al. [159] suggested that probably a minimum fibril content is required to induce intense interactions between fibrils and thus the formation of percolated networks.

Several studies have been published dealing with the preparation and characterization of NFC based-nanocomposites with different polymeric matrices, such as poly(vinyl acetate) [175], hydroxypropyl cellulose [159], viscous polysaccharide matrices in the form of a 50/50 amylopectin-glycerol blends [167], polylactic acid [168-169], polyvinyl alcohol [159,170], polyurethanes [171] and chitosan matrices [172-174]. These NFC-based nanocomposites have been extended into several areas including transparent materials [187,215,221], biomedical applications, and gas barrier films [215]. Bacterial cellulose nanofribrills have also been studied as reinforcing elements in nanocomposites with several polymeric matrices, such as flexible polyurethane elastomers [222], cellulose acetate butyrate [223], acrylic thermosetting resins [186,221], phenolic resins [224], poly(ethylene oxide) [225], plasticized starch [226-227] and polylactic acid [214].

However, the preparation and characterization of cellulose nanofibres and chitosan nanocomposites is still poorly explored. Microfibrillated cellulose (MFC) was used for the first time as chitosan matrix reinforcement by Hosokawa et al. in 1990 [172-173]. However, at that time, MFC dimensions were in the micro scale and were not homogeneous, and only a limited number of parameters such as the effect of the chitosan solution concentration of the film strength and biodegradability were evaluated. More recently, low contents of MFC were also used to enhance the wet properties of chitosan-acetic-acid-salt films [174].

The published studies on the preparation of chitosan-bacterial cellulose composite materials include (i) the modification of the bacterial cellulose biosynthesis condition, by the addition of polyaminosaccharide modifiers into the culture medium [228] and (ii) dipping a dried bacterial cellulose membrane into an acetic acid solution of chitosan [229]. The resulting membranes were characterized and showed valuable features, including superior mechanical properties in a wet and dry state, a high water absorption capacity, a high average surface area, high moisture-keeping properties, as well as bacteriostatic and bactericidal activity [229].

Further studies on transparent nanocomposite films based on chitosan and its derivatives with cellulose nanofibres (e.g. bacterial cellulose and microfibrillated cellulose) through simple and green approaches (without the use of organic solvents), are today a stimulating challenge to optimize their quality and extend their applications.

4 Chitosan and cellulose in paper coating

There has been a growing interest of using chitosan as a coating material in different areas, because of its ease dissolution under mildly acidic conditions, film-forming properties and also because of its recognized antimicrobial activity and antifungal properties [94,230-232]. Besides these properties, chitosan films or coatings have been investigated because of their ability to retard the mass transfer rate (e.g. moisture, oxygen, aromas, oil and solute transports), their flexibility and potential improvement of mechanical and resistance properties of the final materials.

The main application of chitosan coatings is as active edible and biodegradable films to improve the quality, nutritional stability and extend the storage life of food and limit its contamination. The use of coatings is a simple technology that can be applied directly on the food or incorporated in, or coated onto, the food packaging material such as plastic or paper [203,230,233-236].

Chitosan has also been used as invisible film in wound healing dressings [237], as a coating for textile fibre protection and resistance [238-239] and in paper and paperboard coating (e.g. food packaging), as discussed below.

Paper is one of the most important materials invented by human and has adopted numerous functions in our society, for example as an information support, packaging material, among others. However, the paper industry has been under significant pressure because of the global economic decline and competition from alternative media. A dramatic reduction in production and reduced demand for packaging, combined with increased acceptance of electronic media, has led to a significant global oversupply of

paper and paperboard products. It is therefore understandable that during the last few years, a growing interest on the development of new functional paper materials, or on the improvement of the end-user specifications of paper, has been observed in order to achieve, for instance, better surface and optical properties for a superior printability, better gas-barrier and antimicrobial properties for packaging requirements, as well as enhanced mechanical properties for general applications. These properties could be achieved with a thin coating layer, for example.

Paper coating is a process that has undergone a number of developments in the last twenty years. Various formulations have been explored (blends of pigments with synthetic or natural polymers or other additives) in order to improve paper optical and printing properties. Chitosan has been one of these agents, incorporated singularly or blending with specific paper additives such as starch and inorganic fillers.

Therefore, the idea of combining chitosan with paper and paperboard is not new. Chitosan has been previously investigated as a surface coating [117-119,123-124,126,240-244], as well as a bulk paper additive [116,125,245-249], and showed that the well-known aptitude of chitosan to form strong thin films and its structural similarity with cellulose could be successfully applied to deposit them onto paper surfaces. This surface treatment imparts the paper products improved mechanical strength, controls the microbial contamination of packaging materials and improves printability. However, there is a lack of literature in the field of the improvement of functional properties of paper and paperboard via coating with chitosan [243-244,248]. Previous studies focus essentially on the evaluation of the barrier, mechanical and antimicrobial properties of the films, whereas other important parameters were marginally explored or not considered. For example, the improvement of printability is often referred, but, to the best of our knowledge, only one study dealing with the evaluation of the printability of sized kenaf papers has been published so far [242]. Moreover, relevant aspects related to the final applications of paper had never been studied. For instance, chitosan-coated papers display a high chemical and morphological heterogeneity, because of the complexity of the interactions among cellulose fibres, fillers and chitosan, but, these details were not adequately tackled in previous studies.

Moreover, the coating of *E. globulus* paper materials with chitosan had also never been described, nor a comprehensive study of the effect of a water soluble chitosan

derivative as coated paper agent. The pulp and paper industry represents an important sector of the Portuguese economy with *E. globulus* wood representing the most important raw material. This wood is made up of short and very homogenous fibres that provide relevant characteristics for papermaking, such as smoothness, very high bulk, excellent rigidity, good dimensional stability and high resistance when dump [250].

Nanotechnology is a novel and emerging area. Nevertheless, this 'new' concept is not a novelty for paper coating, because "nano-sized particles and pores are everyday business in paper coating" [251].

Despite the unique properties of cellulose nanofibres already pointed out, only recently their potentialities have been explored on paper production. Cellulose nanofibres, used as bulk additives or coating agents, have an enormous advantage in the production of papers with better properties [176,190-191,252-258]. For example, bacterial cellulose coated fibrous materials displayed good properties of gloss, smoothness, ink receptivity and holdout, and surface strength. However, some experimental technical problems were observed in these studies. The bacterial cellulose suspensions tended to undergo phase segregation under shear conditions, as in a size-press machine. The water rich fraction was transferred preferentially to the paper while the main proportion of bacterial cellulose remains in suspension. Some dispersing agents namely carboxymethylcellulose and starch were used to reduce this effect. For this reason, it is important to devise new processes that allow transfer reproducibly desirable amount of cellulose nanofibres onto the paper sheets.

5 Oxypropylation of natural polymeric substrates

The vast quantities of by-products arising from agricultural, marine and forestry activities represent a very promising first generation of natural resources, available for specific chemical modifications aimed at generating novel materials. Two aspects are relevant here, *viz.*, the fact of (i) selecting only the less noble parts of these commodities for the modifications, leaving the more valuable ones for well-established uses (food, timber, papermaking, pharmaceuticals, etc.) and (ii) valorising *all* the components of a given resource through the biorefinery working hypothesis, instead of selecting only that or those which appear to be more valuable. Indeed, a growing number of studies show that the so-called by-products can in fact be the precursors to materials with remarkable properties and high added value [259].

Among the numerous approaches investigated within this context [259-261], only the bulk oxypropylation of natural polymeric substrates is discussed here. Lignin, sugar beet pulp, olive stones and cork powder are secondary products of major biomass-based industrial activities, mainly used today as sources of energy by combustion. In previous studies, they have been efficiently converted by a single-step oxypropylation reaction into liquid viscous polyols [262-270], which are interesting macromonomers for the synthesis of polyurethanes and polyesters [263,271-272]. However, the reaction may be limited only to an outer shell of the substrate. The reaction mechanism remains the same but only the most accessible hydroxyl groups react, forming a thermoplastic sleeve around a pristine, unmodified core [273-276].

These systems are particularly straightforward in terms of their implementation, since they only involve the mixing of the activated solid substrate with propylene oxide (PO) in an autoclave and the subsequent heating of the ensuing suspension until the total consumption of the added PO. The recovery of the final polyol mixture is extremely simple, because it does not require the removal of any solvent or other component, nor any separation or purification procedure. The green connotations of the entire operation are therefore quite relevant. The fact that PO was always totally used up in the oxypropylation represents an element of safety, but, of course, particular care must be taken during these reactions to avoid any loss of control, which might lead to PO contamination.

A schematic representation of this reaction chain extension by propylene oxide is presented in Figure I-11. The number of hydroxyl groups of the substrate is not changed, however, they have moved away from the bulk and are much more accessible.

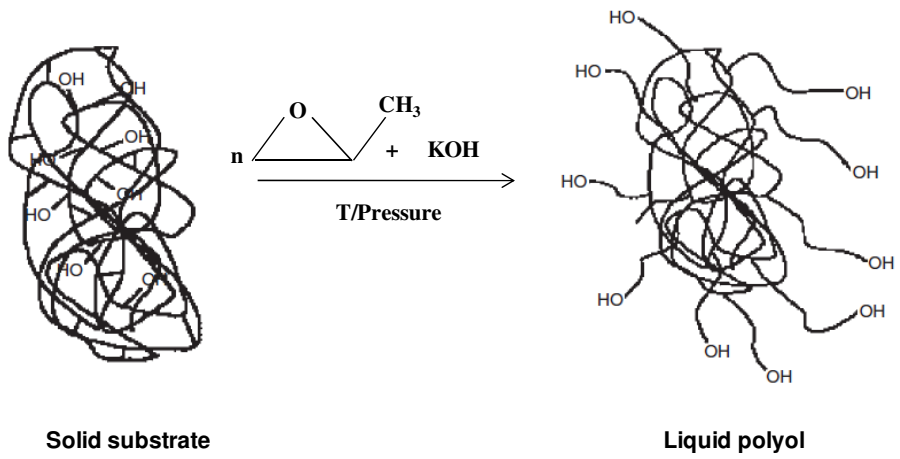

Figure I-11. Schematic representation of the hydroxyl group displacement caused by the oxypropylation reaction (reproduced from ref [277]).

In general, the reaction begins with hydroxyl group activation by the catalyst (typically, KOH) forming an alcoholate group (RO^-). Afterwards, the alcoholate group attacks the oxiranic ring of a PO moiety forming a new oxianion at the end of the chain. The chain-extension occurs until all PO is consumed. The preferred site for attack in PO is the α carbon of the oxiranic ring due to the low steric hindrance (Figure I-12a). The less probable attack of the alcoholate group, that can also occur, is the β position of the oxiranic ring (Figure I-12b) [277-278].

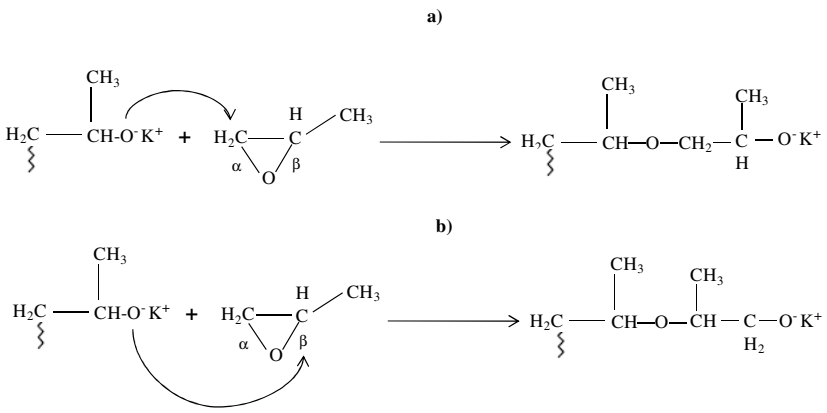

Figure I-12. Representation of the oxypropylation reaction: a) attack at the α carbon and b) attack at the β carbon (reproduced from ref [278]).

The oxypropylation reaction is always accompanied by the occurrence of PO homopolymerisation, which conducting to the formation of oligomeric materials (Figure I-13). The homopolymerisation of PO takes places when some residual moisture is present in the reaction medium. This situation leads to the appearing of OH^- species (e.g., from aqueous KOH) which can directly activate PO.

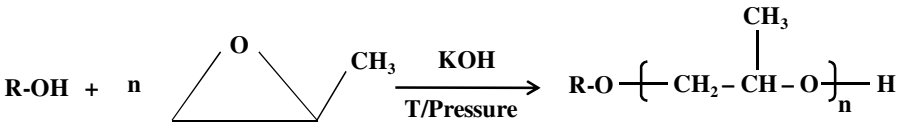

Figure I-13. Secondary reaction occurring during the oxypropylation: homopolymerisation of PO.

This *specific* approach has never been applied to chitin, and only once very succinctly to chitosan [266]. The studies related to the preparation of hydroxypropyl chitin and chitosan bearing very short grafts [279-286] and intended to biomedical applications, all involved the use of a solvent and required therefore a laborious workup, isolation and purification of the final product. The state of affairs prompted to extend to chitin and chitosan the successful approach already applied to other natural polymers, with the aim of valorising the less noble fractions and by-products arising from the industrial process consisting of the isolation of chitin and its conversion into chitosan.

Based on the above arguments concerning the needs of novel materials based on renewable resources and progress in paper science, this thesis aimed developing novel materials based on chitosan and its derivatives with cellulose nanofibres. The combination of these two polysaccharides was explored on the preparation of transparent biocomposite films, on the production of coated paper materials preferably with improved final properties and the optimization of the dispersion and application of BC and NFC onto paper sheets.

With the aim of valorising the less noble fractions and by-products of chitin and chitosan, the possibility of transforming these valuable renewable resources into viscous polyols through a simple oxypropylation reaction was also investigated in the course of this thesis.

.

Part II

Experimental

This second Part is devoted to the description of the raw-materials namely, chitin, chitosan, vegetal nanofibrillated cellulose, bacterial cellulose and paper sheets, and to the explanation of the methods and techniques used to characterize these materials.

This Part also describes the preparation of blends and nanocomposite films based on different chitosan matrices and different cellulose substrates, as well as the application of chitosan and its derivatives as coating formulations on the paper sheets.

Finally, the method use to convert chitin and chitosan into viscous polyols and the techniques used to characterize the ensuing materials are described.

6 Materials and Methods

6.1 Chitin and chitosan

Commercial chitosan samples were kindly provided by Norwegian Chitosan AS (Norway) and gently provided and purchased from Mahtani Chitosan Pvt. Ltd. (India). Chitin was also generously made available by Mahtani Chitosan Pvt. Ltd. (India). An ultra-pure chitosan sample (CHUP), purchased from NovaMatrix, was also used to compare its properties with those of the laboratory-purified samples.

The identification and the suppliers of chitin and chitosan samples as well as their degree of deacetylation (DDA) and molecular weights are listed in Table II-1.

Table II-1. Identification, DDA and suppliers of the chitin and chitosan samples used in this investigation.

Sample	Identification	DDA [%]	Molecular Weight [g/mol]	Supplier
Chitin	**Chitin**	30	600 000	Mahtani Chitosan Pvt. Ltd.
Chitosan	**HCH**	97	350 000	Mahtani Chitosan Pvt. Ltd.
Chitosan	**CH95**	95	543 000	Mahtani Chitosan Pvt. Ltd.
Chitosan	**LCH**	90	90 000	Norwegian Chitosan AS
Chitosan	**CH79**	79	58 000	Norwegian Chitosan AS
Chitosan	**CH67**	67	58 000	Norwegian Chitosan AS
Chitosan	**CHUP**	88	170 000	NovaMatrix

Note 1: the identification assigned to each sample (with exception of sample CHUP) was related to their DDA or to their molecular weight. For example, HCH means chitosan with a high molecular weight and CH79 means chitosan with a DDA of 79%.
Note 2: the DDA and molecular weight values presented in this table were determined in our laboratory.

6.1.1 Purification of chitosan

Before use, all chitosan commercial samples were purified in order to remove the impurities that are associated with the natural crustacean morphologies, rich in lipids, dyes, calcium carbonate and proteins [287].

The purification of the powdered commercial chitosan samples was carried out by successive dissolution-precipitation cycles. Chitosan solutions (0.5% w/v) were prepared by dissolution of the powdered chitosan samples in a 1% (v/v) aqueous CH_3CO_2H (Panreac, 99.7% purity) solution by stirring during 48 h at room temperature to ensure complete dissolution of the polymer by protonation of the amine functions. Then, these solutions were filtered successively through Porafil® membranes (3, 1.2 µm) and precipitated by addition of 10% NaOH (purchased by Fluka, 97% purity) solutions up to a pH of 8.5. The ensuing precipitates were washed with methanol (Fisher Scientific, 99.99% purity)/distilled water mixtures, whose composition was progressively varied from 70/30 to 100/0 (v/v), until a neutral pH. Finally, the samples were air dried at room temperature [75].

The final precipitates were characterized in terms of degree of deacetylation, average molecular weight, surface energy, moisture content, thermal stability, crystallinity, and morphology, as described bellow.

6.1.2 Degree of deacetylation

The degree of deacetylation (DDA, *i.e.* the fraction of amino groups within the chitosan polymeric chain) of all purified chitosan samples was determined by proton Nuclear Magnetic Resonance (^{1}H NMR) following a known procedure [49]. However, for two selected chitosan samples three methods (^{1}H NMR spectroscopy, elemental analysis (EA) [57] and conductometric titration [51]) were used and compared. As mentioned before, several techniques have been used for the determination of DDA. However, ^{1}H NMR is considered the most sensitive and precise technique [47], therefore, it was chosen as a reference method to verify the results obtained from other techniques or to verify the validity of other simpler and inexpensive techniques including those previously mentioned.

^{1}H NMR

To determine the degree of deacetylation of chitosan samples by ^{1}H NMR, using a DRX 300 Brüker spectrometer (300.13 MHz), it was necessary to take in account two important aspects: the solvent used and the scanning temperature, because of the presence of interference signals near to the acetyl groups [48] and of the difficulty in observing the proton present on carbon 1 of the *N*-acetyl glucosamine units due to the proximity of the residual water peak. Regarding the solvent, a mixture of D_2O/HCl (purchased by Acrös Organics, 100% D and Acrös Organics, 37% purity, respectively) (~pH 4) was used, which allowed to separate the relevant peaks used in the calculation of the chitosan DDA. Hydrochloric acid was chosen instead of acetic acid due to the presence of acetyl groups in the last [48-49]. As for the temperature, the scans were made at 85 ºC, in order to decrease the solution viscosity to increase the spectra resolution.

The DDAs were determined by integration of the specific peaks according to Equation II-1.

$$\mathbf{DDA}\ (\%) = \mathbf{1} - \left(\frac{\frac{\mathbf{I_{H7}}}{\mathbf{3}}}{\mathbf{I_{H1} + I_{H1'}}} \right) \times \mathbf{100} \qquad \mathbf{Equation\ II-1}$$

Where, I_{H7} is the integration of the CH_3 protons resounance of the acetyl group and (I_{H1} + $I_{H1'}$) is that of the proton in position 1 of the chitosan glycosidic ring both in a deacetylated (I_{H1}) and in acetylated ($I_{H1'}$) monomer units.

Elemental analysis

The degree of deacetylation of some purified and dried chitosan samples was further verified by elemental analyses using a Leco CNHS-932 Elemental Analyser. Before manipulation, the samples were extensive dried overnight in a vacuum oven in the presence of P_2O_5.

CHN elemental analyses allowed to determine the carbon, hydrogen and nitrogen mass percentages of the chitosan samples. However, since in a chitosan sample it is practically impossible to eliminate all residual water, even using procedures such as lyophilisation, the determination of DDA by this method involved the ratio between the mass percentages of C and N, using the relation, given by Kassai et al. [57] (Equation II-2).

$$\mathbf{DDA}\ (\%) = \mathbf{1} - \left(\frac{\frac{\mathbf{C}}{\mathbf{N}} - \mathbf{5.145}}{\mathbf{6.816} - \mathbf{5.145}} \right) \times \mathbf{100} \qquad \textbf{Equation II} - \mathbf{2}$$

Where, C/N is the percent ratio of carbon and nitrogen in the chitosan sample, and reflected the average value from three determinations. This ratio varies from 5.145 in completely *N*-deacetylated chitosan ($C_6H_{11}O_4N$ repeat unit) to 6.816 in chitin, the fully *N*-acetylated polymer ($C_8H_{13}O_5N$ repeat unit) [57].

Conductometric titration

The conductometric titration method used to determine the DDA is based on the high conductivity of the hydrogen and hydroxyl ions present in a chitosan solution.

The conductivity measurements were carried out as described by Raymond & Marchessault [51] using a CDM 230 MeterLab® conductivitymeter. The dried chitosan samples (25 mg) were dissolved in an acidic solution (2.5 mL of HCl (0.1 M) in 40 mL of water). The titration was performed using a dilute solution of NaOH (0.02 M) that was added slowly (0.2 mL at a time) to the acidic chitosan solution at 18.0 ± 0.1 ºC, until neutrality was achieved. The conductivity measurements were made in duplicate.

The number of free amine groups was determined using the equivalence point value calculated by the volume difference of the two inflection points corresponding to the acid consumed for the protonation of the amino groups. The following equations (Equations II-3 and II-4) were used to determine the DDA of the chitosan samples, by this method.

$$\boldsymbol{\alpha\left(^{eq}/_{g}\right) = \left(\frac{1 - DA}{(1 - DA) \times 161 + 203 \times DA}\right) \leftrightarrow}$$

$$\boldsymbol{DA = \left(\frac{1 - 161\alpha}{1 + 42\alpha}\right)} \qquad \textbf{Equation II} - \textbf{3}$$

$$\boldsymbol{DDA\ (\%) = (100 - DA) \times 100} \qquad \textbf{Equation II} - \textbf{4}$$

Where, α is the number of equivalents per unit mass of the chitosan sample used. The values of 161 and 203 correspond to the completely *N*-deacetylated chitosan ($C_6H_{11}O_4N$ repeat unit) and to fully *N*-acetylated polymer ($C_8H_{13}O_5N$ repeat unit), respectively.

6.1.3 Molecular weight

The molecular weight of all the chitosan samples was determined by viscosimetry. For two selected samples, size exclusion chromatography multi-angle light scattering (SEC-MALS) was also used.

Viscosimetry

To determine the intrinsic viscosity of each chitosan solution, measurements of the flow time of the solvent and of the diluted chitosan solutions were carried out using a glass capillary viscometer (inner capillary diameter 1.0 mm). From a chitosan solution ($C_0 \approx 65$ mg /50 mL), using 0.3M CH_3CO_2H/0.2M CH_3CO_2Na as solvent, four more concentrations of chitosan solutions were prepared ($2C_0/3$; $C_0/2$; $C_0/3$ and $C_0/6$) and used in order to calculate the intrinsic viscosity at 25.0 ± 0.1 ºC. About 8 replicates were performed for each chitosan samples.

The intrinsic viscosity was obtained by extrapolating the reduced viscosity (η_{red}) *vs* concentration data to zero concentration as defined below:

$$[\eta] = (\eta_{red})C \to 0 \qquad \textbf{Equation II} - \textbf{5}$$

The viscosity molecular weight (M_v) was calculated based on Mark-Houwink-Sakurada equation (Equation I-1) using the published Mark-Houwink constants (K and a, see in Table III-5 the values used), which depend on the DDA of the chitosan samples [64].

Size exclusion chromatography (SEC)

The molecular weights of HCH and CHUP were also determined by size exclusion chromatography multi-angle light scattering (SEC-MALS), using a Waters Alliance 2695 (USA) equipped with two online detectors, a differential refractometer and a multi-angle laser light scattering detector (MALLS)-(DAWN HELEOS-II) from Wyatt technologies (USA). The solvent was aqueous acetic acid 0.3M/sodium acetate 0.2M at a flow rate of 50 µL/min and the temperature 30 ºC. Samples were prepared by dissolving the chitosan in aqueous acetic acid 0.3M/sodium acetate 0.2M and then filtering through a 0.45 µm filter (Millipore) after 48 h. The polymer concentration injected was around 0.5 mg/mL. The weight-average molecular weight was obtained from a data collected and analyzed using an ASTRA SEC software (version 4.90, Wyatt Technology Corp. USA). The calculations of molecular weight were carried out according to Zimm's plot.

SEC-MALS profiles, obtained by this method, allowed calculating the weight-average molar mass (M_w), the number-average molar mass (M_n) and of the polydispersity index, Ip, which is the ratio of M_w/M_n.

6.1.4 Surface energy

The chitosan powder samples, before and after the previously described purification, were sequentially Soxhlet-extracted with dichloromethane, *n*-hexane and acetone. The chitosan films were only extracted with acetone. After each extraction, the solution was vacuum evaporated to dryness, and the residues analysed by gas chromatography-mass spectrometry (GC-MS). Before GC-MS analysis, extracts were

silylated in pyridine at 70 ºC for 30 minutes with trimethylchlorosilane in the presence of *N*,*O*-bis(trimethylsilyl)trifluoracetamide, according to a described procedure [288]. The GC-MS analyses of the derivatized extracts were performed using a Trace Gas Chromatograph 2000 Series, equipped with a DB-1 J&W capillary column (30 cm x 0.32 mm, 0.25 µm film thickness, helium as carrier gas (35 cm/s)), which was coupled with a Finnigan Trace MS mass spectrometer. The chromatographic conditions were: initial temperature, 80 ºC for 5 min; heating rate, 5 ºC/min; final temperature, 285 ºC for 15 min; injector temperature, 200 ºC; transfer-line temperature, 280 ºC; split ratio 1:35.

Pellets of both commercial and variously-purified chitosan and chitin samples, as well as of the respective model compounds (D-(+)-glucosamine hydrochloride 99% and *N*-acetyl-D-glucosamine 99% (purchased from Sigma and used as received), were prepared using a Graseby Specac (6 ton during 1 min) laboratory press. Films were obtained by the casting method using 1% w/v solution of the purified chitosan samples in 1% v/v aqueous acetic acid.

Three different test liquids, one apolar and two polar were required for the calculation of the surface energy of the materials. Diiodomethane (Aldrich, 99% purity GC) was chosen as the apolar liquids and water and formamide (Sigma, 99% purity GC) as the polar liquids. The values of the dispersive and polar components to the surface tension of the liquids used for the contact angle measurements are available in the literature [289]. Contact angles (θ) were measured with a "Surface Energy Evaluation System" commercialized by Brno University (Czech Republic). Each θ value (average of 3-5 measurements, with an associated standard deviation of ±2º) was the first captured by the instrument following the drop deposition on the sample surface, which had previously been equilibrated with the vapor of the liquid to be tested. All measurements were carried out at the laboratory temperature, which varied between 23 and 25 ºC. The contact angle values were then used to calculate the dispersive and polar contributions to the surface energy of the samples, using Owens-Wendt's approach [290].

6.1.5 Other properties

The structural characterization of the chitosan samples was assessed by Fourrier Transform Infra Red Spectroscopy (FTIR), ^{1}H NMR spectroscopy and solid state ^{13}C CP-MAS NMR experiments.

The FTIR spectra were taken with a Mattson 7000 FTIR spectrophotometer equipped with a single horizontal Golden Gate ATR cell. The spectra were recorded in transmittance mode from 4000 to 500 cm^{-1}, co-adding 256 scans at 8 cm^{-1} resolution.

^{1}H NMR spectra were recorded as described before in Section 6.1.2. Solid state ^{13}C CP-MAS NMR experiments were performed at 100.62 MHz on a Bruker MSL 400 P spectrometer with a spinning rate of 5 kHz, using the combined technique of magic angle spinning (MAS) and cross-polarization (CP). Taking values from 10 ms to 10 s and a CP contact time of 1 ms.

The thermal stability and crystallinity of the samples were also determined. The thermogravimetric analisys (TGA) were carried out with a Shimadzu TGA 50 analyzer equipped with a platinum cell. Samples were heated at a constant rate of 10 ºC/min from room temperature to 800 ºC under a nitrogen flow of 20 mL/min. The thermal decomposition temperature was taken as the onset of significant (≥ 0.5%) weight loss, after the initial moisture and acetic acid losses (when applicable).

For crystallinity measurements, the powdered samples were gently compacted and analyzed by X-ray diffraction (XRD) using a Philips X'pert MPD diffractometer using Cu Kα radiation.

6.2 Cellulose substrates

6.2.1 Bacterial cellulose

Bacterial cellulose (BC), in the shredded wet form, in a 5 wt% water suspension was supplied by Forschungszentrum für Medizintechnik und Biotechnologie e.V. (Germany). It was produced by the genera *Gluconacetobacter xylinus* in a reactor with

agitated conditions and was also characterized in terms of morphology by scanning electron microscopy (SEM), crystallinity and thermal stability.

SEM micrographs were obtained on a HR-FESEM SU-70 Hitachi equipment operating at 1.5 kV. Samples were mounted on carbon tape and coated with carbon for SEM analysis. The crystallinity and the thermal stability were performed as previously described.

6.2.2 Nanofibrillated cellulose

The nanofibrillated cellulose (NFC) as a 2 wt% water suspension was kindly provided by Professor Lars Berglund at KTH (Stockholm, Sweden). The preparation of NFC is described in detail by Henriksson et al. [164].

NFC was characterized in terms of morphology (SEM), crystallinity and thermal properties using the techniques already described.

6.2.3 Paper sheets

Non commercial A3-size papers sheets (100% *E. globulu*s bleached kraft pulp, produced by AKD-based sizing system) without any surface treatment, produced and supplied by the Grupo Portucel-Soporcel, Figueira da Foz, Portugal, were used as paper substrates for coating assays. This substrate is identified as the control sheet (CS).

The paper materials were characterized in terms of morphology (SEM), mass properties (grammage and apparent density), surface properties (roughness), mechanical properties (tensile strength, bursting strength and surface strength), barrier properties (air permeability and water vapour permeability), optical properties (brightness and opacity), paper lightfastness (ageing essays) and printability (color density, Gamut Area (GA), Inter Colour Bleed and images analysis).

The morphology of the paper materials was assessed by SEM as described in Section 6.2.1.

The grammage was determined in accordance with the ISO 536 standard method, using a Mettler PC 220 analytic balance (±1 mg). The grammage gains were obtained by subtracting the weight of the paper sheet before the coating to the chitosan-coated paper sheets.

The apparent density was calculated using the thickness of the specimens measured according to the TAPPI T411 om-89 method, with a precision micrometer using a Model 51 D2 Lorentzen & Wettre Thickness Tester. The thickness was measured in 10 positions of each specimen.

The Bendetsen roughness was measured according to the ISO 8791 2:1990 standard method, using a Lorentzen & Wettre model 114 L&W Bendtsen® Tester.

Tensile index and stretch at break were determined using a Lorentzen & Wettre model 65-F Alwetron TH1 tensile tester. The preconditioned sheets were cut into 15 mm x 180 mm strips and tested according to the ISO 1924/2 standard method. The initial clamp distance was 100mm and the strain rate 20 mm/s.

Burst Index was determined in accordance with the ISO 2758 standard method, using a Lorentzen & Wettre model 04 BOM Burst-0-Matic.

Surface strength of paper surface was determined by the waxes-pick test according to the TAPPI T459 om-93 standard method.

The Bendtsen air permeability was measured according to the ISO 5636/3:1992 standard method using a Lorentzen & Wettre model 114 L&W Bendtsen® Tester.

The water vapour permeability (WVP) was measured with basis on the ASTM D96-95 standard method, following the "desiccant method". The paper specimens, with a diameter of 6 cm, were sealed to the open mouth of the test cup containing a desiccant, anhydrous calcium chloride pre-dried at 200 ºC for 2 h, using a silicon sealant and four screws symmetrically located around the cup circumference. The cylindrical test cups were made of polymethylmethacrylate and the area of the cup mouth was 19.6 cm^2 and the internal deep was 2 cm. The assembly was placed in a test chamber maintained at 232 ± 3 ºC and at 43% relative humidity using a saturated aqueous magnesium nitrate solution. Air was continuously circulated throughout the chamber with a van at ~160 m/min. Periodic weighings to the nearest 0.1 mg were performed in order to determine the rate of water vapour movement through the specimen into the desiccant. Stable state conditions were assumed when the rate of change in weight of the cup became

constant (~1 h). This constant rate of weight increase was obtained by linear regression. Correlation coefficients for all reported data were 0.98 or higher. The WVP were calculated from the water vapour transmission rate (WVTR) values, assuming a correction method to account for the water vapour partial pressure gradient in the stagnant air layer within the test cup [291]. Three samples of each paper type were tested.

Brightness and Opacity were measured using an Elrepho 2000 data colour unit according to the TAPPI T 452 om-98 and TAPPI T 425 standard methods, respectively.

In order to evaluate the inkjet print quality of the coated papers, a specific print mask form was printed on each paper sample using a HP DESKJET F370 printer (thermal inkjet technology) equipped with standard HP print cartridges (water based, HP21 Black - pigment ; HP22 Tri-colour (C,M,Y) - dye). The printer was set to "paper quality: plain paper" and "print quality: normal". An AvaMouse Handhel Reflection Spectrometer (SpectroCam Avantes World Headquarters) operating in the visible range (380 to 780 nm) was used to assess Gamut area and colour density. The gamut area, assessing the range of reproducible colours, corresponds to the area of the hexagon whose vertices are the pairs (a*,b*), where a* and b* are the CIE Lab coordinates colours obtained for each colour (cyan, yellow, magenta, green, blue and red). The larger the area, the greater the paper potential to reproduce every colour. A PIAS^{TM}-II Personal Image Analysis System based on the ISO/ TEC13660:2001 standard was used to evaluate the Inter Colour Bleed and the image analysis. Inter Colour Bleed occurs at the interface between two different coloured inks (black and yellow, in this case).

Selected coated papers were submitted to a Xénon light source placed inside a camera (SUNTEST XLS+ equipped with a UV filter) at 65 ºC, with an irradiation of 600 W/m^2 during 1h. Two 10×10 cm pieces of each paper sheet were used. The paper lightfasteness was evaluated by the determination of the CIE (International Commission on Illumination) L*, a*, b* (SCAN P:72 standard method) and the whiteness (ISO 11475 standard method). Where, L* represents the lightness of the color (ranging from zero to a hundred of black to white) and a*, b* are the chromaticity values, red/green coordinate and yellow/blue coordinate, respectively. This method is an internal procedure used by Grupo Portucel-Soporcel, Portugal and is based on the standard ISO/CD 14358-2 and ISO 2470 standard methods. The spectrophotometer used was an Elrepho L&W. Four replicates were analysed for each coated paper sample.

The values used were the average of three different measurements on each paper sheet.

7 Synthesis of chitosan derivatives

7.1 Fluorescent chitosan

In order to introduce a certain amount of chromophore groups into the chitosan backbone, which could be conveniently and directly quantified by UV or fluorescence spectroscopy, a fluorescent chitosan derivative (FITC-CH) with a low degree of substitution (~ 2% of the amino groups) was synthesized using fluorescein isothiocyanate (FITC) following the procedure described by Qaqish & Amiji [103].

A 0.5 mg/mL solution of FITC (purchased from Sigma-Aldrich, purity 90% minimum) in methanol was slowly added under continuous stirring to a 1% w/v solution of the purified chitosan in 1% v/v aqueous acetic acid (prepared with 5.0 g of chitosan by stirring for 48 h at room temperature). The condensation between the isothiocyanate groups of FITC and the NH_2 groups of CH was allowed to proceed for 1 h, in the dark, at room temperature. Then, the ensuing FITC-CH derivatives were precipitated in a 10% NaOH aqueous solution and washed with distilled water, until the total disappearance of FITC in the washing medium. The FITC-CH derivative was obtained as a powder by lyophilisation.

The structural characterization of FITC-CH was assessed by FTIR spectroscopy and X-ray diffraction using the methodology described before. The degree of substitution was determined by CHNS elemental analyses using a Leco CNHS-932 Elemental Analyser. For this purpose this chitosan derivative was also extensive dried overnight in a vacuum oven, weighed and then introduced inside a silver capsule. Its molecular weight

was determined by SEC as described in Section 6.1.3. Its optical properties were assessed by UV-vis absorption and luminescence spectroscopy.

UV-vis spectra were recorded with a temperature-controlled Jasco V-560 spectrophotometer using 1 cm Hellma suprasil cells equipped with both 9 and 9.9 mm quartz spacers and a quartz pyrex graded seal. The Beer-Lambert law was applied by measuring the absorbance of increasing concentrations using a solution of FITC or FITC-CH dissolved in a mixture of aqueous acetic acid (1% v/v) and MeOH (Fisher Scientific, 99.99% purity).

The photoluminescence spectra were recorded at room temperature with a modular double grating excitation spectrofluorimeter equipped with a TRIAX 320 Fluorolog-3, Jobin Yvon-Spex emission monochromator and coupled to a R928 Hamamatsu photomultiplier, using the front-face acquisition mode. The excitation source was a 450W Xe arc lamp. The emission spectra were corrected for detection and optical spectral response of the spectrofluorimeter and the excitation spectra were corrected for the spectral distribution of the lamp intensity using a photodiode reference detector.

7.2 Water soluble chitosan

The water soluble chitosan quaternary ammonium derivative (WSCH) was prepared, following the procedure described by Seong et al. [98]. Purified chitosan was dissolved in a 1% acetic acid aqueous solution (250 mL), before adding glycidyltrimethylammonium chloride (GTMAC, Fluka, 90% purity), in a GTMAC/CH molar proportion of 4/1. This stirred mixture was kept at 60ºC for 24 h under a N_2 atmosphere. The ensuing water soluble chitosan derivative (*N*-(*3*-(*N,N,N*-Trimethylamonium)-2-hydroxypropyl) chloride chitosan) was precipitated in ethanol (Sigma-Aldrich, 90% purity) and washed several times with the same solvent.

These conditions were the selected to synthesize WSCH with a DS close to 30%, which is the percentage of substituted amino groups necessary to have a total dissolution of the polymer in water, after testing other conditions varying the chitosan concentration (1-2%), the temperature (50-65 ºC) and the reaction time (24-48 h), in order to optimize the synthesis.

The structural characterization of WSCH was assessed by FTIR spectroscopy, solid state ^{13}C CP-MAS NMR and XRD. The degree of substitution of the modified polymers was determined by ^{1}H NMR spectroscopy, the molecular weights by SEC and the thermal properties by TGA.

8 Preparation of the chitosan-cellulose nanocomposite films

8.1 Preparation of blends

For the preparation of the chitosan and chitosan-cellulose nanocomposite films, chitosan 1.5% (w/v) solutions were first prepared (at pH 4 for CH and pH 7 for WSCH, see Appendix 1), by dissolving the corresponding powdered chitosan samples (two selected chitosan samples, one with a relatively low molecular weight (LCH) and another with a high molecular weight (HCH)) in aqueous acetic acid (1% v/v) or in water (in the case of WSCH).

Then, different amounts of cellulose were added to these solutions. The NFC amounts varied from 5 to 10% (relative to the weight of dry chitosan) for HCH and its water soluble derivative (WSHCH), and from 5 to 60% in the case of LCH. In the case of water soluble low molecular weight (WSLCH) only two different amounts were considered, 10 and 60%.

The contents of BC were 5 and 10% for HCH and WSHCH, and were varied from 5 to 40% for LCH films. In this context, WSLCH was not used.

The maximum amount of cellulose used with each type of chitosan was limited by the final high viscosity of the ensuing mixtures.

The dispersion of the cellulose nanofibres in the chitosan solutions was performed using an Ultra-Turrax unit for 30 minutes at 20 500 rpm. Then, each suspension was degassed under vacuum to remove entrapped air.

8.2 Nanocomposite films

An appropriate mass of both unfilled CH and chitosan-cellulose formulations were transferred onto levelled 10×10 cm^2 square plexiglass plates (Figure II-1) in order to keep both total amount of polymer deposited per casting area unit (3.1×10^{-3} g polymer/cm^2) and thickness (~ 30 μm) constant (see values in Appendix 1). Four films, from each solution and suspension were then prepared by casting at 30 ºC in a ventilated oven for 16 h.

Figure II-1. Plates used in the preparation of the nanocomposite films.

Finally, the films were removed from the moulds and conditioned in a cabinet at 50 ± 5 % relative humidity (RH) and 25 ± 3 ºC for at least 48 h to ensure the stabilization of their moisture content. Before testing, the thickness of all films was measured using a digital micrometer (model MDC-25S, Mitutoya Corp., Tokyo, Japan). Their mean thickness was the average from five measurements taken at different locations of each film samples (see values in Appendix 1).

8.3 Techniques used to characterize the materials

All the unfilled CH and WSCH, and chitosan-cellulose nanocomposite films (CHNFC and CHBC) were characterized by several techniques aiming to assess their

morphology (SEM and AFM), crystallinity (XDR), thermal stability (TGA), mechanical properties (tensile tests and dynamic mechanical analysis (DMA)) and optical properties (transmittance).

SEM, XDR and TGA were assessed as previously explained.

AFM measurements were performed in an Innova AFM Veeco Instrument. The images were scanned in a tapping mode under ambient condition using rectangular silicon cantilevers from Veeco-probes (MMP-12100-10), resonating at about 110 kHz. The samples were mounted on a magnetic puck with double-sided tape and analyzed in ambient air at room temperature.

The tensile tests were performed at room conditions on a TA-Hdi Stable Micro Systems Texture Analyser equipped with fixed grips lined with a thin rubber film at their ends and fitted with a static load cell of 50 N. The film strips were 90 mm long and 10 mm wide. The initial grip separation was set at 50 mm, and the crosshead speed was 0.5 mm/s. Tensile strength, tensile modulus, and elongation to break were obtained using the Instron Series IX software. Fifteen measurements were conducted with each sample in order to obtain an experimental error of about 5%.

In order to study the temperature dependency of the storage modulus, DMA measurements were carried out on a Tritec 2000 DMA Triton equipment operating in the tensile mode. Tests were performed at 1 Hz, an amplitude of 4 μm and a heating rate of 5 ºC/min, from -50 to 165 ºC. Test specimens with a typical size of 0.5 mm x 1 mm were used.

To study the moisture dependency of the storage modulus, DMA measurements were carried out on a Perkin-Elmer DMA7 operating in the tensile mode. A dynamic deformation was applied at a frequency of 1 Hz. The static load was set to 120% of the dynamic load, keeping the amplitude constant at 4 μm. Measurements were performed in humidity scans from 5-90% RH after an initial conditioning at 5% RH for 30 minutes. The scan rate was 1% RH/min. The humidity scan was created by a computer controlled humidifier producing humid air by mixing dry and fully moisture saturated air streams. For both DMA techniques the number of measurements was conducted in order to obtain an experimental error of ± 5% and the average values calculates there from.

The transmittance spectra of the films and nanocomposite films were measured with a UV-vis Spectrophotometer (Perkin-Elmer UV 850) equipped with a 15 cm diameter

integrating sphere bearing the holder in the horizontal position. Spectra were recorded at room temperature in steps of 1 nm, in the range 400–700 nm.

9 Coating experiments

9.1 General conditions

Paper sheets were coated with different solutions namely CH, FITC-CH and WSCH, using a RRC-BW 350 mm pilot size-press MathisLAB reverse roll coater.

The general view of the size-press and the details of the feeding and drying sections are illustrated in Figure II-2.

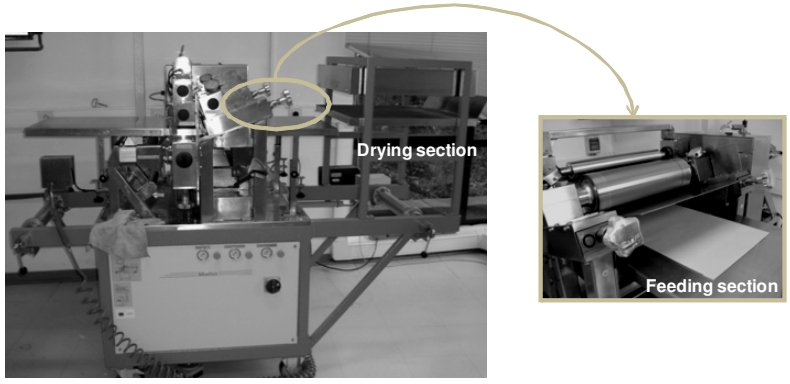

Figure II-2. Size-press (MathisLAB reverse roll coater type RRC-BW 350 mm) used in the coating experiments.

The conditions of the machine operation were always the same *viz.* the coating speed was fixed at 20 m/min and the distance between the cylinders was adjusted depending on the desired chitosan deposited on the paper sheets (adjusting precision ± 1 µm) and different coating levels were applied using CH solutions from 1 to 5 layers on one side of the paper sheet. The ensuing coated papers were then dried for 2 minutes at

100 ºC in the dryer section of the size press, after each layer deposition. Thereafter, an A4 sample was cut out from the inner region of each original A3 sheet in order to eliminate the inevitable irregularities associated with its coated borders.

Before their characterization, all coated papers were conditioned at 23 ± 1 ºC and 50 ± 5% RH for 3 days following the TAPPI T402 om-93 standard method.

Finally, the coated paper sheets were thoroughly characterized by the several techniques described in Section 6.2.3.

9.2 Preparation of chitosan-coated papers using a fluorescent chitosan

The paper sheets were coated with a 2% w/v LCH or FITC-LCH solutions in 1% v/v acetic acid. In order to achieve different coating weights, different coating levels were applied using both LCH and FITC-LCH, with 1 (LCH1 or FITC-LCH1), 2, 3, 4 or 5 layers respectively on one side of the paper sheet. Three replicates were prepared for each condition and each chitosan solution. The coated-based materials were prepared and stored as described before in Section 9.1.

Different approaches were investigated namely reflectance, radiance and luminescence to assess the chitosan macromolecules distribution onto and within paper sheets. The methodology used to assess to luminescence was explained in Section 7.1.

The diffuse reflectance spectra of the paper sheets were measured with a Perkin-Elmer 860 Spectrophotometer equipped with a 15 cm diameter integrating sphere bearing the holder in the bottom horizontal position. They were recorded at room temperature in steps of 1 nm, in the 350–600 nm range with a bandwidth of 2 nm. The instrument was calibrated with a certified Spectralon white standard (Labsphere, North Sutton, USA) and spectra were acquired by inserting before the detector a visible short-wave pass filter (LOT-Oriel 450FL07-50, 450 cut-off wavelength) in order to remove the fluorescence component of the chitosan derivative. The reflectance of both sides of the sheet was measured, which provided two spectra for each sample. The Kubelka–Munk model [292] describes the light penetration in porous media using only two parameters (both with units of cm^{-1}), namely an absorption coefficient, *k*, and an isotropic scattering coefficient, *s*. This

leads to a very simple relationship between infinite reflectance and absorption and scattering coefficients, known as the remission function, *viz.*:

$$F(R_\infty) = (1-R_\infty)^2 / 2R_\infty = k/s \qquad \textbf{Equation II-6}$$

A very important requirement for the use of the Kubelka–Munk model is the homogeneous distribution, both vertically and horizontally, of the absorbed compound in the layer. If the light absorption due to the compound is not excessive, it can be assumed that only the absorption coefficient, but not the scattering coefficient, of the doped medium changes by adding the light-absorbing compound. The absorption coefficient of the system, $k_{tot} = k + k_i$, given by the sum of the absorption coefficient of the medium (k) and that of the compound adsorbed on its solid surface (k_i), is proportional to the molar absorption coefficient of the compound, $\varepsilon_i(\lambda)$ (cm^3/ mol.cm) and to its adsorbed concentration C_i (mol/cm^3).

The radiance measurements and the CIE (x,y) emission colour coordinates were performed using a TOP 100 DTS140-111 Instrument Systems telescope optical probe. The excitation source was a 150 W Xe arc lamp coupled to a TRIAX 180 Jobin Yvon-Spex monochromator. The width of the rectangular excitation spot was set to 2 mm and the diameter used to collect the emission intensity to 0.5 mm. The emission colour coordinates and the radiance of an uncoated paper were also measured. For all the measurements, the experimental conditions (excitation and detection optical alignment) were kept constant to enable the quantitative comparison between the measurements to be carried out. A mapping of the radiance and colour coordinates was performed using 12 paper test pieces (4.0 cm × 4.0 cm) randomly cut off from different regions of the same A4 sheet (as shown in Figure II-3) and 20 measurements were conducted for each sample and their average value calculated. The experimental error was ± 5%.

The grammage gain, the Bendtsen air permeability and the tensile index were also assessed as already described.

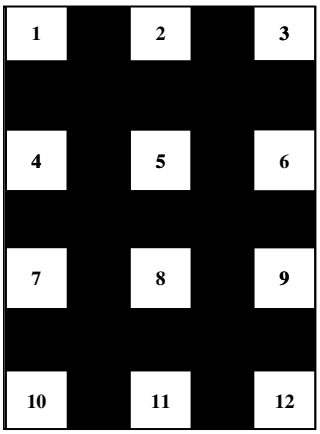

Figure II-3. Map showing the 12 paper pieces (4.0 cm × 4.0 cm) cut off from different regions of the same A4 sheet.

9.3 Preparation of papers coated with CH and WSCH

Paper sheets were coated with LCH and its WSLCH solutions (1% acetic acid and water, respectively) at 2% w/v. Different coating weights were attained by the deposition from 1 (LCH1 or WSLCH1) to 5 coating layers. Blank essays with water (W), a 1% acetic acid solution (AA) and a "mechanical" treatment (MT, without any solution) were also carried out. Five replicates were prepared for each condition and each chitosan solution. The coated-based materials were prepared and stored as described in Section 9.1.

The mass, mechanical, surface, barrier and optical properties, morphology, paper lightfasteness and inkjet print quality of the ensuing coated papers were investigated, assessed and compared.

10 Chitin and chitosan oxypropylation

In this investigation chitin and chitosan were treated with propylene oxide (PO) (Sigma-Aldrich, 99% employed as received).

The oxypropylation reactions were carried out in a 300 cm^3 stainless steel autoclave equipped with stirring, a heating resistance and temperature and pressure sensors (Figure II-4).

Figure II-4. Stainless steel autoclave equipped with stirring, a heating resistance and temperature and pressure sensors.

The chitin and chitosan (CH95) samples (10 g) were preactivated in the reaction vessel with an ethanol/KOH (Merck, 85% purity) solution for 1 hour at room temperature

under a nitrogen atmosphere. The dried activated-substrate was then mixed with PO (40 and 20 ml, respectively for chitin and chitosan) and allowed to react, with constant mechanical stirring at 1000 rpm, at 140 (set 1) and 120 ºC (set 2). The higher amount of PO in the experiments with chitin was employed to guarantee a thorough impregnation of the substrate, which was particularly fluffy. The onset of the oxypropylation reaction was revealed by a rapid increase in temperature (max. 220 ºC) and pressure (max. 15 bar) and its completion by the return of the pressure to its atmospheric value. The reaction time varied between 1 and 2 hours. In all these experiments, no unreacted PO was detected after opening the autoclave.

The viscous products were diluted with dichloromethane and filtered through a highly porous cotton fabric. The solid residues (SR) were washed several times with dichloromethane, dried and weighed in order to determine the percentage of unreacted, or poorly reacted, substrate. The solvent and other volatile components of the filtrates were removed in a rotary evaporator leaving a viscous polyol which was then extracted with n-hexane in order to separate the oxypropylated chitin or chitosan (hexane insoluble material) from the PO homopolymer fraction. The separation procedures were only applied in order to characterize all the products of the reaction. In practice, however, the polyol mixtures can be used as such without any separation or purification.

Some of the solid products were submitted to a second oxypropylation in the same conditions in order to verify whether they were intractable structures or simply residual polysaccharides which had not been sufficiently modified during the first treatment. The fact that in all instances liquid polyols were obtained proved that the latter reason had been the cause of these incomplete oxypropylations.

The two fractions were separated and thoroughly characterized by FTIR and NMR spectroscopy, TGA, DSC, hydroxyl number and viscosity.

The DSC thermograms were traced with a Setaram analyzer scanning at 10 ºC/min in a stream of helium. Scanning at 2 ºC/min gave essentially the same results.

The hydroxyl index number (I_{OH}) is an important parameter in the characterization of polyols intended to polyurethane formulations, since it allows the calculation of the corresponding amount of isocyanate. I_{OH}, by definition, is the number of milligrams of potassium hydroxide equivalent to the hydroxyl content of 1 g of polyol. This parameter was determined according to the ASTM D1638 standard method, which consists in

dissolving the polyol in pyridine (Acrös Organics, 99% purity), treating it with a known excess of phthalic anhydride (Aldrich, 99% purity) under reflux for one hour. Then, the mixture was back-titrated with a solution of sodium hydroxide (0.5 M) (Fluka, 97% purity). The difference between the NaOH volume required for the titration of the blank and that required for the polyol sample allowed the determination of the hydroxyl number. I_{OH}, in mg of KOH/g, was determined according to Equation II-7.

$$\mathbf{I_{OH}} = \frac{\mathbf{(V_1 - V_2) \times C \times 56.1}}{\mathbf{W}} \qquad \textbf{Equation II} - \mathbf{7}$$

Where,V_1 is the NaOH volume required for blank titration and V_2 is the NaOH volume required for polyol sample titration, in mL; C is the NaOH concentration, in mol/L; W is the polyol weight, in g; and 56.1 is the molar mass of KOH in g.

The viscosities of the chitin- and chitosan-based polyols (PL) were measured with a controlled-stress AR 1000 TA rheometer, fitted with a cone-plate geometry (40 mm diameter and 4º angle) at 20 ºC.

Part III
Results and discussion

This Third Part is dedicated to the presentation of the results and their discussion.

Chapter 11 presents the main characteristics of the raw-materials (chitin, chitosan, nanofibrillated cellulose, bacterial cellulose and cellulose substrates) and of the chitosan derivatives.

Chapter 12 describes the preparation and characterization, by several techniques, of nanocomposite films based on different chitosan matrices and different cellulose substrates. These transparent nanocomposite films were prepared through a simple and fully green approach of casting a water-based suspension of chitosan and nanocellulose. In addition, potential applications for these novel materials will be suggested.

Chapter 13 describes the study the distribution of chitosan onto the chitosan-coated paper using a fluorescent chitosan derivative as a tool to assess its spatial and in-depth distribution onto the paper sheet. Then, the effect of the chitosan acidic solution and chitosan quaternization, on the final properties and paper ageing of *E. globulus*-based papers is assessed.

The vast quantities of by-products arising from marine activities represent a very promising first generation of natural resources available for specific chemical modifications aimed at generating novel materials. In this context, chitin and chitosan were converted into viscous polyols through a simple oxypropylation reaction (Chapter 14).

Finally, a general conclusion and suggestions for further work are presented.

11 Chitosan and cellulose substrates: characterization

11.1 Chitin and chitosan

11.1.1 Degree of deacetylation

In this section, the DDA values obtained by three methods (^{1}H NMR spectroscopy, elemental analysis and conductometric titration), are presented, discussed and compared.

^{1}H NMR

The typical ^{1}H NMR spectrum of chitosan in D_2O/HCl at 85 ºC is shown in Figure III-1. The chemical shifts listed in Table III-1 are in agreement with the assignments previously reported [48-49,293].

The chitosan spectrum shows a peak at 2.05 ppm attributed to the *N*-acetyl glucosamine units (H7, $-CH_3$) that survived the saponification of chitin. The signal at 3.22 ppm (H2) and the multiplets from 3.75 to 4.12 ppm (H3 – H6) are attributed to the chitosan glycosidic ring protons and also to residual water in the case of the multiplets. The two signals observed at 4.65 and 4.89 ppm are assigned to the H1' and H1 protons of the *N*-acetyl glucosamine and D-glucosamine units, respectively.

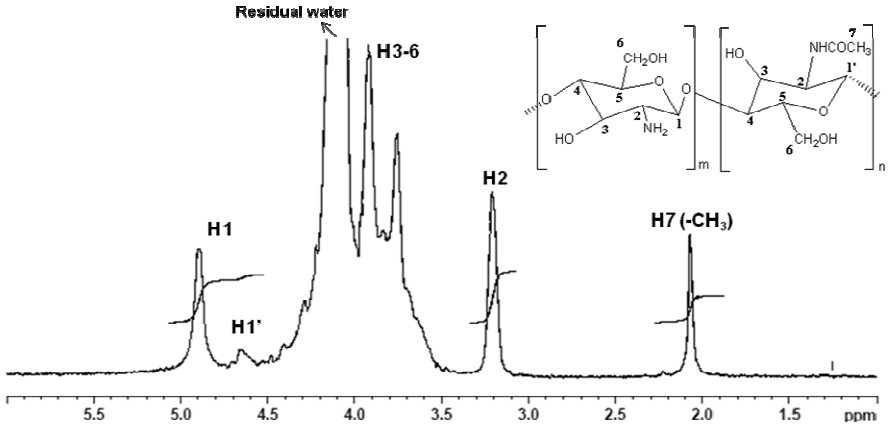

Figure III-1. ^{1}H NMR spectrum of CHUP in D_2O/HCl solution (10 mg/mL) at 85ºC.

The DDA was determined by the integration of specifics peaks according to Equation II-1 and is given in Table III-1.

Table III-1. ^{1}H NMR chemical shifts (ppm) of HCH and CHUP chitosan sample in D_2O/HCl solution at 85ºC.

Sample	Peak	H1+H1'	H2	H7	DDA (%)
HCH	Number of protons	1	1	3	97
	δ (ppm)	4.94	3.26	2.08	
	Integration	1.00	1.04	0.09	
CHUP	Number of protons	1	1	3	88
	δ (ppm)	4.64+4.89	3.22	2.05	
	Integration	1.00	1.05	0.36	

The DDA of each chitosan and chitin determined by this technique are listed in Table III-9. The ^{1}H NMR spectrum of the HCH sample is presented in Appendix 2.

Elemental analysis

Table III-2 gives a selection of results related to the elemental composition of HCH and CHUP, the relative percentage of carbon and nitrogen (C/N) and the corresponding DDA values determined according to Equation II-2.

Table III-2. Elemental composition (C and N) of HCH and CHUP chitosan samples and their C/N ratio.

Chitosan Sample	Weight percent of elements (Experimental)		C/N	DDA (%)
	C (%)	N (%)		
HCH	37.22±0.01	7.16±0.02	5.19	**97**
CHUP	38.57±0.01	7.18±0.01	5.37	**87**

It can be clearly seen that the EA gave values that were in agreement with those obtained by ^{1}H NMR.

Conductometric titration

Figure III-2 shows a typical curve of the conductimetric titration of HCH acidic solution with NaOH.

The curve of the conductivity against the volume of NaOH is divided into three regions, with two inflection points. The first descending portion of the curve corresponds to the neutralization of the free protons present in the solution, and the curvature at the lower end of this portion is attributed to the initial dissociation of the protonated amino groups of chitosan. The first ascending portion is due to the neutralization of the protonated amino groups. A small deviation from linearity was observed during the final phase of neutralization, which coincides with the precipitation of chitosan. The final ascendant portion of the curve corresponds to the increase in the conductance due to the excess of added NaOH.

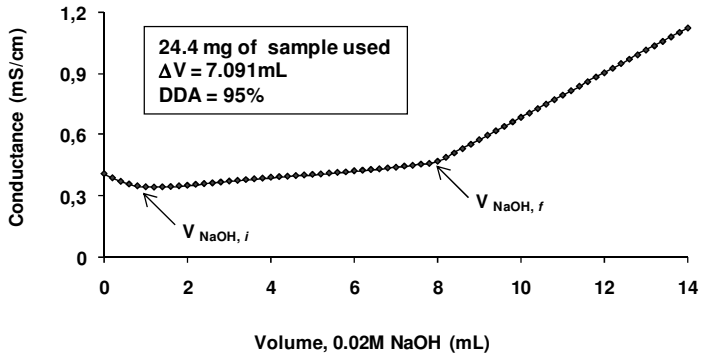

Figure III-2. Typical conductimetrical titration curve for HCH, where it is possible to differentiate the three portions which permit to determine the equivalent amino groups.

As mentioned before, the equivalence was calculated by the difference on the volumes of the two inflectional points of the curve which corresponds to the NaOH volume required to neutralized the free amino groups present in the chitosan, and which permits to calculate its degree of *N*-acetylation (Equations II-3 and II-4, Chapter 6). Table III-3 listed the α values and the DDA of the HCH and CHUP chitosan samples. The DDA results obtained by this method also were in agreement.

Table III-3. DDA values calculated from the conductimetric titrations of HCH and CHUP.

Chitosan Sample	α (eq/g)	DDA (%)
HCH	5.8×10^{-3}	**95**
CHUP	5.1×10^{-3}	**85**

The DDA values determined by these three methods for the two of the chitosans used in this study are compared in Table III-4. These results confirmed that EA and conductometric titration gave DDA values that were in very good agreement with those obtained via ^{1}H NMR. As a result, these simple methods can safely be used for the determination of chitosan DDA, as cited also in literature [56]. For example, the use of solid-state EA method provides a number of advantages such as it not need solvent and sample preparation.

Table III-4. Comparison of the DDA of HCH and CHUP, as determined by ^{1}H NMR, elemental analysis and conductimetric titration.

Sample	DDA values [%]		
	^{1}H NMR	Elemental Analys	Conductimetry
HCH	97	97	95
CHUP	87	87	85

The DDA values used thereafter in this thesis are those obtained by ^{1}H NMR (Table III-9).

11.1.2 Molecular weight

Table III-9 gives the viscosimetric molecular weights of all the chitosan samples. In the case of HCH and CHUP, size exclusion chromatography multi-angle light scattering (SEC-MALS) was also used in order to measure the molecular weight distribution and the polymolecularity index (Ip).

Viscosimetry

The viscosity molecular weight was calculated based on Mark-Houwink-Sakurada Equation II-6, using the published Mark-Houwink constants (K and *a*) presented in ref [57] and listed in Table III-5 taking into account the DDA values of each chitosan sample and chitosan solvent used in this method (0.3 M CH_3CO_2H/ 0.2 M CH_3CO_2Na).

Figure III-3 shows a typical representation of $\eta_{red} = f(C)$ of HCH at 25 ºC. In order to determine the intrinsic viscosity a straight line was fitted to the mean values of η_{red} by the least-squares technique. Intrinsic viscosity was obtained from the intercept of the line at $C = 0$ ($[\eta] = 1349$ mL/g) that was used in Equation II-6 to calculate the molecular weight of HCH.

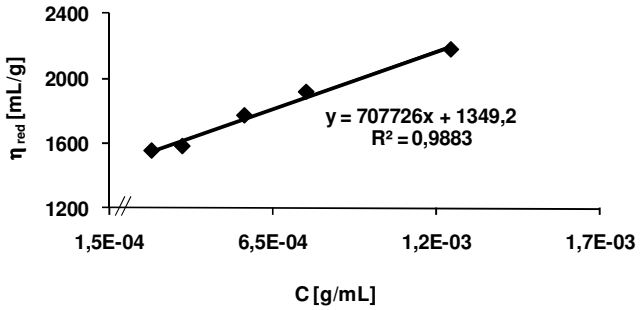

Figure III-3. Representation of $\eta_{red} = f(C)$ of the HCH chitosan sample at 25ºC.

In Table III-5 the relevant data related to the determination of the molecular weight of HCH and CHUP by the present method and the corresponding average values of molecular weight are listed. The weight-average M_v of HCH and CHUP were determined to be 3.5×10^5 and 1.7×10^5, respectively.

Table III-5. Molecular weight and other viscosimetric features determined by viscosimetry of the HCH and CHUP at 25 ºC.

Chitosan Samples	DDA [%]	K	a	[η] [mL/g]	M_v [g/mol]
HCH	> 90	0.082	0.76	1 349	353 000
CHUP	< 90	0.076	0.76	689	170 000

Size exclusion chromatography (SEC)

Figure III-4 shows the SEC-MALS profiles that allowed calculating the weight-average molar mass (M_w), the number-average molar mass (M_n) and the polydispersity index, Ip, of HCH and CHUP samples displayed in Table III-6.

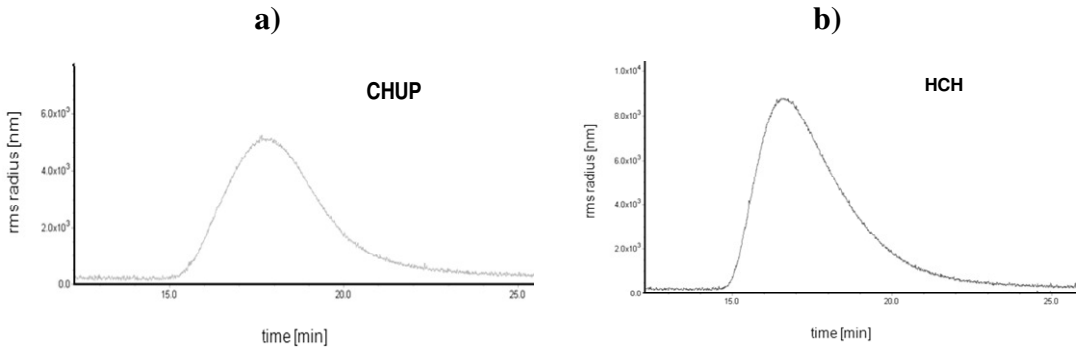

Figure III-4. Molar mass distribution profiles of CHUP a) and HCH b) obtained by SEC-MALS.

The weight-average M_w of HCH and CHUP calculated by this method were 3.2×10^5 and 1.7×10^5, respectively, which were found to be in a very good agreement with those obtained by viscosimetry. These samples presented acceptable polydispersive index.

Table III-6. Molecular weight determined by SEC-MALS for HCH and CHUP chitosan samples.

Chitosan Samples	M_w [g/mol]	M_n [g/mol]	Ip
HCH	316 400	91 977	3.44
CHUP	160 000	68 740	2.45

It was noteworthy that these realy different methods gave similar M_w values. Thus, viscosimetry could be used as a credible, simple and rapid technique to calculate the molecular weight of these polymers compared with the sophisticate techniques like SEC-MALS.

11.1.3 Surface energy

The knowledge of the surface properties, in particular the surface energy of materials is a key aspect in several contexts, such as, in this case, of the use of chitosan as a component in combinations with other polymers, in coatings and as a precursor to novel materials, through its surface or bulk chemical modifiction. Moreover, a bibliographic search related to chitosan surface energy [294-299] revealed some puzzling data, in the

sense that in all the publications in which both the polar and the dispersive components were determined, the former contribution was systematically very low, varying from 1 to 8 mJ/m^2. The values of the latter contribution, mostly around 30 mJ/m^2, were more in tune with a polysaccharide structure and in reasonable agreement among themselves [295-298], with only one [294] much lower figure of 17 mJ/m^2. In another study [299], only the total surface energy was reported with, again, an exceedingly low value of 18 mJ/m^2. All these data were based on contact angle measurements. The use of IGC, which ensures a clear-cut approach to the dispersive component of the surface energy of solids, yielded values of about 50 mJ/m^2 for chitosans with different degrees of deacetylation [300], which are higher than the corresponding values determined by contact angle measurements, a frequently observed difference between the two techniques [301].

Chitosan, cellulose and starch are all polysaccharides, the only difference residing in the replacement of an OH group in each saccharide unit of cellulose by an NH_2 counterpart in chitosan and by the presence of branched structures in starch. Cellulose and starch have similar polymer structures, dominated by OH functions and both the dispersive and the polar components to their surface energy are high, *viz.* 30-40 and 20-30 mJ/m^2, respectively [300,302-303], for different purified materials. These values reflect convincingly the facts that, on the one hand, they refer to macromolecules, hence their high dispersive component and, on the other hand, they are associated with a predominance of OH groups at their surface, hence a high polar contribution.

It is therefore surprising to encounter repeatedly unreasonably modest values for the chitosan surface energy, particularly in relation to the polar component, published by several authors in the last fifteen years, considering moreover their lack of reproducibility from one study to the next. No cross-reference was provided in any of these publications, nor any discussion related to these seemingly abnormal results.

The very low values of the polar contribution to the chitosan surface energy strongly suggested that non-polar impurities were responsible for this anomalous feature. Therefore, a systematic study was undertaken of the surface energy of chitin, chitosan and their respective monomeric counterparts (D-(+)-glucosamine hydrochloride (GlcN) and *N*-acetyl-D-glucosamine (GlcNAc)) using contact angle measurements on films and pellets. A series of purification procedures to assess their effect on the free energy of the ensuing surfaces was carried out, and the residues analysed by GC-MS after derivatization.

Table III-7 shows that the values of the polar component of the surface free energy of the commercial chitosan (HCH, CH95, CH79 and CH67) and chitin samples used in this work were particularly low, thus confirming the general trend related to chitosan previously reported [294-299].

These results are in complete divergence with the corresponding values obtained for the model compounds, namely GlcN and GlcNAc (Table III-7) for which both polar and dispersive components of the surface energy are high and in excellent tune with those of starch and cellulose, *viz.* $\gamma_s^p \approx \gamma_s^d \approx 30$ mJ/m^2. Although GlcN hydrochloride is a water soluble substance, the deposition of water droplet on the surface of its pellets gave enough time to register the corresponding contact angles before any substrate dissolution by diffusion. It seemed therefore most unlikely that, when joined in a macromolecular chain, these structures should behave in such a way, as to lose most of their polarity when exposed to the atmosphere.

Table III-7. Total surface energy, together with its polar and dispersive components, relative to all the pellets prepared from the samples' powders.

	γ_s^p (mJ/m^2)	γ_s^d (mJ/m^2)	γ_s (mJ/m^2)
GlcNAc	29	33	62
GlcN	29	33	62
Chitin	11	41	52
HCH	0.1	41	41
CH95	0.4	38	38
CH79	3	40	43
CH67	~0.0	31	31

This difference in behaviour constituted the first indication corroborating the idea of non-polar impurities present in the commercial polymers, but absent in their monomeric counterparts. The origin of these impurities is clearly associated with the natural crustacean morphologies from which chitin is extracted and then converted into chitosan, that are rich in lipids, dyes, calcium carbonate and proteins [287]. Therefore, different purification procedures to the commercial chitosan and chitin samples were applied in order to detect any increase in surface energy and to identify the ensuing impurities.

First of all, sequential Soxhlet extractions of the chitosan and chitin samples were carried out with *n*-hexane, dichloromethane and acetone. After each Soxhlet extraction, the contributions to the surface energy were assessed on pellets of the residual material, which showed that both the dispersive and the polar components had increased, more so the latter. Figure III-5 and III-6 show the values obtained after the three extractions, which emphasize the drastic increase in γ_s^p with all the samples, albeit in different quantitative proportions. With the "purest" commercial sample according to the manufacturer, HCH, the respective contributions had already reached values close to those of GlcN and other polysaccharides. Moreover, the values obtained for the extracted chitin (Figure III-6), namely γ_s^p=23.2 and γ_s^d=39.1 mJ/m^2 were very similar to those published by Nair et al. [304], *viz.* γ_s^p=20 and γ_s^d=32.6mJ/m^2, using the same approach, and an almost identical value for the dispersive component was reported by Belgacem et al. [303] (γ_s^d=38.3mJ/m^2), using inverse gas chromatography.

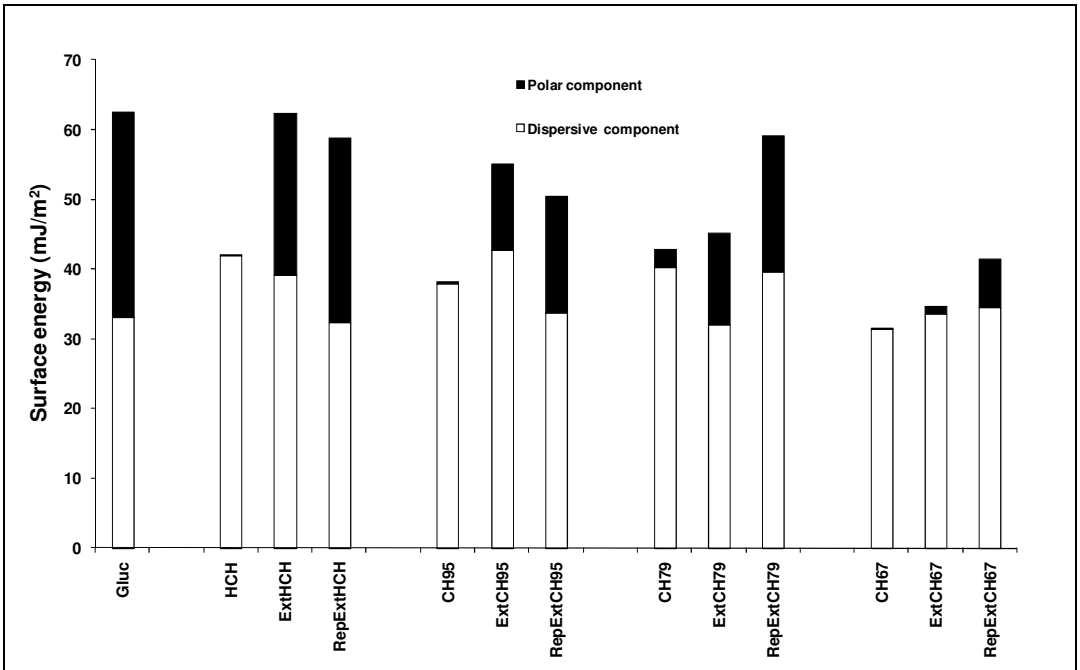

Figure III-5. Variation of the surface energy of the chitosan pellets before and after purification treatments. (Ext – extracted; RepExt – reprecipitated and extracted).

The four chitosan samples were also purified by reprecipitation followed by the same sequential Soxhlet extractions. Once again, Figure III-5 shows that after this double treatment, the polar component was enhanced to higher levels than with the extraction

sequence alone, suggesting that a higher proportion of impurities had been removed. Furthermore, Figure III-5 indicates that, whereas the initial quality of the samples played an important role in the extent of purification level achievable (with HCH attaining surface energies entirely comparable with those of its monomeric structure and of other polysaccharides), the DDA did not appear to be a crucial factor affecting the surface energy, since the CH95 and the CH79 gave similar values for the polar component after the purification steps.

This important aspect is corroborated even more strongly by the fact that the two monomer models gave identical values of γ_s^p and γ_s^d, despite the fact that their structure differs by the presence of relatively less polar acetylamide moiety.

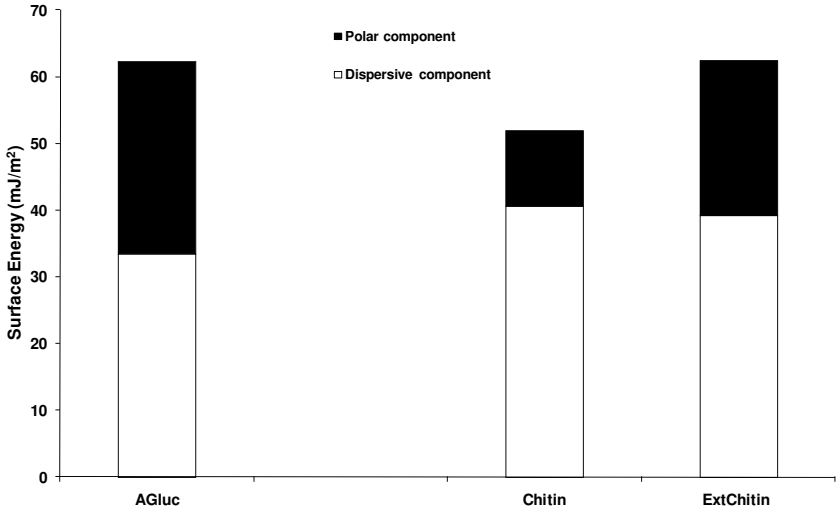

Figure III-6. Variation of the surface energy of the chitin pellets before and after Soxhlet extraction. (Ext – extracted).

In other words, the polar contribution to the surface energy of these substrates, both in a monomeric (NH_3^+, Cl^-, or amide), and a polymeric form (acetate for chitosan films, and also for chitosan precipitated without neutralization, or NH_2 for precipitated and neutralized chitosan), is not significantly affected by the specific nature of this nitrogen-bearing moiety in the presence of the very strong accompanying contribution of the two OH groups. Obviously, these conclusions have nothing to do with the actual *chemical reactivity* of the different *N*-containing groups and only relate to their role in determining the *surface energy* of the corresponding substrates. Figure III-7 shows that the film casting

of both pristine and purified chitosan samples did not provide the same increase in γ_s^p as with pelleted powders. This can be rationalized by considering that, during the slow process of film formation, even minute amounts of residual non-polar impurities were adsorbed efficiently at the liquid surface, just like surfactants, and thereafter remained imprisoned as solid monolayers, a phenomenon which is obviously much less pronounced when chitosan powders are solvent-extracted and/or reprecipitated. The validity of this interpretation was unambiguously proved by scraping the surface of the films of the purified chitosans, an operation which resulted in a drastic decrease in the water contact angle, typically going from 95-110 to 40-60º, the latter values being the same as those measured for GlcN and the purified HCH. This simple experiment provided strong evidence that the non-polar impurities had indeed migrated (almost) entirely to the film surfaces. Interestingly, scraping the surface of the pellets produced a much more modest effect and indeed none at all for GlcN and purified HCH.

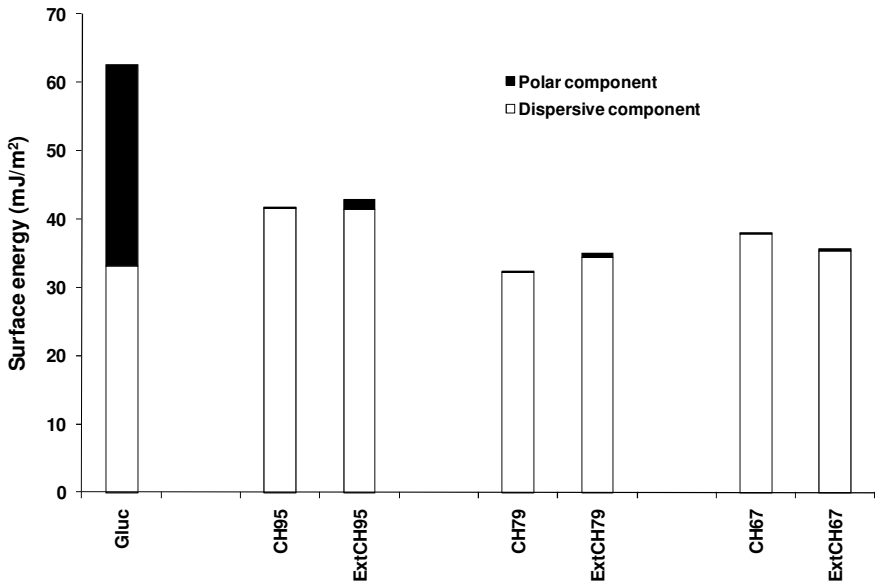

Figure III-7. Variation of the surface energy of some chitosan films before and after Soxhlet extraction. (Ext – extracted).

The possible role of the surface roughness on the contact angle values was assessed by preparing pellets of different surface morphology, by varying the particle size of the sample and the pressure applied in the fabrication of the pellets. No significant trend was encountered, outside the standard contact angle deviation, which suggested that in the

present context the roughness parameter did not influence appreciably the contact angle measurements. As for the scraping experiments, the same doubt arose concerning the inevitable change in surface roughness associated with this operation. In order to check for a possible effect of scraping as such, *i.e.* in the absence of surface impurities, we applied it to a pure cellophane film. Several tests revealed that the contact angle values, compared with those taken on the unscrapted surface, tended to vary randomly with ± 10º, thus ruling out a univocal role of scraping, which could have cast a doubt on our above interpretation related to the removal of low-energy impurities from the surface of chitosan films.

After each Soxhlet extraction, the extracted impurities from both chitosan and chitin, were silylated and analyzed by GC-MS. The most abundant compounds, identified by this technique and reported in Table III-8, had predominantly non-polar structures like higher alkanes, fatty acids and alcohols.

Table III-8. Identification of the main compounds extracted from the chitin and chitosan samples.

Family	Compound	%*
Alkanes	Heptacosane	5.6
	Nonacosane	8.1
	Triacontane	5.8
Alcohols	Glycerol	2.5
	Tetradecanol	0.6
	Hexadecanol	14.0
	(Z-9)-octadecenol	20.0
	Octadecanol	11.5
	Octacosanol	1.0
Fatty acids	tetradecanoic acid	9.7
	hexadecanoic acid	10.6
	oleic acid	4.0
	octadecanoic acid	4.4
	docosanoic acid	0.9
Sterols	Cholesterol	1.5

* Percentage of each impurity related to the total identified amount

These results are entirely in tune with the fact that the chitin and chitosan samples employed in this investigation were extracted from the exoskeleton of crustaceans. This external anatomical feature is constituted by several layers, namely, epicuticle, exocuticle

and endocuticle. The latter two contain the chitin macromolecules and are linked to the former, which contains waxes and paraffines, fatty acids, esters and alcohols [287].

The presence of these impurities in commercial chitin and chitosan constitutes, as clearly shown above, an enormous source of error in the determination of the surface free energy of these biopolymers.

To sum up, the origin of the widely different and anomalous results reported for the surface energy of chitosan showed to be associated with non-polar impurities in even the best-quality commercial samples, giving rise to enormous errors in the determination of the polar component of their surface energy. After their thorough removal, the value of the total surface energy (γ_s), and particularly of its polar component, increased considerably and reached the classical polysaccharide figures of γ_s^d ~30 and γ_s^p ~30 mJ/m^2. The characterization of the impurities by GC-MS analysis indicated the presence of significant amounts of higher alkanes, fatty acids and alcohols and sterols.

11.1.4 Other characteristics

Structural characterization

A typical FTIR-ATR spectrum of chitosan is shown in Figure III-8, characterized by one intense and broad band centred at 3450 cm^{-1}, which is attributed to the axial stretching of the O-H and N-H bonds; one band corresponding to the axial stretching of C-H bonds, near 2860 cm^{-1}; bands centred at 1650 and 1590 cm^{-1}, assigned to the amide I and amide II vibrations, respectively; bands at 1420 and 1380 cm^{-1} resulting from the coupling of C-N axial stretching and N-H angular deformation; and the bands in the range 1150-897 cm^{-1} due to the polysaccharide backbone, including the glycosidic bonds, C-O and C-O-C stretching [38].

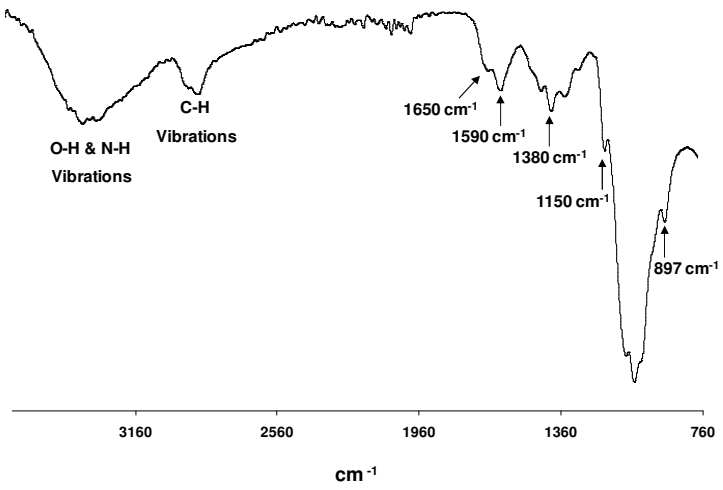

Figure III-8. Typical FTIR-ATR spectrum of a chitosan sample (CHUP).

The peaks in the CP-MAS ^{13}C NMR spectra of a selected chitosan (HCH) displayed in Figure III-9 were assigned according to the literature data [53-54]: $\delta \approx 25$ ppm attributed to the carbon atom of the methyl moieties of the acetamido groups; $\delta \approx 58$ ppm attributed to the C6 and C2 carbons: $\delta \approx 75$ ppm due the C5 and C3 carbons; $\delta \approx 81$ ppm corresponding to the C4 carbon; $\delta \approx 102$ ppm corresponding to the C1 carbon; and finally $\delta \approx 180$ ppm due the C=O of the acetamido groups (taking into account the chitosan structure in Figure III-1 for the C numbering).

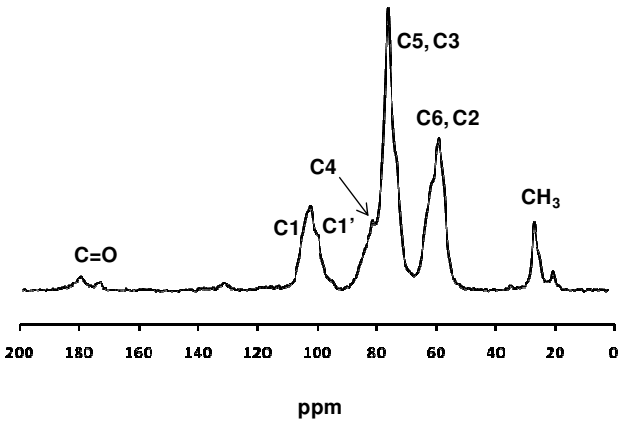

Figure III-9. Typical ^{13}C NMR spectrum of a chitosan sample (HCH).

Crystallinity

A characteristic X-ray diffraction pattern of chitosan powder is shown in Figure III-10, with peaks at around 2θ of 12 and 19º [72], assigned to the crystal form I and II, respectively. A peak at around 2θ of 30º was observed in certain chitosan samples, which was attributed to $CaCO_3$ impurities [22].

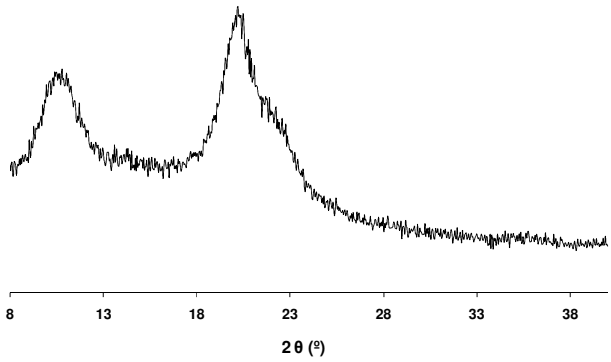

Figure III-10. X-ray diffraction of the a powdered chitosan sample (HCH).

Thermal stability

Figure III-11 shows a typical TGA profile of chitosan. The mass loss at around 100 ºC was associated with the volatilization of water and the maximum degradation step at around 300 ºC assigned to the actual degradation of chitosan [305]. All the others samples displayed similar features, albeit with variable moisture contents.

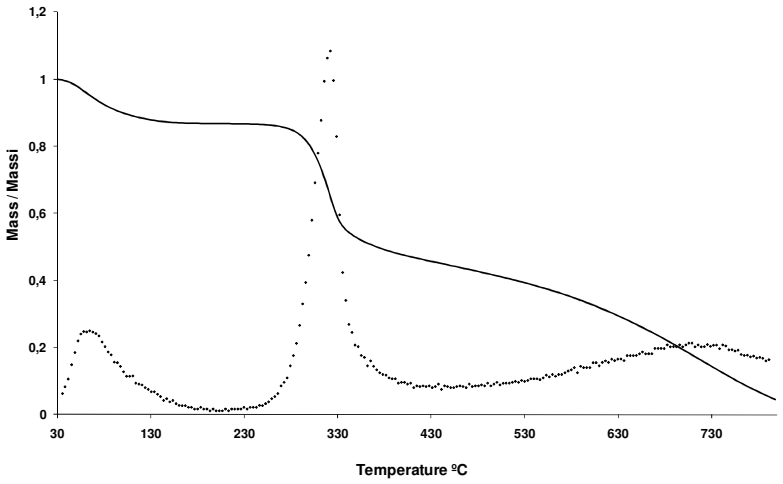

Figure III-11. Thermogram corresponding of powdered chitosan sample HCH containing ~ 11% of moisture.

Table III-9 summarises the main properties of the chitin and chitosan samples used in the present work such as degree of deacetylation, obtained by ^{1}H NMR, molecular weight, obtained by viscosimetry, degree of polymerisation, moisture content, surface energy and colour. This detailed characterazation showed that these samples presented different properties in termrs of DDA and M_w, etc.

Table III-9. Main properties of chitin and chitosan samples.

Sample	DDA [%]	Molecular Weight [g/mol]	DP	Moisture Content [%]	Surface Energy [mJ/m^2]	Colour
Chitin	30	600 000	3 000	8	60	off-white
HCH	97	350 000	2 200	11	60	white
CH95	95	543 000	3 300	6	51	white
LCH	90	90 000	600	10	48	brownish
CH79	79	58 000	400	11	59	yellowish
CH67	67	58 000	400	9	41	off-white
CHUP	88	170 000	1 000	10	-	white

Among these chitosan samples, HCH and LCH were selected for the further studies.

11.2 Chitosan derivatives

11.2.1 Fluorescent chitosan

Fluorescent polymers have potential applications as probes to better understand and optimize some mechanism involving different materials. Fluorescent chitosan derivatives have been applied to some biologically related systems [102-106].

Therefore, in the context of the present thesis, a fluorescent chitosan derivative with a low degree of substitution (DS) was prepared to assess its spatial and in-depth distribution onto cellulosic substrates.

The chitosan sample subjected to this derivatization was LCH. Figure III-12 illustrates the synthesis of FITC-LCH derivative and the aspect of the powdered chitosan without and with UV-vis excitation.

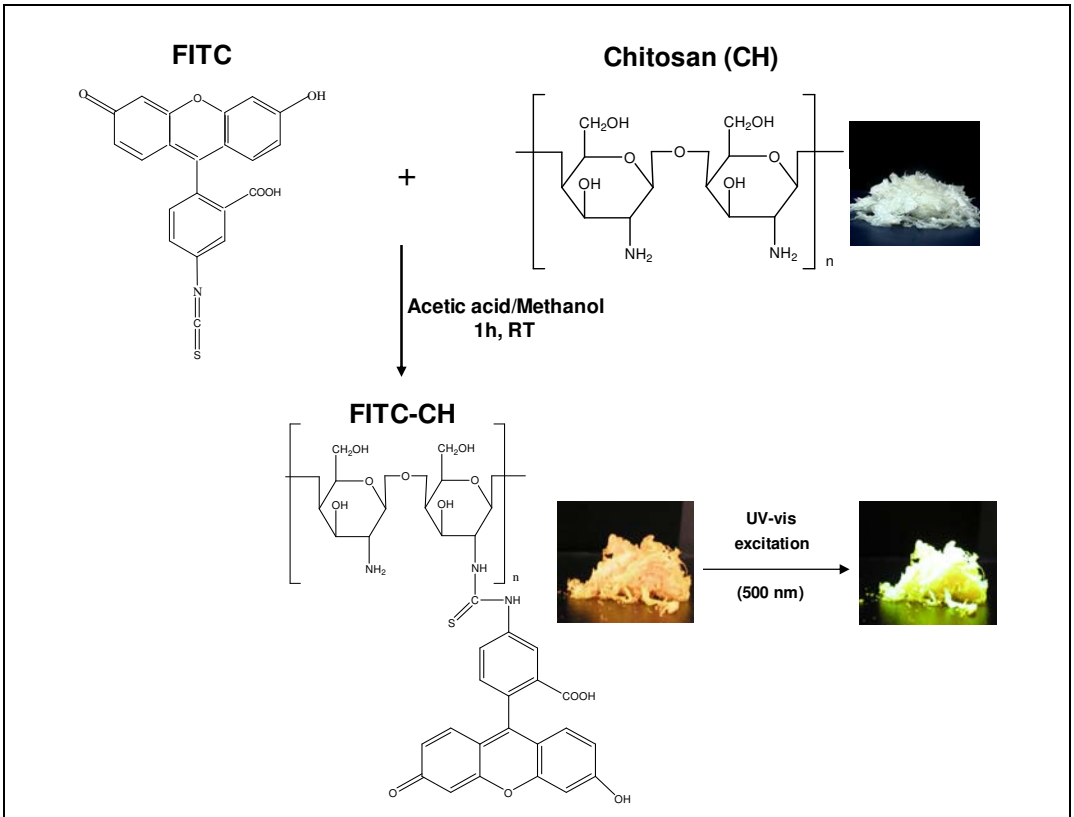

Figure III-12. Schematic illustration of the synthesis of FITC-LCH derivative, and aspect of the final product without and with UV-vis excitation.

Due to their very low DS-values (Table III-10), the conformation of these fluorescent chitosan derivatives is not altered, *i.e.*, the structural polymer properties are not essentially affected, except of course their optical properties.

Chitosan and fluorescent chitosan derivatives were first analysed in terms of structural properties and crystallinity. Only some slight alterations were found in the FTIR-ATR spectrum of FITC-LCH (Figure III-13) compared with that of the unmodified LCH. A new band at 1750 cm^{-1}, characteristic of the carboxyl C=O stretching vibration, was found. The band at 1650 cm^{-1}, characteristic of the $–NH_2$ deformation vibration of chitosan, scarcely changed when compared with that in the spectrum of the unmodified chitosan, because the DS was very low and therefore, the majority of $–NH_2$ persisted.

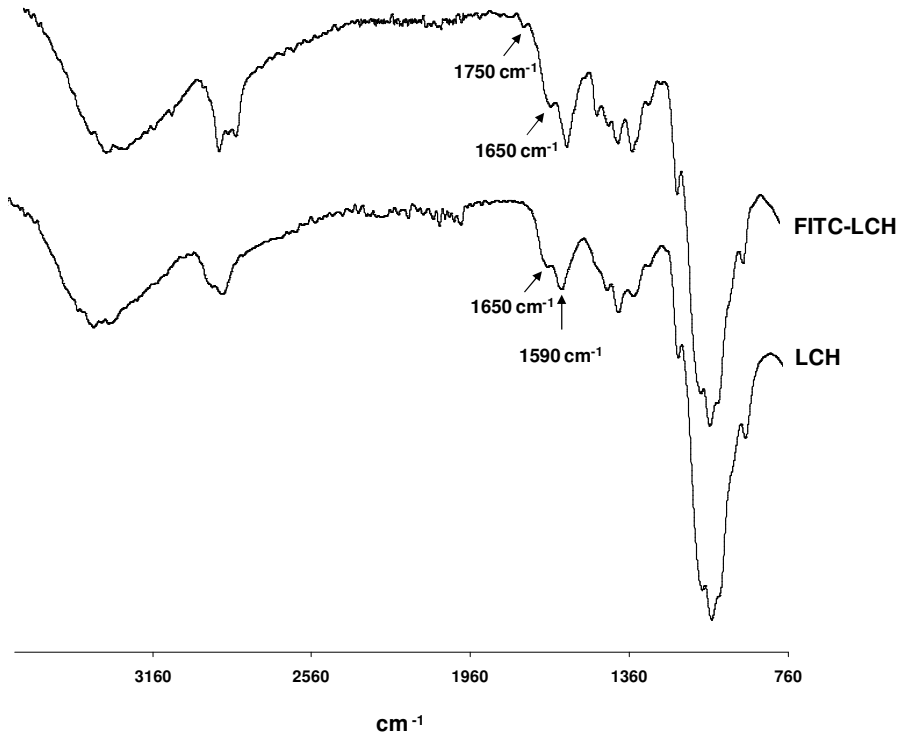

Figure III-13. FTIR-ATR spectra of chitosan (LCH) and fluorescent chitosan derivative (FITC-LCH).

The X-ray diffraction patterns of CH and FITC-CH powders are shown in Figure III-14. Both showed the typical X-ray diffraction patterns of chitosan substrates with peaks at around 2θ of 12 and of 19º [72].

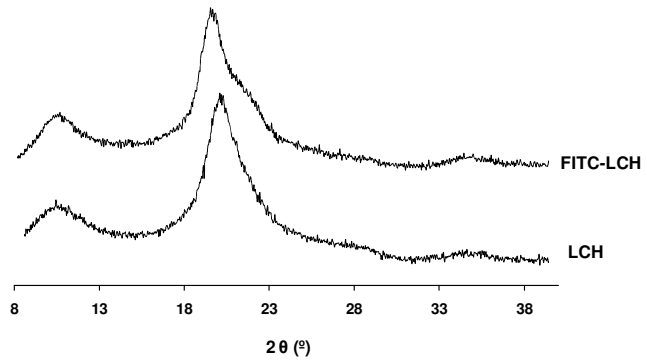

Figure III-14. X-ray diffraction of chitosan (LCH) and fluorescent chitosan derivative (FITC-LCH).

The degree of substitution was determined by elemental analysis and found to be 2.3% (Table III-10).

The molecular weight of the FITC-LCH derivative was only slightly higher than that of the starting chitosan sample (Table III-10). Moreover, the degree of polymerization of the chitosan derivative did not demonstrate significant changes. These results confirmed that the derivatization procedure did not affect the starting properties of the polymer.

Table III-10. Elemental composition, degree of substitution, molecular weight and degree of polymerisation of of LCH and FITC-LCH.

Sample	Elemental Composition [%]				Degree of Substitution	Molecular weight	DP
	C	H	N	S	[%]	[g/mol]	
LCH	39.45	6.61	7.18	-	-	90 000	600
FITC-LCH	41.23	6.25	7.46	0.15	2.3	110 000	650

Figure III-15 shows the spectrum and the molar extinction coefficient of FITC-LCH at the two maximum wavelengths (454 and 479 nm) as obtained by the Beer–Lambert law. These maxima were similar to those exhibits by FITC (445 and 481 nm).

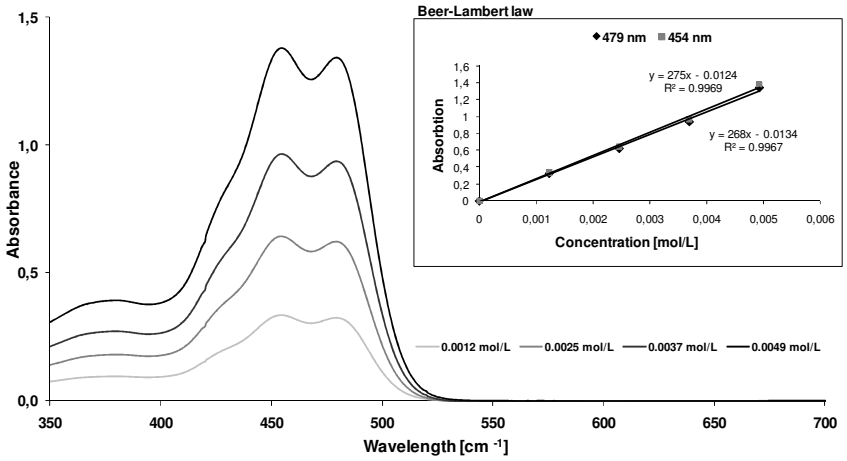

Figure III-15. Absorbance spectra of increasing concentrations of FITC-LCH in aqueous acetic acid and MeOH and illustration of the Beer-Lambert law for the two maxima.

When solid FITC-LCH was submitted to UV excitation the ensuing emission spectra (Figure III-16) were in tune with that of the fluorescein moiety, known to occur around 510-540 nm [106]. Increasing the excitation wavelength from 350 to 500 nm did not modify the position of the emission band, but only its relative intensity, as shown in Figure III-16.

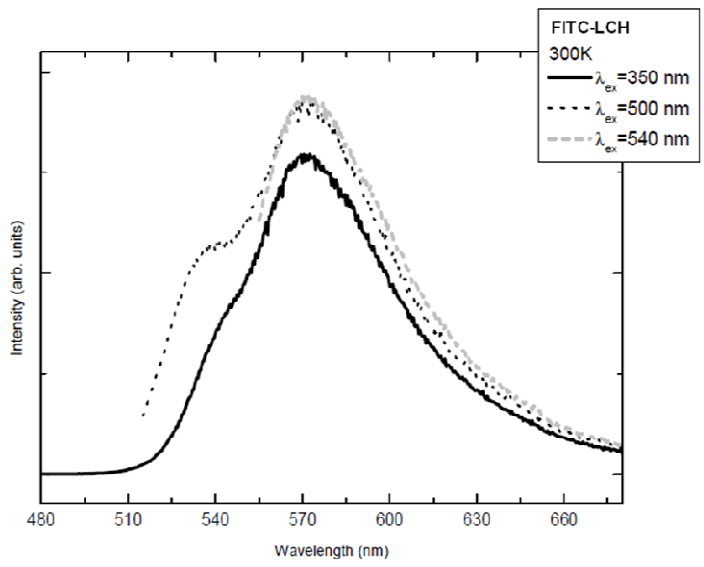

Figure III-16. Fluorescent emission spectra of FITC-CH at different excitation wavelengths.

11.2.2 Water soluble chitosan

Water soluble chitosan quaternary ammonium derivatives are employed in situations where the use of acid solutions constitutes a problem, e.g. in pharmaceutical, biomedical and coating application [306].

The chitosan samples subjected to this derivatization were LCH and HCH. Figure III-17 illustrates the chemical modification of chitosan with glycidyltrimethylammonium chloride (GTMAC).

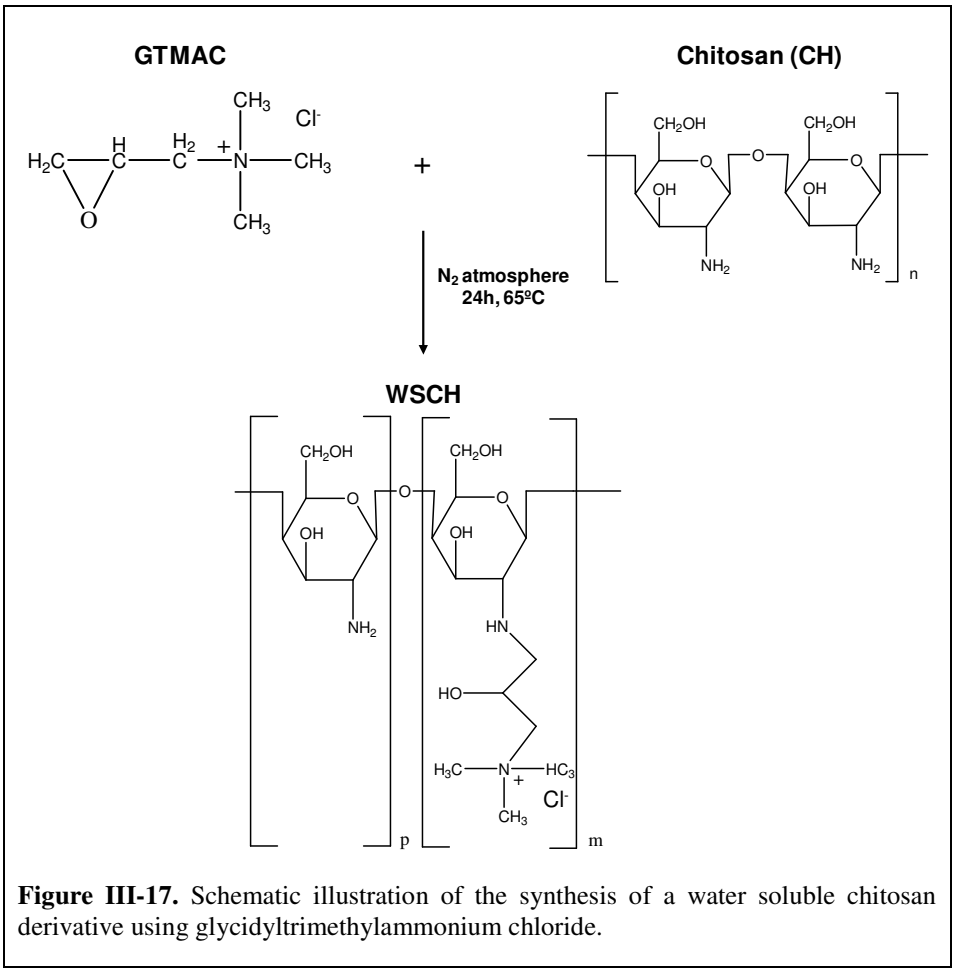

Figure III-17. Schematic illustration of the synthesis of a water soluble chitosan derivative using glycidyltrimethylammonium chloride.

The occurrence of the quaternazation was clearly confirmed by FTIR-ATR, based on appearance of new bands (Figure III-18). An increase of the intensity of the bands at 2820-2980 cm^{-1}, in the FTIR-ATR spectra of both WSLCH (data not shown) and WSHCH, was observed. These bands are attributed to the C-H stretching of CH_2 and CH_3 groups of the alkyl substituent. The other important evidence was the apperence of two intense bands

at 1377 and 1480 cm^{-1}, associated with the C-N stretching mode and the asymmetric angular deformation of the C-H of the trimethylammonium group, respectively. A further main difference was related with the decrease in the intensity of the band at 1590 cm^{-1}, attributed to the angular deformation of the N-H bond of the amino group (due to the change from primary to secondary amine), and the increase of the band at 1650 cm^{-1}. This confirmed the occurrence of the expected *N*-alkylation, rather than the O-alkylation.

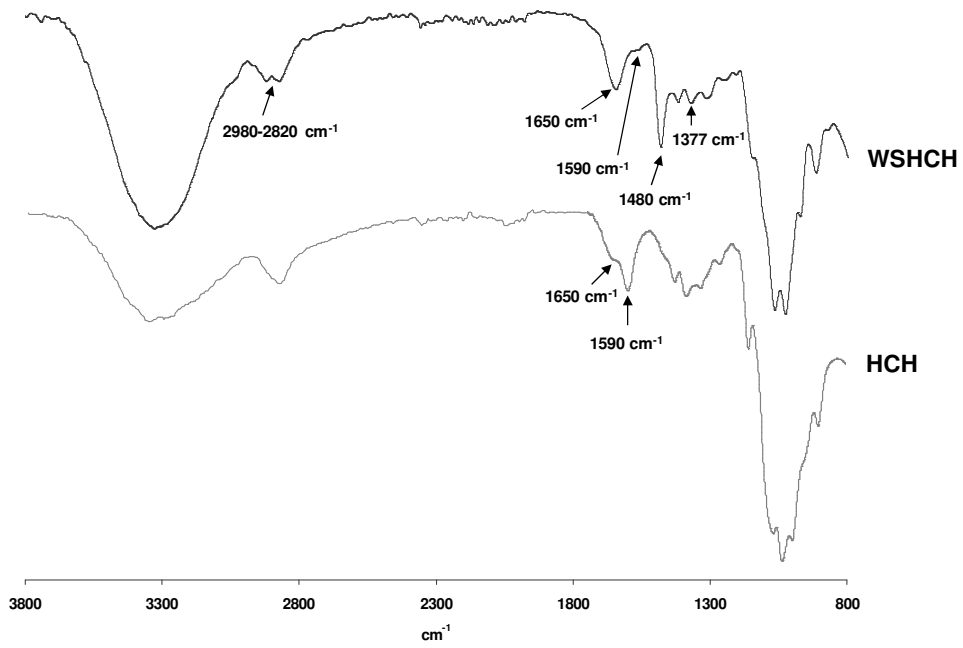

Figure III-18. Typical FTIR-ATR spectra of chitosan (CH) and water soluble chitosan derivative (WSCH, using HCH).

The comparison of the ^{13}C CP-MAS NMR spectra of the chitosan samples before (Figure III-9) and after its reaction with GTMAC (Figure III-19), clearly confirmed the chitosan quaternization, mainly due to the emergence of new peaks at $\delta \approx 55$ ppm attributed to the carbon atoms of the *N*-trimethylated group. Similar results were described in a previous study [307].

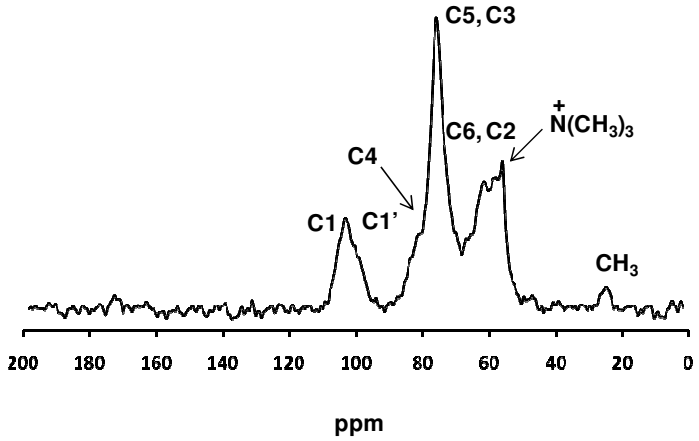

Figure III-19. Typical ^{13}C NMR spectrum of WSHCH.

This chemical modification led to an extensive decline in crystallinity of the chitosan samples, since both WSHCH and WSLCH displayed a diffraction pattern typical of a predominantly amorphous material and had good water-solubility, as previously observed with other water soluble chitosan derivatives with high degrees of substitution [308]. The water soluble derivatives only showed one broad peak at around 2θ of 20º (Figure III-20).

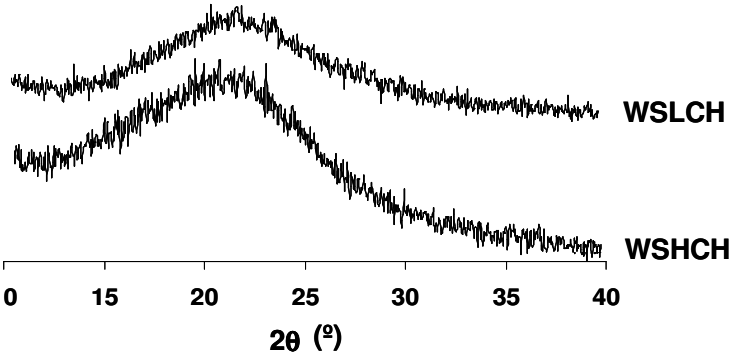

Figure III-20. X-ray diffraction patterns of the two water soluble chitosans.

This lower crystallinity was ascribed to the presence of the grafted moieties, which probably hindered the formation of inter- and intra-molecular hydrogen bonds between the modified chitosan macromolecules.

The degree of substitution was determined by ^{1}H NMR. Table III-11 gives the signal assignments of ^{1}H NMR spectra of both modified chitosans and the corresponding values of the degree of substitution, which were determined based on the following equation:

$$DS = \frac{I_{H1}}{I_{H1} + I_{H1'}} \qquad \text{Equation III} - 1$$

Where I_{H1} is the integration value of the H1 peak attributed to the proton of the unmodified D-glucosamine units, and $I_{H1'}$ that related to the proton of the quaternized monomer units.

Table III-11. Signal assignment of ^{1}H NMR spectra, DS and molecular weight of WSLCH and WSHCH.

Peak		H1	H1'	DS	Mw	DP
δ (ppm)		5.09	4.84	[%]	[g/mol]	
Integration	WSLCH	1.00	0.51	34	180 000	800
	WSHCH	1.00	0.37	27	465 000	2 400

Table III-11 also provides the molecular weights of the WSCH derivatives, which were higher than those of the starting chitosans (Table III-6) because of the alkyl substitution. However, their degree of polymerisation did not change appreciably, as expected.

The water soluble derivatives (WSLCH and WSHCH) were more thermally unstable than their precursors (Figure III-11), since they started to decompose (Td_i) at around 180 ºC with the maximum degradation (Td) step at 260-270 ºC, as given by Table III-12.

Table III-12.Thermogravimetric features of WSLCH and WSHCH.

Samples	Td_i (ºC)	Td (ºC)
WSLCH	199	260
WSHCH	186	270

11.3 Cellulose substrates

11.3.1 Bacterial cellulose

Bacterial cellulose (BC) was obtained in the shredded wet gel form with a moisture content of 95% (Figure III-21a), in contrast with the fibrous aspect of vegetable cellulose. Figure III-21b) clearly shows the tridimensional network of nano and microfibrils with 10-200 nm width of the bacterial cellulose.

Bacterial cellulose showed a typical main double weight-loss feature, with a maximum decomposition temperature in the range of 340-350 ºC (the TGA curve profile is very similar to that of NFC, Figure III-24). The mass losses around 100 ºC were associated with the volatilization of water.

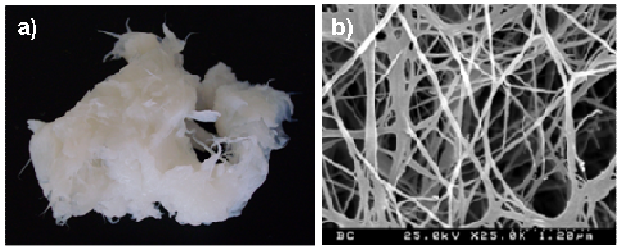

Figure III-21. Fibrillated aspect a) and SEM image (× 25 000) b) of bacterial cellulose.

Figure III-22 shows the typical X-ray diffraction profile of BC, with the main peaks characteristics of Cellulose I (native cellulose) at 2θ of 14.3, 15.9 and 22.6º [151].

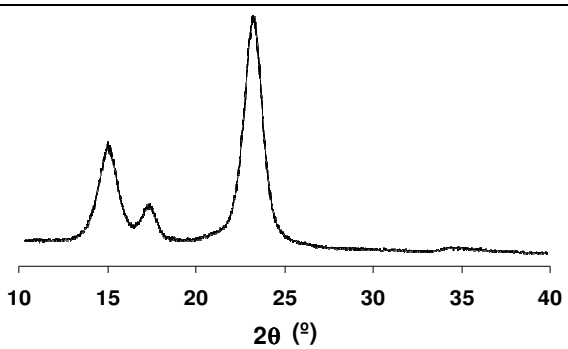

Figure III-22. X-ray diffractogram of BC.

11.3.2 Nanofibrillated cellulose

The NFC used here had the form of a highly swollen gel with 98% humidity (Figure III-23a), with highly microfibrillated nanofibres bearing a large aspect ratio, *viz.* 15–30 nm wide and several micrometers long. There was also a fraction of shorter nanofibres with thickness of 5–10 nm (Figure III-23b). This high aspect ratio is particular interesting because providing better reinforcing effects, as will be discussed later.

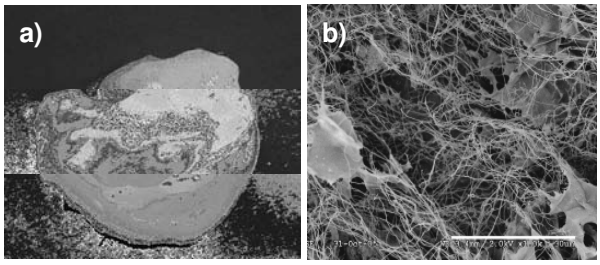

Figure III-23. NFC aspect a) and SEM image b). The scale of the bar in image b) is 30 μm.

The dried NFC displayed a typical double-weight loss profile with the most pronounced degradation step at around 340 ºC (Figure III-24) [130]. Again, the mass loss observed around 100 ºC was associated with the volatilization of the residual moisture.

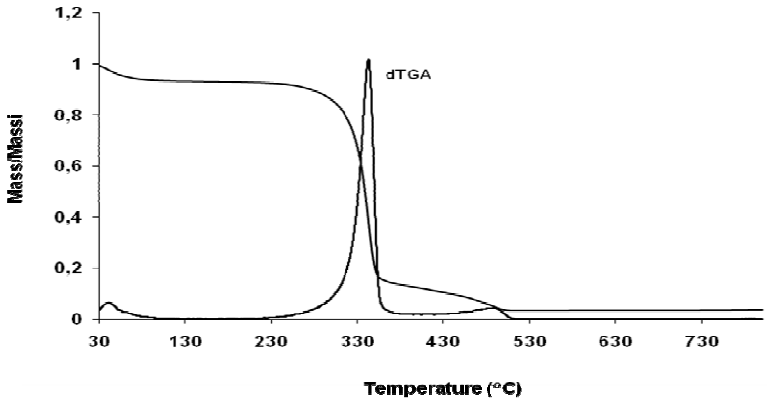

Figure III-24. TGA and dTGA of NFC.

Figure III-25 shows the X-ray diffraction profile of NFC that also presented the typical peaks of Cellulose I (native cellulose). However the intensity of the peak changed and BC showed to be more crystalline than NFC.

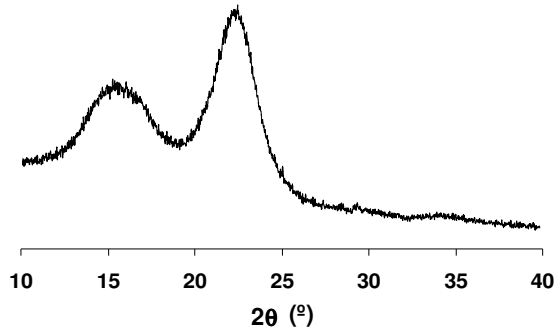

Figure III-25. X-ray diffractograms of NFC.

11.3.3 Paper sheets

The A3-size papers sheets of 100% *Eucalyptus globulus* bleached kraft pulp used in the coating experiments had a average grammage of 75 g/m^2 and an average thickness of 100 µm. Figure III-26 shows the SEM image of this paper where is possible to observe its main constituents namely the fibres and the fillers (precipitated calcium carbonate).

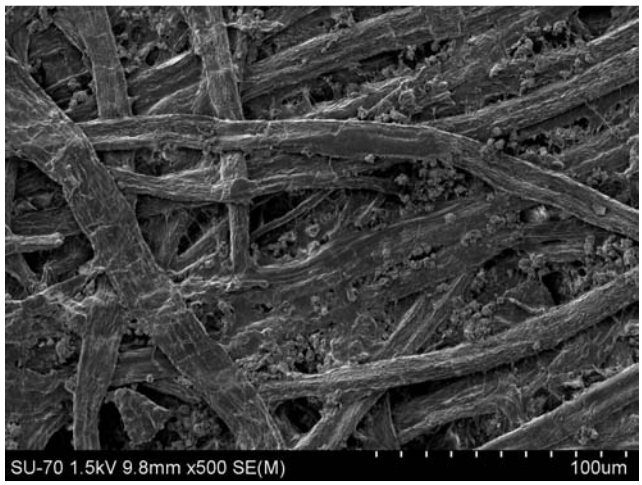

Figure III-26. SEM images (× 500) of control sheet (CS).

These characterized materials, chitin, chitosan, cellulose nanofibres and paper, were then used to prepare novel materials in both nanocomposite films and coating formulations for paper. Finally, chitin and chitosan were also used to produce viscous polyols by oxypropylation. Table III-12 lists the different applications of each raw-material and chitosan derivatives.

Table III-12. Summary of the applications of each raw-material and chitosan derivatives.

Materials	Chapter 12 Nanocomposite Films	Chapter 13 CH-coated Papers	Chapter 14 Oxypropylation
LCH	✓	✓	×
HCH	✓	✓	×
WSLCH	✓	✓	×
WSHCH	✓	✓	×
FITC-LCH	×	✓	×
CH95	×	×	✓
NFC	✓	✓	×
BC	✓	✓	×
CS	×	✓	×

12 Chitosan-cellulose nanocomposite films

This chapter discusses materials prepared by combining the two polysaccharides which form the basis of this thesis.

The identification of all chitosan-cellulose nanocomposite films prepared is given in Table III-13.

Table III-13 Identification of the chitosan and chitosan-cellulose nanocomposite films.

Film Identification	Chitosan Sample	% of Cellulose
Unfilled chitosan films		
HCH	High molecular weight	-
LCH	Low molecular weight	-
WSHCH	High molecular weight (water soluble derivative)	-
WSLCH	Low molecular weight (water soluble derivative)	-
Nanocomposite Films with NFC		
HCHNFC5	High molecular weight	5
HCHNFC10	High molecular weight	10
HCHNFC20	High molecular weight	20
LCHNFC5	Low molecular weight	5
LCHNFC10	Low molecular weight	10
LCHNFC20	Low molecular weight	20
LCHNFC30	Low molecular weight	30
LCHNFC40	Low molecular weight	40
LCHNFC50	Low molecular weight	50
LCHNFC60	Low molecular weight	60
WSHCHNFC5	High molecular weight (water soluble derivative)	5
WSHCHNFC10	High molecular weight (water soluble derivative)	10
WSHCHNFC20	High molecular weight (water soluble derivative)	20
WSLCHNFC10	Low molecular weight (water soluble derivative)	10
WSLCHNFC60	Low molecular weight (water soluble derivative)	60
Nanocomposite Films with BC		
HCHBC5	High molecular weight	5
HCHBC10	High molecular weight	10
LCHBC5	Low molecular weight	5
LCHBC10	Low molecular weight	10
LCHBC20	Low molecular weight	20
LCHBC30	Low molecular weight	30
LCHBC40	Low molecular weight	40
WSHCHBC5	High molecular weight (water soluble derivative)	5
WSHCHBC10	High molecular weight (water soluble derivative)	10

12.1 Morphology

Scanning electron microscopy (SEM) was used to observe the surface of the polymeric films and chitosan-cellulose nanocomposite films. The selected SEM micrographs showed that all unfilled CH and WSCH films had similar surface morphologies, displaying a dense, homogeneous and smooth structure, without bubbles, tracks or aggregated domains (Figure III-27 and III-28). A selection of SEM micrographs of the surface of LCHNFC and LCHBC nanocomposite films filled with 5%, 10% and 40% of BC and NFC is shown in Figure III-27. The random orientation and the good dispersion of the cellulose nanofibrills of the surface of the chitosan matrices is quite clear even for high reinforcement contents (LCHBC40 and LCHNFC40). The SEM micrographs also provided evidence for the characteristic tridimensional fibrillar network of BC of the surface of the nanocomposite films.

A structure of fibrils and fibril bundles evenly distributed and forming a percolated/interconnected network is clearly visible in the materials with a high cellulose contents (Figure III-27). Percolation here refers to the idea that adjacent fibril/fibril bundles were in contact with each other at some point and that this led to a continuous network of fibrils within the matrix.

The surface differences in terms of smoothness, is clearly visible between nanocomposites with a low and a high cellulose content (Figure III-27 and III-28). This fact is probably attributed to a lower solvent evaporation rate associated with the high cellulose fibres content. In fact, the drying process of the chitosan-cellulose blends prepared with low cellulose content was faster than that of those with high cellulose content.

In conclusion, SEM micrographs provided evidence of the good dispersion of the cellulose fibrils (NFC and BC) in the chitosan matrices, without noticeable aggregates, even for high reinforcement contents.

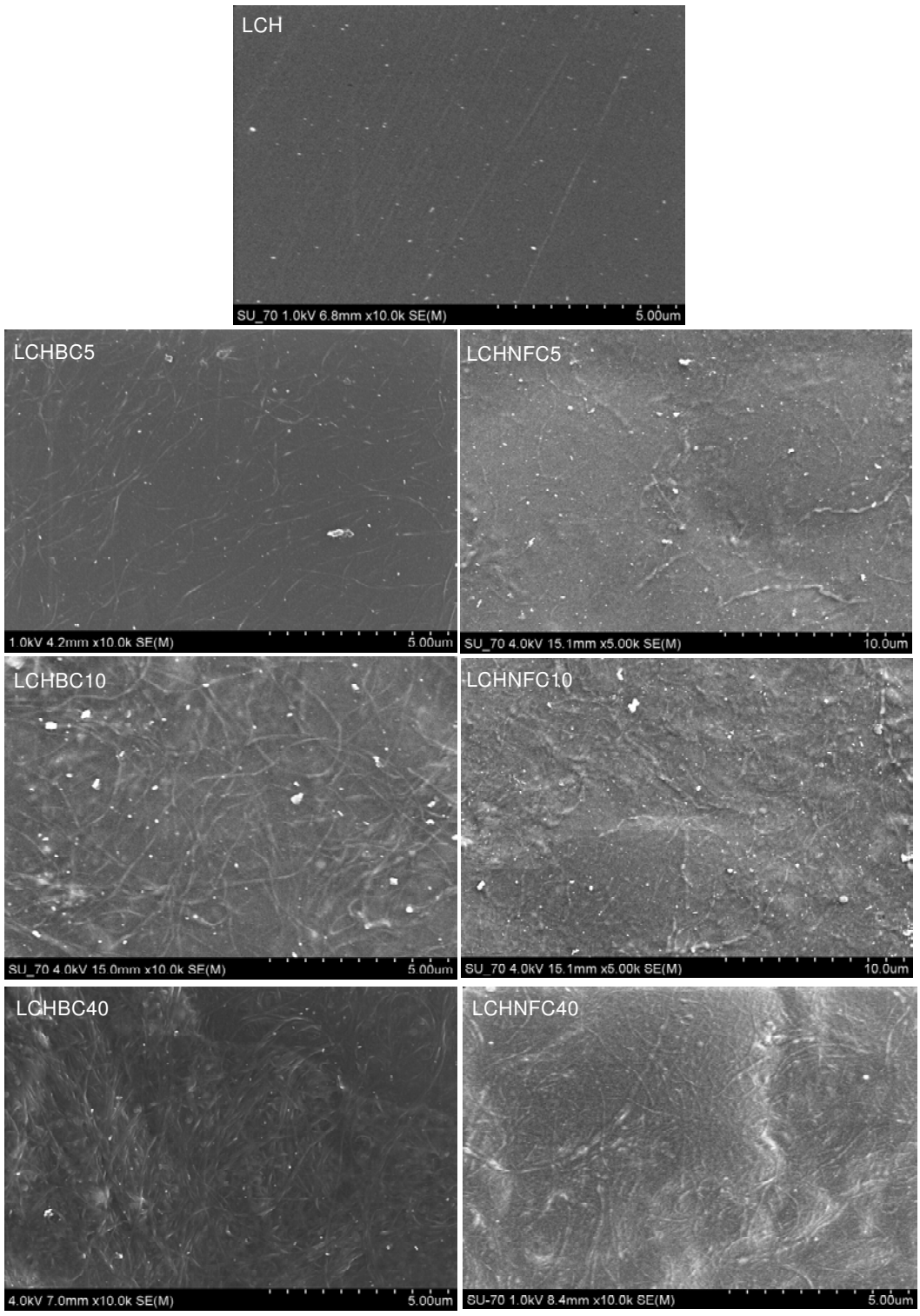

Figure III-27. SEM micrographs of the surface of LCH films and LCHNFC and LCHBC nanocomposite films filled with 5%, 10% and 40% of cellulose.

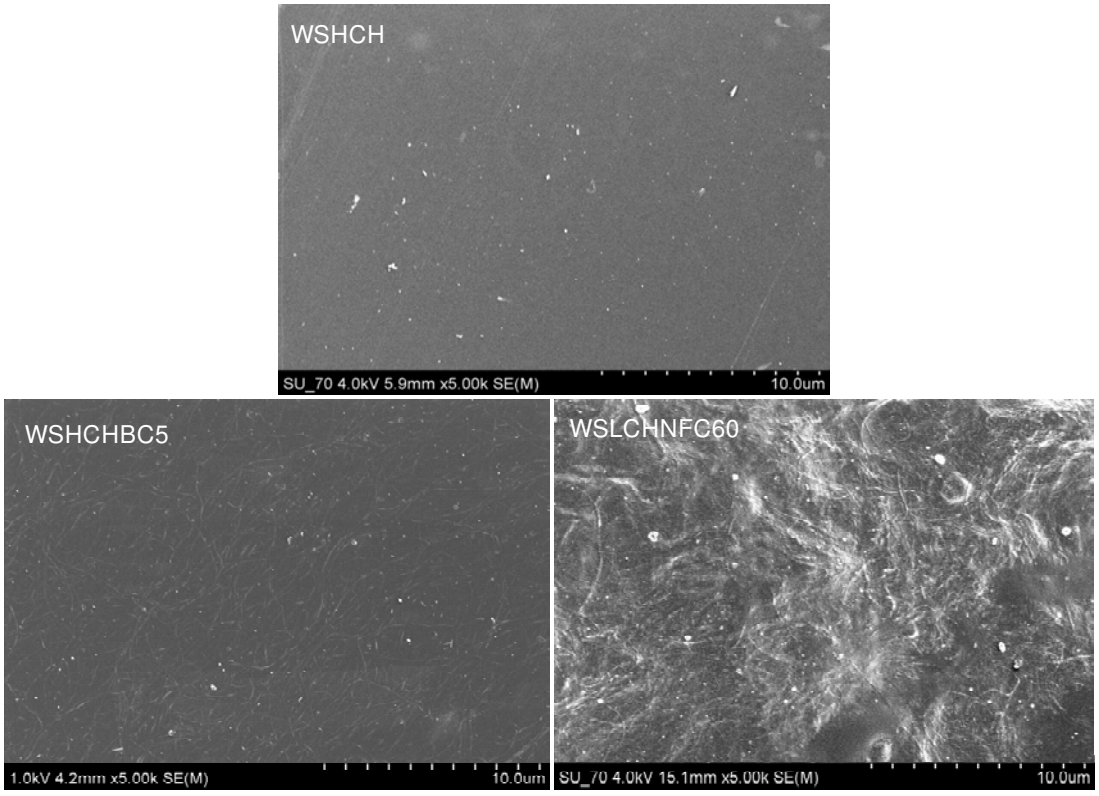

Figure III-28. SEM micrographs of the surface of WSHCH, WSHCHBC5 and WSLCHNFC60 nanocomposite films.

The analysis of the surface morphology of the films was complemented by the acquisition of AFM images. The AFM technique, in topography or phase mode, provides the dimensions of the particles in feature length, width, and average height.

The results showed that pure chitosan films displayed nanometer scale textured surfaces. Contrary to the SEM analysis, the images acquired by AFM showed some differences between the two pure chitosan films (HCH and LCH) and also between the chitosan films and their corresponding water soluble chitosan films, particularly in terms of scale. With respect to the pure chitosan films, these differences might be related to the fact that chitosan samples did not have the same origin, non the same processing, thus displaying dissimilar characteristics and properties (Figure III-29 and III-30).

The images in phase and in topography, using a magnification of 2×2 μm^2, showed that the surface of both LCH and HCH films consisted of tightly packed, grain-like particles (Figure III-29). However, LCH showed well-defined particles with a homogeneous size of 100-300 nm, instead of the non distinct particles of the HCH film

which displayed particles with different scales. Similar chitosan morphology were observed in a previous study [309].

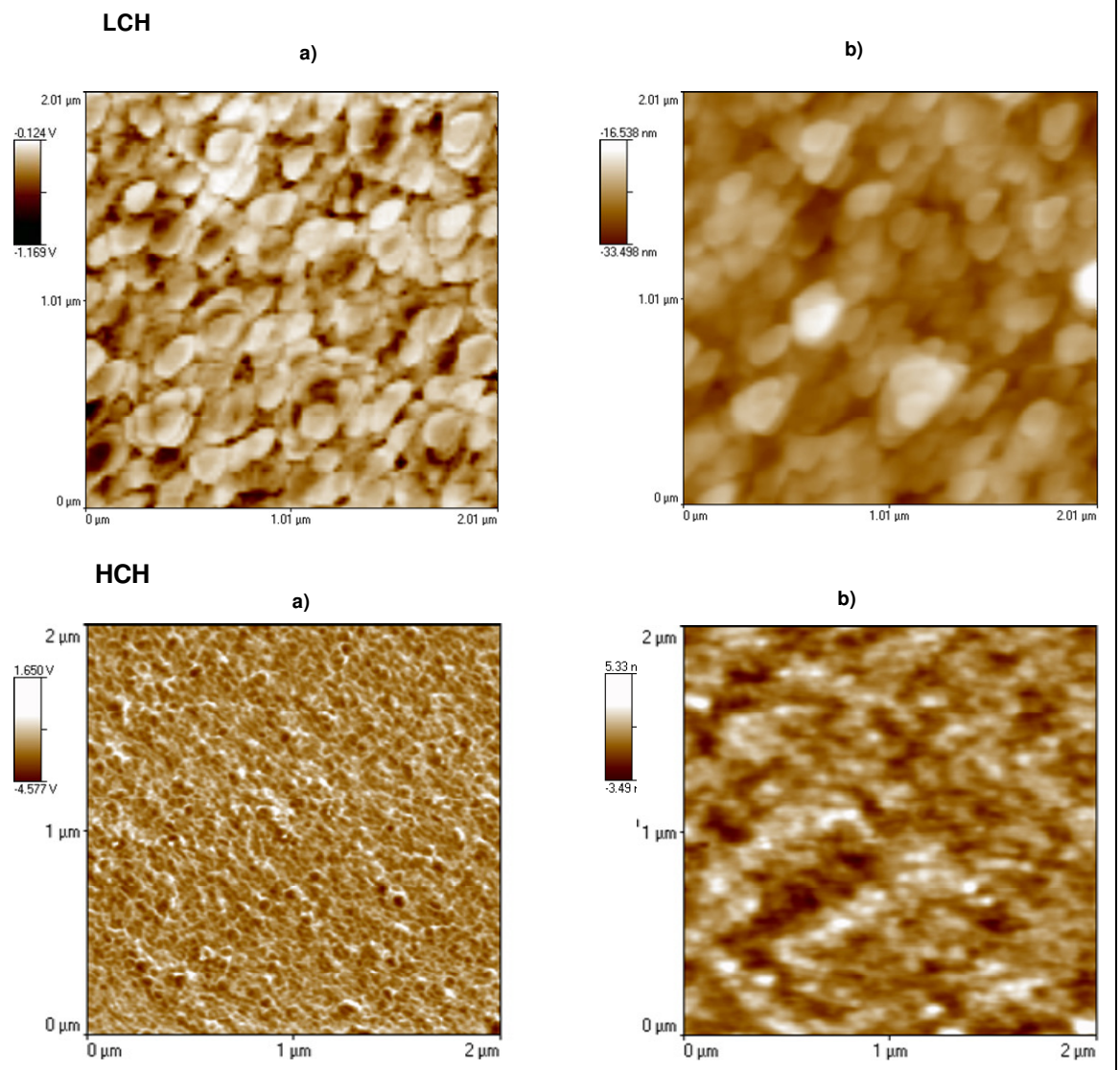

Figure III-29. Contrast phase a) and topographic b) AFM images of the surface of LCH and HCH films.

The chemical modification of chitosan with glycidyltrimethylammonium chloride induced an alteration of the surface of HCH films (Figure III-30). The image, in the phase mode displayed a topography composed of granules which had smaller size compared to those of the HCH pure samples. In order to analyze in detail this change of the morphology, an image with a higher magnification was acquired (1×1 µm^2). At this

magnitude in contrast phase, it is possible to observe a topography dominated by small structures composed by very tiny holes (8-5 nm).

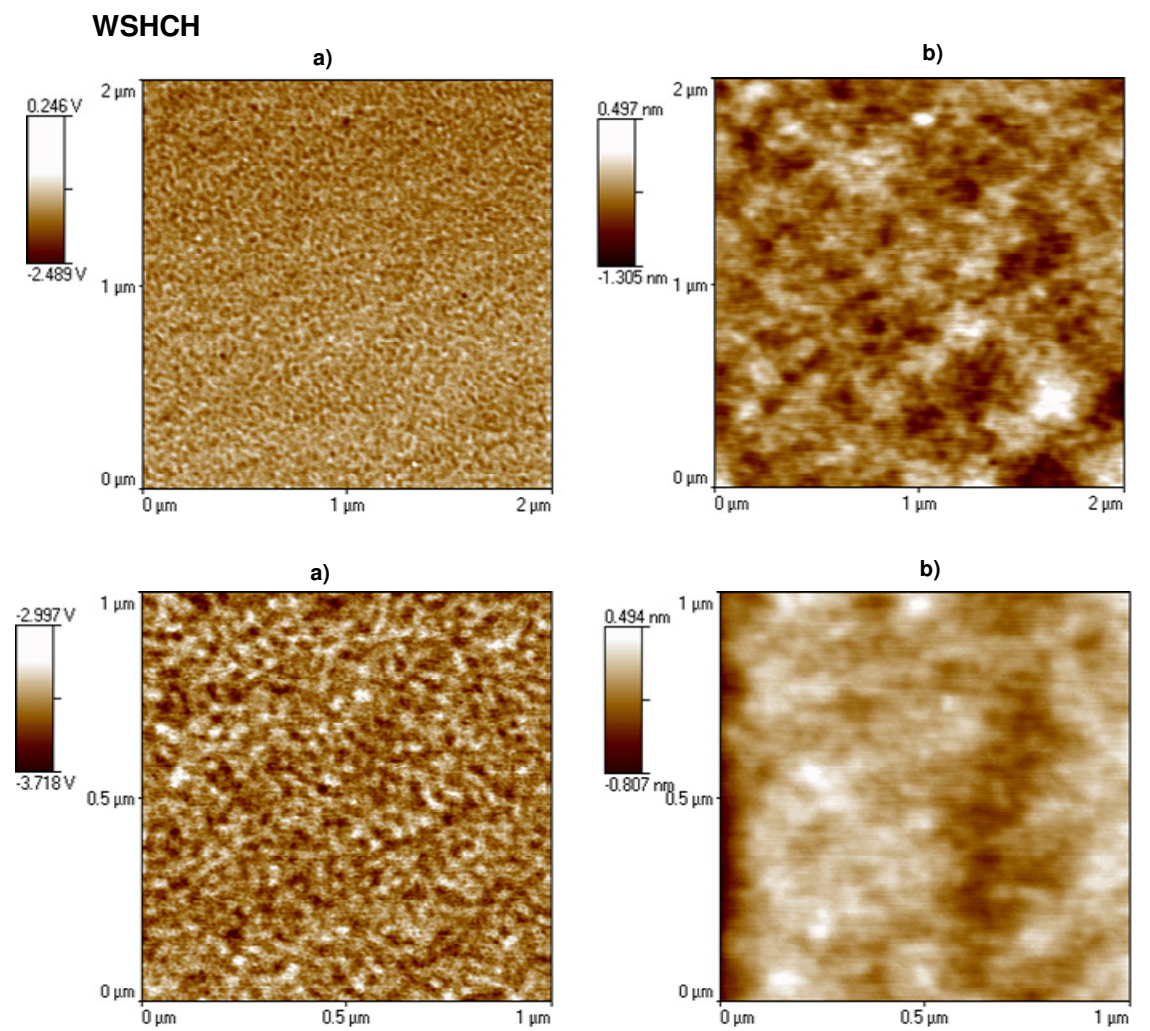

Figure III-30. AFM phase a) and topographic b) images of the surface of the modified chitosan WSHCH film at 2 µm and 1 µm of magnitude.

The surface of the chitosan-cellulose nanocomposite films was also studied by AFM. Both CHBC and CHNFC films displayed a homogeneous and dense structure that consisted of a randomly assembled nanofibrils of BC or NFC in the CH matrices.

Obviously, for the films with a low NFC and BC content the granular morphology of the chitosan matrix (100-300 nm) predominates, while for composite films with a high content of cellulose, the fibril morphology of the NFC (5-100 nm) and BC (10-200 nm) dominate (Figure III-31 and III-32).

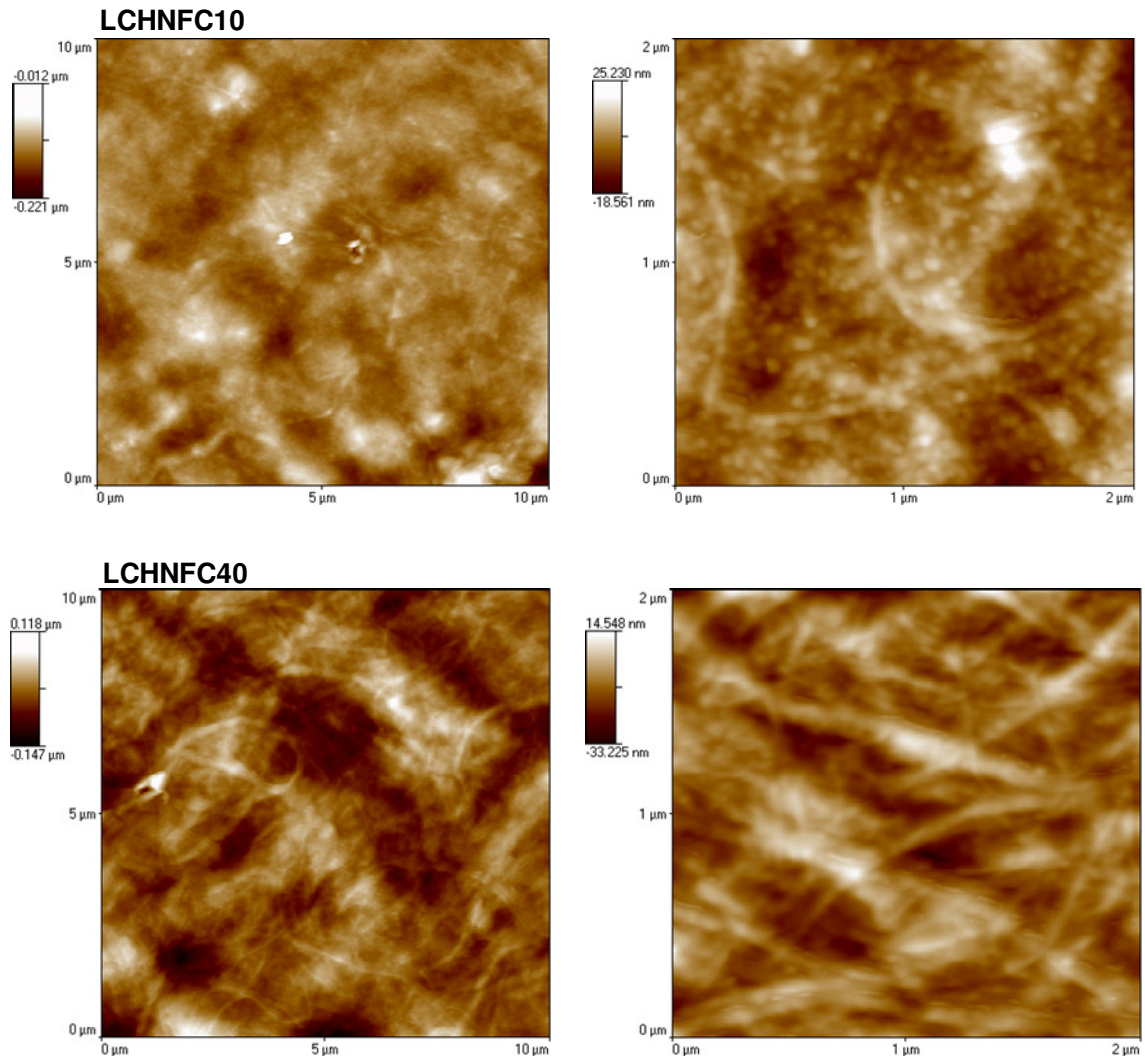

Figure III-31. AFM (topography mode) images of the surface of LCHNFC10 and LCHNFC40 films with two different magnifications, at 10 µm and 2 µm.

The uniform structure of these films was a good indication of their structural integrity, and, consequently, an indication of good mechanical properties.

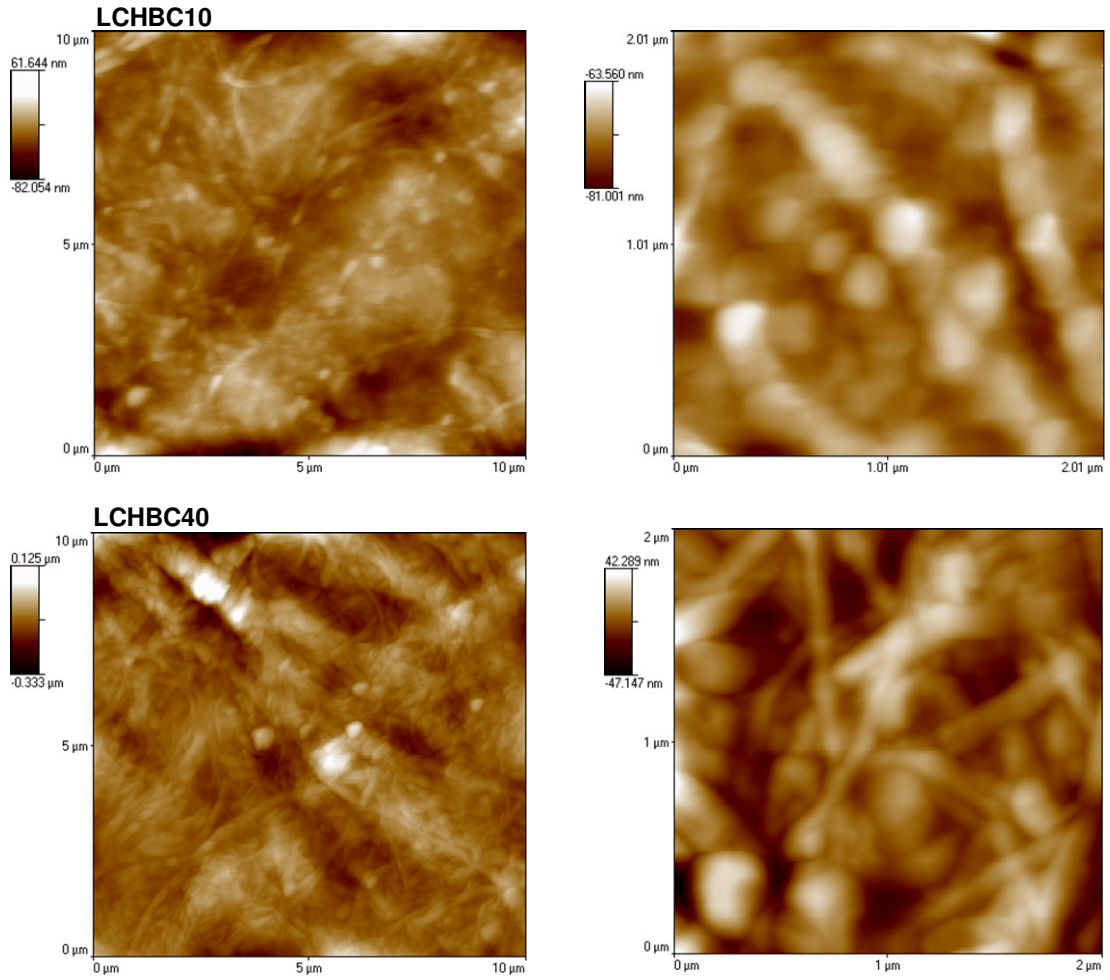

Figure III-32. AFM topographic images of the surface of LCHBC10 and LCHBC40 films at two different magnifications (10 and 2 µm).

12.2 Chemical structure

CP-MAS ^{13}C NMR

Solid state ^{13}C NMR spectroscopy was used to investigate the chemical structure of the CH, WSCH and the nanocomposite films. The evaluation of the chitosan and corresponding water soluble derivatives spectra was already done in Sections 11.1.4 and 11.2.2, respectively. Appendix 3 gives interpreted ^{13}C NMR spectra of the selected CH and WSCH films.

Figure III-33 shows the ^{13}C NMR spectra of LCHNFC and LCHBC nanocomposite films which displayed typical peaks of both polysaccharide components (chitosan and cellulose), and obviously their intensity was proportional to the content of each polysaccharide. As expected, the peak corresponding to C1 of the main polysaccharide (CH) had a displacement for 105 ppm (closer to cellulose value of $\delta \approx 105$ ppm that corresponds to the anomeric carbon), and both C4, and C6 peaks of cellulose were well defined in the nanocomposite films structure. In the case of cellulose, the signals from C4 atoms are in the range of 79-92 ppm, from C2, C3 and C5 in range of 72-79 ppm and finally the C6 peak was at a chemical shift of ≈ 64 ppm [130,170,310].

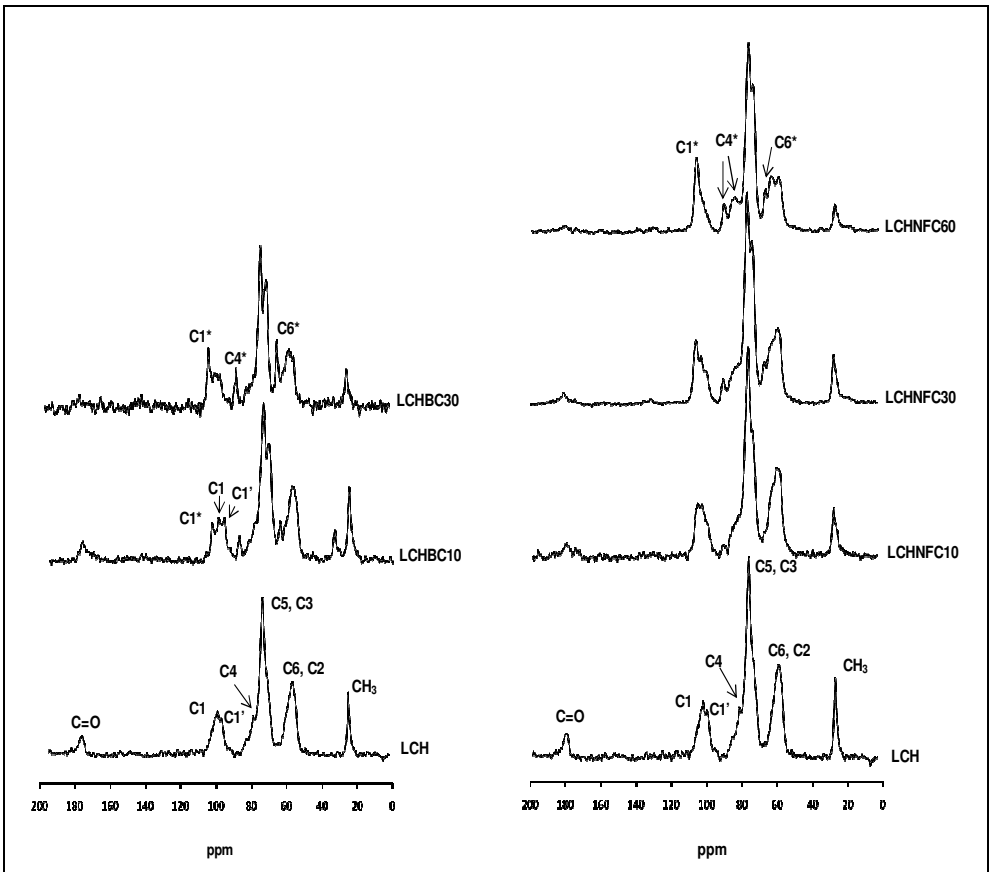

Figure III-33. CP-MAS ^{13}C NMR spectra of LCH and of nanocomposite films with different amounts of BC and NFC. (Note: C* corresponding to the cellulose signals)

Similar results, in terms of typical peaks and displacement, of both polysaccharides were found in the case of the nanocomposite films prepared with HCH and WSCH after the addition of BC and NFC (see spectra in Appendix 3).

12.3 Crystallinity

Figure III-34 shows the X-ray diffraction patterns of the unfilled LCH and HCH films together with those of the corresponding WSLCH and WSHCH films. The diffractograms of the formers showed the typical pattern of chitosan substrates, as in the case of the powdered chitosan samples, with major peaks at around 2θ of 12 and of 19º, indicating that the HCH film was much more crystalline than the LCH counterpart.

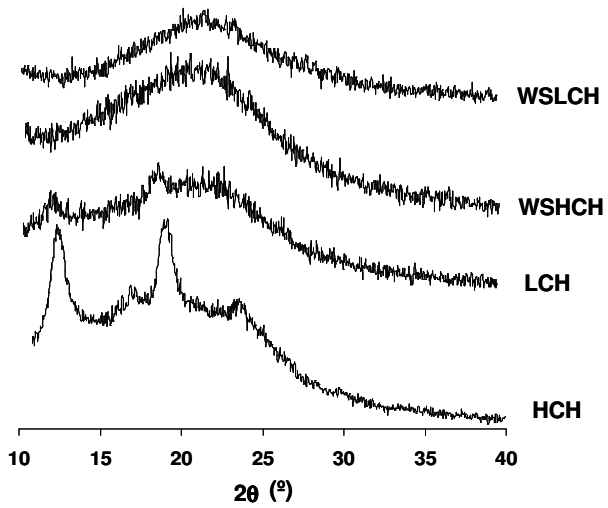

Figure III-34. X-ray diffractograms of unfilled CH and WSCH films.

As with the powdered water soluble chitosan samples, the X-ray diffractograms of the WSCH films, showed that the chemical modification had led to an extensive decline of their crystallinity.

The X-ray diffractograms of all the CHNFC and CHBC nanocomposites displayed typical diffraction peaks of both polysaccharide components, and, as expected, their intensity was proportional to the content of each polysaccharide. The incorporation of NFC seemed not to affect the crystallinity of the chitosan matrices, since no relevant changes on their diffraction profiles were observed (Figure III-35). However, the incorporation of BC seemed to promote the crystallization of chitosan, since the peaks at 2θ of 12 and 19º appeared in the diffractogram of WSHCHBC films (Figure III-36). This phenomenon is probably explained by the organized deposition of chitosan chains at the surface of the crystalline domains of the bacterial cellulose nanofibrils.

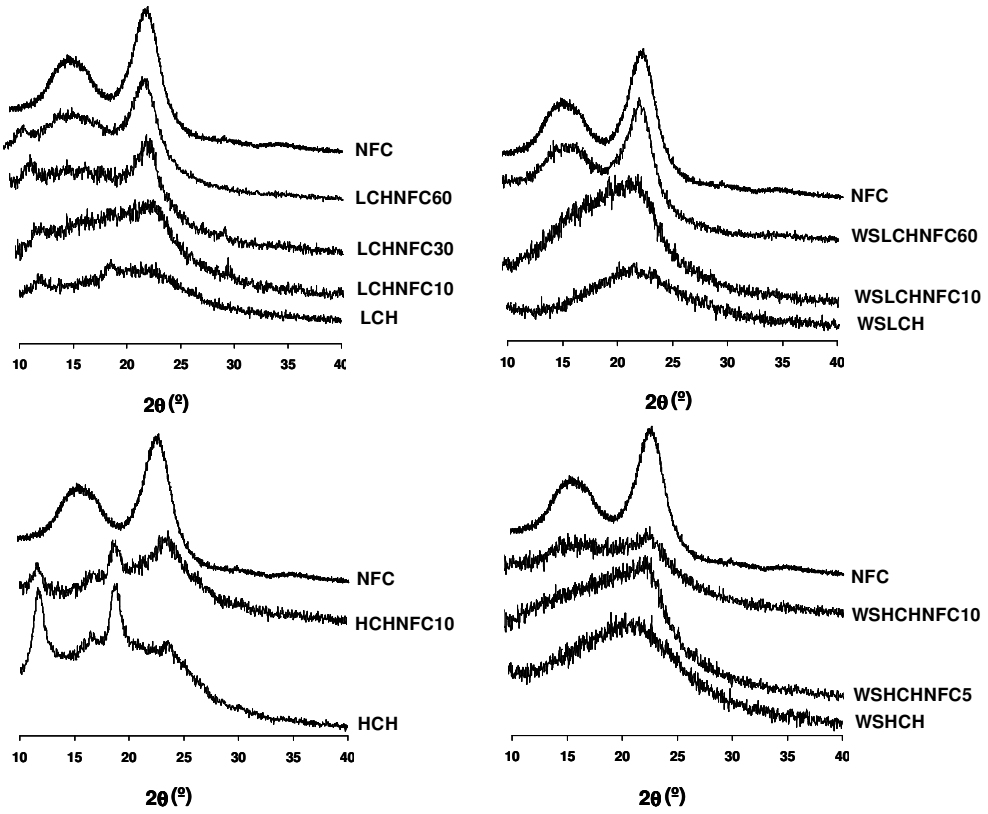

Figure III-35. X-ray diffractograms of NFC, CH and WSCH unfilled films and LCHNFC, WSLCHNFC, HCHNFC and HCHNFC nanocomposites.

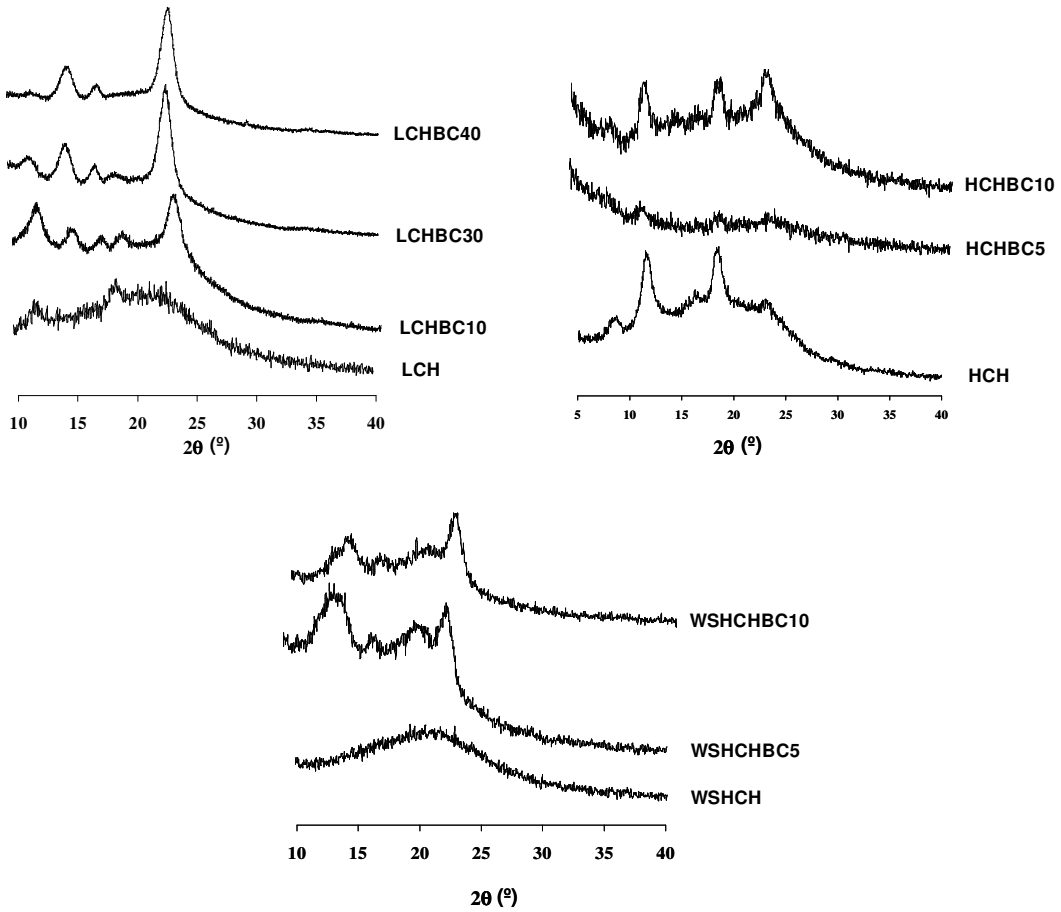

Figure III-36. X-ray diffractogram of CHBC nanocomposite films.

12.4 Thermal stability

Figure III-37 shows the thermograms of HCH and LCH and their corresponding water soluble derivatives films. In the former the two mass losses observed at around 100 ºC and 200 ºC, were associated with the volatilization of water and acetic acid, respectively. The maximum degradation step at 300 ºC was assigned to the degradation of chitosan [305]. The films prepared with WSHCH and WSLCH were more unstable than their unmodified precursors, since they started to decompose at around 180 ºC with the maximum degradation step at 260-270 ºC as previously described. Obviously, in these cases the loss of acetic acid was not observed because the films were cast from pure water.

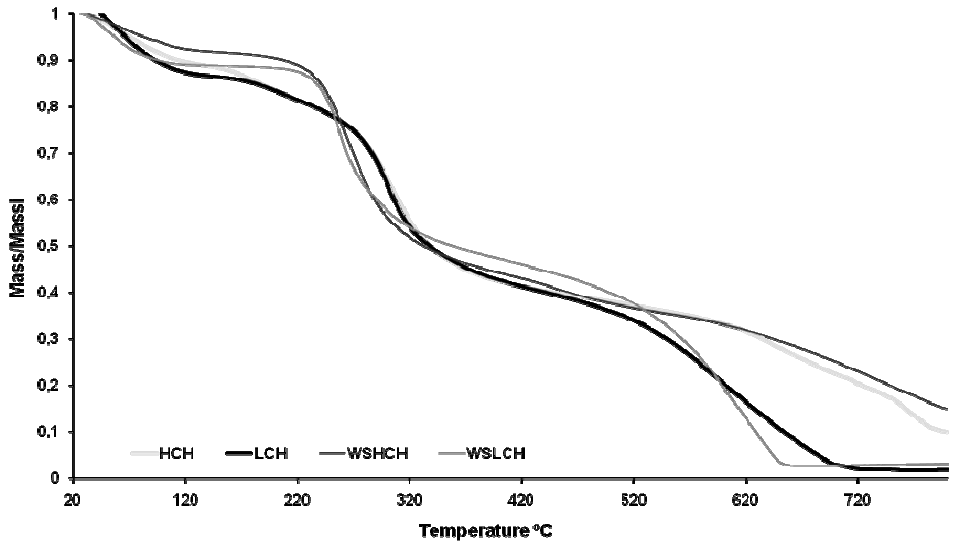

Figure III-37. TGA curves of LCH, HCH, WSLCH and WSHCH.

In general, the TGA tracings of the CHNFC and CHBC nanocomposite films (Figures III-38 and III-39 and Appendix 4) were a combination of those of chitosan and cellulose presenting double weight loss step profiles. The relevant thermal data (Td_i, Td_1 and Td_2) are listed in Table III-14, where, Td_i is the initial degradation temperature and Td_1 and Td_2 are the maximum first and second degradation temperatures, respectively. The incorporation of NFC into the CH matrices resulted, in most cases, in a considerable increase in thermal stability (increments of 10-40 ºC in the Td_i). For example, an increase in the Td_i from 227 ºC in the unfilled LCH film up to 271 ºC in filled LCHNFC50 nanocomposite films, and a Td_1 raising from 304 ºC to 313 ºC for the same materials. However, only a slight increase in the Td_i (around 10 ºC in some cases) was observed with the nanocomposite films prepared with BC.

Table III-14. Thermogravimetric features of the NFC, CH, WSCH and their nanocomposites.

Samples	Td_i (ºC)	Td_1 (ºC)	Td_2 (ºC)
NFC & BC	240	340(33)	
HCH	229	306(40)	-
LCH	227	304(41)	-
WSHCH	186	270(31)	-
WSLCH	199	260(27)	-
LCHNFC5	248	308(41)	365(53)
LCHNFC10	271	312(40)	365(53)
LCHNFC20	269	307(38)	365(53)
LCHNFC30	270	313(38)	367(54)
LCHNFC40	273	314(34)	370(51)
LCHNFC50	271	313(31)	370(51)
LCHNFC60	246	305(31)	366(51)
WSLCHNFC10	223	256(37)	301(57)
WSLCHNFC60	223	297(34)	354(47)
HCHNFC5	234	304(45)	350(57)
HCHNFC10	232	307(40)	364(55)
WSHCHNFC5	213	277(34)	330(51)
WSHCHNFC10	194	279(36)	339(53)
LCHBC5	237	302(40)	370(60)
LCHBC10	237	304(41)	370(60)
LCHBC30	239	300(34)	379(56)
LCHBC40	239	301(35)	379(55)
HCHBC5	225	294(38)	- [a]
HCHBC10	226	260(35)	- [a]
WSHCHBC5	231	280(28)	- [a]
WSHCHBC10	230	276(27)	- [a]

[a] Td_2 overlapped with Td_1. The numbers in parentheses refer to the percentage of volatilization attained at both Td_1 and Td_2.

Theses results are a good indication of the good dispersion and high compatibility between the two polysaccharide components, resulting in composite materials with enhanced thermal stability. Moreover, the addition of NFC or BC also produced a slight

decrease in moisture content, particularly for high NFC contents, where the residual moisture decreased from 10-11% for unfilled films to 8% for nanocomposite ones. The observed reduction in moisture could be due to strong molecular interactions between cellulose nanofibres and the chitosan matrix.

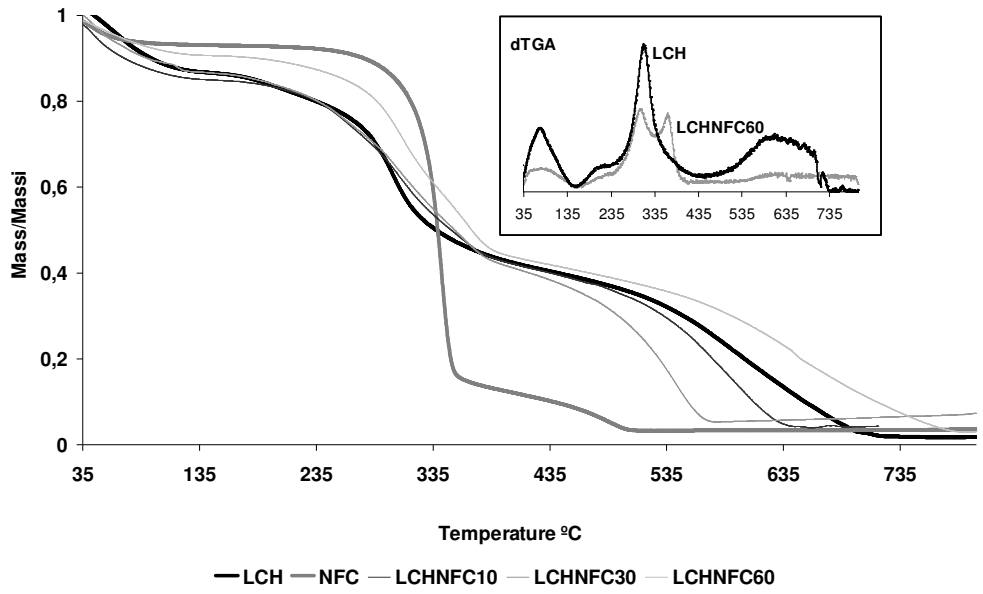

Figure III-38. TGA curves of NFC, LCH and selected LCHNFC nanocomposite films with different NFC contents (10, 30 and 60%), with the corresponding dTGA plots of LCH and LCHNFC60.

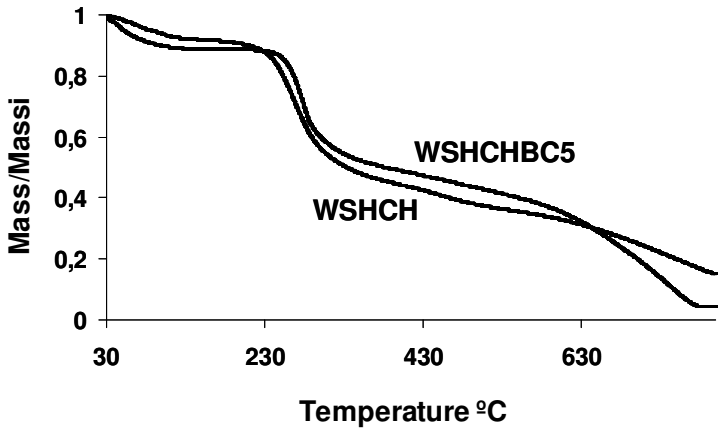

Figure III-39. TGA curves of WSHCH and WSHCHBC5.

12.5 Optical properties

The optical properties of the unfilled and chitosan-cellulose nanocomposite films (approximately 30 μm thick) were evaluated by measuring their transmittance in the range 400-700 nm.

The transmittance in this range was about 90% for HCH and WSHCH and about 80% for LCH and WSLCH (Figure III-40 and III-41). This difference was probably related to the light-brownish colour of the pristine LCH sample due to trace amounts of coloured impurities, which however could be removed, if required, using adequate purification procedures [10]. The slightly higher transmittance values obtained with the WSCH derivatives in relation to the corresponding unmodified CH films was probably associated with the chitosan modification procedure that implied a purification step.

In all cases (CH and WSCH films), the transmittance of the films was not affected by the incorporation of 5% of cellulose nanofibrils (NFC and BC). However, for CH films with NFC and BC contents equal to, or higher, than 10%, a reduction in the transmittance was observed (Figure III-40 and III-41). In the case of NFC, the transmittance was reduced from nearly 90% in the CH films to the lower value of 20% for LCHNFC60. For nanocomposite films filled with contents of BC equal or higher than 10%, the transmittance decreased to 80% and 70%, respectively for HCH/ WSHCH and LCH composite films. The transmittance results also indicated some differences among the nanocomposite films: those with BC showed higher transmittance than that of counterparts with NFC, because, BC is pure cellulose without residual lignin or hemicelluloses.

The transmittance values of the chitosan substrates [311] and also of the CH films filled with NFC [174] are in good agreement with previously published data.

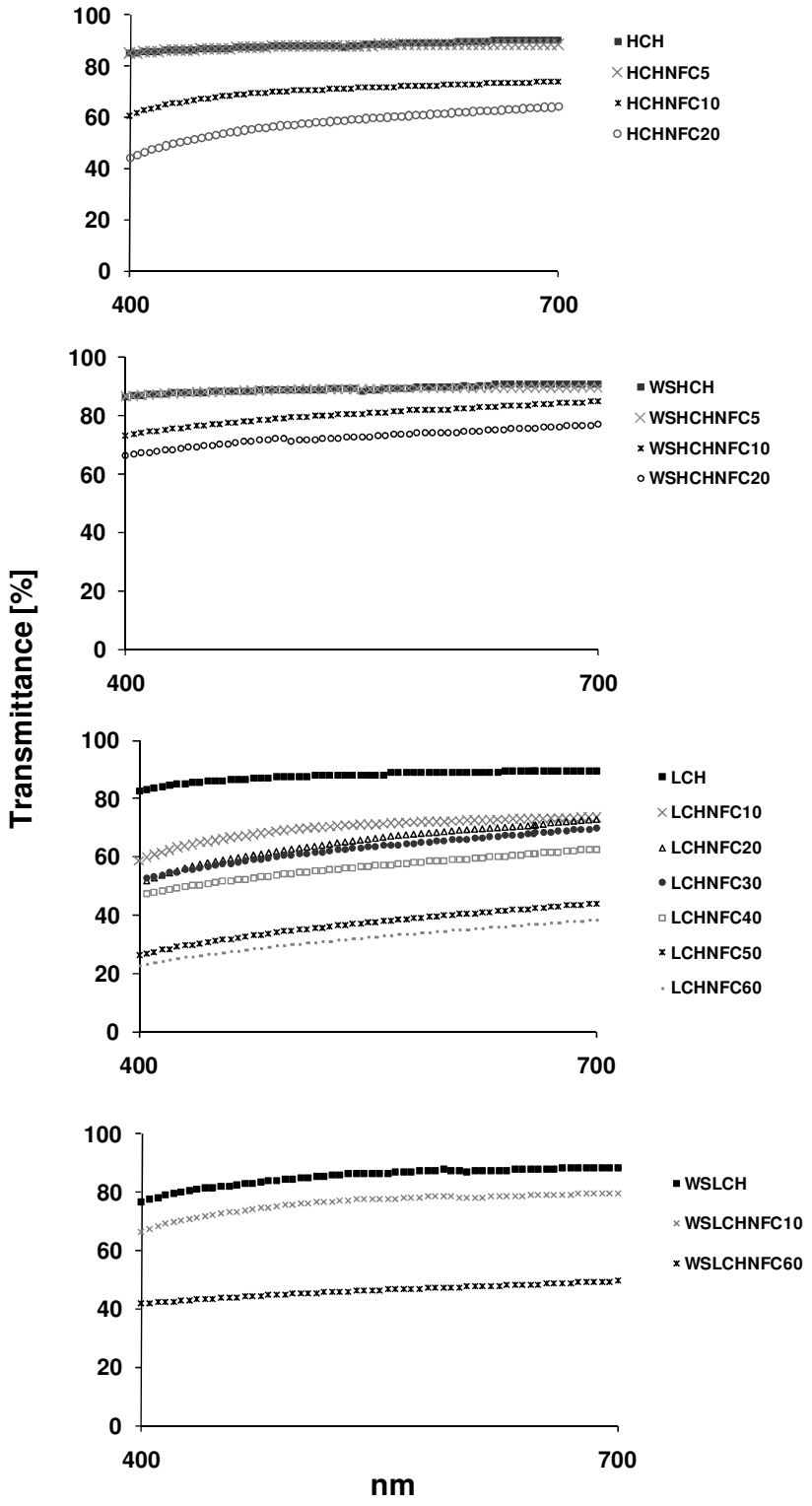

Figure III-40. Transmittance of unfilled CH films and of the corresponding CHNFC and WSCHNFC nanocomposites with different NFC contents.

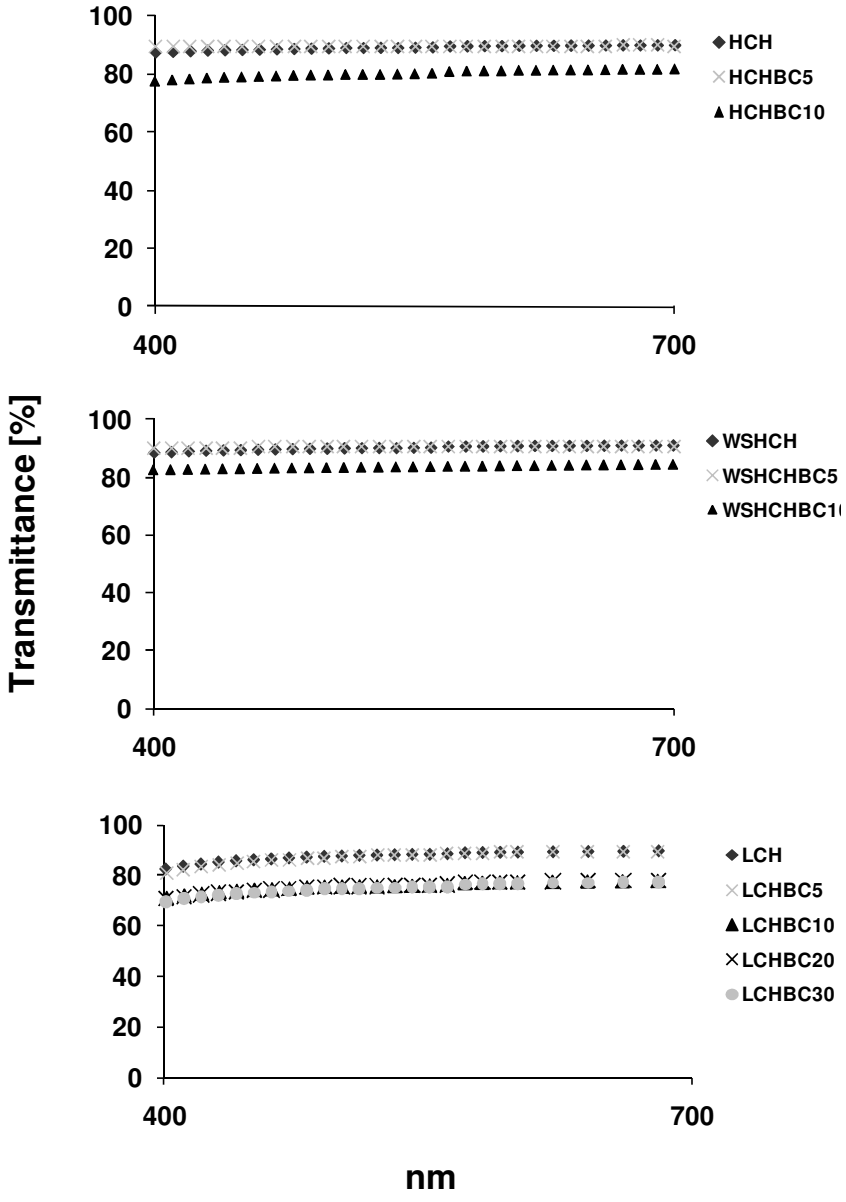

Figure III-41. Transmittance of unfilled CH films and of some corresponding CHBC nanocomposites with different BC contents.

The high transparency of CH and its nanocomposite films was visually evidenced by the photos showed in Figure III-42 and III-43. Similarities of chitosan films with or without NFC or BC were observed at this macroscopic level.

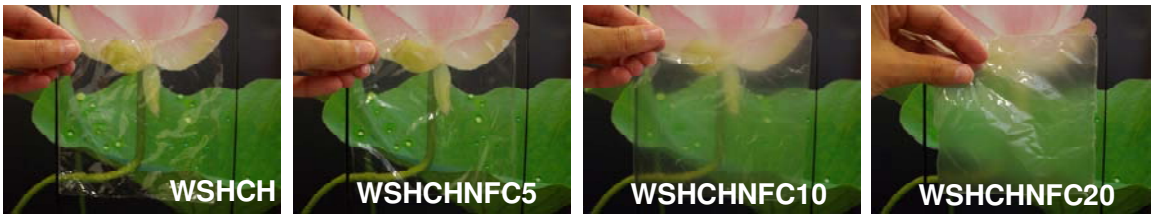

Figure III-42. Images of the WSHCH and of its nanocomposite films containing different percentages of NFC.

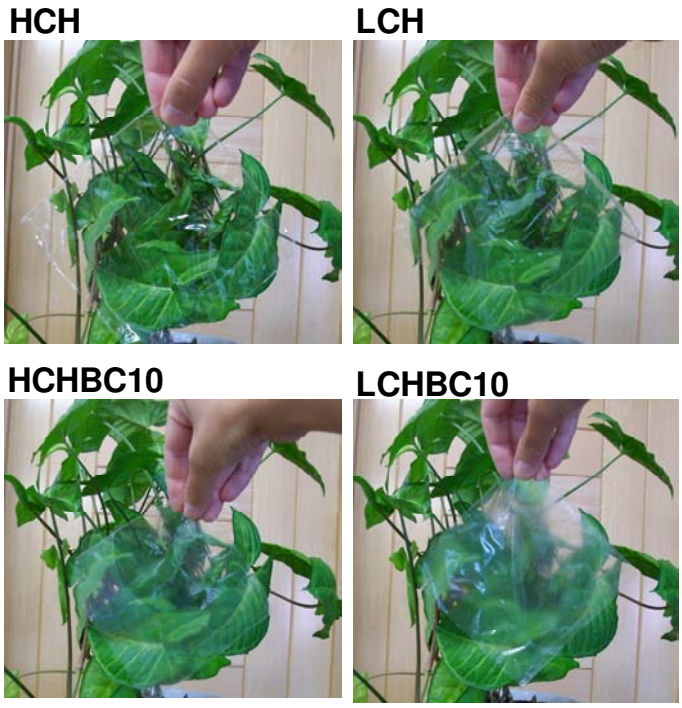

Figure III-43. Images of the LCH and HCH and of their corresponding nanocomposite films containing 10% of NFC.

The regular nature of the transparency over all the films suggested that the NFC and BC nanofibres were well dispersed within the CH and WSCH matrices, as previously observed by SEM and AFM.

12.6 Mechanical properties

Tensile tests

The effect of the NFC and BC content, chitosan DP and quaternization on the large strain behaviour of nanocomposite films was studied up to their failure. The Young's modulus, tensile strength and elongation at break, determined from the typical stress-strain curves, are displayed in Figure III-44 and III-45.

HCH showed a higher Young's modulus than LCH, confirming that the decrease in the CH DP negatively affected its mechanical performance [312]. Previous studies reported values of Young's modulus, stress and elongation to break of the same order, depending again on the chitosan degree of polymerization [313-315]. For example, HCH showed higher elongation at break than LCH, with values of elongation at break of 34% and 27% for first and second films, respectively; and of 30% and 21% for their respectively water soluble derivatives, WSHCH and WSLCH. The WSCH derivatives displayed the lowest modulus, confirming that the chemical functionalization clearly affected the mechanical behaviour of the CH substrates, obviously associated with the drastic decrease of crystallinity previously observed by X-ray diffraction. These results were also found in previous studies with other chitosan quaternary salts [307].

The reinforcement effect of NFC or BC on the mechanical properties of the CHNFC nanocomposite films was evaluated up to their failure, as a function of the each nanofibre content.

As can be seen in Figure III-44a), the Young's modulus of the CHNFC nanocomposite films increased considerably with the NFC content, keeping constant the relative order of absolute values for the starting chitosans. The maximum amount of NFC used was limited to 20% for HCH and WSHCH, and, in these cases, the maximum increment on the Young's modulus was of 78% and 150%, respectively. However, when higher incorporations of NFC were possible, up to 60% in the case of LCH and WSLCH, the increases in the Young's modulus were correspondingly higher, *viz.* 200% and 320%, respectively. The tensile strength measurements (Figure III-44b) of the studied nanocomposite films were in agreement with the evolution of the Young's modulus.

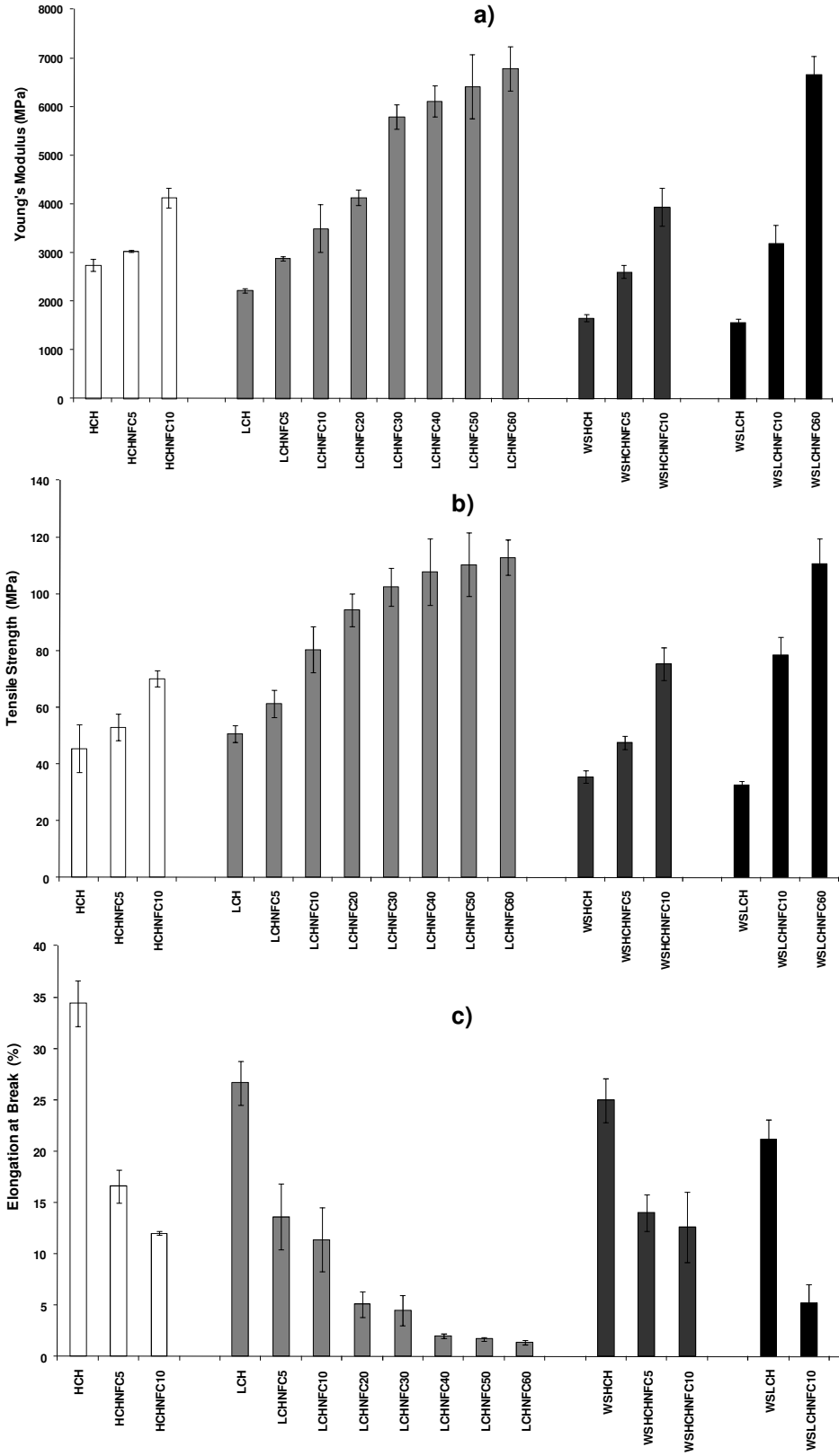

Figure III-44. Young's modulus, stress and elongation to break of the CH and CHNFC films.

Finally, the incorporation of NFC into the CH matrices caused a significant decrease in the maximum strain, which was proportional to the NFC content (Figure III-44c). Thus, for quite high NFC loads (40, 50 and 60%), the films became very brittle.

Actually, this increment in the mechanical performance by the incorporation of NFC has been observed in various composite materials with other kind of matrices, such as polylactic acid [168], polyvinyl alcohol [170] and starch [167], among others.

As previously mentioned, the preparation of composite films with nanofibrillated cellulose and chitosan is not pioneering and previous studies [173-174] had shown a slight improvement in the mechanical resistance of these materials, when compared with those obtained with chitosan alone. However, in this work it was possible to prepare and characterize transparent chitosan films reinforced with high contents (up to 60%) of NFC, contrasting with the small amounts used in preceding studies. Moreover, the use of water soluble chitosan derivates reinforced with NFC is also described here for the first time.

The Young's modulus of the CHBC composite films also increased considerably with the BC content (Figure III-45a). At a fibre content of 10%, the Young's modulus was 40, 32 and 114% higher than that of the unfilled CH substrates, respectively for the HCHBC, LCHBC and WSHCHBC films. The increment was particularly relevant for the WSHCHBC films, which can be related to the observed increase in crystallinity of this mainly amorphous matrix, after incorporation of the BC nanofibrils.

Moreover, the LCHBC films with higher BC contents (30 and 40%) gave Young's modulus similar to those of HCHBC and WSHCHBC films with only 10% of cellulose nanofibrils. These results indicated that the HCH and WSHCH matrices are more suitable for the preparation of transparent nanocomposite films with high mechanical performance. The incorporation of BC also promoted a considerable increase in the tensile strength of the nanocomposite films (Figure III-45b) and a significant decrease in the elongation at break (Figure III-45c), which was more pronounced for higher cellulose contents, as already observed with NFC. One way to increase the nanocomposite films flexibility is to use a plasticizer (e.g. glycerol) in order to reduce polymer chain-to-chain interactions. Nevertheless, a previous study [173] related to the effect of plasticizers on the strength of composites films, demonstrated that the tensile strength decreased with an increase in plasticizer content, because the plasticizer inhibits the bonding between chitosan and cellulose.

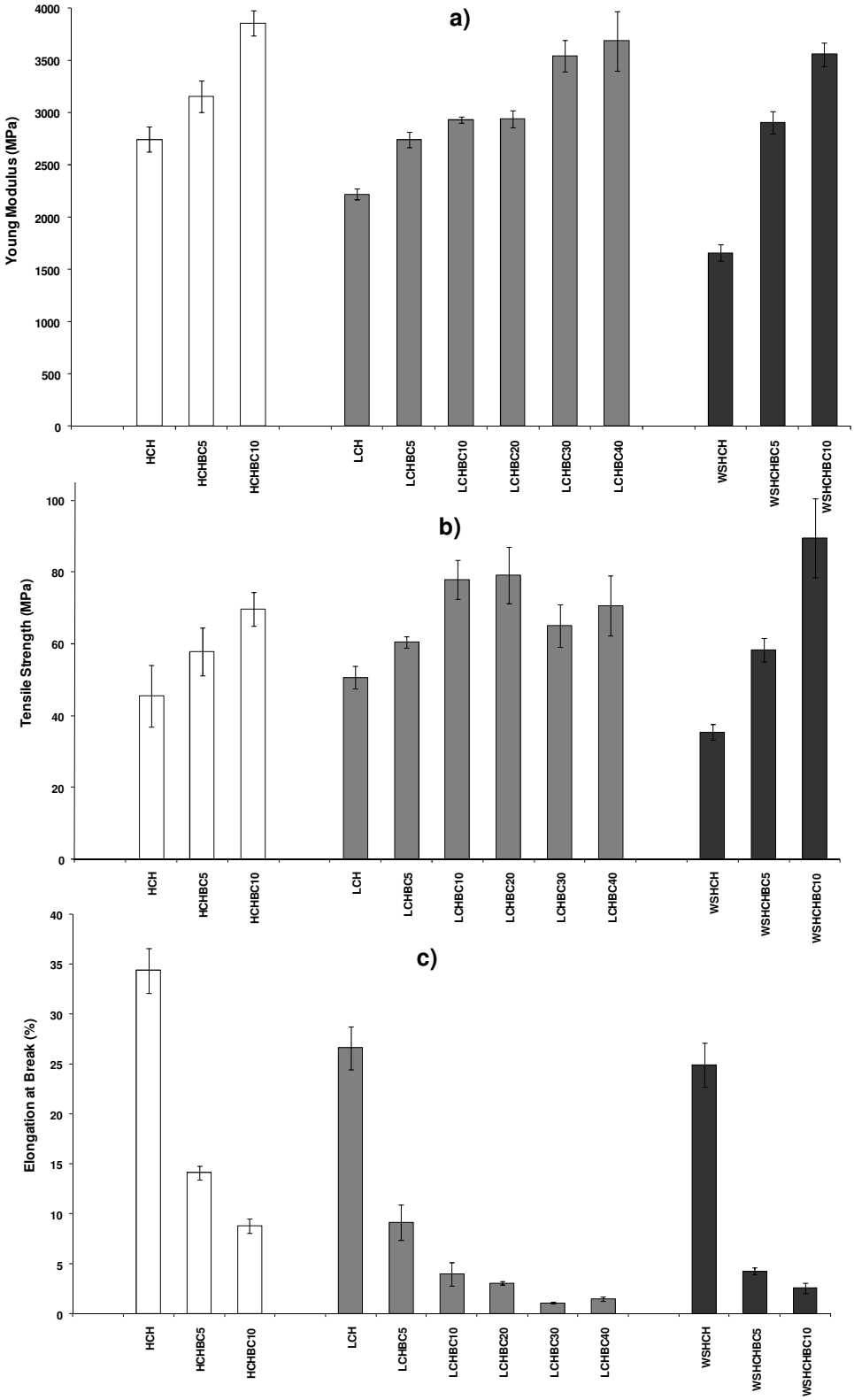

Figure III-45. Young's modulus, tensile strength and elongation to break of CH and corresponding nanocomposite films with different BC contents.

Enormous increments in the mechanical performance of several composite materials have been previously reported by the incorporation of BC nanofibres (or other nanocellulose substrates) in other kind of matrices, such as acrylic resins [316], flexible polyurethane elastomers [222] and phenolic resins [224], among others.

The superior mechanical properties of all CHNFC and CHBC films compared with those of the unfilled chitosan matrices, confirmed the good interfacial adhesion and the strong interactions between the two components. These results can be explained by the inherent nanofibrillar morphology of NFC and BC and the similar chemical structures of the two polysaccharides.

Globally, the tensile properties of CHNFC nanocomposites are better than those of CHBC counterparts. This behaviour could be due to the better dispersion of NFC nanofibres into the chitosan matrices, because of the fact that in this substrate the nanofibrills are almost totally individualized, as well as due to the higher aspect ratio of NFC compared with that of bacterial cellulose [216].

Dynamic mechanical analysis

The mechanical properties of the chitosan films and chitosan-cellulose nanocomposite films were also studied by dynamic mechanical analysis. Two different experiments were carried out, one to evaluate the effect of the temperature on the dynamic-mechanical behaviour, varying the temperature from -50 to 165 ºC and another to assess the effect of the humidity at 30 ºC, by varying the relative humidity from 10 to 80%. The latter was only performed for the unfilled chitosan films and for their CHNFC nanocomposite.

Figure III-46 shows the temperature dependence of the storage modulus at 1 Hz of CH and WSCH films. The curves of the storage modulus *vs* temperature of HCH and LCH showed two main relaxations, at 0-40 ºC and 125-155 ºC, typical of CH substrates. The first transition is normally assigned to the β relaxation associated with local movements of side groups in chitosan [198], while the transition occurring for higher temperatures, designated as the α relaxation, reflects the glass transition temperature of amorphous chitosan [198]. There were no obvious glass transition observed for the WSCH derivatives.

The storage modulus of the LCH films was lower than that of the HCH and the WSLCH derivative displayed the lowest storage modulus.

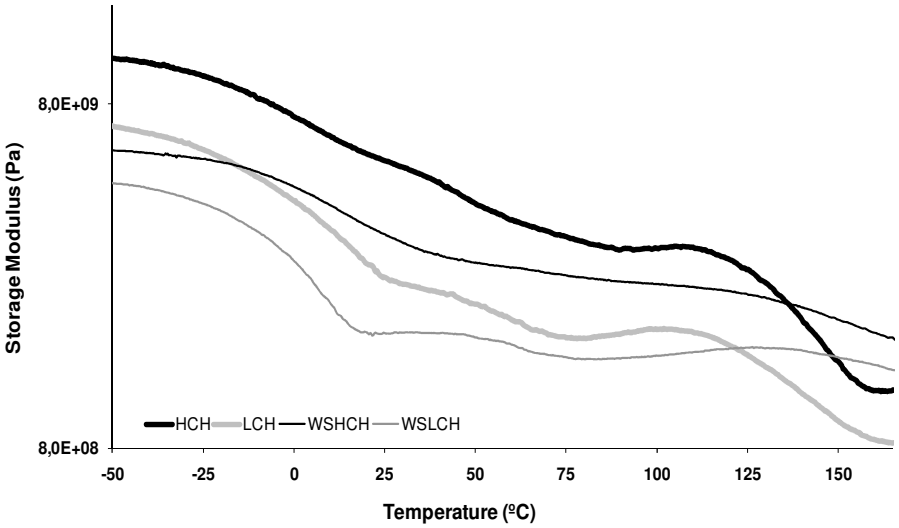

Figure III-46. Temperature dependence of the storage modulus of LCH, HCH, WSLCH and WSHCH films.

The incorporation of NFC and BC increased considerably the storage modulus in the entire temperature range and did not affect the main transitions of chitosan, as illustrated in Figure III-47 for LCH and WSLCH films filled with different amounts of NFC.

The storage modulus of LCHNFC nanocomposite films increased by 24% and 90%, when filled with 10 and 60% of NFC content, respectively, when compared with the unfilled LCH film at 25 ºC, while at a temperature above Tg, the storage modulus increased 300% and 500%, for LCHNFC10 and LCHNFC60, respectively. This behaviour could be attributed to the formation of a percolating system of cellulose nanofibres linked by hydrogen bonding.

The storage modulus of the nanocomposite films (LCHNFC and WSLCHNFC) was essentially independent of temperature. However, this effect was more relevant for reinforcements higher than 10% of NFC (Figure III-47). This feature was observed before with other polymeric matrices [168-169], suggesting that the NFC network interconnected by hydrogen bonds resists the applied stress independent of the softening of chitosan.

Similar results were observed in the case of bacterial cellulose (see the storage modulus of the nanocomposite films in Appendix 5).

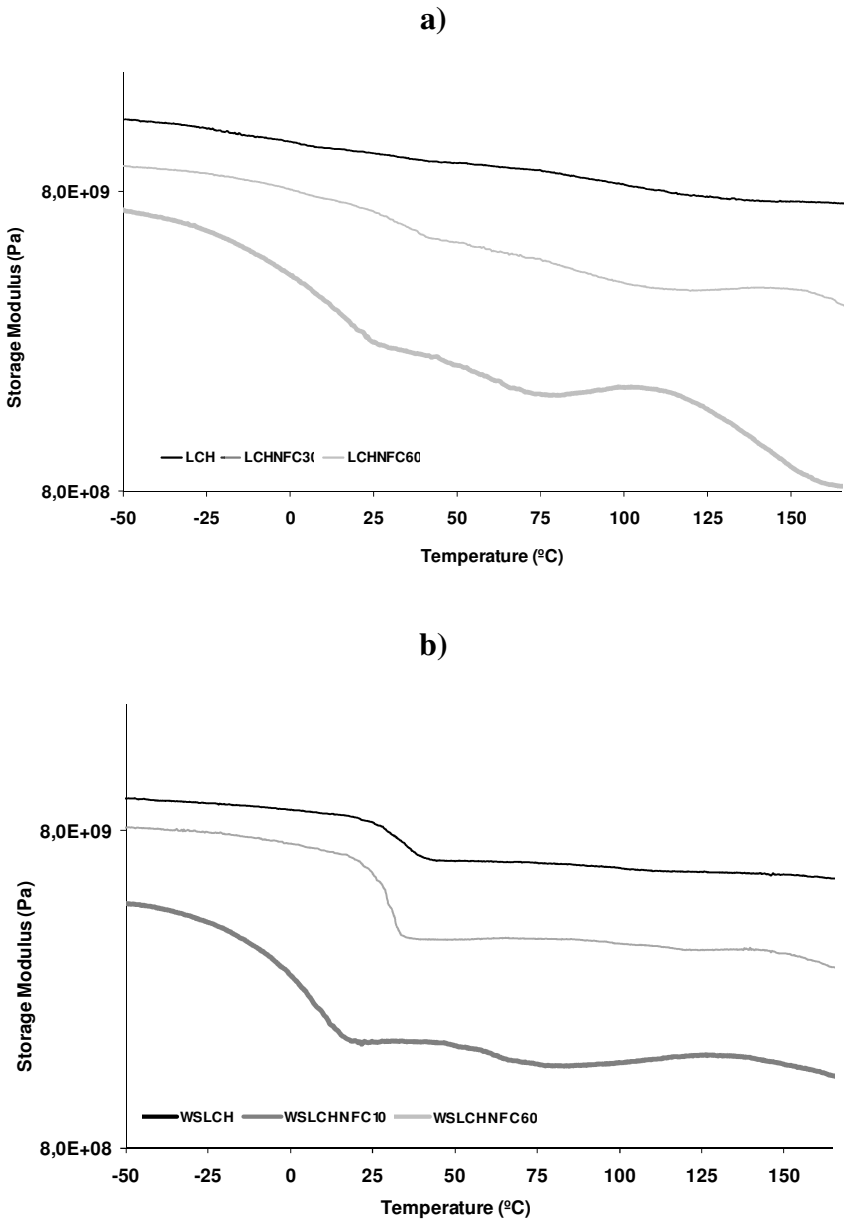

Figure III-47. Temperature dependence of the storage modulus of LCHNFC a) and WSLCHNFC b) films with different amounts of NFC.

Figure III-48 and III-49 illustrate the effect of the relative humidity on the dynamic mechanical properties of CH films and of the corresponding CHNFC nanocomposites, respectively. As can be seen in Figure III-48, CH and WSCH showed a quite different

behaviour with respect to the stiffness variation with increasing humidity. Both displayed a decrease of the storage modulus with the relative humidity. However, the WSCH films displayed a more significant reduction at low humidity values due to their high moisture sensitivity related to the incorporation of the quaternary ammonium moieties.

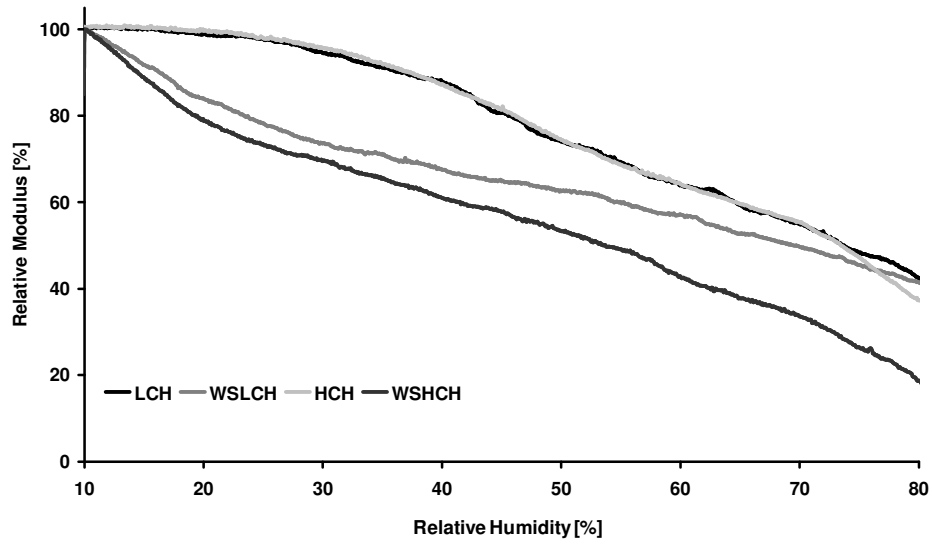

Figure III-48. Moisture dependence of the relative modulus at 30 ºC for CH and WSCH films.

The softening behaviour of the CH and WSCH nanocomposite films was not affected by the incorporation of 10% of NFC. For contents higher than 10%, an improved moisture resistance was observed, as can be observed in Figure III-49.

These results are in excellent agreement with previous works reporting on the incorporation of MFC and NFC into several polymeric matrices, such as PLA, PVA and starch, among others [168-170,174], and of BC [224].

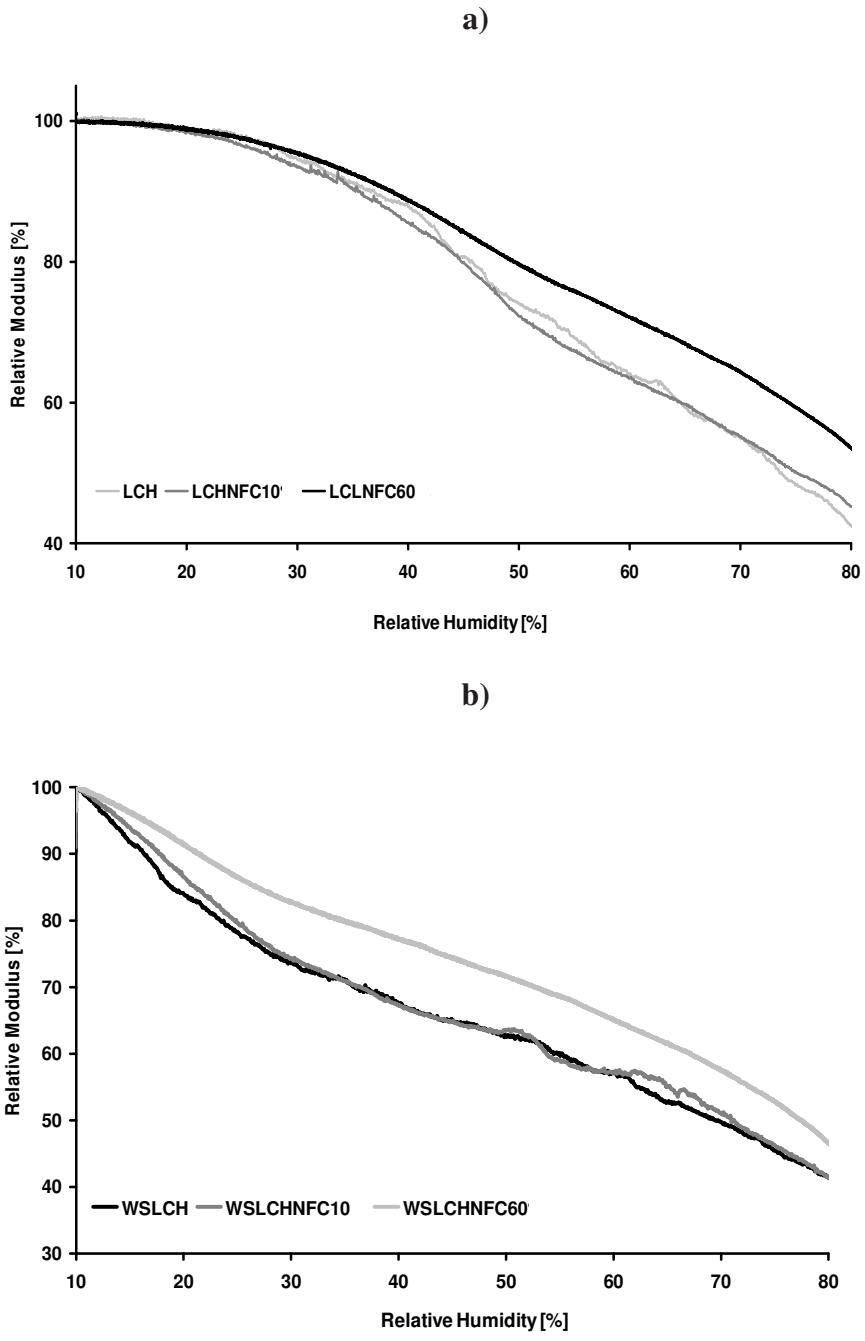

Figure III-49. Moisture dependence of the relative modulus at 30 ºC for a) LCHNFC and b) WSLCHNFC.

12.7 Final considerations

Transparent chitosan-nanofribrillated cellulose (CHNFC) and chitosan-bacterial cellulose (CHBC) nanocomposite films were prepared by simply casting water (or 1% acetic solutions) suspensions of chitosan with different contents of NFC (up to 60%) and BC (up to 40%).

Their often high transmittance, varying between 90 and 20% depending on the type of chitosan and NFC and BC content indicated that the dispersion of the cellulose nanofibres into the chitosan matrices was quite good. CHBC showed higher transmittance than CHNFC, because of the higher purity of BC.

These materials were in general very homogenous and presented better thermal stability and mechanical properties than the corresponding unfilled chitosan samples. The higher molar mass chitosans showed higher elongation at break than that of the corresponding water soluble derivatives, WSHCH and WSLCH. Also, the nanocomposite films prepared with HCH showed higher elongation at break than with LCH. In addition, the nanocomposite films prepared with NFC and BC also presented better thermo-mechanical properties than the unfilled chitosan films. The superior mechanical properties of all CHNFC and CHBC films compared with those of the unfilled CH films, confirmed the good interfacial adhesion and the strong interactions between the two components.

13 Chitosan-coated papers

13.1 Evaluation of the chitosan distribution onto the paper sheet using a fluorescent chitosan

Paper materials, including chitosan-coated papers, display a high chemical and morphological heterogeneity, because of the complexity of the interactions among cellulose fibres, fillers and chitosan. As these intricacies had not been tackled by previous studies, a look into this topic in a more systematic fashion, calling upon the use of a fluorescent chitosan derivative as a tool to assess its spatial and in-depth distribution onto the paper sheet, was considered. Fluorescent chitosan derivatives have been applied to some biologically related systems [102-106]; however, studies reporting the use of this chitosan derivative as pointer in papermaking science are scarce.

To evaluate the distribution of chitosan deposited layer-by-layer onto conventional paper sheets in terms of both spreading and penetration, it was essential to establish that papers coated with the *same amount* of either LCH or FTIC-LCH (Table III-15) would give properties which were not affected by the presence of the fluorescent substituents on the macromolecules, except of course for the features purposely associated with the introduction of these moieties. In order to assess this point, it was necessary to compare the grammage gain (Table III-15), air permeability (Table III-15) and tensile index (Table III-16) of differently coated sheets and to verify that the changes in this property as a function of the number of deposited layers was the same for both chitosans used.

As clearly suggested by the data given in Table III-15 and III-16 the two chitosans induced the same quantitative effects in these parameters within experimental error.

Table III-15. Grammage gain and Bendtsen air permeability of LCH and FITC-LCH-coated papers.

	Grammage Gain [g/m^2]					
	CS	**1 layer**	**2 layers**	**3 layers**	**4 layers**	**5 layers**
LCH	-	1.5 ± 0.2	2.5 ± 0.2	3.2 ± 0.3	3.9 ± 0.2	4.6 ± 0.3
FITC-LCH		1.5 ± 0.0	2.6 ± 0.3	3.3 ± 0.2	4.1 ± 0.2	4.9 ± 0.4
	Bendtsen Air Permeability [µm/Pa.s]					
LCH	9.6 ± 0.3	8.0 ± 0.2	3.3 ± 0.2	0.8 ± 0.1	0.2 ± 0.0	0.0 ± 0.0
FITC-LCH		8.1 ± 0.1	3.5 ± 0.1	0.9 ± 0.0	0.2 ± 0.0	0.0 ± 0.0

Table III- 16. Tensile Index of CS, LCH and FITC-LCH-coated paper in machine (MD) and cross direction (CD).

	Tensile Index [N.m/g]					
	CS	**LCH1**	**LCH2**	**LCH3**	**LCH4**	**LCH5**
MD	88.4 ± 1.1	100 ± 1.2	110 ± 1.2	114 ± 0.3	115 ± 0.7	117 ± 0.8
CD	26.0 ± 0.4	28.7 ± 0.4	31.8 ± 1.0	34.0 ± 1.8	35.3 ± 0.7	37.5 ± 0.4
	CS	**FITC-LCH1**	**FITC-LCH2**	**FITC-LCH3**	**FITC-LCH4**	**FITC-LCH5**
MD	88.4 ± 1.1	99.7 ± 1.0	105 ± 0.6	110 ± 0.9	113 ± 0.5	114 ± 0.7
CD	26.0 ± 0.4	29.1 ± 0.8	32.9 ± 0.6	34.4 ± 1.1	35.9 ± 0.4	38.7 ± 0.2

The actual variations in these two properties will be discussed in Section 13.2 together with the effect of other parameters.

13.1.1 Reflectance

To gain some understanding of the role of the presence of chitosan layers in terms of its penetration within the paper sheet, visible diffuse reflectance measurements were carried out on both sides (coated and uncoated) of the FITC-LCH-coated papers bearing up to five different layers. The same reflectance spectrum was measured between 400 and 600 nm for all the paper sheets, both at their CS coated and uncoated sides, using two

random pieces cut out of each sheet. The CS remission function (with an intensity lower than 0.01 between 420 and 570 nm) was deduced from all the spectra of the coated paper sheets. Figure III-50 clearly shows a saturation of the intensity of the reflectance signal on both sides of the paper after the third layer.

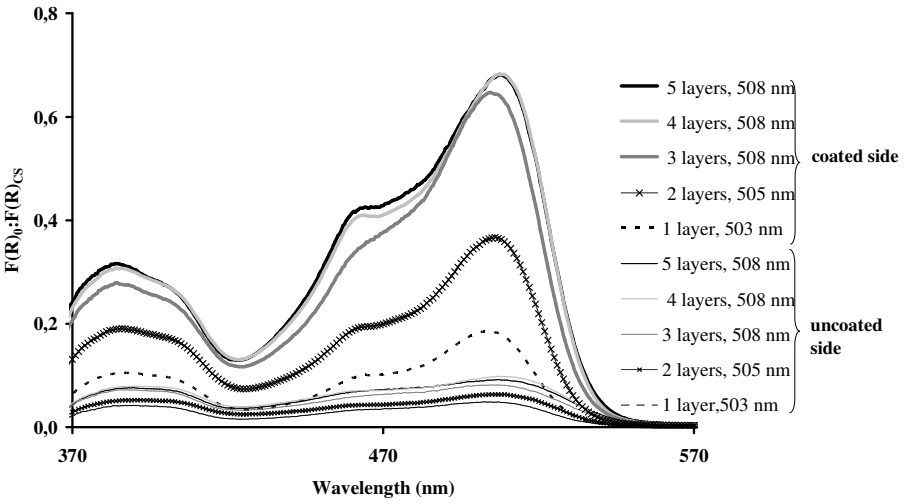

Figure III-50. Visible diffuse reflectance spectra of coated and uncoated side of FITC-LCH coated paper for one to five chitosan layers.

Figure III-51 displays a linear increase in the Kubelka-Munk function at 507 nm for the first three layers, followed by its stabilization for the two additional ones, suggesting that chitosan had attained a complete surface coverage and hence a constant reflectance intensity. This hypothesis was confirmed by the similar variation of the maximum wavelength intensity with the number of layers for the coated and uncoated paper sheets shown in Figure III-50.

The variation in reflectance (in the range of 503-508 nm) for the first three layers is related to the interaction of chitosan with the paper components (mainly cellulose fibres), which induced a modification of the environment of the chitosan derivative and a shift in the absorption wavelength. For the fourth and fifth layers, the wavelength maximum stayed at 508 nm, given the fact that the coverage of the paper surface had reached completion.

The fact that the fluorescent chitosan derivative was also detected on the *uncoated* side of the sheets confirmed that it had penetrated progressively throughout the paper thickness all the way to the other side.

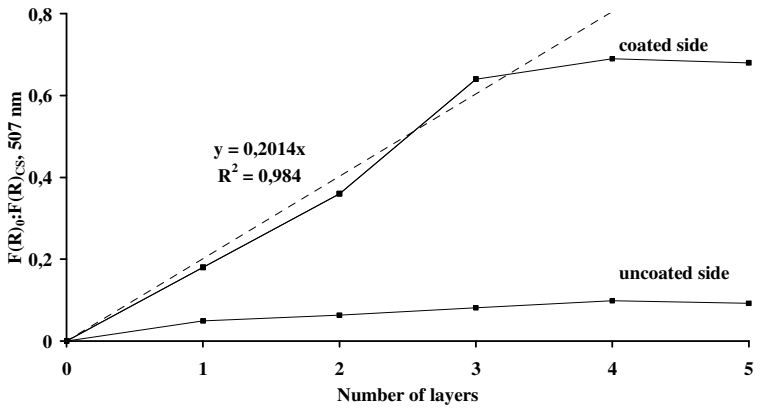

Figure III-51. Intensity variation at 507 nm of the remission function for the coated and uncoated side of FITC-LCH coated paper with the number of the chitosan layers.

13.1.2 Luminescence

Figure III-52A compares the emission features of the uncoated and coated paper sheets submitted to UV excitation. For all of them, the spectra displayed a main broad band with two components peaking around 430 nm, attributed to the optical brighteners agents present in the paper sheets. For the FITC-LCH-coated sheets, an additional emission band peaking at higher wavelengths was detected. This coating-related emission was in tune with that of the fluorescein moiety, known to occur around 510-540 nm [106].

Increasing the excitation wavelength from 370 to 500 nm (Figure III-52B), no change in the energy of the emission bands was measured, but only an enhancement in the relative intensity of the high-wavelength component. As the number of FITC-LCH deposited layers increased from 1 to 5, the fluorescein-related emission exhibited a bathochromic shift from 531 to 538 nm (Figure III-52A and B), attributed to the increase in the fluorescein concentration, as already observed for other dye compounds [317-318].

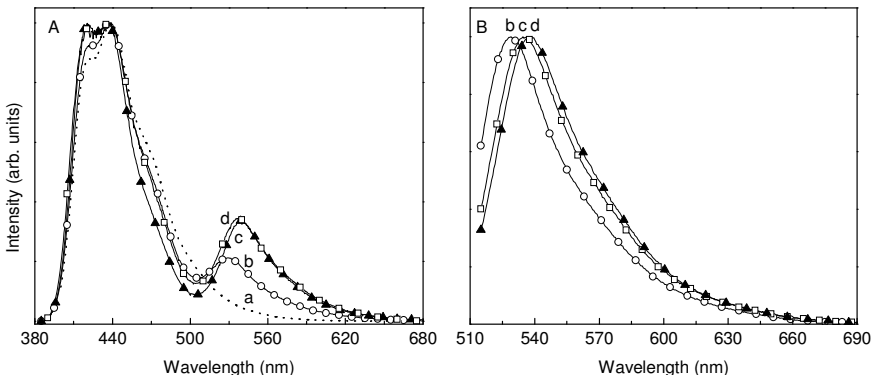

Figure III-52. Emission spectra of the CS (a, dotted line) and of the FITC-LCH1 (b, open circles), FITC-LCH3 (c, solid triangles) and FITC-LCH5 (d, open squares) sheets excited at (A) 370 nm and (B) 500 nm.

The effect of the coating on the emission features of the paper sheet under UV/vis excitation energies were quantified through the estimation of the CIE (x,y) colour coordinates. Figure III-53 shows the chromaticity diagram for the emission colour of the CS as well as the FITC-LCH1 and FITC-LCH3 sheets under two selected excitation wavelengths.

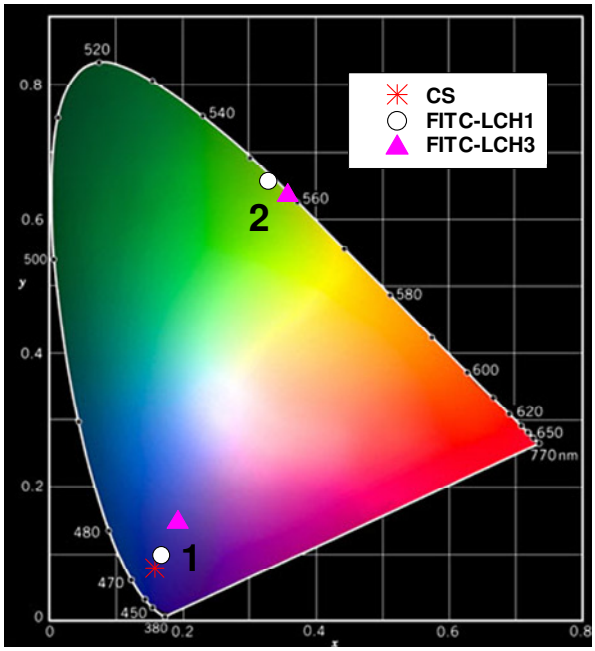

Figure III-53. CIE chromaticity diagram (1931) showing the emission colour coordinates of the CS as well as of the FITC-LCH1 and FITC-LCH3 excited at (1) 370 nm and (2) 500 nm.

The colour coordinates of the FITC-LCH5 paper were omitted because they resembled those of the FITC-LCH3 homologue. The emission colour coordinates of the CS were independent of the excitation wavelength and located in the purplish-blue region of the diagram. Under UV excitation, the emission colour coordinates of the FITC-LCH samples deviated towards the centre of the diagram due to the contribution of the chitosan-related emission component (Figure III-53). Under visible excitation, the emission colour coordinates were close to pure colours within the green region. By controlling the number of deposited layers and by varying the excitation wavelength from 370 nm to 500 nm, the emission colour coordinates could be readily tuned from the purplish-blue (FITC-LCH1, (0.19,0.09)) to the bluish-purple (FITC-LCH3, (0.20,0.14)) regions and from the yellowish-green (FITC-LCH1, (0.33,0.65)) to the yellow-green (FITC-LCH3, (0.36,0.63)) spectral regions, respectively.

The emission properties of the coated paper sheets were further quantified by the measurement of the radiance under UV-vis excitation (370 and 500 nm). The average values found for FITC-LCH1, FITC-LCH3 and FITC-LCH5 were 0.040, 0.029, and 0.027 $\mu W/cm^2sr$ at 370 nm and 3.471, 4.465 and 5.311 $\mu W/cm^2sr$ at 500 nm, respectively. Using the 370 nm excitation, the highest radiance value for the FITC-LCH1 was due to the higher relative contribution of the uncoated paper intrinsic emission to the overall photoluminescence features. Increasing the number of coating layers from 1 to 3 to 5, the radiance values decreased, indicating a more efficient coating. The similarity between the radiance values for FITC-LCH3 and FITC-LCH5 suggest that beyond 3 layers, a saturation of the paper coating was attained, as the diffuse reflectance spectra had pointed out. By exciting selectively the FITC-LCH-related emission, the radiance values increased progressively (up to 20-30%) with the number of deposited layers, indicating a correspondingly higher contribution of the FITC-LCH centres for the luminescence features. For both excitation wavelengths, the standard deviation was within the experimental error, confirming a homogeneous distribution of the deposited fluorescent chitosan.

13.1.3 Final remarks

This study proves that the distribution of chitosan onto the chitosan-coated paper is uniform and this macromolecule does not have a preferential way to cover the surface of the paper. Chitosan penetration into the sheets occurs progressively in the first layers, after the formation of a coating is observed on the paper sheet. Both techniques, reflectance and luminescence, show a saturation of the FITC-CH-coated paper after 3 layers.

According to these results, the next section will present and discuss the important effect of chitosan-coated paper on the final properties of the paper, using LCH and WSLCH in the conditions used in this work.

13.2 Effect of chitosan and chitosan quaternization on the final properties of chitosan-coated papers

As described before, the idea of combining chitosan with paper materials is not new. This combination is known to impart the paper products with better mechanical properties and printability and to control the microbial contamination of paper-based materials.

However, as previously referred, chitosan is not soluble in neutral aqueous media, but can be chemically modified in order to enhance its aqueous solubility at neutral pH. In fact, water soluble chitosan derivatives have been often used in retention- and drainage-aid agent and wet-end papermaking systems because of their strong interaction with cellulosic substrates or mineral fillers [250,319-323]. However, their use as coating agents is still poorly explored, since only one work dealing with the preparation and evaluation of the mechanical properties of coated papers by a spray deposition technique has been published so far [324].

This section reports the preparation and comparison of *E. globulus*-based papers coated with chitosan and a water soluble chitosan derivative, in order to avoid the use of acetic acid solutions and the consequent cellulose chains hydrolysis and paper ageing.

13.2.1 Morphology

The morphology of the CS, LCH and WSLCH papers was investigated by SEM using different magnifications (×150, ×500 and ×1500) and views (coated side, uncoated side and cross section).

The SEM images of the LCH coated papers (from Figure III-54 to III-56) clearly showed the features of their three major components, *viz*. the fibres, the inorganic fillers and the chitosan film, the latter being particularly evident when three or more CH layers were applied. The most interesting feature, however, has to do with the uniformity of the chitosan film over all the examined surfaces, which corroborates the spectroscopic observations and discussed in Section 12.1.

However, although the surface of the fibres was completely CH-coated when three or more layers were applied, the polymer did not fill completely the paper pores on its 3D structure, even with five layers. The presence of chitosan on the back of the sheet, shown in Figure III-54b confirms that this polymer did penetrate through the fibre network. As expected, this effect was strongly dependent on the number of deposited chitosan layers, particularly for the first three applications.

The information provided by the images obtained at higher magnifications (Figure III-55) was particularly instructive because it showed that as the number of chitosan layers increased, its well-known film-forming aptitude achieved a progressively more continuous morphology leading to a smooth surface coverage which incorporated both fibres and fillers. Particularly visible in these micrographs is the growing evenness of the sheet surface, as the thickness of the added polymer increases, which of course is a major feature in terms of the decrease in surface roughness (rugosity) and hence, most probably, of improved printing quality.

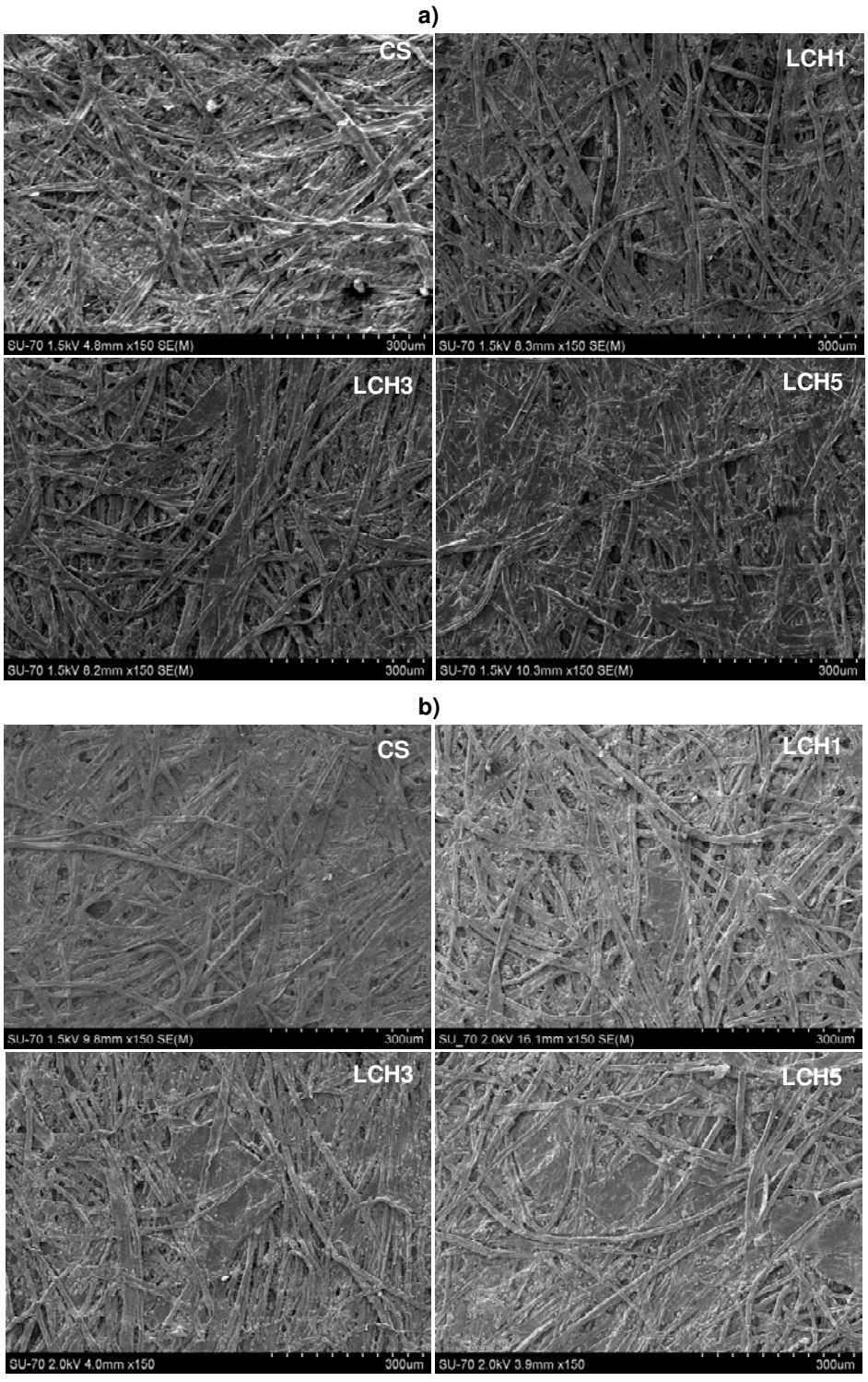

Figure III-54. SEM surface views (×150) of the CS, LCH1-, LCH3- and LCH5-coated papers from the coated a) and uncoated sides b).

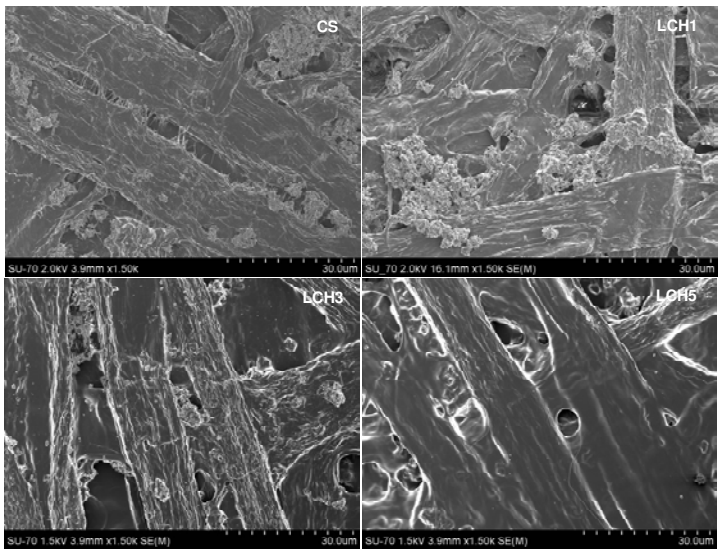

Figure III-55. SEM surface views (×1500) of the CS, LCH1-, LCH3- and LCH5-coated papers from the coated side.

The observation of the cross-section images (Figure III-56), revealed a progressive compaction of the fibres under the influence of a growing number of chitosan layers, a "gluing" effect which confirmed that the polymer did indeed penetrate within the paper sheet, to an extent that obviously depended on the number of its successive additions. This intimate interaction between the two polysaccharides is not surprising, given their structural affinity which translates into a pronounced tendency to form intermolecular hydrogen bonds.

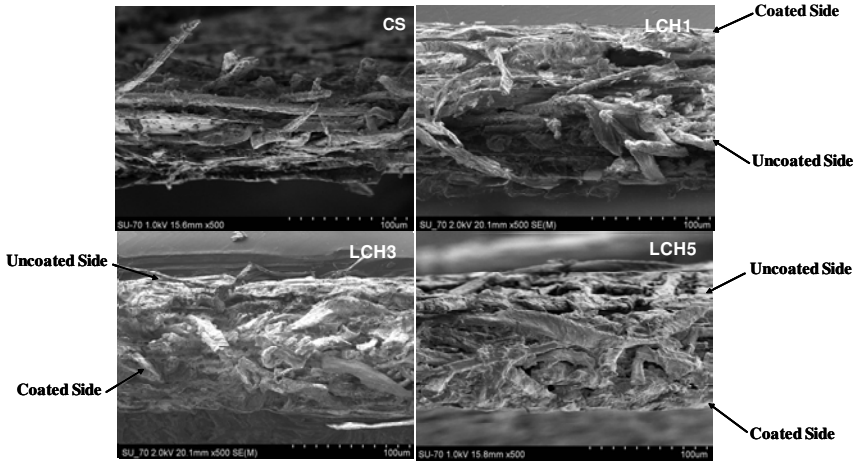

Figure III-56. Microscopic views (×500) of the CS, LCH1-, LCH3- and LCH5-coated papers observed from the cross-sectional.

Similar morphologies were also observed with the water soluble chitosan derivative (Figure III-57). This chitosan coating becomes particularly evident with the increasing number of chitosan layers, as previously demonstrated with LCH, certainly due to the well-known film-forming aptitude of chitosan derivative since the degree of quaternization investigated in this work did not affect this intrinsic property.

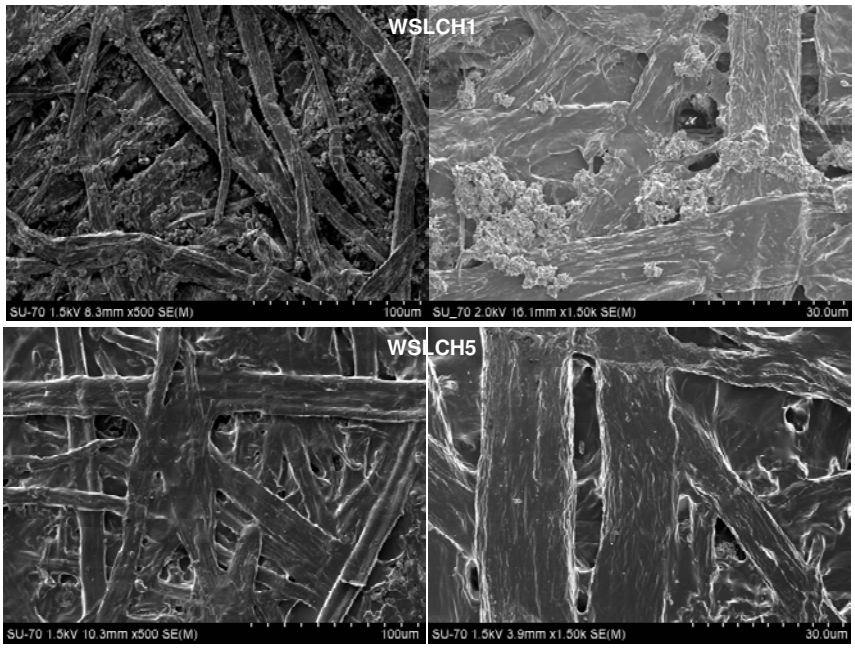

Figure III-57. Microscopic views (×500 and ×1 500) of the WSLCH1- and WSLCH5-coated papers.

13.2.2 Mass properties

The average grammage of the control paper sheet (CS) was 74.2 ± 0.2 g/m^2. For sheets treated with water (W) and 1% aqueous acetic acid solution (AA), a decrease in grammage was observed (0.4-0.5 g/m^2), independent of the number of layers (see Appendix 6). The same effect was also observed for the mechanical treatment (MT, see Appendix 6). These results can be explained by the removal of fine surface particles during the first coating layer.

Therefore, the grammage values, obtained with CH and WSCH (Table III-17), were corrected for this loss.

Table III- 17. Grammage, grammage gain and apparent density values of LCH- and WSLCH-coated papers.

	Grammage [g/m^2]				
	1 layer	**2 layers**	**3 layers**	**4 layers**	**5 layers**
LCH	75.8 ± 0.2	76.8 ± 0.2	77.4 ± 0.3	78.2 ± 0.2	78.9 ± 0.3
WSLCH	75.8 ± 0.3	76.5 ± 0.2	77.5 ± 0.2	77.9 ± 0.1	78.6 ± 0.1
	Grammage Gains [g/m^2]				
LCH	1.5 ± 0.1	2.5 ± 0.2	3.2 ± 0.3	3.9 ± 0.1	4.6 ± 0.3
WSLCH	1.6 ± 0.1	2.2 ± 0.2	3.0 ± 0.2	3.6 ± 0.2	4.3 ± 0.2
	Apparent Density [g/cm^3]				
LCH	0.74± 0.01	0.75± 0.01	0.75± 0.01	0.77± 0.01	0.77± 0.00
WSLCH	0.73± 0.00	0.74± 0.00	0.74± 0.01	0.75± 0.01	0.76± 0.01

As expected, the grammage gains, and consequently the grammage values, obtained with the chitosan based solutions increased linearly with the number of layer at rates of 0.76 and 0.68 g/m^2 for CH and WSCH coating, respectively as previously reported by Despond et al. [124]. However, the first layer originated a most significant grammage gain (1.5%), which could be explained by the easier penetration of the chitosan solutions through the discontinuous pristine paper network, whose pores and voids probably became less accessible after the first coating.

The average apparent density of CS was 0.74 ± 0.01 g/m^{3}and this value was not affected by the "blank" essays. Nevertheless, this parameter was only slightly affected by the LCH and WSLCH coating (Table III- 17). This phenomenon could be attributed to the penetration of the chitosan into the cellulose matrix in the first coating layer and to the chitosan continuous film forming (layer by layer) in the others coatings.

13.2.3 Roughness

Surface analysis, including roughness estimation, is particularly important in printing papers and packaging boards, because parameters like roughness affect such optical properties of paper as gloss and ink penetration.

The Bendtsen roughness of the CS was 330 ± 15 mL/min on both sides of the sheet. When the paper was treated with water or the aqueous acetic acid (1%) solution, this value

decreased to 250 mL/min, independent of the number of layers, probably due to the mechanical stress associated with the coating procedure that promoted the surface arrangement of the paper components (Appendix 7).

In the case of LCH and WSLCH-coated papers, the roughness decreased progressively with the number of layers (Figure III-58), because of the good film-forming capacity of chitosan, particularly after 3 coating layers. The chitosan film laminated the voids in the fibre network, thus reducing its roughness, as already showed by SEM. No significant differences were observed between the LCH and WSLCH-coated papers.

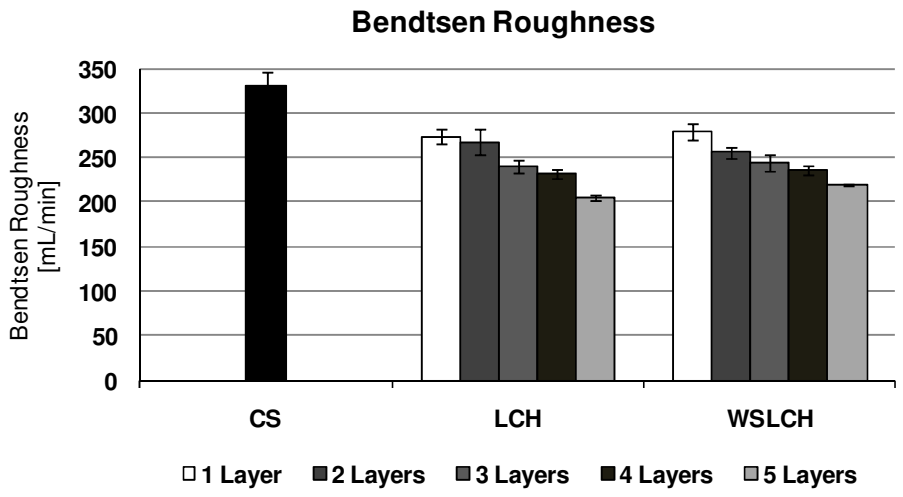

Figure III-58. Bendtsen Roughness of LCH- and WSLCH-coated papers.

13.2.4 Mechanical properties

Tensile Strength

Chitosan coating had a positive impact on all strength properties and, particularly, on the tensile index. Table III-18 gives the absolute values of tensile index and Figure III-59 its gain in percentage. Moreover, this behaviour was more pronounced in the cross-machine direction (CD) than in the machine direction (MD), as will be discussed below. The water and the acetic acid treatments decreased the tensile index in both machine and cross-machine direction (values in Appendix 8). This was probably, due to the establishment of hydrogen bonds with water or the acetic acid molecules and to the

acid-catalyzed hydrolysis of the cellulose chain (cleavage of 1,4-glycosidic bond) in the latter case. In fact, the tensile index loss was more pronounced after the acetic acid treatment than that with water. The tensile indexes values of both LCH and WSLCH-coated papers were therefore corrected for these losses.

Table III-18. Tensile index and stretch at break of control sheet and LCH- and WSLCH-coated papers in machine (MD) and cross-machine direction (CD).

	Tensile Index [N.m/g]					
	CS	**1 Layer**	**2 Layers**	**3 Layers**	**4 Layers**	**5 Layers**
			LCH			
MD	88.4 ± 1.1	100.3 ± 1.2	110.1 ± 0.8	114.2 ± 0.3	115.1 ± 0.7	117.4 ± 0.8
CD	26.0 ± 0.4	28.7± 0.4	31.8 ± 1.0	34.0 ± 1.8	35.3 ± 0.7	37.5 ± 0.4
			WSLCH			
MD	88.4 ± 1.1	95.9 ± 1.2	104.2 ± 1.3	111.1 ± 1.3	113.6 ± 1.7	116.9 ± 0.9
CD	26.0 ± 0.4	28.6 ± 0.9	30.7 ± 1.0	33.8 ± 1.2	34.09± 1.3	35.09± 1.4
	Stretch at Break [%]					
			LCH			
MD	2.0 ± 0.1	2.7 ± 0.1	2.9 ± 0.1	3.0 ± 0.0	3.3 ± 0.1	3.4 ± 0.1
CD	3.1 ± 0.1	4.4 ± 0.3	4.7 ± 0.4	5.0 ± 0.1	5.1 ± 0.4	5.2 ± 0.0
			WSLCH			
MD	2.0 ± 0.1	2.7 ± 0.1	2.8 ± 0.2	3.0 ± 0.0	3.2 ± 0.1	3.3 ± 0.2
CD	3.1 ± 0.1	4.1 ± 0.1	4.7 ± 0.4	4.8 ± 0.0	5.1 ± 0.3	5.3 ± 0.1

The paper coating with LCH and WSLCH did not promote the same reinforcing effect in the MD as in the CD, because of the high resistance of the fibres themselves and because of their rigid lengthways in the MD. In the MD, the tensile index increased with the number of LCH and WSLCH layers deposited, but was slightly more pronounced for LCH coating in the first three layers. However, after the third layer the tensile index gain tended to a plateau with both LCH and WSLCH (Figure III-58).

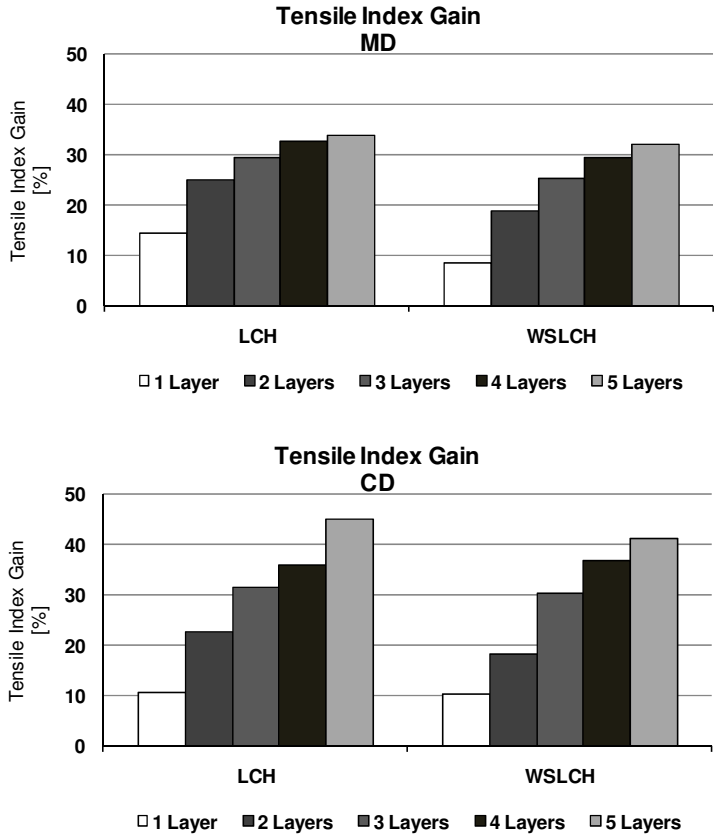

Figure III-59. Tensile index gain of LCH- and WSLCH-coated papers in MD and CD.

The reinforcing effect observed in the CD, even if less intense in absolute value (Table III-18) is considerably more relevant in % of tensile index gain (Figure III- 59), which is ascribed to the good film-forming ability and flexibility of LCH and WSLCH that strengthened the cellulose fibres inter-bonds (see Figure III-55 and III-57). In the literature, some authors found the same results, *viz*. a positive impact on the mechanical properties after coating the paper with chitosan and water soluble chitosan derivatives [244,324]. However, for other authors this impact was not so significant [123,126,241].

Although coating experiments are not often used to improve the tensile properties, which for paper materials are intrinsically good enough, with the improvement in tensile properties demonstrated here, it could be possible to decrease considerably the energy consumption associated with the beating.

The stretch at break also increased with increasing in the LCH and WSLCH coating weights (Table III-18). Gains of 60 and 70% were in fact observed for papers with 5 layers of chitosan or water soluble chitosan (see Appendix 8).

Bursting Strength

The effect of chitosan coating on the burst index (an important parameter in packaging products) is shown in Figure III-60. In this case, the "blank" essays showed just a slight negative influence on the mechanical properties and only after 3 or more coating layers (e.g. CS 3.15 $kPa.m^2.g^{-1}$, W5 or AA5 3.03 $kPa.m^2.g^{-1}$, values in Appendix 8). The LCH and WSLCH coatings improved considerably the paper bursting strength, particularly for one single coating layer. This result is partly attributed to the penetration of chitosan into the fibres network and also to the high compatibility between chitosan and the cellulose fibres resulting in the formation of a continuous film incorporating the fibres.

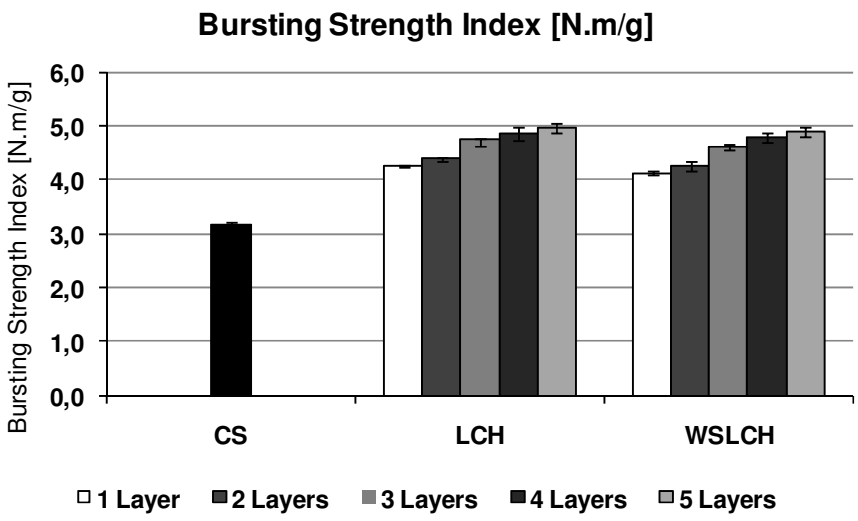

Figure III-60. Bursting strength index of CS, LCH- and WSLCH-coated papers.

Surface Strength

The paper surface strength is a property that refers to the surface fibres and fillers bonding to the paper sheet network. This parameter is particularly relevant during printing

and the frequent rewetting of the paper sheets. Here, the paper surface strength was determined by the wax pick method and the results are shown in Table III-19.

This method is based on a series of hard calibrated waxes (numbered from 2 A to 26 A) with adhesive power were detached from the paper surface. The wax with the highest number in the series that does not damage the surface of the paper is the numerical evaluation of surface strength. The numbering of waxes increases in proportion to its power of adhesion.

Table III-19. Surface strength of LCH- and WSLCH-coated papers.

	Surface Strength [A]				
	1 layer	**2 layers**	**3 layers**	**4 layers**	**5 layers**
LCH	16	18	18	20	20
WSLCH	16	18	18	20	20

The surface strength of the CS was 14 A and this value was not affected by the water and the acetic acid treatments. However, it increased 2 A and 6 A wax numbers for papers coated with 1 and 5 layers of LCH or WSLCH, respectively. The LCH and WSLCH films covered the cellulose fibres and the fillers and consequently increased their adhesion. These observations are in agreement with previously reported results for chitosan coatings [240].

13.2.5 Barrier properties

Air Permeability

Figure III-61 displays the Bendtsen air permeability of the paper sheets before and after the LCH and WSLCH coating experiments.

The water and acetic acid treatments caused a slight increase in the air permeability, which was probably due to a little disruption of the fibre network and a consequent increment in paper porosity. However, the paper coating with both LCH and WSLCH promoted a considerable and progressive decrease in air permeability, as the amount of chitosan increased, attaining very low values (near the detection limit of the method used)

for four and five coating layers. In these cases, the chitosan filled the pores and begun to develop an almost continuous chitosan film, as confirmed by the SEM analysis (see Figure III-55 and III-57).

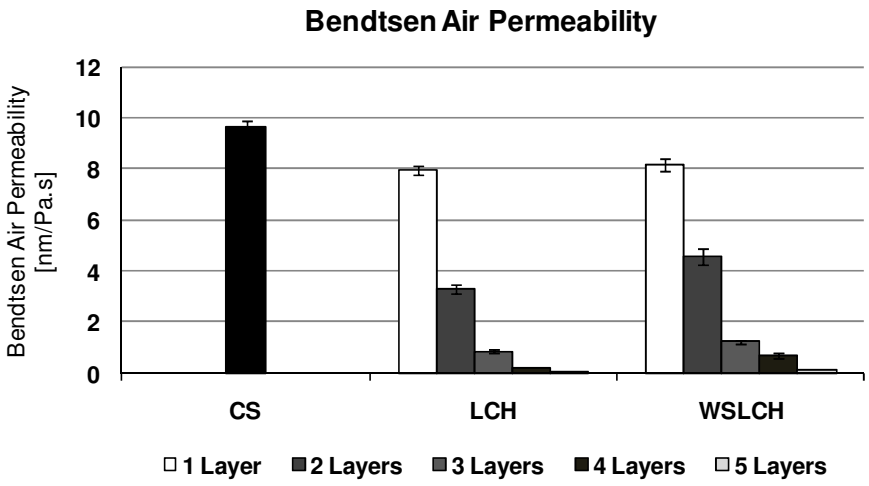

Figure III-61. Bendtsen air permeability of LCH- and WSLCH-coated papers.

Water Vapour Permeability

No significant differences in the water vapour permeability (WVP) were observed between the CS and the LCH and WSLCH-coated papers for one and three coating layers (Table III-20).

Table III-20. WVP values for CS and LCH- and WSLCH-coated papers.

	WVP [10^{-2} mm g/h kPa m]			
	CS	**1 Layer**	**3 Layers**	**5 Layers**
LCH	3.24 (±0.04)	3.22 (±0.03)	3.20 (±0.06)	1.85 (±0.06)
WSLCH		3.20 (±0.10)	3.28 (±0.06)	4.06 (±0.09)

However, for five LCH coating layers, the WVP decreased by about 45% because, as already referred, after 3 layers the chitosan deposited onto paper sheets forms an almost continuous film and also may contribute to the increase of polymer-polymer interactions,

thus decreasing the WVP. Another probable reason for this observation is the presence of impurities inherent to the chitosan sample as described before, which provide a surface hydrophobization of the paper sheets. On the other hand, as expected, in the case of WSLCH, the opposite was observed (for five layers), because WSLCH is much more sensitive to water vapour due to its ionic character.

13.2.6 Optical properties

LCH and with WSLCH coating of paper sheets showed only a modest influence on their opacity, but reduced appreciably their brightness. Brightness is one of the optical terms used in paper industry to describe the quality of white paper for printing, and is defined as the percent reflectance of blue light, centred at 457 nm.

The CS opacity was 92.6% and the values obtained for the LCH and WSLCH-coated papers, as well as for the "blank" assays, were in the range of 92.2% - 93.1% (values in Appendix 9).

The appreciable loss of brightness observed after the chitosan paper coating (Figure III-62 see values in Appendix 9) was mainly influenced by the brownish colour of the chitosan samples that "covered" in part the optical additives. This aspect was more pronounced for LCH, since during the quaternization of chitosan, and subsequent isolation steps, involved in the preparation of WSLCH, an appreciable part of such impurities were removed. Nevertheless, this situation could be easily overcome by using a purer chitosan, as will be discussed in the next section.

Moreover, in the case of the LCH coated papers, the brightness reduction was also strongly promoted by the presence of residual acetic acid. The significant loss of the brightness of LCH coated paper in relation to the papers only "coated" with AA, was probably due to the fact that the acetic acid evaporation is more difficult in the presence of chitosan and also to the brownish chitosan colour (Figure III-62). These results are in agreement with those reported by Lertsutthiwong et al. [240], who used chitosan as a surface sizing agent and also observed a considerable reduction in the ISO brightness.

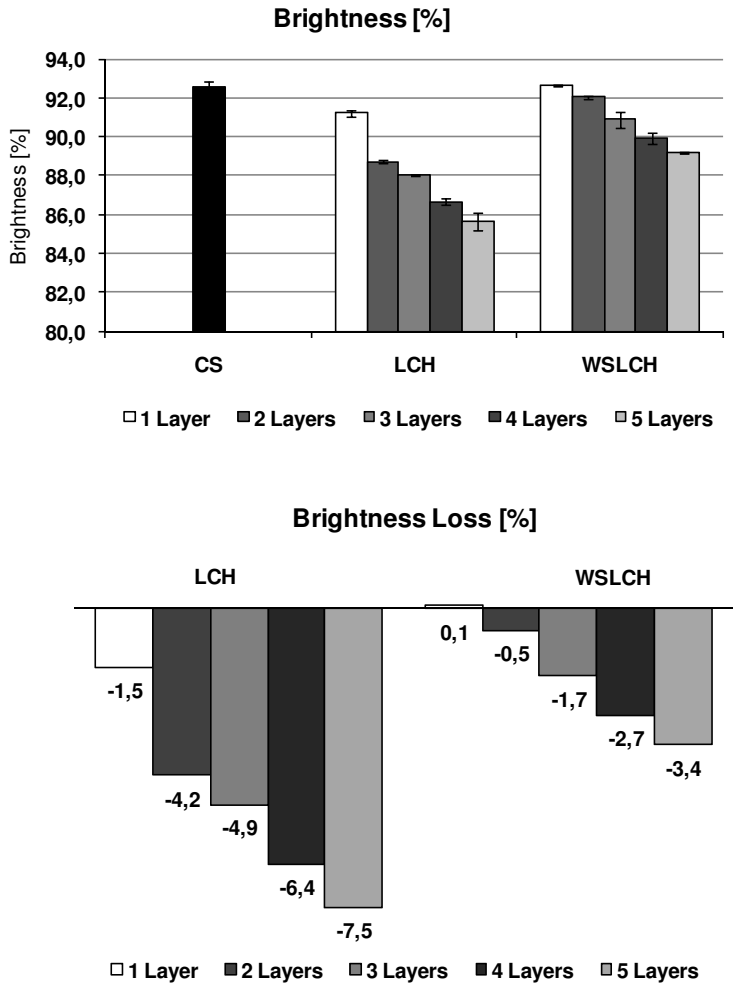

Figure III-62. Brightness and brightness loss of LCH- and WSLCH-coated papers.

13.2.7 Paper lightfastness

In order to evaluate the lightfastness (paper ageing) of the LCH and WSLCH-coated papers, their optic parameters CIE L*, a*, b* and whiteness were measured before and after being exposed to a light source under controlled conditions. The results were expressed in terms of the colour difference (ΔE) and delta whiteness (see Figure III-63 and values in Appendix 10). Whiteness, like brightness, is also widely used to describe the quality of white papers. However, whiteness refers to the extent that paper diffusely reflects light of all wavelengths throughout the visible spectrum (400-700 nm).

The parameter ΔE was calculated according to the expression:

$$\Delta E = \sqrt{(\Delta L)^2 + (\Delta a)^2 + (\Delta b)^2}$$ **Equation III- 2**

Where, ΔL, Δa and Δb are the algebraic differences before and after being exposed to a light source. Figure III-63 illustrates the lightfastness of the CS and different chitosan coated paper materials, including the blank essays, for 1, 3 and 5 layers.

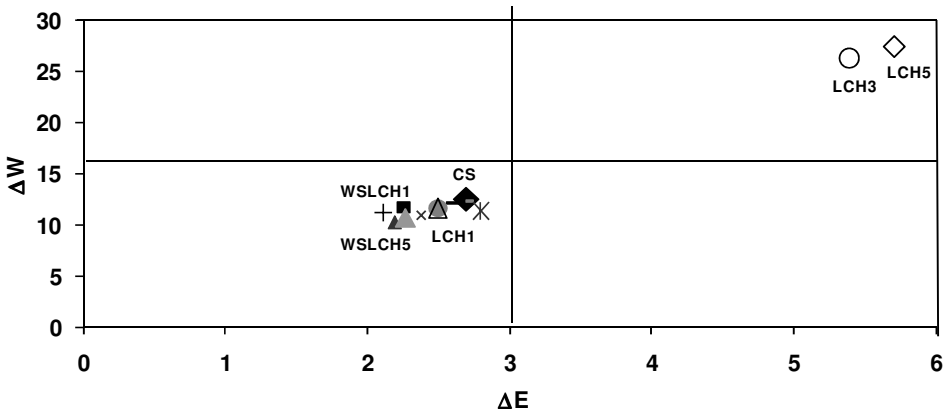

FigureIII-63. Lightfastness of CS and LCH- and WSLCH-coated papers.

The paper sheets treated with water or acetic acid had approximately the same lightfastness as the CS, meaning that they do not have a detrimental effect. However, it was possible to observe a negative tendency for the papers treated with acetic acid when the number of layers increased, and an inverse trend with respect to the water treated papers, probably because the water "cleaned" some of the acid that remained on the surface of the paper. The LCH-coated papers showed a considerable increase in the lightfastness when the number of layers increased (3 and 5 layers) certainly because of the presence of residual acetic acid that did not evaporate due to the formation of the LCH film and also to the optical properties of this coated papers, as previously discussed. It is known that environments with low pH affects the ageing of paper [325]. On the other hand, the WSLCH coated papers showed an improvement on the lightfastness in relation to the CS.

Therefore, it seems that the WSLCH acts like a protecting coating against the ageing of paper. The coating formulations to be applied to long-life, permanent papers and to those for archival, should be acid-free and have a pH slightly above 7 [325]. This parameter is very important, given market requirements in terms of better printability, superior brightness and whiteness and paper quality/durability.

13.2.8 Inkjet print quality

Paper and paperboard coating is normally used to improve printability. This parameter is influenced by such surface properties as porosity, smoothness and surface strength, as well as by the brightness and opacity. Colour density, Gamut Area (GA), Inter Colour Bleed and image analysis are the most widely used parameters to access inkjet print quality. A mask was used to evaluate the inkjet print quality of the chitosan-coated papers.

Colour Density

Colour density (the "richness" of the colour) is largely determined by the ink penetration in the z-direction, *i.e.* a high density is achieved when the dye is fixed near the surface at the point of impact [326]. In general, all chitosan-coated papers displayed higher colour densities than the CS (Table III-21 for black colour and Appendix 11). These results are in good agreement with previous studies [240,242]. This behaviour is in part associated with the decrease in paper porosity, as confirmed by the increase in the air resistance after the chitosan coating. Besides, the interactions established between the inks and chitosan also play an important role.

Table III-21. Colour density of black of CS a commercial paper and chitosan-coated papers.

	Colour Density of black						
	CS	**Commercial Paper**	**1 Layer**	**2 Layers**	**3 Layers**	**4 Layers**	**5 Layers**
LCH	1.28±0.02	1.37±0.02	1.47±0.01	1.49±0.02	1.54±0.01	1.59±0.01	1.61±0.02
WSLCH			1.41±0.01	1.48±0.02	1.47±0.01	1.49±0.01	1.48±0.02

Gamut Area

The addition of LCH had a positive effect on the GA (Table III-22) for low coating weights (one layer, Figure III-64), but for three or more layers the GA values drastically decreased, probably due to the increase in the acidic environment and to the decrease in the optical properties (brightness and whitness) of the papers with increasing numbers of LCH layers. It is known that low-pH media (below about 4.5), originated for example by acidic formulations such as the LCH ones, can retard or prevent the ink drying or cause ink chalking [325].

However, in the case of WSLCH, the GA increased from below 7400 (CS) to 8000, without important variations between the different coating layers. WSLCH seemed more appropriate in terms of colour printing, probably because of the greater polar feature provided to the paper surface by a more hydrophilic coating, which resulted in a higher affinity with the water-based inks. On the other hand, it is interesting to note that, according to the coordinates of each point of the graphics in Figure III-64, all samples reproduce each colour almost in the same way.

The positive tendency of GA values of blank assays could be related to the increase in surface "cleanliness" of paper with the number of layers (see results in Appendix 11).

Table III-22. Gamut Area of CS, a commercial paper and chitosan-coated papers.

	Gamut Area						
	CS	**Commercial Paper**	**1 Layer**	**2 Layers**	**3 Layers**	**4 Layers**	**5 Layers**
LCH	7415±22	7224±30	7667±20	7630±32	7045±22	6610±18	6335±18
WSLCH			8063±31	8043±39	8056±43	7984±37	7937±29

Moreover, the increase in GA is probably also a consequent of the aptitude of chitosan to form a film on the paper surface, resulting in a reduction in its porosity and in ink penetration. The inks have a strong tendency to penetrate into the pores and also to spread around the fibres, which tends to reduce their intensity and colour density on the surface of the paper sheets and consequently the GA. These results showed that small quantities of chitosan could modify the inkjet print quality of the paper sheet.

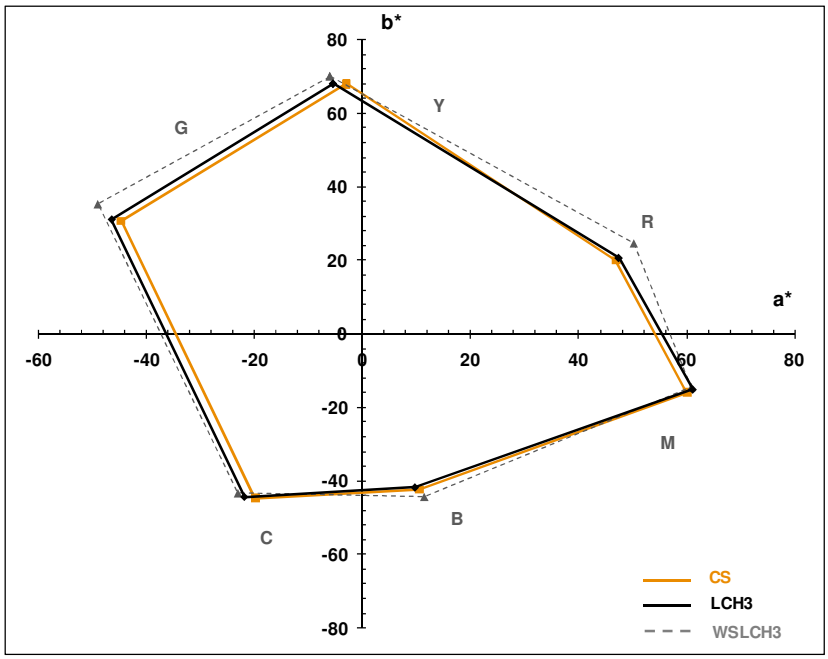

FigureIII-64. Gamut area of CS, LCH1- and WSLCH3-coated papers. The characters G, Y, R, M, B and C means green, yellow, red, magenta, blue and cyan, respectively.

Inter Colour Bleed

The good film-forming ability of both LCH and WSLCH is also quite important on the reduction of the Inter Colour Bleed (Table III-23, Figure III-65 and Appendix 12). However, in the case of the WSLCH-coated papers, this effect was not so pronounced, because of the high affinity of this chitosan derivative to the water-based inks.

Table III-23. Inter Colour Bleed of CS, LCH- and WSLCH-coated papers.

	Inter Colour Bleed						
	CS	**Commercial Paper**	**1 Layer**	**2 Layers**	**3 Layers**	**4 Layers**	**5 Layers**
LCH	46±2	45±1	50±2	43±2	44±2	38±1	32±1
WSLCH			56±3	50±39	48±1	47±2	49±2

The high Inter Colour Bleed values for the first layer could be explained by the affinity of the ink with chitosan solutions that go through the voids and paper pores promoting the spreading.

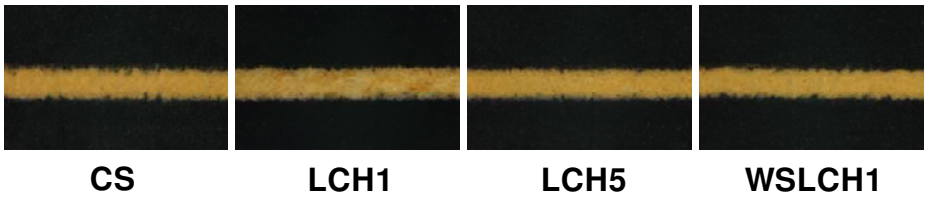

Figure III-65. Examples of Inter Colour Bleed images of CS, LCH1-, LCH5- and WSLCH1-coated papers.

Images Analysis

The effect of the LCH and WSLCH-coated papers on the spreading of the black dots and lines was also measured. Line and dots spreading occurs mainly when the surface of paper consists of disconnected features. However, once again, the good film-forming ability of both LCH and WSLCH derivative contributed to the reduction of the black dot and horizontal line spreading (Figure III-66). Nevertheless, the results, even if higher than those of commercial papers (Appendix 12), are still somewhat distant from the desired dimensions (Figure III-66).

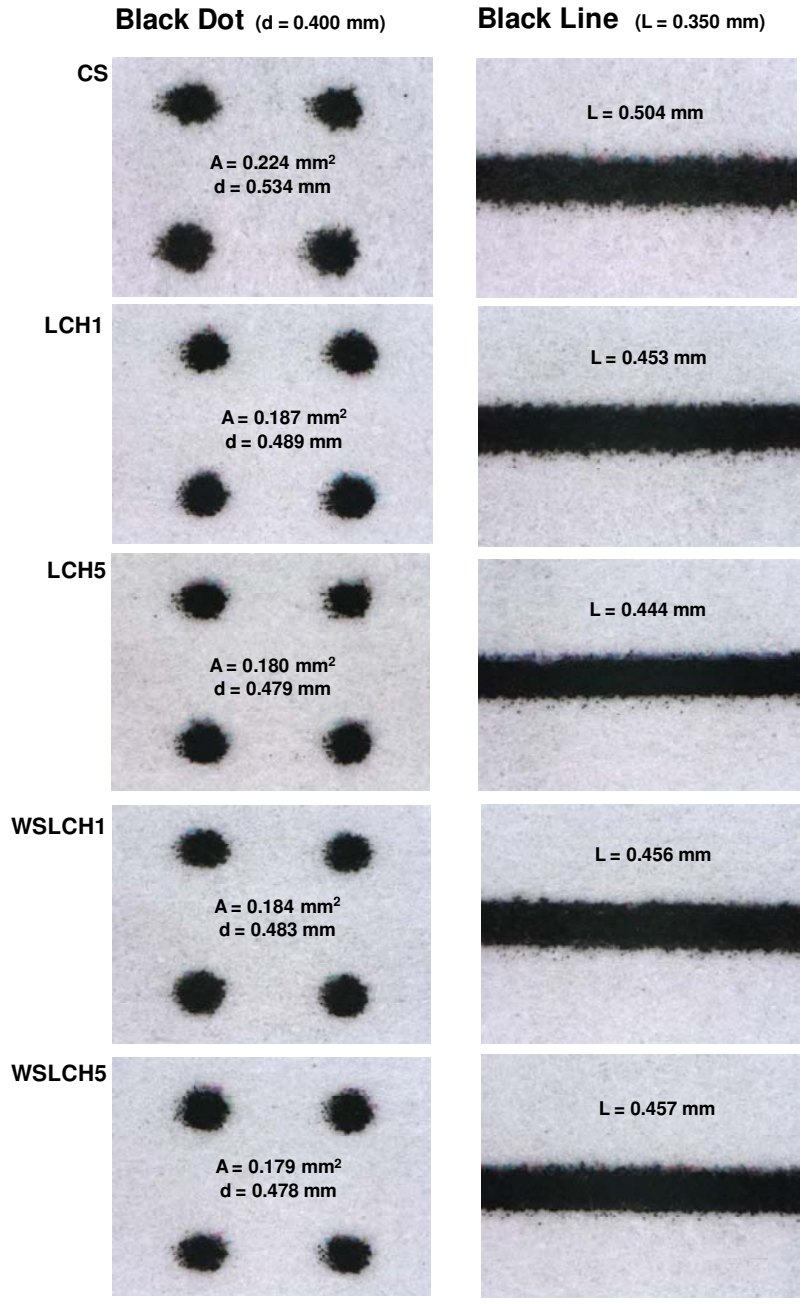

FigureIII-66. Pictures of black dots and black lines of CS and selected LCH- and WSLCH-coated papers (d=0.400m and L=0.350mm are de ideal values for these parameters).

To sum up, chitosan is associated with a significant improvement of the inkjet print quality of paper with better results than with commercial papers

(see Appendices 13 and 14). In particular, the water soluble chitosan derivative had a higher impact in terms of Gamut Area and colour density.

13.2.9 Final considerations

This study has shown that coating of *E. Globulos*-based paper sheets with both LCH and WSLCH derivatives had a positive impact in the final properties of the coated papers namely in terms of mechanical properties, roughness, air permeability and inkjet print quality, and that the quantitative improvement of the mentioned properties was dependent on the number of deposited chitosan layers. Furthermore, the WSLCH derivative coated papers showed superior brightness, ageing stability and ink jet print quality than those coated with LCH. This behaviour is probably associated with the absence of residual acetic acid in these coating formulations. In sum, this investigation showed that the use of water soluble chitosan derivatives on paper coating processes represents a promising and sustainable approach for the development of new functional paper materials.

14 Chitin and chitosan oxypropylation

The purpose of this investigation was to establish the feasibility of converting chitin and chitosan into viscous polyols via a simple oxypropylation reaction, without any attempt to optimize the processes through a systematic study of the role of each parameter (Figure III-67). The mechanism of these bulk oxypropylations calls upon the activation of some of the substrate OH groups by a Brønsted or Lewis base to produce the corresponding oxianions, from which PO oligomers are grafted by its ring-opening anionic polymerization. Because transfer reactions inevitably occur in this process, the formation of some PO homopolymer (PPO) always accompanies the actual oxypropylation.

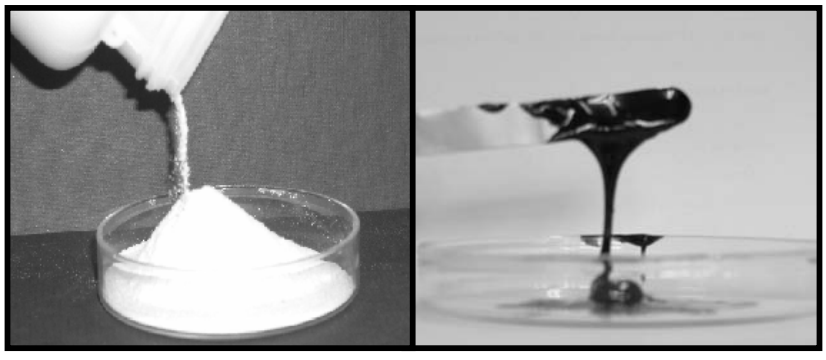

Figure III-67. Chitin powder and the ensuing viscous polyol via oxypropylation reaction.

With the conditions described in Chapter 9, the extent of oxypropylation of both chitin and chitosan was relatively high, but not complete, as measured by the relatively modest amounts of unreacted or poorly oxypropylated solid residues (5-15% and ~25%, respectively for chitin and chitosan). The lower reactivity of chitosan was interpreted on

the basis of its higher cohesive energy [303] arising from the very strong intermolecular hydrogen bonds involving both its OH and NH_2 groups, because the reoxypropylation of the corresponding solid residue gave the same result (~25% of unreacted material), suggesting that the added amount of PO had not been the limiting factor in the first treatment. It is important to emphasize here that there is no doubt in our minds that the systematic study of both these systems will provide the appropriate conditions insuring total conversion of the substrates into liquid products.

As mentioned in Chapter 9, the oxypropylation of OH-containing substrates, such as polysaccharides, inevitably gives two products, namely the oxypropylated macromolecules and some PPO [262-265,268]. Their relative proportion, which depends on the reaction conditions, obviously influences the physical properties, as well as the reactivity of these polyol mixtures. It has been shown that these two polymers can be efficiently separated by extracting the reaction mixture with n-hexane [265], since the HP fraction is selectively removed by this solvent. In the present study, the proportion of HP formed was systematically around ~40%, in close agreement with that obtained with other natural substrates oxypropylated under similar reaction conditions [263,265,271].

14.1 Structural properties

FTIR

Figure III-68 shows typical FTIR spectra of chitosan and the two liquid polyol fractions (HP and PL) resulting from its oxypropylation. As expected, the spectrum of HP displayed the same bands as those of a commercial sample of PPO, *viz*. around 3380 cm^{-1}, assigned to the OH stretching modes; in the range 2870-2970 cm^{-1} for the C-H stretching modes of the aliphatic CH_3 CH_2 and CH groups; an increase in the band at 1370 cm^{-1} confirming the introduction of CH_3 groups; and around 1080 cm^{-1} for the C-O-C moieties [327]. The spectrum of the chitosan PL also showed the latter features, plus an additional peak around 1590 cm^{-1}, assigned to the N-H deformation mode of primary amines [327], arising from the chitosan monomer units. These results corroborated the occurrence of the

oxypropylation reaction through the grafting of PPO chains onto the polysaccharide backbone and the efficiency of the use of n-hexane as a discriminating solvent.

The two polyol fractions obtained in the oxypropylation of chitin also presented different FTIR spectra, but with the carbonyl amide band at 1680-1630 cm^{-1}, resulting from the chitin monomer units, as the main distinguishing feature (Appendix 13).

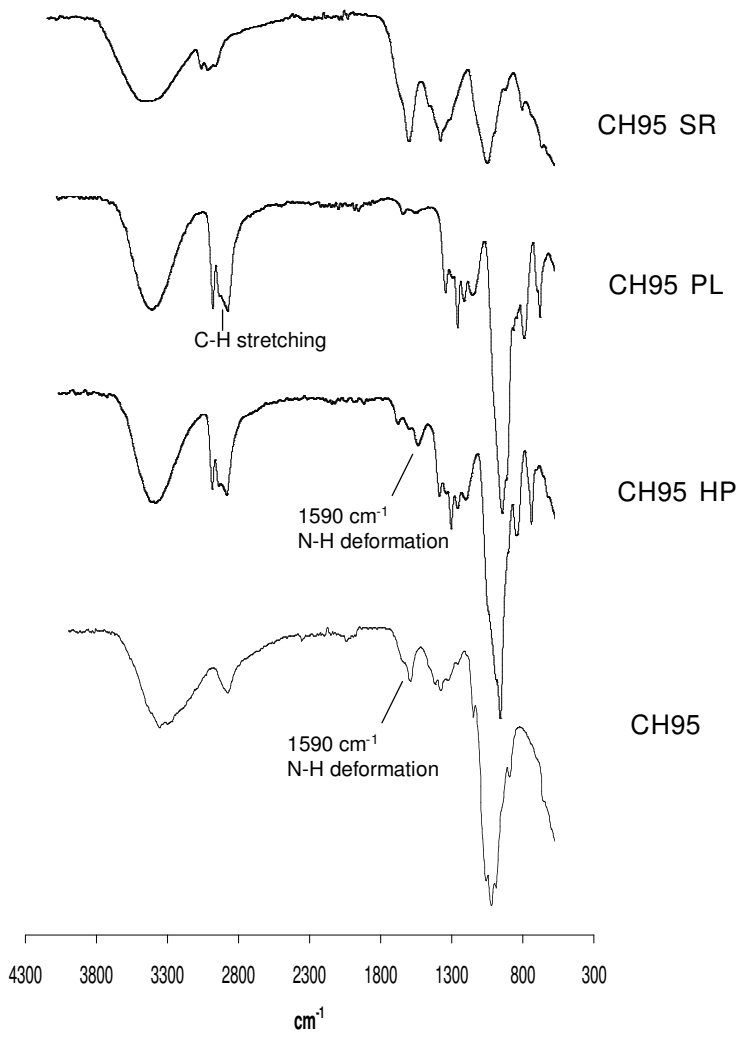

Figure III-68. Typical FTIR spectra of chitosan, the two liquid polyol fractions (HP and PL) and the solid residue (SR) resulting from its oxypropylation at 140 ºC.

^{1}H NMR

Figure III-69 shows typical ^{1}H NMR spectra of chitosan and of the two chitosan-related products, following the extraction with n-hexane. The ^{1}H spectrum of chitosan, obtained in an acidic solution at 50 ºC, is in close agreement with previously published spectra [48,52].

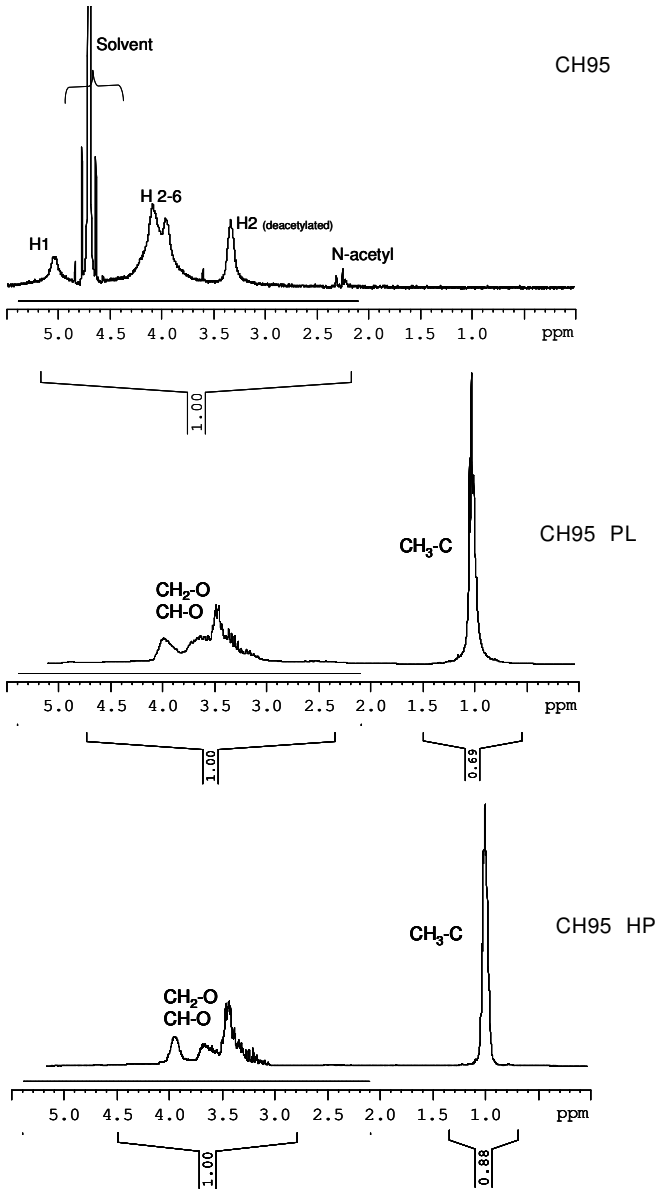

Figure III-69. ^{1}H NMR spectra of CH95 (dissolved in CD_3CO_2D (1%)/D_2O) and of the two fractions (HP and PL, dissolved in $CDCl_3$) obtained after its oxypropylation at 120 ºC. Chemical shifts are expressed in δ (ppm) values relative to tetramethylsilane (TMS) as the internal reference.

On the other hand, the soluble material gave a spectrum very similar to that of commercial PPO, except for a slightly higher integration in the 3-5 ppm region, characteristic of CH-O and CH_2-O protons, compared with that of the methyl groups around 1 ppm, suggesting that small amounts of the oxypropylated chitosan had also been extracted, since for PPO alone those integrations are identical. The spectrum of the n-hexane-insoluble polyol showed, as expected, a higher contribution of the ether-type peaks, reflecting the presence of the chitosan backbones. In the case of the corresponding products relative to the oxypropylation of chitin, the extracted material gave a spectrum virtually identical to that of PPO, whereas that of the residue showed a less pronounced relative integration of the ether protons, compared with the chitosan-based counterpart. These results corroborated the previous indication related to the lower reactivity of chitosan in these oxypropylation conditions.

14.2 Elemental analysis

Table III-26 gives a selection of results related to the elemental analysis of the different fractions isolated following the oxypropylation of both substrates. The low, but non-zero nitrogen content of the HP fractions confirmed the conclusions drawn from the ^{1}H NMR spectra concerning the fact that n-hexane actually extracted the PPO and a very small amount of oxypropylated substrate, more so in the case of chitosan. The nitrogen content of the oxypropylated chitin and chitosan fractions was however much higher than that of their corresponding homopolymeric fractions, as expected for these truly grafted samples.

In addition, the nitrogen contents of the solid residues were lower than those of the initial substrates, but higher than those of the corresponding n-hexane insoluble products, confirming that the residues were composed mainly of weakly oxypropylated chitin or chitosan, as already suggested on the basis of the FTIR analysis and of the reoxypropylation experiments. Interestingly, these second experiments gave, not only a similar percentage of solid residue, but also elemental analyses which replicated those related to the corresponding first run, as shown in Table III-26.

Table III-26. Elemental composition of the fractions isolated following the oxypropylation of chitin and chitosan at 140 ºC and 120 ºC. ROx refers to the reoxypropylation experiments.

Sample	C [%]	N [%]	H [%]
Chitin	41.87	6.03	6.41
CH95	37.22	7.16	6.86
Chitin HP (set 1)	57.79	0.42	9.90
Chitin HP (set 2)	57.42	0.47	10.22
Chitin PL (set 1)	56.25	1.82	8.79
Chitin PL (set 2)	55.24	1.84	8.25
SR chitin	52.54	2.57	8.10
ROx chitin HP	57.72	0.47	9.70
ROx chitin PL	53.19	1.59	8.46
CH95 HP (set 1)	53.09	1.21	10.16
CH95 HP (set 2)	54.85	0.65	9.86
CH95 PL (set 1)	54.29	2.23	8.45
CH95 PL (set 2)	53.75	2.67	8.20
SR CH95	42.36	4.54	6.55
ROx CH95 HP	56.16	0.41	9.79
ROx CH95 PL	47.52	2.04	7.67

14.3 Thermal stability

The two fractions resulting from the oxypropylation of these natural substrates showed in all cases markedly different TGA profiles (Figure III-70). Thus, the HP fractions displayed a typical single weight loss and a maximum decomposition temperature at 240-290 ºC, characteristic of PPO. On the other hand, the oxypropylated counterparts gave profiles which were a combination of those of the corresponding natural polymer and of PPO, with two main losses at 250-270 and 350-370 ºC, indicating that the grafted architecture of these materials did not alter their thermal degradation in relation to their separate components.

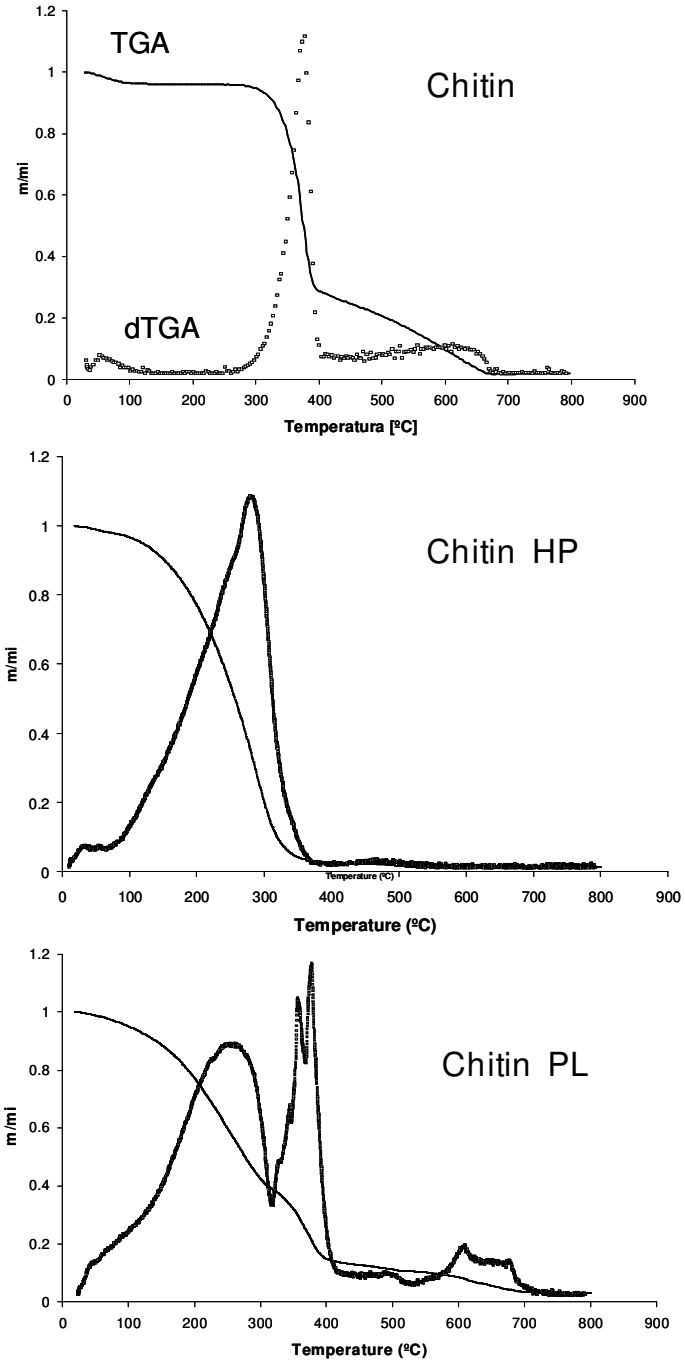

Figure III-70. TGA thermograms of the two fractions (HP and PL) obtained from the oxypropylation of chitin at 140 ºC.

14.4 DSC

The Tg of the HP products were consistently around -75 ºC, *i.e.* the typical value for low molecular-weight PPO (Figure III-71). The n-hexane-insoluble products gave Tg values of about -55 ºC for both oxypropylated polysaccharides (Figure III-71). This increase in Tg reflects the stiffening role of the natural polymer backbone, but the modest increment suggests that the PPO grafts played a predominant plasticizing role in these structures. These results are in good agreement with those previously published for similar products obtained in the oxypropylation of other natural substrates [263-264].

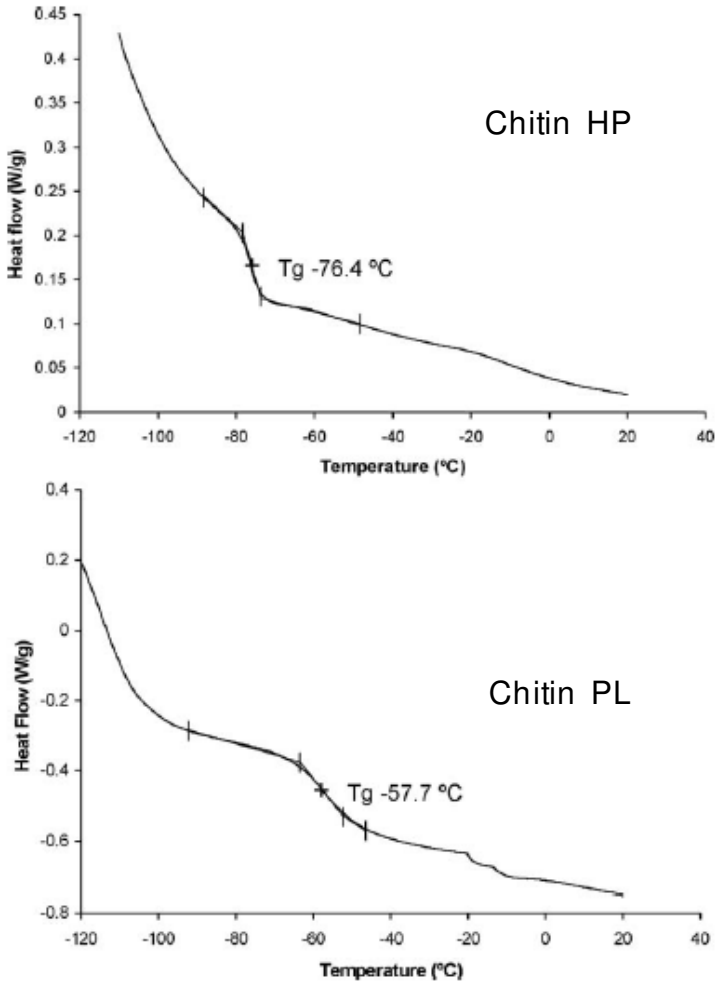

Figure III-71. DSC thermograms of the two fractions (HP and PL) obtained from the oxypropylation of chitin at 140 ºC.

14.5 Viscosity

The viscosities of chitosan's PLs (50 000 Pa.s) were some 5 times higher than those of chitin's homologues. This further confirmed the lower reactivity of the former polysaccharide. Of course, all the polyol mixtures before extraction were some 100 times less viscous, given the low viscosity of the accompanying PPO oligomers.

Hence, these mixtures, as recovered after the oxypropylation reaction, without any separation or purification, are the actual polyols which constitute the interesting macromonomers to be exploited in polycondensations based on the use of their OH groups. The oxypropylated polymer has a high OH functionality, indeed the same as that of the substrate, since the grafting reaction only brings the OH group out of its initial core structure. The PPO has an OH functionality of two and will therefore act as a chain extender during the polycondensation reactions in which the grafted polymer is responsible for branching and ultimately cross-linking.

14.6 I_{OH}

The values of I_{OH} were about 80 for chitin (at 120 ºC) and 100 for chitin (at 140 ºC); and about 90 and 130 for CH95 at 120 and 140 ºC, respectively. This index increased with increasing reaction temperature and the values are different depending on the sample (chitin or chitosan). Considering the purpose of valorizing these industrial by-products, it is important that the I_{OH} values are within the range of commercial materials, and in fact, these values are close to those of commercial polyols usually employed to prepare polyurethanes.

14.8 Final remarks

This study provides irrefutable qualitative evidence about the possibility of transforming chitin and chitosan into viscous polyol mixtures by an extremely simple process which only involves the activated substrate and propylene oxide. It is very

important to underline that the various separation procedures described above were only applied in order to characterise the different products of these reactions. This process bears "green" connotations, given that it requires no solvent, leaves no by-products and no specific operations (separation, purification, etc.) are needed to isolate the entire reaction product. In all instances, the reaction product was a viscous liquid made up of oxypropylated chitin or chitosan and PO homopolymer. Polyols produced using the formulations deduced from the optimisation study presented I_{OH} and viscosity values close to those of commercial polyols typically employed in rigid polyurethane synthesis.

15 General Conclusions and Perspectives

15.1 Conclusions

The outcome of this study was encouraging because it gave clear indications about both the possibility of the development of new materials based on chitosan and cellulose fibres, in the context of relatively simple and green processes, and the interest of valorising chitosan in the form of industrial residues in a rational manner by the oxypropylation reaction.

This investigation confirmed the importance in the purification of commercial chitosan samples because of the presence of some non-polar impurities, even in the best-quality commercial samples, which are at origin of the widely different and anomalous results reported for the surface energy of chitosan. All the commercial samples of these polymers were shown to contain impurities, confirmed by GC-MS (higher alkanes, fatty acids and alcohols and sterols), that gave rise to enormous errors in the determination of the polar component of their surface energy. After their careful removal, the value of the total surface energy increased considerably and reached the classical polysaccharide figures. Given the rapidly growing interest in the development and applications of materials based on chitosan, the clarification of such a relevant ambiguity represents an important contribution to this realm.

Chitosan-cellulose nanofibre (BC and NFC) combinations were investigated in two different approachs: as formulations for the preparation of transparent chitosan-bacterial cellulose (CHBC) and chitosan-nanofibrillated cellulose (CHNFC) nanocomposite films and as coating formulations for paper sheets.

Transparent chitosan-cellulose nanofibre composite films (CHNFC, CHBC, WSCHNFC and WSCHBC) were prepared by a simple and green procedure based on casting water (or 1% acetic solutions) suspensions of chitosan with different contents of NFC, up to 60%, and BC, up to 40%. The transparency indicated that the dispersion of the NFC and BC into the chitosan matrices was quite good. The nanocomposite films prepared with BC showed higher transmittance than the corresponding films prepared with NFC, because of the higher purity of BC.

These materials were in general very homogenous and presented better thermo-mechanical and mechanical properties than the corresponding unfilled chitosans. With the NFC and BC addition to the chitosans matrices, tensile strength and modulus were completely dominated by the NFC and BC network. The superior mechanical properties of all CHNFC and CHBC films, compared with those of the unfilled CH films, confirmed the good interfacial adhesion and the strong interactions between the two components. These results can be explained by the inherent morphology of BC with its nanofibrillar network, the high aspect ratio of NFC and the similar structures of the two polysaccharides. The nanocomposite films presented better thermal stability than the corresponding unfilled chitosan films.

The nanocomposites prepared with the high-DP water soluble chitosan are particularly interesting for future studies, since they have an attractive combination of properties, including a high optical transparency.

Globally, the properties of CHNFC nanocomposite films were better than those displayed by similar chitosan films reinforced with BC nanofibrils. This behaviour could be due to the better dispersion of NFC into the chitosan matrices, related to the individual fibre morphology, contrasting with the tridimensional network fibres structure of BC, as well as to the higher aspect ratio of the NFC compared with BC.

The prominent properties of these nanocomposite films could be exploited for several applications, such as in transparent functional, biodegradable and anti-bacterial packaging, electronic devices and biomedical applications.

When compared to other studies, the present approach showed significants advantages, namely because it was not necessary to dissolve the cellulose fibres, avoiding the use of solvents and preserving the fibres structure and all of their properties in the obtained materials, while keeping the materials transparent.

Paper is widely used as an information cultural and advertising medium in our society. However, paper is being challenged by modern technology. Thus, in order to maintain its position, paper quality needs to be improved. This may require a reorganization of the paper structure or the addition of functional properties to paper surfaces. The present thesis investigated some alternatives to improve paper quality. First, the distribution of chitosan deposited at the paper surface by several layers, was assessed using a fluorescent chitosan derivative, and showed that the chitosan distribution was uniform and did not have a preferential way to cover the paper surface. Chitosan penetration into the sheets occurred progressively in the first layers and thereafter a film formation onto the paper sheet was observed. The experimental approach presented here to assess the chitosan distribution on chitosan-coated papers may be certainly extrapolated to the study of other paper-coating agents.

The effect of chitosan and water soluble chitosan derivative on the final properties of the paper was then investigated. The results indicated that both chitosan and water soluble chitosan derivative coatings had a positive influence in the final properties of *E .globulus* coated papers that was quite dependent on the number of deposited chitosan layers. However, the water soluble chitosan derivative promoted superior brightness, ageing stability and inkjet print quality than those coated with chitosan.

Consequently, the use of water soluble chitosan derivatives on paper coating processes represents a promising and sustainable approach for the development of new functional paper materials (e.g. papers with antimicrobial properties) or on the improvement of the end-user specifications of paper (e.g. better optical properties and superior printability) for packaging requirements and general applications.

Concerning the valorisation of the less noble fractions or by-products of chitin and chitosan, this short study demonstrated the possibility of transforming these renewable resources into viscous polyol mixtures through a simple oxypropylation reaction. In practice, the polyol mixtures are simply removed *as such* from the reaction vessel, without the need of any other operation. These polyols constitute viable macromonomers for the synthesis of polyurethanes, polyethers or polyesters replacing the petroleum-based counterparts. In other words, these systems are a good example of green chemistry in that they do not require any solvent, leave no residue and call upon the exploitation of renewable resources. The ensuing polyols showed properties close to those of commercial polyols typically employed in synthesis of rigid polyurethane foams.

The information acquired from this study can contribute to produce novel high-performance and environmentally sustainable intelligent and functional materials from renewable resources. For example, we can envisage the interest of producing transparent electro-active membranes or papers.

15.2 Perspectives

The work carried out constitute an important instrument on the development of novel materials from biomass using chitosan and cellulose fibres as nanocomposite films and as paper coatings and therefore contribute to the emergent effort on the search of new materials designed as '*green materials'*. Nevertheless, several additional topics for further research were raised by the present work namely:

- The use of AFM to study the morphology of WSCH films using derivatives with different degrees of substitution to understand the different morphologies of these materials when compared with those of CH films;
- The study of the gas permeability of the nanocomposite films using the gas to which food packaging should show specific permeability or unpermeability like oxygen, carbon dioxide and nitrogen. Additionaly, the antibacterial and fungicidial properties should be also considered;

- The study of new coating formulations based on chitosan and its derivatives and cellulose nanofibres in combination with the additives usually used in papermaking, namely starch, fillers (e.g. $CaCO_3$), sizing agents (e.g. ASA, AKD), among others, on the final properties of the papers;
- The use of the latter formulations as wet-end additives on the papermaking and the evaluation of the final properties of the papers;
- The study of the reaction kinetics between polyols derived from the oxypropylation of chitin and chitosan and isocyanates, including aliphatic and aromatic structures as well as mono- and difunctional molecules. Moreover, the preparation of rigid polyurethane foams using the chitin and chitosan polyols shoud be also considered;
- The using of the chitin and chitosan polyols as plasticizers of the nanocomposite films instead of glycerol, for instance.

References

[1] A. Gandini and M.N. Belgacem, in Monomers, Polymers and Composites from Renewable Resources, M.N. Belgacem and A. Gandini (eds.) Elsevier, London, **2008**, pp. 1-16.

[2] A. Gandini, Polymers from renewable resources: A challenge for the future of macromolecular materials, *Macromolecules*, 41, **2008**, 9491-9504.

[3] J.T.P. Derksen, F.P. Cuperus and P. Kolster, Renewable resources in coatings technology: a review, *Progress in Organic Coatings,* 27, **1996**, 45-53.

[4] L. Yu and L. Chen, in Biodegradable Polymer Blends and Composites from Renewable Resources, L. Yu, John (ed.) Wiley & Sons, New Jersey, **2009**, pp. 1-13.

[5] A.K. Mohanty, M. Misra and L.T. Drzal, Sustainable Bio-Composites from Renewable Resources: Opportunities and challenges in the green materials world, *Journal of Polymers and the Environment*, 10, **2002**, 19-26.

[6] A. Uihlein, S. Ehrenberger and L. Schebek, Utilisation options of renewable resources: a life cycle assessment of selected products, *Journal of Cleaner Production*, 16, **2008**, 1306-1320.

[7] S. Warwel, F. Bruse, D. Demes, M. Kunz and M.R. Klass, Polymers and surfactants on the basis of renewable resources, *Chemosphere,* 43, **2001**, 39-48.

[8] L. Yu, K. Dean, and L. Li, Polymer blends and composites from renewable resources *Progress in Polymer Science*, 31, **2006**, 576-602.

[9] K.G. Satyanarayana, G.G.C. Arizaga, F. Wypych, Biodegradable composites based on lignocellulosic fibers: an overview, *Progress in Polymer Science*, 34, **2009**, 982-1021.

[10] C. Peniche, W. Argüelles-Monal and F.M. Goycoolea, in Monomers, Polymers and Composites from Renewable Resources, M.N. Belgacem and A. Gandini (eds.) Elsevier, London, **2008**, pp. 517-542.

[11] S.P. Campana-Filho and J. Desbrières, in Natural polymers and agrofibres based composites, E. Frollini, A. Leão and L. Mattoso (eds.), Embrapa Instrumentação Agropecuária, São Carlos, **2000**, pp. 41-71.

[12] M. Rinaudo, Chitin and chitosan: Properties and applications, *Progress in Polymer Science*, 31, **2006**, 603-632.

[13] R.A.A. Muzzarelli, Chitin, Pergamon Press, Oxford, **1976**.

[14] Y.B. Wu, S.H. Yu, F.L. Mi, C.W. Wu, S.S. Shyu, C.K. Peng and A.C. Chao, Preparation and characterization on mechanical and antibacterial properties of chitsoan/cellulose blends, *Carbohydrate Polymers*, 57, **2004**, 435-440.

[15] L. Hong, Y.L. Wang, S.R. Jia, Y. Huang, C. Gao and Y.Z. Wan, Hydroxyapatite/bacterial cellulose composites synthesized via a biomimetic route, *Materials Letters*, 60, **2006**, 1710-1713.

[16] J. Yin, K. Luo, X. Chen, and V.V. Khutoryanskiy, Miscibility studies of the blends of chitosan with some cellulose ethers, *Carbohydrate Polymers*, 63, **2006**, 238-244.

[17] S.Z. Rogovina and G.A. Vikhoreva, Polysaccharide-based polymer blends: methods of their production, *Glycoconjugate Journal*, 23, **2006**, 611-618.

[18] M.A.S.A. Samir, F. Alloin and A. Dufresne, Review of recent research into cellulosic whiskers: their properties and their application in nanocomposite field, *Biomacromolecules*, 6, **2005**, 612-626.

[19] A.K. Mohanty, M. Misra and L.T. Drzal, Surface modification of natural fibers and performance of resulting biocomposites: an overview, *Composite Interfaces*, 8, **2001**, 313-343.

[20] G.A.F. Roberts, Chitin Chemistry, The Macmillan Press Ltd, Hong Kong, **1992**.
[21] F.M. Goycoolea, W. Argüelles-Monal, C. Peniche and I. Higuerra-Ciapara, in Novel Macromolecules in Food Systems, G. Doxastakis and V. Kiosseoglou (eds.) Elsevier, Thessaloniki, Greece, **2000**, pp. 265-307.
[22] A.P. Abram and I. Higuera, in Quitina y quitosano: obtencion, caracterizacion y aplicaciones, A.P. Abram (ed.) Pontificia Universidad Católica del Perú, Perú, vol. 1, **2004**, pp. 23-71.
[23] M. Terbojevich and R.A.A. Muzzarelli, Chitosan, Woodhead Publisshing Limited, Cambridge, **2000**.
[24] C. Peniche, PhD Thesis, Universidad de La Habana, **2006**.
[25] J. Desbrières, Chitine et chitosane, *L'actualité chimique*, 11-12, **2002**, 39-44.
[26] G.A.F. Roberts, in 21st Newsletter of Euchis European Chitin Society News Letter European Chitin Society, 21, **2006,** pp. 5.
[27] M.N.V.R. Kumar, R.A.A. Muzzarelli, C. Muzzarelli, H. Sashiwa and A.J. Domb, Chitosan chemistry and pharmaceutical perspectives, *Chemical Reviews*, 104, **2004**, 6017-6084.
[28] C. Jeuniaux and M. F. Voss-Foucart, Chitin biomass and production in the marine environment, *Biochemical Systematics and Ecology*, 19, **1991**, 347-356.
[29] D. Raabe, C. Sachs and P. Romano, The crustacean exoskeleton as an example of a structurally and mechanically graded biological nanocomposite material, *Acta Materialia*, 53, **2005**, 4281-4292.
[30] R.A.A. Muzzarelli, The Polysaccharides, Academic Press, New York, **1985**.
[31] Chitin in Nature and Technology, R.A.A. Muzzarelli, C. Jeuniaux and G.W. Gooday (eds.) Plenum Press, New York, **1986**.
[32] Chitin Enzymology, R.A.A. Muzzarelli (ed.) Atec, Italy, **1993**.
[33] H.K. No and P. Meyers, in Chitin Handbook, R.A.A. Muzzarelli and M.G. Peter (eds.) European Chitin Society, Grottammare, **1997**, pp. 475.
[34] F.M. Goycoolea, E. Agulló and R. Mato, in Quitina y quitosano: obtención, caracterizatión y aplicaciones, A. P. Abram (ed.) Pontificia Universidad Católica del Perú, Perú, vol. 3, **2004**, pp. 103-154.
[35] F. Shahidi and R. Abuzaytoun, in Advances in food and nutrition research, Elsevier, vol. 49, **2005**, pp. 93-135.
[36] A. Martinou, V. Bouriotis, B.T. Stokke and K.M. Värum, Mode of action of chitin deacetylase from Mucor rouxii on partially *N*-acetylated chitosans, *Carbohydrate Research*, 311, **1998**, 71-78.
[37] M.N.V.R. Kumar, A review of chitin and chitosan applications, *Reactive and Functional Polymers*, 46, **2000**, 1-27.
[38] W. Argüelles-Monal and A.H. Caballero, in Quitina y Quitosano: obtención, caracterización y aplicaciones, A. P. d. Abram (ed.) Pontifica Universidad Católica del Perú, Perú, vol. 4, **2004**, pp. 155-206.
[39] Q. Li, E.T. Dunn, E.W. Grandmaison and M.F.A. Goosen, in Applications of chitin and chitosan, M.F.A. Goosen (ed.) Technomic publishing CO., INC., Lancaster, USA, **1997**, pp. 3-21.
[40] G.K. Moore and G.A.F. Roberts, Determination of the degree of. *N*-acetylation of chitosan, *International Journal of Biological Macromolecules*, 2, **1980**, 115-116
[41] J.G. Domszy and G.A.F. Roberts, Evaluation of infrared spectroscopic techniques for analysing chitosan, *Makromolekulare Chemie*, 186, **1985**, 1671-1677.

[42] M. Miya, R. Iwamoto, S. Yoshikawa and S. Mima, I.r. spectroscopic determination of CONH content in highly deacylated chitosan, *International Journal of Biological Macromolecules*, 2, **1980**, 323-324.

[43] A. Baxter, M. Dillon, K.D.A. Taylor and G.A.F. Roberts, Improved method for IR determination of the degree of *N*-acetylation of chitosan, *International Journal of Biological Macromolecules*, 14, **1992**, 166-169.

[44] S. Aiba, Studies on chitosan: 1. Determination of the degree of *N*-acetylation of chitosan by ultraviolet spectrophotometry and gel permeation chromatography, *International Journal of Biological Macromolecules*, 8, **1986**, 173-176.

[45] R.A.A. Muzzarelli and R. Rocchetti, Determination of the degree of Acetylation of chitosans by first derivative ultraviolet spectrophotometry, *Carbohydrate Polymers*, 5, **1985**, 461-472.

[46] Y. Inoue, in Chitin Handbook, R.A.A. Muzzarelli and M.G. Peter (eds.) European Chitin Society, Grottammare, **1997**, pp. 133-136.

[47] M.R. Kasaai, Determination of the degree of *N*-acetylation for chitin and chitosan by various NMR spectroscopy techniques: a review, *Carbohydrate Polymers*, 79, **2010**, 801-810.

[48] A. Hirai, H. Odani and A. Nakajima, Determination of degree of deacetylation of chitosan by ^{1}H NMR spectroscopy, *Polymer Bulletin*, 26, **1991**, 87-94.

[49] J. Desbrières, C. Martinez and M. Rinaudo, Hydrophobic derivatives of chitosan: Characterization and rheological behaviour, *International Journal of Biological Macromolecules*, 19, **1996**, 21-28.

[50] A. Ebert and H.-P. Fink, in Chitin Handbook, R.A.A. Muzzarelli and M. G. Peter (eds.), European Chitin Society, Grottammare, **1997**, pp. 137-143.

[51] L. Raymond, F.G. Morin and R.H. Marchessault, Degree of deacetylation of chitosan using conductimetric titration and solid-state NMR, *Carbohydrate Research*, 246, **1993**, 331-336.

[52] K.M. Värum, M.W. Anthonsen, H. Grasdalen and O. Smidsrod, Determination of the degree of *N*-acetylation and the distribution of *N*-acetyl groups in particular *N*-acetylated chitins (chitosans) by high-field NMR spectroscopy, *Carbohydrate Research*, 217, **1991**, 19-27.

[53] M.L. Duarte, M.C. Ferreira, M.R. Marvão and J. Rocha, Determination of the degree of acetylation of chitin materials by ^{13}C CP/MAS NMR spectroscopy, *International Journal of Biological Macromolecules*, 28, **2001**, 359-363.

[54] L. Heux, J. Brugnerotto, J. Desbrières, M.F. Versali and M. Rinaudo, Solid state NMR for determination of degree of acetylation of chitin and chitosan, *Biomacromolecules*, 1, **2000**, 746-751.

[55] I. García-Alonso, C. Peniche and J.M. Nieto, Determination of the degree of acetylation of chitin and chitosan by thermal analysis, *Journal of Thermal Analysis*, 28, **1983**, 189-193.

[56] Z.M. dos Santos, A.L.P.F. Caroni, M.R. Pereira, D.R. da Silva and J.L.C. Fonseca, Determination of deacetylation degree of chitosan: a comparation between conductometric titration and CHN elemental analysis, *Carbohydrate Research*, 344, **2009**, 2591-2595.

[57] M.R. Kasaai, J. Arul and G. Charlet, Intrinsic viscosity-molecular weight relationship for chitosan, *Journal of Polymer Science, Part B*, 38, **2000**, 2591-2598.

[58] M.R. Kasaai, Various methods for determination of the degree of *N*-acetylation of chitin and chitosan: a review, *Journal of Agricultural and Food Chemistry*, 5, **2009**, 1667-1676.
[59] R.A.A. Muzzarelli, C. Lough and M. Emanuelli, The molecular weight of chitosan studied by laser light scattering, *Carbohydrate Research*, 164, **1987**, 433-442.
[60] A. Domard and M. Rinaudo, Preparation and characterization of fully deacetylated chitosan, *International Journal of Biological Macromolecules*, 5, **1983**, 49-52.
[61] M. Terbojevich and A. Cosani, in Chitin Handbook, R.A.A. Muzzarelli and M.G. Peter (eds.), European Chitin Society, Grottammare, **1997**, pp. 87-101.
[62] A. Isogai, in Chitin Handbook, R.A.A. Muzzarelli and M.G. Peter (eds.), European Chitin Society, Grottammare, **1997**, pp. 103-108.
[63] W.A. Bough, W.L. Salter, A.C.M. Wu and B.E. Perkins, Influence of manufacturing variables on the characteristics and effectiveness of chitosan products. I. Chemical composition, viscosity, and molecular-weight distribution of chitosan products, *Biotechnology and Bioengineering*, 20, **1978**, 1931-1943.
[64] M. Rinaudo, M. Milas and L. Dung, Characterization of chitosan. Influence of ionic strength and degree of acetylation on chain expansion, *International Journal of Biological Macromolecules*, 15, **1993**, 281-285.
[65] G.G. Maghami and G. A. F. Roberts, Evaluation of the viscometric constants for chitosan, *Makromolekulare Chemie*, 189, **1988**, 195-200.
[66] O. Philippova, E. Volkov, N. Sitnikova, A. Khokhlov, J. Desbrières and M. Rinaudo, Two types of hydrophobic aggregates in aqueous solutions of chitosan and its hydrophobic derivative, *Biomacromolecules*, 2, **2001**, 483-490.
[67] G.A.F. Roberts and J. Domszy, Determination of the viscometric constants for chitosan, *International Journal of Biological Macromolecules,* 4, **1982**, 374-377.
[68] P. Meyer and G.W. Pankow, *Helvetica Chimica Acta*, 18, **1935**, 589.
[69] D.A. Rees, E.R. Morris, D. Thom and J.K. Madden, The polysaccharides, Academic Press, Inc., New York, **1982**.
[70] T. Sannan, K. Kurita and Y. Iwakura, *Makromolekulare Chemie*, 178, **1977**, 3202.
[71] G.L. Clark and A.F. Smith, Research article X-ray diffraction studies of chitin, chitosan, and derivatives, *Journal of Physical Chemistry*, 40, **1937**, 863.
[72] R.J. Samuels, Solid state characterization of the structure of chitosan films, *Journal of Polymer Science Part B: Polymer Physics*, 7, **1981**, 1081-1105.
[73] V.K. Mourya and N.N. Inamdar, Chitosan-modifications and applications: Opportunities galore, *Reactive and Functional Polymers*, 68, **2008**, 1013-1051.
[74] M. Rinaudo, G. Pavlov and J. Desbrières, Influence of acetic acid concentration on the solubilization of chitosan, *Polymer*, 25, **1999**, 7029-7032.
[75] M. Rinaudo, G. Pavlov and J. Desbrières, Solubilization of chitosan in strong acid medium, *International Journal of Polymer Analysis and Characterization*, 3, **1999**, 267-276.
[76] P. Sorlier, A. Denuziere, C. Viton and A. Domard, Relation between the degree of acetylation and the electrostatic properties of chitin and chitosan, *Biomacromolecules*, 3, **2001**, 765-772.
[77] K.M. Värum, M.H. Ottoy and O. Smidsrod, Water-solubility of partially *N*-acetylated chitosans as a function of pH: effects of chemical composition and depolymerization, *Carbohydrate Polymers*, 25, **1994**, 65-70.

[78] A. Montembault, C. Viton and A. Domard, Rheometric study of the gelation of chitosan in aqueous solution without cross-linking agent, *Biomacromolecules*, 2, **2005**, 653-662.

[79] H. Yi, L.Q. Wu, W.E. Bentley, R. Ghodssi, G.W. Rubloff, J.N. Culver and G.F. Payne, Biofabrication with chitosan, *Biomacromolecules*, 6, **2005**, 2881-2894.

[80] M.G. Zhang and W. Gorski, Electrochemical sensing platform based on the carbon nanotubes/redox mediators-biopolymer system, *Journal of the American Chemical Society*, 127, **2005**, 2058-2059.

[81] D. Wei, W. Sun, W. Qian, Y. Ye and X. Mac, The synthesis of chitosan-based silver nanoparticles and their antibacterial activity, *Carbohydrate Research*, 344, **2009**, 2375-2382.

[82] C.A. Constantine, K.M. Gattas-Asfura, S.V. Mello, G. Crespo, V. Rastogi, T.C. Cheng, J.J. DeFrank and R.M. Leblanc, Layer-by-layer biosensor assembly incorporating functionalized quantum dots., *Langmuir*, 19, **2003**, 9863-9867.

[83] M. Terbojevich, A. Cosani and R.A.A. Muzzarelli, Molecular parameters of chitosans depolymerized with the aid of papain, *Carbohydrate Polymers*, 29, **1996**, 63-68.

[84] R.A.A. Muzzarelli, M. Tomasetti and P. Ilari, Depolymerization of chitosans with the aid of papain, *Enzyme and Microbial Technology*, 16, **1994**, 110-114.

[85] B.K Choi, K.Y. Kim, Y.J. Yoo, S.J. Oh, J.H. Choi and C.Y. Kim, In vitro antimicrobial activity of a chitooligosaccharide mixture against *Actinobacillus actinomycetemcomitans* and *Streptococcus mutans, International Journal of Antimicrobial Agents,* 18, **2001**, 553–557.

[86] H. Sashiwa, S. Fujishima, N. Yamano, N. Kawasaki, A. Nakayama, E. Muraki, M. Sukwattanasinitt, R. Pichyangkura and S. Aiba, Enzymatic production of *N*-acetyl-D-glucosamine from chitin. Degradation study of *N*-acetylchitooligosaccharide and the effect of mixing of crude enzymes, *Carbohydrate Polymers*, 51, **2003**, 391-395.

[87] C.K.S. Pillai, W. Paul and C.P. Sharma, Chitin and chitosan polymers: Chemistry, solubility and fiber formation, *Progress in Polymer Science*, 34, **2009**, 641-678.

[88] A.B.V. Kumar, M.C. Varadaraj, R.G. Lalitha and R.N. Tharanathan, Low molecular weight chitosan: preparation with the aid of papain and characterization, *Biochimica et Biophysica Acta*, 1670, **2004**, 137-146.

[89] K. Kurita, Controlled functionalization of polysaccharide chitin, *Progress in Polymer Science*, 26, **2001**, 1921-1971.

[90] K.V.H. Prashanth and R.N. Tharanathan, Chitin/chitosan: modifications and their unlimited application potential: an overview, *Food Science and Technology,* 18, **2007**, 117–131.

[91] S.H. Lim and S.M. Hudson, Review of chitosan and its derivatives as antimicrobial agents and their uses as textile chemicals, *Journal of Macromolecules Science: Part C: Polymer Reviews*, 2, **2003**, 223 – 269.

[92] H. Sashiwa and S. Aiba, Chemically modified chitin and chitosan as biomaterials, *Progress in Polymer Science*, 29, **2004**, 887–908.

[93] M. Zhang and H.-X. Ren, Structural modification and application of chitosan, *Journal of Clinical Rehabilitative Tissue Engineering Research*, 11, **2007**, 9817–9820.

[94] R.A.A. Muzzarelli, Modified chitosans and their chemical behavior, *American Chemistry Society, Division of Polymer Chemistry*, 31, **1990**, 626.

[95] R. Jayakumar, M. Prabaharan, R.L. Reis and J.F. Mano, Graft copolymerized chitosan: present status and applications, *Carbohydrate Polymers,* 62, **2005**, 142–158.
[96] Y.W. Cho, Y.N. Cho, S.H. Chung, G. Yoo and S.W. Ko, Water-soluble chitin as a wound healing accelerator, *Biomaterials*, 20, **1999**, 2139-2145.
[97] US Patent N°4921949*,* **1982**.
[98] H.S. Seong, H.S. Whang and S.W. Ko, Synthesis of a quaternary ammonium derivative of chito-oligosaccharide as antimicrobial agent for cellulosic fibers, *Journal of Applied Polymer Science*, 76, **2000**, 2009-2015.
[99] J. Cho, J. Grant, M. Piquette-Miller and C. Allen, Synthesis and physicochemical and dynamic mechanical properties of a water-soluble chitosan derivative as a biomaterial, *Biomacromolecules*, 7, **2006**, 2845-2855.
[100] R.A.A. Muzzarelli and F. Tanfani, The *N*-permethylation of chitosan and the preparation of*N*-trimethyl chitosan iodide, *Carbohydrate Polymers*, 5, **1985**, 297-307.
[101] A. Domard, M. Rinaudo and C. Terrassin, Adsorption of chitosan and a quaternized derivative on kaolin, *Journal of Applied Polymer Science,* 38, **1989**, 1799-1806.
[102] O. Gåserød, O. Smidsrød and G. Skjåk-Bræk, Microcapsules of alginate-chitosan - I A quantitative study of the interaction between alginate and chitosan, *Biomaterials*, 19, **1998**, 1815-1825.
[103] R.B. Qaqish and M.M. Amiji, Synthesis of a fluorescent chitosan derivative and its application for the study of chitosan-mucin interactions, *Carbohydrate Polymers*, 38, **1999**, 99-107.
[104] Y. Fang, G. Ning, D. Hu and J. Lu, Synthesis and solvent-sensitive fluorescence properties of a novel surface-functionalized chitosan film: potential materials for reversible information storage, *Journal of Photochemistry and Photobiology A: Chemistry,* 135, **2000**, 141-145.
[105] K. Tømmeraas, S.P. Strand, W. Tian, L. Kenne and K.M. Vårum, Preparation and characterisation of fluorescent chitosans using 9-anthraldehyde as fluorophore, *Carbohydrate Research*, 336, **2001**, 291-296.
[106] X. Guan, X. Liu and Z. Su, Preparation and photophysical behaviors of fluorescent chitosan bearing fluorescein: Potential biomaterial as temperature/pH probes, *Journal of Applied Polymer Science*, 104, **2007**, 3960-3966.
[107] A. Juneau, A. Georgalas and R. Kapino, Chitosan in cosmetics: technical aspects when formulating, *Cosmetic Toil*, 116, **2001**, 73-80.
[108] S. Hirano, C. Itakura, H. Seino, Y. Akiyama, I. Nonaka, N. Kanbara and T. Kawakami, Chitosan as an ingredient for domestic animal feeds, *Journal of Agricultural and Food Chemistry*, 38, **1990**, 1214-1217.
[109] C. Peniche, M. Aguilar, I. Aranaz, A. Mayorga, I. Paños, J. Román and C. Tapia, in Quitina y quitosano: obtención, caracterización y aplicaciones, A. P. Abram (ed.) Pontificia Universidad Católica del Perú, Perú, vol. 6, **2004**.
[110] E. Agulló, L. Albertengo, A.P. Abram, M. Rodríguez and F. Valenzuela, in Quitina y quitosano:obtención, caracterización y aplicaciones, A. P. Abram (ed.) Pontificia Universidad Católica del Perú, vol. 5, **2004**.
[111] A.J. Rigby and S. Anand, Nonwovens in medical and healthcare products. II. Materials and applications, *Technical Textiles International,* 8, **1996**, 24-29.
[112]. S. Rajendran and S.C. Anand, Developments in medical textiles, *Textile Progr*ess, 32, **2002**, 1-42.

[113] S. Hirano, Chitin and chitosan as novel biotechnological materials, *Polymer International,* 48, **1999**, 732-734.
[114] A.A. Desai, Biomedical implantable materials sutures, *Asian Textile Journal*, 14, **2005**, 54-56.
[115] G. Doxastakis and V. Kiosseoglou (eds.), in Novel Macromolecules in food systems, Elsevier, vol. 41, **2000**, pp. 265-307.
[116] M. Gällstedt and M.S. Hedenqvistb, Packaging-related mechanical and barrier properties of pulp-fiber-chitosan sheets, *Carbohydrate Polymers*, 63, **2006**, 46-53.
[117] M. Gällstedt, A. Brottman and M. Hedenqvist, Packaging-related properties of protein-and chitosan-coated paper, *Packaging Technology and Science*, 18, **2005**, 161-170.
[118] F. Ham-Pichavant, G. Sèbe, P. Pardon and V. Coma, Fat resistance properties of chitosan-based paper packaging for food applications, *Carbohydrate Polymer*, 61, **2005**, 259-265.
[119] C.H. Lee, D.S. An, H.J. Park and D.S. Lee, Wide-spectrum antimicrobial packaging materials incorporating nisin and chitosan in the coating, *Packaging Technology and Science*, 16, **2003**, 99-106.
[120] E. Guibal, Interactions of metal ions with chitosan-based sorbents: a review, *Separation and Purification Technology*, 38, **2004**, 43-74.
[121] E. Guibal, C. Milot and J. Roussy, Influence of hydrolysis mechanism on molybdate sorption using chitosan, *Water Environment Research*, 71, **1999**, 10.
[122] A. Bhatnagar and M. Sillanpää, Applications of chitin- and chitosan-derivatives for the detoxification of water and wastewater- a short review, *Advances in Colloid and Interface Science*, 152, **2009**, 26-38.
[123] N. Bordenave, S. Grelier, F. Pichavant and V. Coma, Water and moisture susceptibility of chitosan and paper-based materials: structure-property relationships, *Journal of Agricultural and Food Chemistry*, 55, **2007**, 9479-9488.
[124] S. Despond, E. Espuche, N. Cartier and A. Domard, Barrier properties of paper-chitosan and paper-chitosan-carnauba wax films, *Journal of Applied Polymer Science*, 98, **2004**, 704-710.
[125] M. Mucha and D. Miskiewicz, Chitosan blends as fillers for paper, *Journal of Applied Polymer Science*, 77, **2000**, 3210-3215.
[126] J. Vartiainen, R. Motion, H. Kulonen, M. Rättö, E. Skyttä and R. Ahvenainen, Chitosa-coated paper: effects of nisin and different acids on the antimicrobial activity, *Journal of Applied Polymer Science*, 94, **2004**, 986-993.
[127] E. Heuser, The chemistry of cellulose, Wiley, New York, **1944**.
[128] E. Sjöström, Wood Chemistry - fundamentals and applications, Academic Press Inc., USA, **1981**.
[129] E. Sjöström and U. Westermark, Chemical composition of wood and pulps: basic constituents and their distribution, E. Sjöström and R. Alén (eds.) Springer-Verlag, Berlin, Germany, **1999**.
[130] D. Klemm, T. Heinze and W. Wagenknecht, Comprehensive Cellulose Chemistry, Wiley-VCG, Weinheim, Germany, **1998**.
[131] D.N.S. Hon, Cellulose: a random walk along its historical path, *Cellulose*, 1, **1994**, 1-25.
[132] T.T. Teeri, H. Brumer III, G. Daniel and P. Gatenholm, Biomimetic engineering of cellulose-based materials, *Trends Biotechnology*, 25, **2007**, 299-306.

[133] R.D. Preston, The physical biology of the plant cell wall, Chapman and Hall, London, **1974**.
[134] E. Pecoraro, D. Manzani, Y. Messaddeq and S. J. L. Ribeiro, in Monomers, Polymers and Composites from Renewable Resources, A. Gandini and M. N. Belgacem (eds.) Elsevier, London, vol. 17, **2008**, pp. 369-383.
[135] A. Dufresne, in Monomers, Polymers and Composites from Renewable Resources, A. Gandini and M. N. Belgacem (eds.) Elsevier, London, vol. 19, **2008**, pp. 401-418.
[136] J. Schurz, Trends in polymer science: a bright future for cellulose, *Progress in Polymer Science*, 24, **1999**, 481-483.
[137] R. Rowell, J. Han and J. Rowell, in Natural polymers and agrofibres composites, E. Frollini, A. Leão and L. Mattoso (eds.) Embrapa Instrumentação Agropecuária, Brazil, **2000**, pp. 115-134.
[138] A. Bledzki and J. Gassan, Composites reinforced with cellulose based fibres, *Progress in Polymer Science*, 24, **1999**, 221-274.
[139] W.L. Earl and D.L. VanderHart, Observations by high-resolution carbon-13 nuclear magnetic resonance of cellulose I related to morphology and crystal structure, *Macromolecules*, 3, **1981**, 570-574.
[140] A. Ishikawa, T. Okano and J. Sugiyama, Fine structure and tensile properties of ramie fibres in the crystalline form of cellulose I, II, III(I) and IV(I), *Polymer*, 38, **1997**, 463-468.
[141] H.P. Fink, B. Philipp, D. Paul, R. Serimaa and T. Paakkari, The structure of amorphous cellulose as revealed by wide-angle X-ray scattering, *Polymer*, 28, **1987**, 1265-1270.
[142] A.C. O'Sullivan, Cellulose: the structure slowly unravels, *Cellulose*, 4, **1997**, 173-207.
[143] S. Dimitriu, Polysaccharides: structural diversity and functional versatility, Marcel Dekker, Inc., New York, **1998**.
[144] A. Sarko and R. Muggli, Packing analysis of carbohydrates and polysaccharides. III. valonia cellulose and cellulose II, *Macromolecules*, 7, **1974**, 486-494.
[145] F.J. Kolpak and J. Blackwell, Determination of the structure of cellulose II, *Macromolecules*, 9, **1976**, 273-278.
[146] R.H. Atalla and D. L. VanderHart, Native cellulose: a composite of two distinct crystalline forms, *Science*, 223, **1984**, 283-285.
[147] Y. Wang and L. Zhang, in Biodegradable Polymer Blends and Composites from Renewable Resources, L. Yu (ed.) Wiley, New Jersay, vol. 6, **2009**, pp. 129-161.
[148] T. Heinze and K. Petzold, in Monomers, Polymers and Composites from Renewable Resources, A. Gandini and M.N. Belgacem (eds.) Elsevier, London, vol. 16, **2008**, pp. 343-368.
[149] S. Richardson and L. Gorton, Characterisation of the substituent distribution in starch and cellulose derivatives, *Analytica Chimica Acta*, 497, **2003**, 27-65.
[150] L. Liu, Bioplastics in food packaging: Innovative technologies for biodegradable packaging, Accessed February, www.iopp.orgpagesindex.cfm **2007**.
[151] D.N.S. Hon, in Polysaccharides in medical applications, S. Dimitriu (ed.) Marcel Dekker, Sherbrooke, New York, **1996**, pp. 87.
[152] R.C.R. Nunes and L.L.Y. Visconde, in Natural polymers and agrofibres based composites, E. Frollini, A. Leão and L. Mattoso (eds.) Embrapa Inst. Agropecuária, São Carlos, **2000**.

[153] K. Joseph, L. Mattoso, R. D. Toledo, S. Thomas, L. H. Carvalho, L. Pothen, S. Kala and B. James, in Natural polymers and agrofibres based composites, E. Frollini, A. Leão and L. Mattoso (eds.) Embrapa Inst. Agropecuária, São Carlos, **2000**.

[154] M.N. Belgacem and A. Gandini, in Natural fibre reinforced polymer composites from macro to nanoscale, S. Thomas and L. A. Pothan (eds.) Old City Publishing, vol. 3, **2009**.

[155] M.N. Belgacem and A. Gandini, The surface modification of cellulose fibres for use as reinforcing elements in composite materials, *Composite Interface*, 12, **2005**, 41-75.

[156] C. S. R. Freire and A. Gandini, Recent advances in the controlled heterogeneous modification of cellulose for the development of novel materials, *Cellulose Chemistry and Technology*, 40, **2006**, 691-698.

[157] A. Gandini and M.N. Belgacem, Modified cellulose fibres as reinforcing fillers for macromolecular matrices, *Macromolecular Symposia.* 221, **2005**, 257-270.

[158] D. Fengel and G. Wegener, Wood- chemistry, ultrastructure, reactions, Walter de Gruyter, Berlin, New York, **1989**.

[159] T. Zimmermann, E. Pöhler and T. Geiger, Cellulose fibrils for polymer reinforcement, *Advanced Engineering Materials*, 6, **2004**, 754-761.

[160] A.F. Turbak, F.W. Snyder and K.R. Sandberg, Microfibrillated cellulose, *Journal of Applied Polymer Science: Applied Polymer Symposium*, 37, **1983**, 815-827.

[161] F.W. Herrick, R.L. Casebier, J.K. Hamilton and K.R. Sandberg, Microfibrillated Cellulose: morphology and accessibility, *Journal of Applied Polymer Science: Applied Polymer Symposium,* 37, **1983**, 797-813.

[162] A.N. Nakagaito and H. Yano, The effect of morphological changes from pulp fiber towards nano-scale fibrillated cellulose on the mechanical properties of high-strength plant fiber based composites, *Applied Physics A: Materials Science & Processing*, 78, **2004**, 547-552.

[163] M. Pääbkkö, M. Ankerfors, H. Kosonen, A. Nykänen, S. Ahola, M. Osterberg, J. Ruokolainen, J. Laine, P.T. Larsson, O. Ikkala and T. Lindström, Enzymatic hydrolysis combined with mechanical shearing and high-pressure homogenization for nanoscale cellulose fibrils and strong gels, *Biomacromolecules*, 8, **2007**, 1934-1941.

[164] M. Henriksson, G. Henriksson, L.A. Berglund and T. Lindström, An environmentally friendly method for enzyme-assisted preparation of microfibrillated cellulose (MFC) nanofibers, *European Polymer Journal*, 43, **2007**, 3434-3441.

[165] A.N. Nakagaito and H. Yano, Novel high-strength biocomposites based on microfibrillated cellulose having nanoorder-unit web-like network structure, *Applied Physics A: Materials Science & Processing*, 80, **2005**, 155-159.

[166] H. Yano and S. Nakahara, Bio-composites produced from plant microfiber bundles with a nanometer unit web-like network, *Journal of Materials Science*, 39, **2004**, 1635–1638.

[167] A.J. Svagan, M.A.S.A Samir and L.A. Berglund, Biomimetic polysaccharide nanocomposites of high cellulose content and high toughness, *Biomacromolecules*, 8, **2007**, 2556-2563.

[168] A. Iwatake, M. Nogi and H. Yano, Cellulose nanofiber-reinforced polylactic acid, *Composites Science and Technology.*, 68, **2008**, 2103-2106.

[169] L. Suryanegara, A. Nakagaito and H. Yano, The effect of crystallization of PLA on the thermal and mechanical properties of microfibrillated cellulose-reinforced PLA composites, *Composites Science and Technology*, 69, **2009**, 1187-1192.
[170] J. Lu, T. Wang and T. Drzal, Preparation and properties of microfibrillated cellulose polyvinyl alcohol composite materials, *Composites Part A: Applied Science and Manufacturing*, 39, **2008**, 738-746.
[171] M.O. Seydibeyoglu and K. Oksman, Novel nanocomposites based on polyurethane and micro fibrillated cellulose, *Composites Science and Technology*, 68, **2008**, 908-914.
[172] J. Hosokawa, M. Nishiyama, K. Yoshihara, T. Kubo and A. Terabe, Reaction between chitosan and cellulose on biodegradable composite film formation, *Industrial & Engineering Chemistry Research*, 30, **1991**, 788-792.
[173] J. Hosokawa, M. Nishiyama, K. Yoshihara and T. Kubo, Biodegradable film derived from chitosan and homogenized cellulose, *Industrial and Engineering Chemistry Research*, 29, **1990**, 800-805.
[174] D. Nordqvist, J. Idermark, M. Hedenqvist, M. Gällstedt, M. Ankerfors and T. Lindström, Enhancement of the wet properties of transparent chitosan-acetic acid-salt films using microfibrillated cellulose, *Biomacromolecules*, 8, **2007**, 2398-2403.
[175] A. Boldizar, C. Klason, J. Kubat, P. Näslund and P. Saha, Prehydrolyzed cellulose as reinforcing filler for thermoplastics, *International Journal of Polymer. Materials*, 11, **1987**, 229-262.
[176] K. Syverud and P. Stenius, Strength and barrier properties of MFC films, *Cellulose*, 16, **2009**, 75-85.
[177] M. Andresen and P. Stenius, Water-in-oil emulsions stabilized by hydrophobized microfibrillated cellulose, *Journal of Dispersion Science and Technology,* 28, **2007**, 837-844.
[178] A. Steinbüchel and Y. Doi (eds.), Biotechnology of Biopolymers, Wiley-VCH Verlag GmbH & Co. KGaA, Weinheim, **2005**.
[179] M. Shoda and Y. Sugano, Recent advances in bacterial cellulose production, *Biotechnology and Bioprocess Engineering*, 10, **2005**, 1-8.
[180] P.R. Chawla, I.B. Bajaj, S.A. Survase and R.S. Singhal, Microbial cellulose: fermentative production and applications, *Food Technology and Biotechnology*, 47, **2009**, 107-124.
[181] A. Hirai, M. Tsuji and F. Horii, TEM study of band-like cellulose assemblies produced by Acetobacter xylinum at 4 °C, *Cellulose*, 9, **2002**, 105-113.
[182] D. Klemm, D. Schumann, U. Udhardt and S. Marsch, Bacterial synthesized cellulose - artificial blood vessels for microsurgery, *Progress in Polymer Science,* 26 **2001**, 1561-1603
[183] Y. Tomita and T. Kondo, Influential factors to enhance the moving rate of *Acetobacter xylinum* due to its nanofiber secretion on oriented templates *Carbohydrate Polymers*, 77, **2009**, 754-759
[184] J. George, K.V. Ramana, S.N. Sabapathy and A.S. Bawa, Physico-mechanical properties of chemically treated bacterial (*Acetobacter xylinum*) cellulose membrane, *World Journal of Microbiology and Biotechnology*, 21, **2005**, 1323-1327.
[185] J. George, K.V. Ramana, S.N. Sabapathy, J.H. Jagannath and A.S. Bawa, Characterization of chemically treated bacterial (*Acetobacter xylinum*) biopolymer:

Some thermo-mechanical properties, *International Journal of Biological Macromolecules*, 37, **2005**, 189-194.

[186] S. Ifuku, M. Nogi, K. Abe, K. Handa, F. Nakatsubo and H. Yano, Surface modification of bacterial cellulose nanofibers for property enhancement of optically transparent composites. Dependence on acetyl-group DS, *Biomacromolecules*, 8, **2007**, 1973-1978.

[187] M. Nogi, K. Handa, A.N. Nakagaito and H. Yano, Optically transparent bionanofiber composites with low sensitivity to refractive index of the polymer matrix, *Applied Physics Letters*, 87, **2005**, 243110-3.

[188] M. Nogi, S. Ifuku, K. Abe, K. Handa, A.N. Nakagaito and H. Yano, Property enhancement of optically transparent bionanofiber composites by acetylation *Applied Physics Letters*, 89, **2006**, 233123-3.

[189] M. Nogi and H. Yano, Transparent nanocomposites based on cellulose produced by bacteria offer potential innovation in the electronics device industry, *Advanced Materials*, 20, **2008**, 1849-1852.

[190] JP Patent No. 10273891, **1998**

[191] European Patent EP0289993, **1988**.

[192] KR Patent, No. 20030065916, **2003**.

[193] J. Shah and Jr. R.M. Brown, Towards electronic paper displays made from microbial cellulose, *Applied Microbiology and Biotechnology*, 66 **2005**, 352-355.

[194] A. Budhiono, B. Rosidi, H. Taher and M. Iguchi, Kinetic aspects of bacterial cellulose formation in nata-de-coco culture system, *Carbohydrate Polymers*, 40, **1999**, 137-143.

[195] US Patent No. 4960763, **1990**.

[196] US Patent No. 4912049, **1990**.

[197] H.N. Pei, X.G. Chen, Y. Li and H.Y. Zhou, Characterization and ornidazole release in vitro of a novel composites films prepared with chitosan/poly(vinyl alcohol)/alginate, *Journal of Biomedical Materials Research Part A*, 85A, **2008**, 566-572.

[198] M. Mucha and A. Pawlak, Themal analysis of chitosan and its blends, *Thermochimica Acta*, 427, **2005**, 69-76.

[199] A. Pawlak and A. Mucha, Thermogravimetric and FTIR studies of chitosan blends, *Thermochimica Acta*, 396, **2003**, 153-166.

[200] K. Sakurai, T. Maegawa and T. Takahashi, Glass transition temperature of chitosan and miscibility of chitosan/poly(N-vinyl pyrrolidone) blends *Polymer*, 41, **2000**, 7051-7056.

[201] H. Kiuchi, W. Kai and Y. Inoue, Preparation and characterization of poly(ethylene glycol) crosslinked chitosan films, *Journal of Applied Polymer Science*, 107, **2008**, 3823-3830.

[202] M.M. Amiji, Permeability and blood compatibility properties of chitosan-poly(ethylene oxide) blend membranes for hemodialysis, *Biomaterials*, 16, **1995**, 593-599.

[203] F. Sébastien, G. Stéphane, A. Copinet and V. Coma, Novel biodegradable films made from chitosan and poly(lactic) acid with antifungal properties against mycotoxinogen strains, *Carbohydrate Polymers*, 65, **2006**, 185-193.

[204] T. Bourtoom and M.S. Chinnan, Preparation and properties of rice starch-chitosan blend biodegradable films, *LWT-Food Science and Technology*, 41, **2008**, 1633-1641.

[205] A. Sionkowska, M. Wisniewski, J. Skopinska, C.J. Kennedy and T.J. Wess, The photochemical stability of collagen–chitosan blends, *Journal of Photochemistry and Photobiology A:Chemistry*, 162, **2004**, 545-554.
[206] C.G.A. Lima, R.S. Oliveira, S.D. Figueiro, C.F. Wehmann, J.C. Goes and A.S.B. Sombra, DC conductivity and dielectric permittivity of collagen-chitosan films, *Materials Chemistry and Physics*, 99, **2006**, 284-288.
[207] L. Fang and S.H. Goh, Miscible chitosan/tertiary amide polymer blends, *Journal of Applied Polymer Science*, 76, **2000**, 1785-1790.
[208] Y.K. Twu, H.I. Huang, S.Y. Chang and S.L. Wang, Preparation and sorption activity of chitosan/cellulose blend beads, *Carbohydrate Polymers*, 54, **2003**, 425-430.
[209] M. Hasegawa, A. Isogai, F. Onabe, M. Usuda and R. H. Atalla, Characterization of cellulose-chitosan blend films, *Journal of Applied Polymer Science*, 45, **1992**, 1873-1879.
[210] I.S. Lima, A.M. Lazarin and C. Airoldi, Favorable chitosan/cellulose film combinations for copper removal from aqueous solutions *International Journal of Biological Macromolecules*, 36, **2005**, 79-83.
[211] C.-M. Shih, Y.-T. Shield and Y.K. Twu, Preparation and characterization of cellulose/chitosan blend films, *Carbohydrate Polymers*, 78, **2009**, 169-174.
[212] M. Phisalaphong and N. Jatupaiboon, Biosynthesis and characterization of bacteria cellulose–chitosan film, *Carbohydrate Polymers*, 74, **2008**, 482-488.
[213] J.M. Urreaga and M.U. de la Orden, Chemical interactions and yellowing in chitosan-treated cellulose, *European Polymer Journal*, 42, **2006**, 2606-2616.
[214] Y. Kim, R. Jung, H.S. Kim and H.J. Jin, Transparent nanocomposites prepared by incorporating microbial nanofibrils into poly(L-lactic acid), *Current Applied Physics*, 9, **2009**, S69-S71.
[215] H. Fukuzumi, T. Saito, T. Wata, Y. Kumamoto and A. Isogai, Transparent and high gas barrier films of cellulose nanofibers prepared by TEMPO-mediated oxidation, *Biomacromolecules*, 10, **2009**, 162-165.
[216] H.M.C. de Azeredo, Nanocomposites for packaging applications, *Food Research International* 42, **2009**, 1240-1253.
[217] Y. Shimazaki, Y. Miyazaki, Y. Takezawa, M. Nogi, K. Abe, S. Ifuku and H. Yano, Excellent thermal conductivity of transparent cellulose nanofiber / epoxy resin nanocomposites, *Biomacromolecules*, 8, **2007**, 2976-2978.
[218] R. Jung, H.S. Kim, Y. Kim, S.M. Kwon, H.S. Lee and H.J. In, Electrically conductive transparent papers using multiwalled carbon nanotubes, *Journal of Polymer Science. Part. B*, *Polymer Physics*, 46, **2008**, 1235-1242.
[219] M. Nogi, S. Iwamoto, A.N. Nakagaito and H. Yano, Optically transparent nanofiber paper, *Advanced Materials*, 21, **2009**, 1595-1598.
[220] M.A. Hubbe, O.J. Rojas, A.L. Lucia and M. Sain, Cellulosic nanocomposites: A review, *Bioresources*, 3, **2008**, 929-980.
[221] H. Yano, J. Sugiyama, A.N. Nakagaito, M. Nogi, T. Matsuura, M. Hikita and K. Handa, Optically transparent composites reinforced with networks of bacterial nanofibers, *Advanced Materials*, 17, **2005**, 153-155.
[222] J. Bicerano and J.L. Brewbaker, Reinforcement of polyurethane elastomers with microfibers having varying aspect ratios, *Journal of the Chemical Society, Faraday Transactions*, 91, **1995**, 2507-2513.

[223] W. Gindl and J. Keckes, Tensile properties of cellulose acetate butyrate composites reinforced with bacterial cellulose, *Composites Science and Technology*, 64, **2004**, 2407-2413.
[224] A.N. Nakagaito, S. Iwamoto and H. Yano, Bacterial cellulose: the ultimate nano-scalar cellulose morphology for the production of high-strength composites, *Applied Physics A- Materials Science & Processing*, 80, **2005**, 93-97.
[225] E.E. Brown and M.P.G. Laborie, Bioengineering bacterial cellulose/poly(ethylene oxide) nanocomposites, *Biomacromolecules*, 9, **2008**, 3427-3428.
[226] Y.Z. Wan, H.L. Luo, F. He, H. Liang, Y. Huang and X.L. Li, Mechanical, moisture absorption, and biodegradation behaviors of bacterial cellulose fibre-reinforced starch biocomposites, *Composite Science and Technology*, 69, **2009**, 1212-1217.
[227] I.M.G. Martins, S.P. Magina, L. Oliveira, C.S.R. Freire, A.J.D. Silvestre, C.P. Neto and A. Gandini, New biocomposites based on thermoplastic starch and bacterial cellulose, *Composites Science and Technology*, 69, **2009**, 2724-2733.
[228] D. Ciechanska, Multifunctional bacterial cellulose/chitosan composite materials for medical applications, *Fibres & Textile in Eastern Europe*, 12, **2004**, 69-72.
[229] V. Dubey, L.K. Pandey and C. Saxena, Pervaporative separation of ethanol/water azeotrope using a novel chitosan-impregnated bacterial cellulose membrane and chitosan-poly(vinyl alcohol) blends, *Journal of Membrane Science.*, 251, **2005**, 131-136.
[230] F. Shahidi, U. J. K. Arackchi and Y. J. Jeon, Food applications of chitin and chitosans, *Trends in Food Science and Technology*, 10, **1999**, 37-51.
[231] M.C. Chen, G.H.C. Yeh and B.H. Chiang, Antimicrobial and physicochemical properties of methylcellulose and chitosan films containing a preservative, *Journal of Food Processing and Preservation*, 20, **1996**, 379-390.
[232] C. Caner, P.J. Vergano and J.L. Willes, Chitosan film mechanical and permeation properties as affected by acid, plasticizer, and storage, *Journal of Food Science,* 63, **1998**, 1049-1053.
[233] A.E. Ghaouth, J. Arul, R. Ponnampalam and M. Boulet, Chitosan coating effect on storability and quality of fresh strawberries, *Journal of Food Science*, 56, **1991**, 1618-1621.
[234] C. Han, Y. Zhao, S.W. Leonard and M. G. Traber, Edible coatings to improve storability and enhance nutritional value of fresh and frozen strawberries (Fragaria ananassa) and raspberries (Rubus ideaus), *Postharvest Biology and Technology*, 33, **2004**, 67-78.
[235] C. Caner and O. Cansiz, Effectiveness of chitosan-based coating in improving shelf-life of eggs, *Journal of the Science of Food Agriculture*, 87, **2007**, 227-232.
[236] J.M. Lagaron, P. Fernandez-Saiz and M.J. Ocio, Using ATR-FTIR spectroscopy to design active antimicrobial food packaging structures based on high molecular weight chitosan Polysaccharide, *Journal of Agriculture and Food Chemistry*, 55, **2007**, 2554-2562.
[237] T.A. Khan, K.K. Peh and H.S. Ch'ng, Mechanical, bioadhesive strength and biological evaluations of chitosan films for wound dressing, *Journal of Pharm. Pharmaceut. SCI.*, 3, **2000**, 303-311.
[238] X.D. Liu, N. Nishi, S. Tokura, N. Sakairi, Chitosan coated cotton fibres: preparation and physical properties, *Carbohydrate Polymers*, 44, **2001**, 233-238.
[239] H. Struszczyk, in Chitin Handbook, R.A.A. Muzzarelli and M.G. Peter (eds.) European Chitin Society, Atec Edizioni, Grottammare, Italy, **1997**, pp. 437-440.

[240] P. Lertsutthiwong, M.M. Nazhad, S. Chandrkrachang and W.F. Stevens, Chitosan as a surface sizing agent for offset printing paper, *Appita Journal*, 57, **2004**, 274-280.
[241] H. Kjellgren, M. Gällstedt, G. Engström and L. Järnström, Barriers and surface properties of chitosan-coated greaseproof paper, *Carbohydrate Polymers*, 65, **2006**, 453-460.
[242] A. Ashori and W.D. Raverty, Printability of sized Kenaf (*Hibiscus cannabinus*) papers, *Polymer-Plastics Technology and Engineering*, 46, **2007**, 683-687.
[243] C. Andersson, New ways to enhance the functionality of paperboard by surface treatment – A review, *Packaging Technology Science*, 21, **2008**, 339-373.
[244] J. Kuusipalo, M. Kaunisto, A. Laine and M. Kellomäki, Chitosan as a coating additive in paper and paperboard, *Tappi Journal*, 4, **2005**, 17-21.
[245] H. Li, Y. Du and Y. Xu, Adsorption and complexation of chitosan wet-end additives in papermaking systems, *Journal of Applied Polymer Science*, 91, **2004**, 2642-2648
[246] M. Laleg and I.I. Pikulik, Wet-web strength increase by chitosan, *Nordic Pulp and Paper Research Journal*, 3, **1991**, 99-109.
[247] L. Allen, M. Polverari, B. Levesque and W. Francis, Effect of system closure on retention and drainage aid performance in TMP newsprint manufacture, *Tappi Journal*, 82, **1999**, 188-195.
[248] A. Ashori, J. Harun, W. Zin and M. Yusoff, Enhancing dry-strength properties of kenaf (*Hibiscus cannabinus*) paper through chitosan, *Polymer-Plastics Technology and Engineering*, 45, **2006**, 125-129.
[249] J. Shen, Z.Q. Song, X.R. Qian and C.J. Song, presented in part at the 2nd Internacional papermaking and environment conference, Tianjin, **2008**.
[250] A. Mimms, M.J. Kocurek, J.A. Pyatte and E.E. Wright (eds.) Kraft Pulping- A compilation of notes, Tappi Press, Atlanta, **1993**.
[251] P.A.C. Gane, Nanoscience in paper coating technology, 7th International Paper and Coating Chemistry Symposium, **2009**.
[252] JP Patent No. 8049188, **1996**.
[253] International Patent WO 93/11182, **1993**.
[254] US Patent No. 5637197, **1997**.
[255] M. Henriksson, L. A. Berglund, P. Isaksson, T. Lindström and T. Nishino, Cellulose nanopaper structures of high toughness, *Biomacromolecules*, 9, **2008**, 1579-1585.
[256] Y. Matsuda and F. Onabe, Swelling and adsorption properties of microfibrillated cellulose, *Society of Fiber Science and Technology*, 53, **1997**, 79-85.
[257] K. Mörseburg and G. Chinga-Carrasco, Assessing the combined benefits of clay and nanofibrillated cellulose in layered TMP-based sheets, *Cellulose*, 16, **2009**, 795-806.
[258] H.J. Xiu, Z.J. Wang and J.B. Li, Effect of bacterial cellulose on paper property, 2nd International Symposium on Technologies of Pulping, Papermaking and Biotechnology on Fiber Plants, Nanjing, **2004**.
[259] D.S. Argyropoulos (ed.), Materials, Chemicals, and Energy from Forest Biomass, ACS Symposium Series 954, Washington, **2007**.
[260] C.V. Stevens and R. Verhé, (eds.), Renewable Bioresources, John Wiley, New York, **2004**.

[261] A.J. Ragauskas, C.K. Williams, B.H. Davison, G. Britovsek, J. Cairney, C.A. Eckert, W. J. Frederick, J. P. Hallett, D. J. Leak, C. L. Liotta, J. R. Mielenz, R. Murphy, R. Templer and T.T., The path forward for biofuels and biomaterials, *Science*, 311, **2006**, 484-489.

[262] M. Evtiouguina, A.M. Barros, J.J. Cruz-Pinto, C.P. Neto, M.N. Belgacem, C. Pavier and A. Gandini, The oxypropylation of cork residues: preliminary results, *Bioresource Technology*, 73, **2000**, 187-189.

[263] M. Evtiouguina, A. Barros-Timmons, J.J. Cruz-Pinto, C.P. Neto, M.N. Belgacem and A. Gandini, Oxypropylation of cork and the use of the ensuing polyols in polyurethane formulations, *Biomacromolecules*, 3, **2002**, 57-62.

[264] C. Pavier and A. Gandini, Oxypropylation of sugar beet pulp. 1. Optimisation of the reaction, *Industrial Crops and Products*, 12, **2000**, 1-8.

[265] C. Pavier and A. Gandini, Oxypropylation of sugar beet pulp. 2. Separation of the grafted pulp from the propylene oxide homopolymer, *Carbohydrate Polymers*, 42, **2000**, 13-17

[266] P. Velazquez-Morales, J.F. Le Nest and A. Gandini, Polymer electrolytes derived from chitosan/polyether networks, *Electrochimica. Acta*, 43, **1998**, 1275-1279.

[267] A. Gandini, M.N. Belgacem, Z.X. Guo and S. Montanari, in Chemical Modification, Properties, and Usage of Lignin, T.Q. Hu (ed.), Kluwer Academy/Plenum Publishers, **2002**, pp. 57-80.

[268] H. Nadji, C. Bruzzese, M.N. Belgacem, A. Benaboura and A. Gandini, Oxypropylation of lignins and preparation of rigid polyurethane foams from the ensuing polyols, *Macromolecules Materials and Engineering*, 290, **2005**, 1009-1016.

[269] C.A. Cateto, M.F. Barreiro, A.E. Rodrigues and A. Belgacem, Optimization study of lignin oxypropylation in view of the preparation of polyurethane rigid foams, *Industrial and Engineering. Chemistry Research*, 48, **2009**, 2583-2589.

[270] M. Matos, M.F. Barreiro and A. Gandini, Olive stone as a renewable source of biopolyols, *Industrial Crops and Products*, in press, **2010**.

[271] M. Evtiouguina, A. Gandini, C.P. Neto and M.N. Belgacem, Urethanes and polyurethanes based on oxypropylated cork: 1. Appraisal and reactivity of products, *Polymer International*, 50, **2001**, 1150-1155.

[272] C. Pavier and A. Gandini, Urethanes and polyurethanes from oxypropylated sugar beet pulp - I. Kinetic study in solution, *European Polymer Journal*, 36, **2000**, 1653-1658.

[273] A. Gandini, A.A.S. Curvelo, D. Pasquini and A.J. de Menezes, Direct transformation of cellulose fibres into self-reinforced composites by partial oxypropylation, *Polymer*, 46, **2005**, 10611-10613.

[274] A.J. de Menezes, D. Pasquini, A.A.S. Curvelo and A. Gandini, Novel thermoplastic materials based on the outer-shell oxypropylation of corn starch granules *Biomacromolecules*, 8, **2007**, 2047-2050.

[275] A.J. de Menezes, D. Pasquini, A.A.S. Curvelo and A. Gandini, Self-reinforced composites obtained by the partial oxypropylation of cellulose fibers. 1. Characterization of the materials obtained with different types of fibers, *Carbohydrate Polymers*, 76, **2009**, 437-442.

[276] A.J. de Menezes, D. Pasquini, A.A.S. Curvelo and A. Gandini, Self-reinforced composites obtained by the partial oxypropylation of cellulose fibers. 2. Effect of

catalyst on the mechanical and dynamic mechanical properties, *Cellulose*, 16, **2009**, 239-246.
[277] A. Gandini and M.N. Belgacem, in Monomers, Polymers and Composites from Renewable Resources, M. N. Belgacem and A. Gandini (eds.) Elsevier, London, ch. 12, **2008**.
[278] C. A. Cateto, PhD Thesis, FEUP/PAGORA-INP, **2008**.
[279] Y. Wan, K.A. M. Creber, B. Peppley and T.V. Bui, Ionic conductivity and tensile properties of hydroxyethyl and hydroxypropyl chitosan membranes, *Journal of Polymer Science, Part B*, 42, **2004**, 1379-1397.
[280]. D. Asahina, T. Matsubara, Y. Miyashita and Y. Nishio, Synthesis of hydroxypropyl derivatives of chitin and chitosan and observation of phase behavior of their aqueous solutions, *Sen-I Gakkaishi*, 56, **2000**, 435-442.
[281] S.J. Kim, S.S. Kim and Y.M. Lee, Synthesis and characterization of ether-type chitin derivatives, *Macromolecules Chemistry and Physics*, 195, **1994**, 1687-1693.
[282] S.S. Kim, S.J. Kim, Y.D. Moon and Y.M. Lee, Thermal-characteristics of chitin and hydroxypropyl chitin, *Polymer*, 35, **1994**, 3212-3216.
[283] Y. Liu, G. Chen and K.A. Hu, Synthesis, characterization and structural analysis of polylactide grafted onto water-soluble hydroxypropyl chitin as backbone, *Journal of Material Science Letters*, 22, **2003**, 1303-1305.
[284] I.K. Park and Y.H. Park, Preparation and structural characterization of water-soluble O-hydroxypropyl chitin derivatives, *Journal of Applied Polymer Science*, 80, **2001**, 2624-2632.
[285] Y.F. Peng, B.Q. Han, W.S. Liu and X. Xu, Preparation and antimicrobial activity of hydroxypropyl chitosan. Carbohydrate Research, *Journal of Carbohydrate Research* , 340, **2005**, 1846-1851.
[286] W.M. Xie, P.X. Xu, W. Wang and Q. Liu, Preparation and antibacterial activity of a water-soluble chitosan derivative, *Carbohydrate Polymers*, 50, **2002**, 35-40.
[287] A.C. Neville, Springer-Verlag, Berlin, **1975**, pp. 7-60.
[288] C.S.R. Freire, A.J.D. Silvestre, C. Pascoal Neto and J.A.S. Cavaleiro, Lipophilic extractives of the inner and outer barks of *Eucalyptus globulus*, *Holzforschung*, 56, **2002**, 143-149.
[289]. C. Della Volpe and S.J. Siboni, Some reflections on acid-base solid surface free energy theories, *Journal of Colloid Interface Science*, 195, **1997**, 121-136.
[290] D.K. Owens and R.C. Wendt, Estimation of the surface free energy of polymers, *Journal of Applied Polymer Science*, 13, **1969**, 1741-1747.
[291] A. Gennadios, C.L. Weller and C.H. Gooding, Measurement errors in water-vapor permeability of highly permeable, hydrophilic edible films, *Journal of Food Engeneering*, 21, **1994**, 395-409.
[292] P. Kubelka and P.Z. Munk, Optics of Coloring *Tech Phys*, 12, **1931**, 593-601.
[293] M. Rinaudo, P. Le Dung, C. Gey and M. Milas, Substituent distribution on *O*, *N*-carboxymethylchitosan by ^{1}H and ^{13}C NMR, *International Journal of Biological Macromolecules*, 14, **1992**, 122-128.
[294] D.W.S. Wong, F.A. Gastineau, K.S. Gregorski, S.J. Tillin and A.E. Pavlath, Chitosan-lipid films: microstructure and surface energy, *Journal of Agricultural and Food Chemistry*, 40, **1992**, 540-544.
[295] M. Rillosi and G. Buckton, Modelling mucoadhesion by use of surface energy terms obtained from the Lewis acid-Lewis base approach. II. Studies on anionic, cationic and unionisable polymers, *Pharmacological Research*, 12, **1995**, 669-675.

[296] H. Yamatoto, A. Nishida and K. Ohkawa, *Colloids and Surfaces A*, 149, **1999**, 553-559.
[297] I.F. Amaral, P.L. Granja, L.V. Melo, B. Saramago and M.A. Barbosa, *Journal of Applied Polymer Science*, 102, **2006**, 276-284.
[298] A. Sionkowska, H. Kaczmarek, M. Wisniewski, J. Skopinska, S. Lazare and V. Tokarev The influence of UV irradiation on the surface of chitosan films, *Surface Science*, 600, **2006**, 3775-3779.
[299] M. Yun, Y.L. Jia, Y.L. Shang, F.H. Liao, J.R. Li, S.H. Zhang and O. Zhang, Crosslinked chitosan doped with Y2(CO3)3 and surface energy and electro rheological properties *Journal of Applied Polymer Science*, 105, **2007**, 2427-2432.
[300] H. Angellier, S. Molina-Boisseau, M.N. Belgacem and A. Dufresne, Chemical surface modification of waxy maize starch nanocrystals, *Langmuir*, 21, **2005**, 2425-2433.
[301] M.N. Belgacem and A. Gandini, in E. Pefferkorn (ed.), Interfacial Phenomena in Chromatography, M. Dekker, N.Y, vol. 2, **1999**, pp.44.
[302] A. Gandini and M. N. Belgacem, Cellulose fibre reinforced polymer composites, Old City Publishing, Philadelphia, vol. 3, **2007**.
[303] M.N. Belgacem, A. Blayo and A. Gandini, Surface characterization of polysaccharides, lignins, printing ink pigments, and ink fillers by Inverse Gas Chromatography, *Journal of Colloid Interface Science*, 182, **1996**, 431-436.
[304] K.G. Nair and A. Dufresne, Crab shell chitin whiskers reinforced natural rubber nanocomposites.3. Effect of chemical modification of chitin whiskers, *Biomacromolecules*, 4, **2003**, 1835-1842.
[305] M.J. Zohuriaan and F. Shokrolahi, Thermal studies on natural and modified gums, *Polymer Testing*, 23, **2004**, 575-579.
[306] A. Béin and M. R.V. Calsteren, Antimicrobial films produced from chitosan, *International Journal of Biological Macromolecules*, 26, **1999**, 63-67.
[307] D. Britto and O.B.G. Assis, Synthesis and mechanical properties of quaternary salts of chitosan based films for food application, *International Journal of Biological Macromolecules*, 41, **2007**, 198-203.
[308] G. Ma, D. Yang, Y. Zhou, M. Xiao, J.F. Kennedy and J. Nie, Preparation and characterization of water-soluble N-alkylated chitosan, *Carbohydrate Polymers*, 74, **2008**, 121-126.
[309] Z. Zheng, L. Zhang, L. Kong, A. Wang, Y. Gong and X. Zhang, The behavior of MC3T3-E1 cells on chitosan/poly-L-lysine composite films: Effect of nanotopography, surface chemistry, and wettability, *Journal Biomedical Materials Research- A*, 89, **2009**, 453-465.
[310] S. L. Maunu, Progress in Nuclear Magnetic Ressonance Spectroscopy, Elsevier, Amsterdam, vol. 40, **2002**, pp. 151.
[311] A. Larena and D.A. Caceres, Variability between chitosan membrane surface characteristics as function of its composition and environmental conditions, *Applied Surface Science*, 238, **2004**, 273-277.
[312] R.H. Chen and H. D. Hwa, Effect of molecular weight of chitosan with the same degree of deacetylation on the thermal, mechanical, and permeability properties of the prepared membrane, *Carbohydrate Polymers*, 29, **1996**, 353-358.
[313] M.E.S. Miranda, C. Marcolla, C.A. Rodrígues, H.M. Wilhelm, M.R. Sierakowski, T.M.B. Bresolin and R.A. Freitas, Chitosan and *N*-carboxymethylchitosan:

I. the role of *N*-carboxymethylation of chitosan in the thermal stability and dynamic mechanical properties of its films, *Polymer International*, 55, **2006**, 969-977.

[314] R. Lamim, R.A. Freitas, E.I. Rudek, H.M. Wilhelm, O.A. Cavalcanti and T.M. Bresolin, Films of chitosan and N-carboxymethylchitosan. Part II. Effect of plasticizers on thier physicochemical properties, *Polymer International*, 55, **2006**, 961-968.

[315] C. Santos, P. Seabra, B. Veleirinho, I. Delgadillo and J.A. Lopes-da-Silva, Acetylation and molecular mass effects on barrier and mechanical properties of shortfin squid chitosan membranes, *European Polymer Journal*, 42, **2006**, 3277-3285.

[316] E. Trovatti, A.L. Oliveira, C.S.R. Freire, A.J.D. Silvestre, C. Pascoal Neto, J.J. Cruz Pinto and A. Gandini, Novel bacterial cellulose-acrylic resin nanocomposites, *Composites Science Technology*, *in press*, **2010**.

[317] A. Anedda, C.M. Carbonaro, F. Clemente, R. Corpino, S. Grandi, A. Magistris and P.C. Mustarelli, Rhodamine 6G–SiO2 hybrids: A photoluminescence study, *Journal of Non-Crystalline Solids*, 351, **2005**, 1850-1854.

[318] L.T. Canham, Laser dye impregnation of oxidized porous silicon on silicon wafers, *Applied Physics Letters*, 63, **1993**, 337-339.

[319] H. Chi, H. Li, W. Liu and H. Zhan, The retention- and drainage-aid behavior of quaternary chitosan in papermaking system, *Colloids and Surfaces A: Physicochemical and Engineering Aspects* 297 **2007**, 147-153.

[320] R. Belalia, S. Grelier, M. Benaissa and V. Coma, New Bioactive Biomaterials Based on Quaternized Chitosan, *Journal of Agricultural and Food Chemistry*, 56, **2008**, 1582-1588.

[321] H. Li, Y. Du, X. Wu and H. Zhan, Effect of molecular weight and degree of substitution of quaternary chitosan on its adsorption and flocculation properties for potential retention-aids in alkaline papermaking, *Colloids and Surfaces A: Physicochemical and Engineering Aspects*, 242, **2004**, 1-8.

[321] H. Li, Y. Du, Y. Xu, H. Zhan and J. F. Kennedy, Interactions of cationized chitosan with components in a chemical pulp suspension, *Carbohydrate Polymers*, 58, **2004**, 205-214.

[322] Z. Liu and Y. Z. Sang, 3rd International Symposium on Emerging Technologies of Pulping and Papermaking, Guangzhou, China, **2006**.

[323] M. Hasegawa, A. Isogai and F. Onabe, Alkaline sizing with alkylketene dimers in the presence of chitosan salts, *Journal of Pulp and Paper Science,* 23, **1997**, 528-531

[324] L.N. Yu, Z. Long and R. Zhang, 2nd International Papermaking and Environment Conference, Tianjin, **2008**.

[325] W.H. Bureau, What the printer should know about paper, GATF, Graphic Arts Technical Foundation, USA, **1989**.

[326] E. Svanholm and G. Ström, Influence of polyvinyl alcohol on inkjet printability, International Printing & Graphic Arts Conference, **2004**.

[327] L.J. Bellamy, The infrared spectra of complex molecules, Chapman and Hall, London, Third ed, **1975**.

Appendices

Appendix 1

pH, weight, thickness of chitosan and nanocomposite films

Samples	pH	Mass (g)	Thickness (μm)
		Chitosan	
HCH	**4.10±0.05**	**0.320±0.05**	**29.6±0.9**
LCH	**4.03±0.01**	**0.309±0.03**	**29.3±0.8**
WSHCH	**6.89±0.01**	**0.305±0.02**	**30.5±0.7**
WSLCH	**6.95±0.03**	**0.312±0.04**	**29.5±0.8**
		CHNFC	
HCHNFC5	**4.19±0.05**	**0.307±0.05**	**30.6±0.3**
HCHNFC10	**4.22±0.08**	**0.312±0.03**	**29.9±0.5**
LCHNFC5	**4.17±0.03**	**0.305±0.04**	**30.2±0.1**
LCHNFC10	**4.05±0.00**	**0.303±0.06**	**30.5±0.5**
LCHNFC20	**4.04±0.01**	**0.310±0.02**	**30.7±0.2**
LCHNFC30	**4.01±0.01**	**0.321±0.03**	**32.1±0.3**
LCHNFC40	**4.06±0.01**	**0.305±0.01**	**31.2±0.3**
LCHNFC50	**4.08±0.00**	**0.313±0.05**	**32.0±0.5**
LCHNFC60	**4.07±0.01**	**0.313±0.07**	**32.1±0.7**
WSHCHNFC5	**6.93±0.01**	**0.300±0.04**	**30.9±0.1**
WSHCHNFC10	**7.00±0.05**	**0.315±0.05**	**31.2±0.7**
WSLCHNFC10	**6.98±0.03**	**0.308±0.01**	**30.5±0.6**
WSLCHNFC60	**6.81±0.08**	**0.321±0.03**	**31.5±0.4**
		CHBC	
HCHBC5	**4.08±0.01**	**0.304±0.01**	**29.5±0.5**
HCHBC10	**4.08±0.00**	**0.317±0.04**	**30.7±0.4**
LCHBC5	**4.10±0.05**	**0.325±0.06**	**33.1±0.2**
LCHBC10	**4.09±0.06**	**0.330±0.02**	**31.7±0.6**
LCHBC20	**4.08±0.04**	**0.314±0.02**	**29.9±0.7**
LCHBC30	**4.07±0.00**	**0.335±0.03**	**32.3±0.6**
LCHBC40	**4.08±0.01**	**0.326±0.01**	**32.1±0.3**
WSHCHBC5	**6.93±0.02**	**0.309±0.05**	**31.6±0.2**
WSHCHBC10	**6.95±0.05**	**0.321±0.02**	**31.8±0.2**

Appendix 2

^{1}H NMR spectrum of CH in D_2O/HCl solution (10 mg/mL) at 85ºC

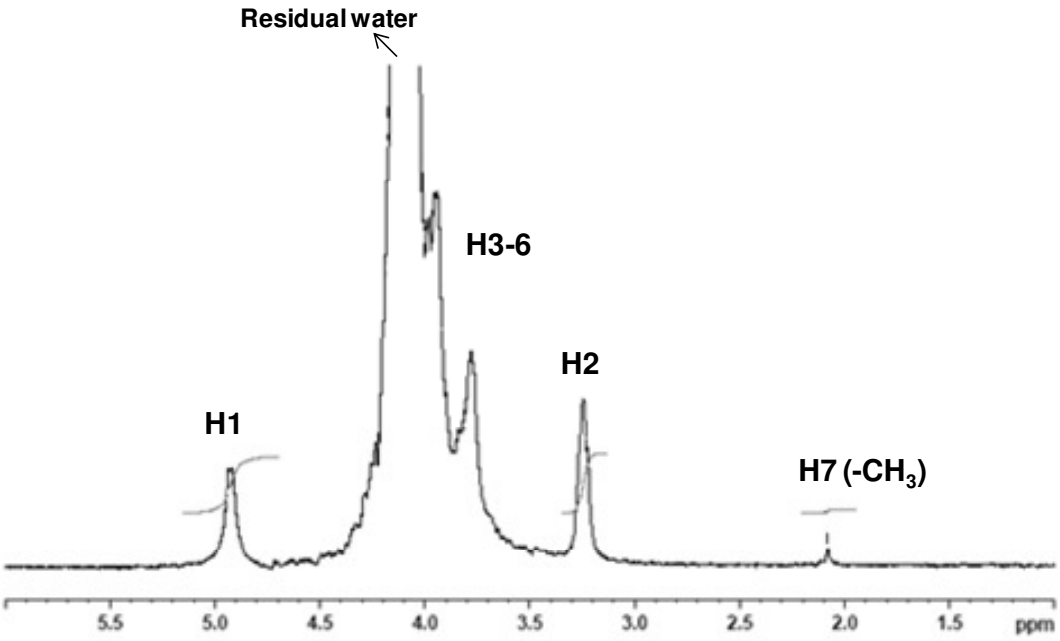

Note: Due to the elevated DDA values, the peak corresponding of the *N*-acetyl glucosamine units (H1') is very small.

Appendix 3

^{13}C CP-MAS NMR spectra of chitosan samples and of their quaternary ammonium salt derivatives

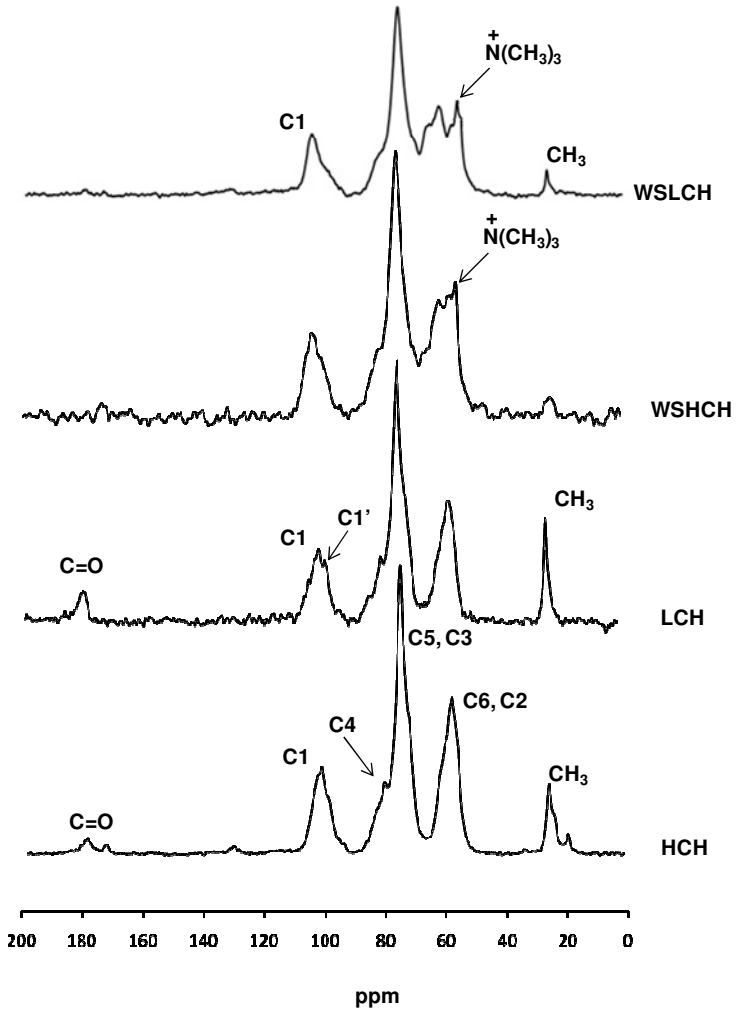

^{13}C CP-MAS NMR spectra of HCH before and after blending with 10% of BC and NFC

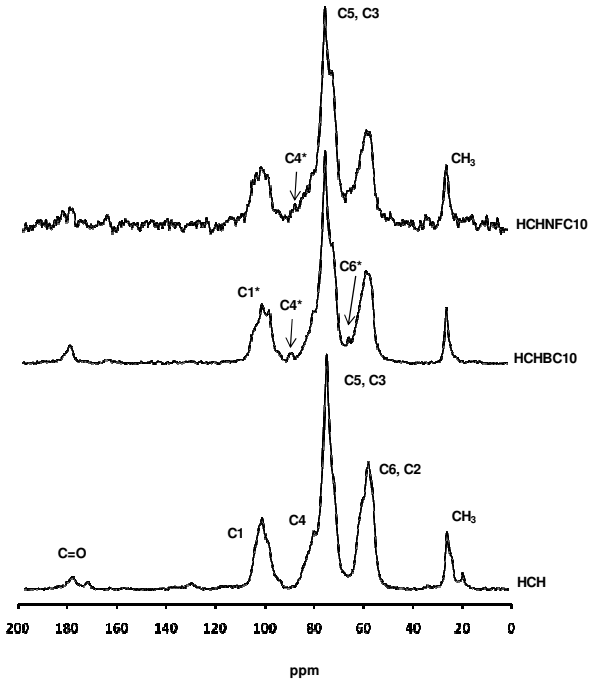

^{13}C CP-MAS NMR spectra of WSHCH and WSHCHBC10 films

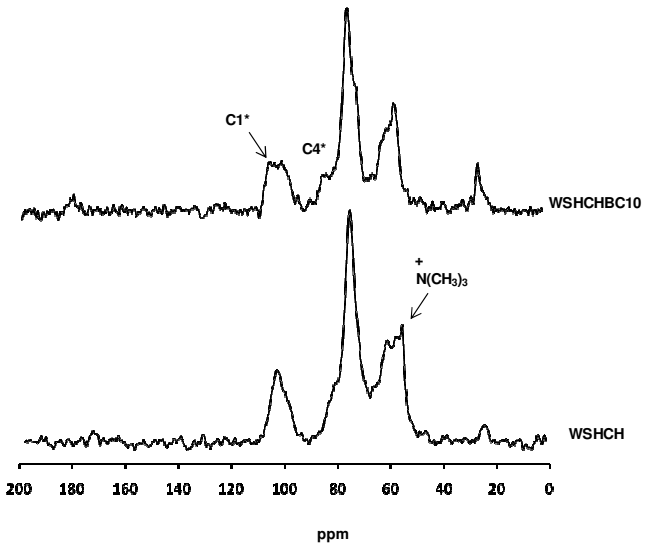

Note: C* corresponding to cellulose signals

^{13}C CP-MAS NMR spectra of WSLCH, WSHCHBC10 and WSHCHBC60 films

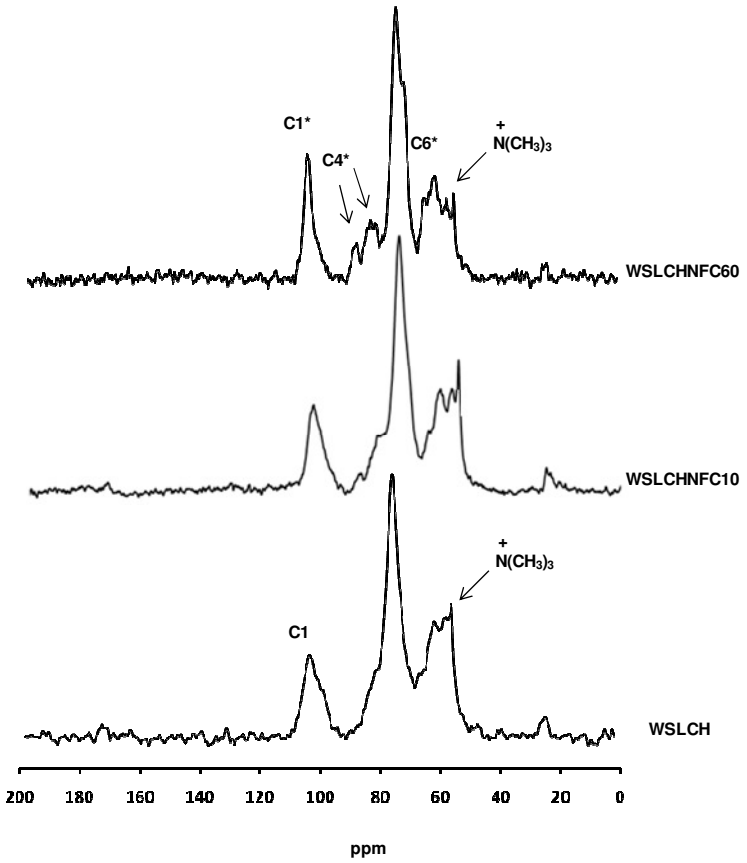

Note: C* corresponding to cellulose signals

Appendix 4

TGA curves of NFC, LCH, WSLCHNFC10 and WSLCHNFC60 with the corresponding dTGA plots of WSLCH and WSLCHNFC60

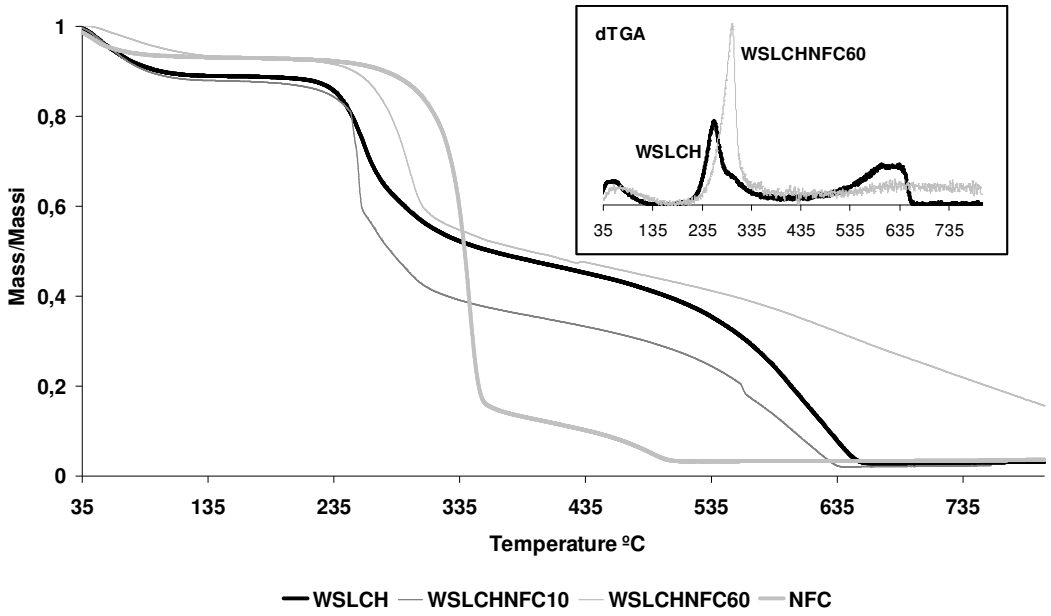

Appendix 5

Temperature dependence of the storage modulus of LCH a) and HCH b) films filled with different contents of bacterial cellulose (10 and 30%)

a)

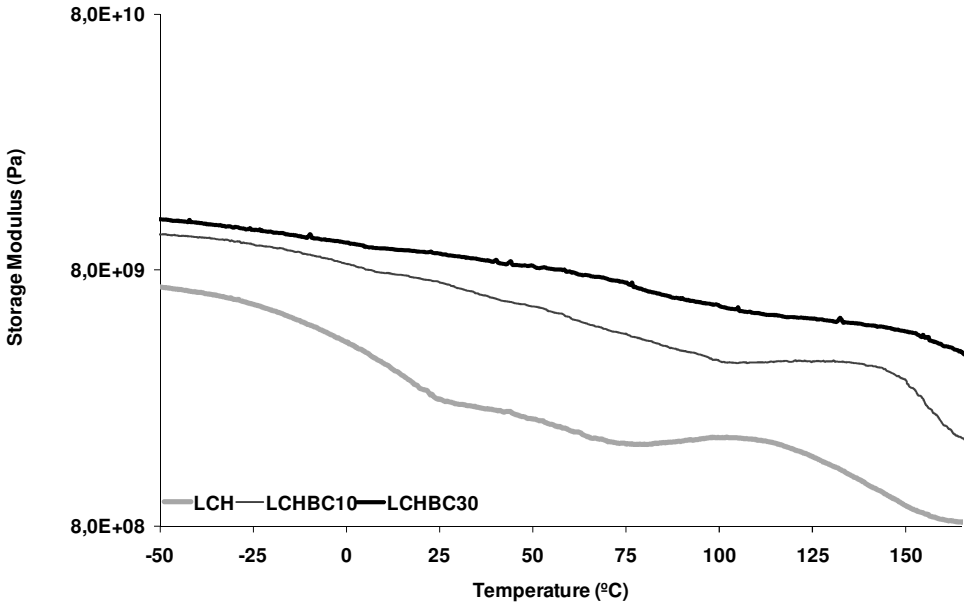

b)

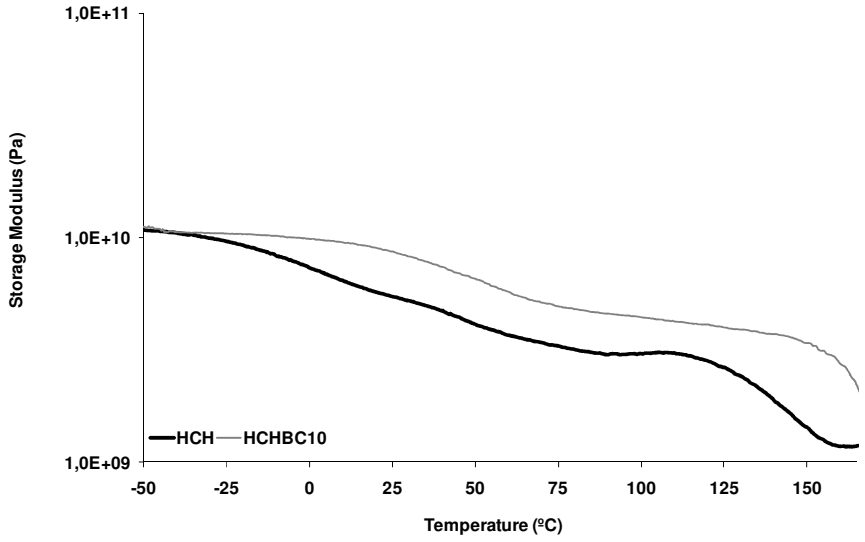

Temperature dependence of the storage modulus of WSHCH and WSHCHNFC10

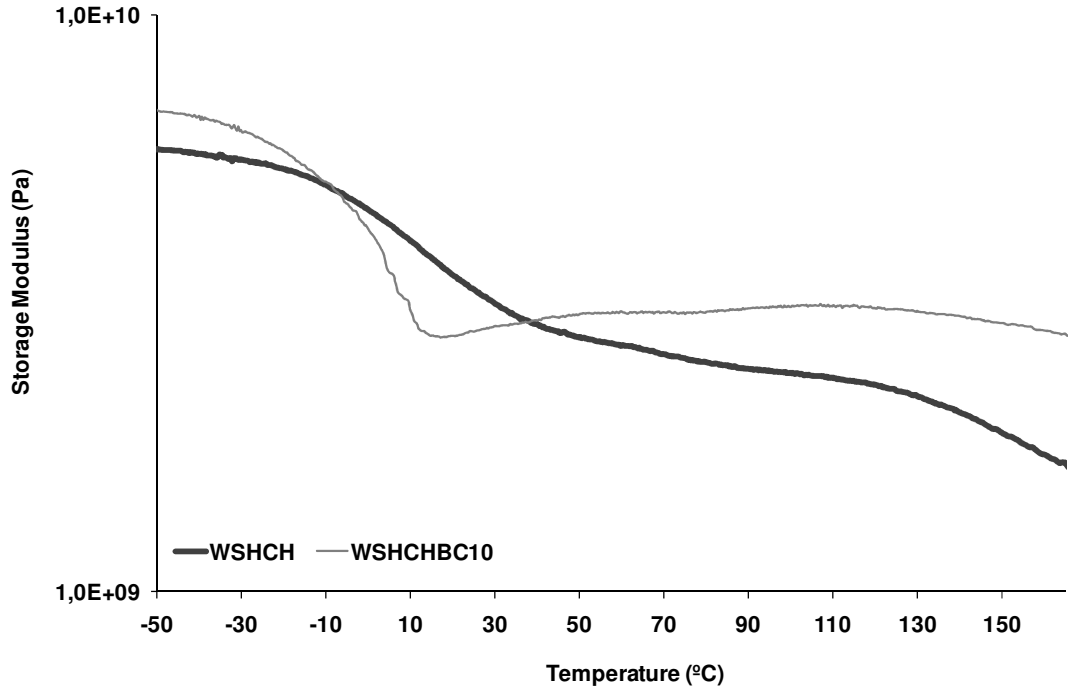

Appendix 6

Grammage, grammage gains and apparent density of chitosan-coated papers

	1 layer	2 layers	3 layers	4 layers	5 layers
Grammage [g/m^2]					
AA	73.8 ± 0.4	74.0 ± 0.1	73.8 ± 0.4	73.9 ± 0.3	73.8 ± 0.2
W	73.7 ± 0.4	73.7 ± 0.5	73.8 ± 0.4	73.8 ± 0.4	73.8 ± 0.1
MT	73.8 ± 0.2	-	73.7 ± 0.3	-	73.9 ± 0.4
LCH	75.8 ± 0.2	76.8 ± 0.2	77.4 ± 0.3	78.2 ± 0.2	78.9 ± 0.3
WSLCH	75.8 ± 0.3	76.5 ± 0.2	77.5 ± 0.2	77.9 ± 0.1	78.6 ± 0.1
FITC-LCH	76.0 ± 0.5	77.3 ± 0.3	77.8 ± 0.2	78.5 ± 0.2	79.2 ± 0.4
HCH	75.9 ± 0.2	-	-	-	-
WSHCH	76.1 ± 0.2	-	-	-	-
Grammage Gain [g/m^2]					
AA	-0.4	-0.5	-0.4	-0.4	-0.5
W	-0.4	-0.4	-0.3	-0.4	-0.4
MT	-0.7	-	-0.5	-	-0.5
LCH	1.5	2.5	3.2	3.9	4.6
WSLCH	1.6	2.2	3.0	3.6	4.3
FITC-LCH	1.5	2.6	3.3	4.1	4.9
HCH	1.8	-	-	-	-
WSHCH	2.0	-	-	-	-
Apparent Density [g/cm^3]					
AA	0.73± 0.01	0.74± 0.01	0.74± 0.01	0.73± 0.00	0.73± 0.01
W	0.74± 0.01	0.74± 0.01	0.74± 0.01	0.73± 0.01	0.73± 0.01
MT	-	-	-	-	-
LCH	0.74± 0.01	0.75± 0.01	0.75± 0.01	0.77± 0.01	0.77± 0.00
WSLCH	0.73± 0.00	0.740± 0.00	0.74± 0.01	0.75± 0.01	0.76± 0.01
FITC-LCH	-	-	-	-	-

Appendix 7

Bendtsen roughness of chitosan-coated papers

	Bendtsen Roughness (smooth side) [mL/min.]				
	1 layer	**2 layers**	**3 layers**	**4 layers**	**5 layers**
AA	253±23	242±18	237±8	243±10	250±20
W	252±24	243±10	241±16	247±13	240±14
MT	-	-	-	-	-
LCH	274±8	262±8	241±14	232±11	205±13
WSLCH	279±9	256±9	244±6	235±5	219±11
FITC-LCH	-	-	-	-	-

Appendix 8

Mechanical properties of chitosan-coated papers

	1 layer	2 layers	3 layers	4 layers	5 layers
Tensile Index (MD) [N.m/g]					
AA	86.2±2.0	85.02±1.3	81.8±0.8	80.4±1.7	79.2±1.3
W	86.8±0.6	86.6±0.5	84.9±2.8	84.6±1.2	84.33±5.29
MT	89.1±2.8	-	89.0±0.5	-	86.6±1.8
LCH	100.3±1.2	110.1 ± 0.8	114.2 ± 0.3	115.1 ± 0.7	117.4 ± 0.8
WSLCH	95.9±1.2	104.2 ± 1.3	111.1 ± 1.3	113.6 ± 1.7	116.9 ± 0.9
FITC-LCH	99.7 ± 1.0	105 ± 0.6	110 ± 0.9	113 ± 0.5	114 ± 0.7
Tensile Index (CD) [N.m/g]					
AA	25.4±0.3	25.5±0.3	25.4±0.7	24.7±0.3	24.4±0.1
W	25.5±0.1	25.5±0.1	25.1±0.1	25.1±0.5	25.0±0.2
MT	25.4±1.1	-	26.6±0.8	-	26.3±0.6
LCH	28.7±0.4	31.8±1.0	34.0 ± 1.8	35.3 ± 0.7	37.5 ± 0.4
WSLCH	28.6±0.9	30.7±1.0	33.8 ± 1.2	34.1±1.3	35.1±1.4
FITC-LCH	29.1±0.8	32.9±0.6	34.4±1.1	35.9±0.4	38.7±0.2
Tensile Index Gain (MD) [%]					
AA	-2.4	-3.8	-7.5	-9.0	-10.4
W	-1.8	-2.1	-4.0	-4.2	-4.6
MT	0.2	-	0.1	-	-2.5
LCH	14.3	25.0	29.3	32.6	33.7
WSLCH	8.5	18.8	25.2	29.4	31.8
FITC-LCH	12.8	19.6	24.1	28.2	28.3
Tensile Index Gain (CD) [%]					
AA	-1.9	-1.9	-2.3	-5.1	-6.1
W	-1.8	-1.9	-3.3	-3.5	-3.7
MT	-2.8	-	1.7	-	0.7
LCH	10.5	22.5	31.2	35.8	44.9
WSLCH	10.2	18.0	30.3	36.8	40.9
FITC-LCH	11.9	26.5	32.4	38.3	49.0

	1 layer	2 layers	3 layers	4 layers	5 layers
Stretch at Break (MD) [%]					
AA	2.0 ±0.0	2.0 ±0.0	1.9 ±0.0	1.9 ±0.1	1.9 ±0.1
W	2.0 ±0.0	2.0 ±0.1	2.0 ±0.0	2.0 ±0.1	2.0 ±0.1
MT	-	-	-	-	-
LCH	2.7 ± 0.1	2.9 ± 0.1	3.0 ± 0.0	3.3 ± 0.1	3.4 ± 0.1
WSLCH	2.7 ± 0.1	2.8 ± 0.2	3.0 ± 0.0	3.2 ± 0.1	3.3 ± 0.2
FITC-LCH	-	-	-	-	-
Stretch at Break (CD) [%]					
AA	3.0 ±0.0	3.0 ±0.0	3.0 ±0.1	3.0 ±0.1	3.0 ±0.1
W	3.1 ±0.0	3.1 ±0.0	3.1 ±0.1	3.1 ±0.1	3.1 ±0.1
MT	-	-	-	-	-
LCH	4.4 ± 0.3	4.7 ± 0.4	5.0 ± 0.1	5.1 ± 0.4	5.2 ± 0.0
WSLCH	4.1 ± 0.1	4.7 ± 0.4	4.8 ± 0.0	5.1 ± 0.3	5.3 ± 0.1
FITC-LCH	-	-	-	-	-
Stretch at Break Gain (MD) [%]					
AA	-2.3	-3.0	-6.0	-6.5	-7.0
W	-1.8	-1.7	-1.3	-1.8	-1.3
MT	-	-	-	-	-
LCH	31.7	42.6	47.5	61.6	65.3
WSLCH	29.3	36.2	41.7	55.8	62.3
FITC-LCH	-	-	-	-	-
Stretch at Break Gain (CD) [%]					
AA	-2.8	-3.5	-2.5	-2.5	-2,5
W	-0.8	-1.2	-1.2	-1.1	-1.3
MT	-	-	-	-	-
LCH	43.0	52.5	59.6	62.8	68.8
WSLCH	32.6	51.1	55.3	65.4	71.3
FITC-LCH	-	-	-	-	-

	Bursting strength index [N.m/g]				
	1 layer	**2 layers**	**3 layers**	**4 layers**	**5 layers**
AA	3.1 ±0.0	3.1 ±0.0	3.1 ±0.0	3.0 ±0.0	3.0 ±0.0
W	3.1 ±0.1	3.1 ±0.1	3.0 ±0.0	3.0 ±0.0	3.0 ±0.1
MT	-	-	-	-	-
LCH	4.3±0.0	4.4±0.0	4.8±0.1	4.9±0.1	5.0±0.2
WSLCH	4.1±0.1	4.3±0.1	4.6±0.1	4.8±0.1	4.9±0.1
	Bursting strength Gain [%]				
AA	-1.5	-2.8	-3.1	-3.9	-4.2
W	-1.3	-2.4	-3.8	-3.7	-3.7
MT	-	-	-	-	-
LCH	35.2	39.1	51.0	54.4	57.6
WSLCH	31.1	35.2	46.6	57.4	61.0
FITC-LCH	-	-	-	-	-

Appendix 9

Brightness, whiteness and opacity of chitosan-coated papers

Brightness [%]					
	1 layer	**2 layers**	**3 layers**	**4 layers**	**5 layers**
AA	90.7±0.0	90.7±0.1	90.5±0.2	90.5±0.1	90.3±0.3
W	92.5±0.1	91.9±0.1	91.8±0.6	91.8±0.2	91.8±0.4
MT	-	-	-	-	-
LCH	91.2±0.2	88.7±0.1	88.0±0.0	86.7±0.2	85.7±0.5
WSLCH	92.6±0.0	92.0±0.1	90.9±0.4	89.9±0.3	89.2±0.1
FITC-LCH	-	-	-	-	-
Brightness Gain [%]					
AA	-2.0	-2.1	-2.3	-2.3	-2.5
W	-0.1	-0.7	-0.9	-0.8	-0.9
MT	-	-	-	-	-
LCH	-1.5	-4.2	-4.9	-6.4	-7.5
WSLCH	0.1	-0.6	-1.8	-2.2	-3.0
FITC-LCH	-	-	-	-	-
Whiteness [%]					
	1 layer	**2 layers**	**3 layers**	**4 layers**	**5 layers**
AA	144.9±1.2	-	147.7±1.2	-	146.1±1.8
W	149.4±2.0	-	148.2±1.0	-	147.4±1.1
MT	-	-	-	-	-
LCH	146.4±1.8	-	140.1±1.1	-	133.6±1.5
WSLCH	148.0±1.3	-	147.3±0.9	-	147.9±0.7
FITC-LCH	-	-	-	-	-

Opacity [%]					
	1 layer	**2 layers**	**3 layers**	**4 layers**	**5 layers**
AA	93.1±0.2	92.9±0.4	93.0±0.1	93.1±0.0	92.6±0.1
W	92.4±0.0	92.6±0.2	92.4±0.0	92.5±0.4	92.2±0.1
MT	-	-	-	-	-
LCH	92.1±0.1	92.3±0.2	92.4±0.5	92.7±0.2	92.9±0.0
WSLCH	92.8±0.2	92.5±0.3	92.7±0.2	92.6±0.2	92.9±0.1
FITC-LCH	-	-	-	-	-

Appendix 10

Lightfastness of chitosan-coated papers

		Before	After	Delta	ΔE
CS	L	93,62	93,19	0,43	**2,70**
	a	2,53	2,00	0,53	
	b	-14,27	-11,66	-2,61	
	Whit.	149,02	136,58	12,44	
	Brigh.	104,24	99,22	5,02	

		Before	After	Delta	ΔE
AA1	L	93,29	92,93	0,36	**2,38**
	a	2,47	1,94	0,53	
	b	-13,48	-11,19	-2,29	
	Whit.	144,89	133,99	10,90	
	Brigh.	102,01	97,80	4,21	

		Before	After	Delta	ΔE
AA3	L	93,51	93,02	0,49	**2,69**
	a	2,39	1,90	0,49	
	b	-14,02	-11,42	-2,60	
	Whit.	147,73	135,49	12,24	
	Brigh.	103,65	98,64	5,01	

		Before	After	Delta	ΔE
AA5	L	94,45	93,00	1,45	**2,80**
	a	2,36	1,90	0,46	
	b	-13,67	-11,32	-2,35	
	Whit.	146,08	134,77	11,31	
	Brigh.	102,96	98,34	4,62	

		Before	After	Delta	ΔE
W1	L	93,57	93,14	0,43	**2,61**
	a	2,57	2,08	0,49	
	b	-14,38	-11,85	-2,53	
	Whit.	149,41	137,34	12,07	
	Brigh.	104,25	99,33	4,92	

		Before	After	Delta	ΔE
W3	L	93,54	93,15	0,39	**2,50**
	a	2,48	2,00	0,48	
	b	-14,12	-11,70	-2,42	
	Whit.	148,24	136,68	11,56	
	Brigh.	103,80	99,17	4,63	

		Before	After	Delta	ΔE
W5	L	93,50	93,12	0,38	**2,12**
	a	2,46	1,96	0,50	
	b	-13,95	-11,93	-2,02	
	Whit.	147,41	136,31	11,10	
	Brigh.	103,41	99,03	4,38	

		Before	After	Delta	ΔE
LCH1	L	93,16	92,75	0,41	**2,50**
	a	2,28	1,82	0,46	
	b	-13,85	-11,43	-2,42	
	Whit.	146,36	134,78	11,58	
	Brigh.	102,57	97,94	4,63	

		Before	After	Delta	ΔE
LCH3	L	92,11	90,95	1,16	**5,40**
	a	1,63	1,61	0,02	
	b	-11,41	-6,14	-5,27	
	Whit.	133,55	107,38	26,17	
	Brigh.	96,54	86,28	10,26	

		Before	After	Delta	ΔE
LCH5	L	92,59	91,55	1,04	**5,71**
	a	1,96	1,9	0,06	
	b	-12,66	-7,05	-5,61	
	Whit.	140,06	112,79	27,27	
	Brigh.	99,47	88,95	10,52	

		Before	After	Delta	ΔE
WSLCH1	L	93,38	92,97	0,41	**2,25**
	a	2,32	1,93	0,39	
	b	-14,12	-11,94	-2,18	
	Whit.	147,97	136,36	11,61	
	Brigh.	103,43	98,76	4,67	

		Before	After	Delta	ΔE
WSLCH3	L	93,21	92,84	0,37	**2,20**
	a	2,32	1,93	0,39	
	b	-14,04	-11,91	-2,13	
	Whit.	147,32	137,11	10,21	
	Brigh.	102,92	98,8	4,12	

		Before	After	Delta	ΔE
WSLCH5	L	93,12	92,7	0,42	**2,27**
	a	2,37	1,97	0,40	
	b	-14,2	-12,01	-2,19	
	Whit.	147,9	137,31	10,59	
	Brigh.	102,94	98,56	4,38	

Appendix 11

Gamut area & color density of CS coated with chitosan and water soluble chitosan derivative

Samples	Gamut Area	Colour Density			
		Cyan	Magenta	Yellow	Black
CS	7415 ± 22	1.06 ± 0.03	0.982± 0.01	1.04 ± 0.03	1.28± 0.02
Commercial Paper	7224 ± 30	1.16 ± 0.02	1.07± 0.03	1.02 ± 0.02	1.37± 0.02
AA1	7477 ± 20	1.02 ± 0.02	0.99 ± 0.01	1.06 ± 0.03	1.36± 0.03
AA3	7488 ± 15	1.05 ± 0.03	1.00 ± 0.01	1.07 ± 0.04	1.34± 0.02
AA5	7510 ± 11	1.08 ± 0.02	1.01 ± 0.02	1.10 ± 0.04	1.37± 0.03
W1	7395 ± 23	1.06 ± 0.04	1.00 ± 0.02	1.08 ± 0.03	1.30± 0.02
W3	7376 ± 17	1.07 ± 0.03	1.00 ± 0.02	1.10 ± 0.03	1.28± 0.01
W5	7546 ± 19	1.07 ± 0.02	1.01 ± 0.01	1.11 ± 0.02	1.28± 0.03
2.0% of LCH and WSLCH					
LCH1	7667 ± 20	1.17± 0.02	1.12± 0.01	1.12± 0.01	1.47± 0.01
LCH2	7630 ± 32	1.14± 0.01	1.11± 0.02	1.10± 0.02	1.49± 0.02
LCH3	7045 ± 22	1.07± 0.02	1.05± 0.02	1.05± 0.03	1.54± 0.01
LCH4	6610 ±18	1.04± 0.03	1.01± 0.03	1.02± 0.02	1.59± 0.01
LCH5	6335 ± 18	0.98± 0.01	0.96± 0.01	1.00± 0.01	1.61± 0.02
WSLCH1	8063±31	1.16± 0.01	1.09± 0.01	1.07± 0.03	1.41± 0.01
WSLCH2	8043±39	1.12± 0.03	1.07± 0.02	1.02± 0.02	1.48± 0.02
WSLCH3	8056±43	1.11± 0.01	1.07± 0.01	1.05± 0.01	1.47± 0.01
WSLCH4	7984±37	1.10± 0.03	1.05± 0.03	1.05± 0.02	1.49± 0.01
WSLCH5	7937±29	1.12± 0.02	1.09± 0.01	1.08± 0.01	1.48± 0.03

Appendix 12

Inter color bleed, black dot and horizontal line

Samples	ITCB	Black Dot		Black Horizontal Line (mm)
		Area (mm^2)	Diameter(mm)	
CS	46±2	0.224±0.001	0.534±0.003	0.504±0.001
Commercial Paper	45±1	0.202±0.002	0.507±0.002	0.505±0.002
AA1	43±1	0.199±0.002	0.503±0.003	0.488±0.002
AA3	42±2	0.197±0.001	0.501±0.002	0.484±0.001
AA5	49±1	0.195±0.001	0.498±0.001	0.469±0.001
W1	48±2	0.203±0.003	0.509±0.002	0.503±0.001
W3	49±2	0.204±0.002	0.509±0.001	0.496±0.002
W5	56±3	0.202±0.001	0.508±0.003	0.516±0.001
2.0% of LCH and WSLCH				
LCH1	50±2	0.183±0.001	0.489±0.002	0.453±0.001
LCH2	43±2	0.184±0.002	0.485±0.001	0.454±0.003
LCH3	44±2	0.182±0.001	0.485±0.001	0.451±0.002
LCH4	38±1	0.182±0.002	0.481±0.003	0.449±0.001
LCH5	32±1	0.180±0.003	0.479±0.001	0.444±0.002
WSLCH1	56±3	0.184±0.001	0.483±0.003	0.457±0.001
WSLCH2	50±4	0.186±0.002	0.487±0.002	0.455±0.002
WSLCH3	48±1	0.183±0.001	0.481±0.001	0.455±0.001
WSLCH4	47±2	0.180±0.001	0.480±0.003	0.457±0.003
WSLCH5	49±2	0.179±0.003	0.478±0.001	0.456±0.002

Appendix 13

FTIR spectra of chitin, the two liquid polyol fractions (HP and PL) and the SR resulting from its oxypropylation at 140 ºC

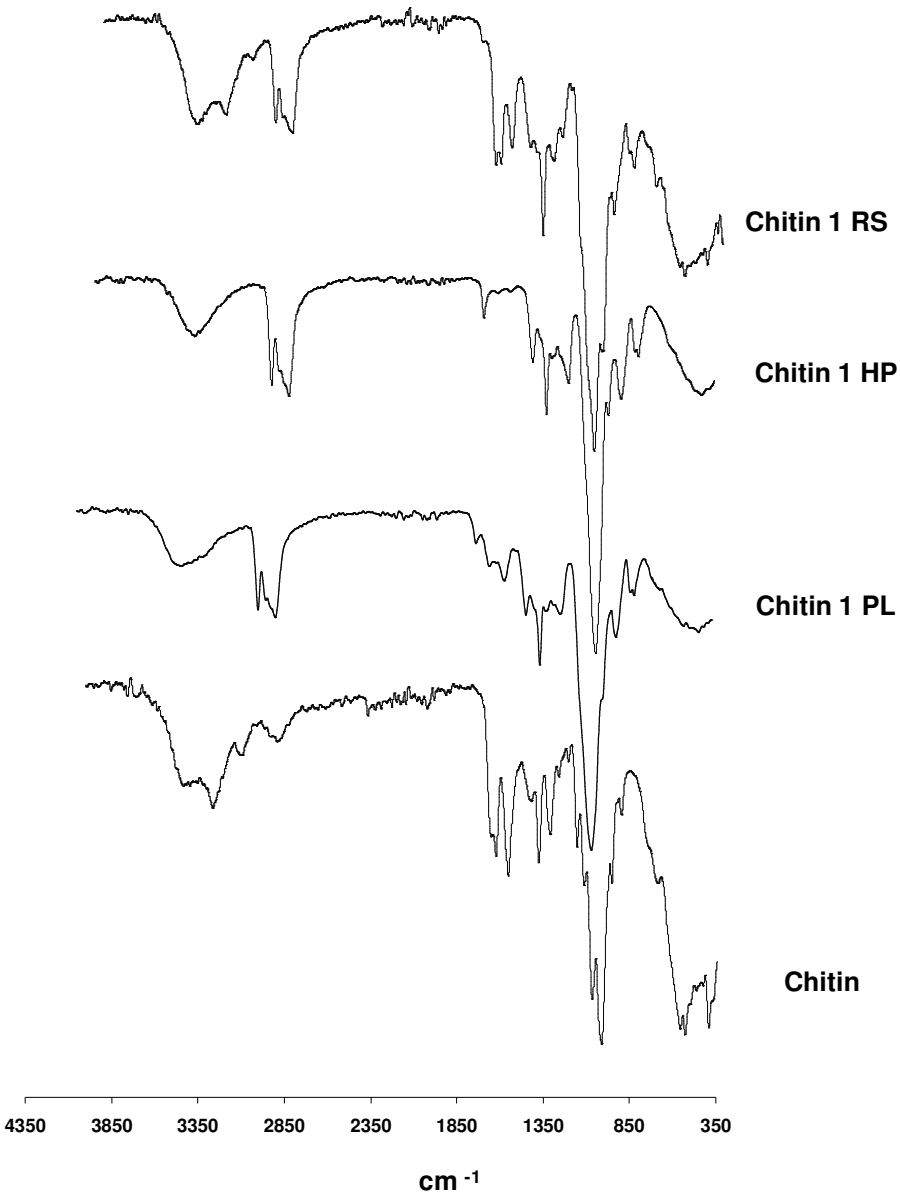

Appendix 14

Original papers

Susana C.M. Fernandes, Carmen S. R. Freire, Armando J. D. Silvestre, Jacques Desbriéres, Alessandro Gandini and Carlos Pascoal Neto, Production of coated papers with improved properties by using a water soluble chitosan derivative , *Industrial and Engineering Chemistry Research*, 49, **2010**, 6432-6438.

Susana C.M. Fernandes, Carmen S. R. Freire, Armando J. D. Silvestre, Carlos Pascoal Neto, Alessandro Gandini, Lars A. Berglund and Lennart Salmén, Transparent chitosan films reinforced with a high nanocellulose content, *Carbohydrate Polymer*, 81, **2010**, 394-401.

Susana C.M. Fernandes, Ana Lúcia Oliveira, Carmen S. R. Freire, Armando J. D. Silvestre, Carlos Pascoal Neto, Alessandro Gandini and Jacques Desbriéres, Novel Transparent nanocomposite Films Based on Chitosan and Bacterial Cellulose, *Green Chemistry*, 11, **2009**, 2023-2029.

Susana C.M. Fernandes, Carmen S. R. Freire, Armando J. D. Silvestre, Carlos Pascoal Neto, Alessandro Gandini, Jacques Desbriéres, Sylvie Blanc, Rute A. S. Ferreira and Luís D. Carlos, A study of the distribution of chitosan onto and within A paper sheet using a fluorescent chitosan derivative, *Carbohydrate Polymer*, 78, **2009,** 760-766.

Ana G. Cunha, Susana C.M. Fernandes, Carmen S.R. Freire, Armando J.D. Silvestre, Carlos Pascoal Neto, Alessandro Gandini, What is the real value of chitosan's surface energy? *Biomacromolecules*, 9, **2008**, p. 610-614.

Susana Fernandes, Carmen Sofia Freire, Carlos Pascoal Neto and Alessandro Gandini, The bulk oxypropilation of chitin and chitosan and the characterization of the ensuing polyols, *Geeen Chemistry*, 10, **2008**, p. 93-97.

Patents

Susana C.M. Fernandes, C.S.R. Freire, Armando J. D. Silvestre, C. Pascoal Neto and A. Gandini, *Aqueous Coating Compositions for Use in Surface Treatment of Cellulosic Substrates*, number PCT/IB2009/055622, deposit at 9th December **2009** at INPI – Instituto Nacional da Propriedade Industrial as Internacional Patent.

Susana C.M. Fernandes, C.S.R. Freire, Armando J. D. Silvestre, C. Pascoal Neto and A. Gandini, *Aqueous Coating Compositions for Use in Surface Treatment of Cellulosic Substrates*, number PT 104 702, deposit at 31st July **2009** at INPI – Instituto Nacional da Propriedade Industrial as National Patent.